Universidade de Aveiro Departamento de Biologia
2012

Marta Filipa Gomes Rodrigues

Análise dos Efeitos de Factores Climáticos e Antropogénicos na Ria de Aveiro

Effects of the Climatic Factors and Anthropogenic Actions in the Ria de Aveiro

Universidade de Aveiro Departamento de Biologia
2012

Marta Filipa Gomes Rodrigues

Análise dos Efeitos de Factores Climáticos e Antropogénicos na Ria de Aveiro

Effects of the Climatic Factors and Anthropogenic Actions in the Ria de Aveiro

Tese apresentada à Universidade de Aveiro para cumprimento dos requisitos necessários à obtenção do grau de Doutor em Biologia, realizada sob a orientação científica do Doutor Henrique Queiroga, Professor Auxiliar com Agregação do Departamento de Biologia da Universidade de Aveiro, e da Doutora Anabela Oliveira, Investigadora Principal do Núcleo de Tecnologias de Informação em Hidráulica e Ambiente do Laboratório Nacional de Engenharia Civil.

Apoio financeiro da FCT através da Bolsa de Doutoramento SFRH/BD/41033/2007.

o júri

presidente

Doutor Domingos Moreira Cardoso
professor catedrático da Universidade de Aveiro

Doutor António Eugénio de Melo Baptista
full professor da Division of Environmental and Biomolecular Systems, Institute of Environmental Health, Oregon Health & Science University, USA

Doutora Vanda Costa Brotas Gonçalves
professora catedrática da Universidade de Lisboa

Doutor Amadeu Mortágua Velho da Maia Soares
professor catedrático da Universidade de Aveiro

Doutor Henrique José de Barros Brito Queiroga
professor auxiliar com agregação da Universidade de Aveiro

Doutora Alexandra Maria Francisco Cravo
professora auxiliar do Centro de Investigação Marinha e Ambiental da Faculdade de Ciências e Tecnologia da Universidade do Algarve

Doutora Anabela Pacheco de Oliveira
investigadora principal do Laboratório Nacional de Engenharia Civil

Doutor Luís Ivens Ferraz Saavedra Portela
investigador auxiliar do Laboratório Nacional de Engenharia Civil

agradecimentos

A realização deste trabalho não teria sido possível sem o apoio de várias pessoas e instituições, às quais não posso deixar de agradecer.

Aos meus orientadores, Professor Henrique Queiroga, Doutora Anabela Oliveira e Professora Vanda Brotas, por toda a dedicação, motivação, e disponibilidade que demonstraram durante o decurso da tese. Um agradecimento especial ao Professor Henrique e à Doutora Anabela por toda a energia que tiveram nas campanhas de campo, e à Professora Vanda pelo apoio e conhecimentos transmitidos no trabalho laboratorial.

Ao Doutor André Fortunato, meu tutor no Laboratório Nacional de Engenharia Civil (LNEC), pela disponibilidade e por todos os comentários e sugestões, sempre construtivas. Agradeço ainda a participação nas campanhas.

Ao LNEC pelo acolhimento, pelo co-financiamento através do projecto *Análise integrada de processos físicos, químicos e ecológicos na zona costeira*, e pela disponibilização dos recursos necessários, entre os quais o *cluster* MEDUSA.

À Fundação para a Ciência e Tecnologia pelo financiamento, através da bolsa SFRH/BD/41033/2007.

À Universidade de Aveiro (UA) e ao Centro de Oceanografia da Faculdade de Ciências da Universidade de Lisboa (CO-FCUL) pela disponibilização de todos os recursos necessários para a realização do trabalho de campo e laboratorial.

À Fundação Luso-Americana para o Desenvolvimento pelo apoio através do projecto BGEM.

A todos os colegas do LNEC, da UA e do CO-FCUL pela participação nas campanhas, pelo apoio no traballho laboratorial e pelos conhecimentos transmitidos na utilização de alguns equipamentos: Xavier Bertin, Alphonse Nahon, Nicolas Bruneau, Ana Ré, Rui Marques, Aldiro Pereira, Bruna Silva, Sofia Tavares, João Carvalho, Sandra Plecha, Carolina Sá, Filipe Neves, Tânia Diniz e Bernardo Duarte. Um agradecimento especial ao Professor João Dias pela disponibilização do correntómetro.

Aos colegas do Núcleo de Estuários e Zonas Costeiras, em particular à Alda Silveira por todo o apoio com as burocracias de preparação das campanhas e ao Simões Pedro pela digitalização da marina.

Aos Professores Joseph Zhang e António Melo Baptista, pela disponibilização e actualização do código do modelo SELFE. Ao Professor Joseph Zhang agradeço também o apoio dado no desenvolvimento do modelo acoplado.

À Professora Maria Dolores Manso, pela disponibilização dos dados atmosféricos da estação meteorológica da UA.

Ao Eng. José Nordeste da Portucel-Soporcel pela informação disponibilizada sobre a Fábrica de Cacia.

Ao Eng. João Dragão da SIMRIA pela informação disponibilizada sobre o funcionamento deste sistema.

Aos colegas e amigos Alberto Azevedo, Lígia Pinto e Martha Guerreiro um agradecimento especial. Ao Alberto e à Lígia pelas longas discussões sobre o SELFE. Ao Alberto agradeço ainda a participação nas campanhas e o apoio no uso do Python. À Martha agradeço todo o apoio dado na preparação e execução das campanhas.

À minha família por estarem sempre ao meu lado.

Aos meus pais pelo amor e pela força que me transmitiram ao longo da vida.

Ao Rodrigo por tudo.

Obrigada.

palavras-chave

estuários, clorofila *a*, nutrientes, oxigénio dissolvido, modelação numérica, séries temporais longas, alterações climáticas, subida do nível do mar, aumento da temperatura do ar, regimes hidrológicos, intervenções antrópicas

resumo

A compreensão dos impactes das alterações climáticas é fundamental para a gestão a longo do prazo dos ecossistemas estuarinos. Esta compreensão só poderá ser efectiva considerando a variabilidade climática natural e o papel relativo das intervenções antropogénicas nestes ecossistemas. Assim, a presente dissertação analisa a influência das alterações climáticas e pressões antropogénicas na qualidade da água e dinâmica ecológica da Ria de Aveiro com base numa abordagem integrada, que combinou a análise de séries temporais dos últimos 25 anos e a modelação numérica de elevada resolução de cenários futuros de alterações climáticas e intervenções antropogénicas.

A componente de modelação de qualidade da água e ecológica foi melhorada a vários níveis. A análise de sensibilidade do modelo 3D hidrodinâmico-ecológico ECO-SELFE aplicado à Ria de Aveiro e a revisão das constantes de semi-saturação para absorção de nutrientes pelo fitoplâncton contribuíram para a precisão e robustez das aplicações. A concentração do fitoplâncton foi significativamente influenciada pelas taxas de crescimento do fitoplâncton e de mortalidade e excreção do zooplâncton, e apresentou uma sensibilidade reduzida à variação das constantes de semi-saturação na gama identificada para as diatomáceas. O acoplamento do ECO-SELFE a um modelo de campo próximo e a integração do ciclo do oxigénio aumentaram a sua capacidade de representação dos processos e das escalas espaciais relevantes. A validação do ECO-SELFE foi realizada com base num conjunto de campanhas específicas realizadas no canal de Mira. Os padrões espaciais e temporais observados para as várias variáveis (clorofila a, nutrientes, oxigénio dissolvido, salinidade, temperatura da água, correntes e níveis) foram simulados com erros menores ou semelhantes aos obtidos neste tipo de aplicações.

A análise dos padrões de variabilidade espacial e temporal da qualidade da água e ecológica na Ria de Aveiro a diferentes escalas, efectuada com base nos dados históricos de 1985 a 2010 complementados pelas campanhas realizadas, sugeriu uma influência combinada da variabilidade climática e das acções antropogénicas. Os cenários futuros de alterações climáticas e intervenções antropogénicas simulados evidenciaram uma influência mais significativa das alterações climáticas quando comparadas com os efeitos das acções antropogénicas analisadas. As variações mais significativas são previstas para os cenários de subida do nível do mar, seguidos dos cenários de alterações dos regimes hidrológicos, evidenciando o papel da circulação (maré e caudal fluvial) no estabelecimento da qualidade da água e dinâmica ecológica na laguna. Para os cenários de subida do nível do mar são previstos decréscimos significativos da clorofila *a* e dos nutrientes a jusante e nas zonas intermédias do canal, e um aumento significativo da salinidade a montante. Estas alterações poderão favorecer modificações da composição e distribuição das comunidades, afectando a cadeia alimentar e causando uma progressão para montante de espécies marinhas. Os resultados sugerem ainda que os efeitos poderão ser mais significativos em estuários pouco profundos.

keywords

estuaries, chlorophyll *a*, nutrients, dissolved oxygen, numerical modelling, long time series, climate change, sea level rise, air temperature rise, hydrological regimes, anhtropic interventions

abstract

Understanding the impacts of climate change is essential to ensure the long-term management of estuarine ecosystems. This understanding will only be reliable if the systems' natural variability and the relative role of anthropogenic pressures are considered. Thus, this thesis evaluates the influence of climate change and anthropogenic pressures on the water quality and ecological dynamics of the Aveiro lagoon based on an integrated approach, combining the analysis of long time series from the past 25 years and high-resolution numerical modelling of future scenarios of climate change and anthropogenic interventions in the lagoon.

The water quality and ecological modelling component was improved at several levels. The sensitivity analysis of the 3D hydrodynamic-ecological model ECO-SELFE applied in the Aveiro lagoon and the review of the half-saturation constants for nutrients uptake by phytoplankton contributed to the precision and robustness of the applications. Phytoplankton concentration was significantly influenced by the phytoplankton growth and zooplankton mortality and excretion rates, and presented a low sensitivity to the half-saturation constants variation within the range reviewed for diatoms. ECO-SELFE's coupling to a near field model and its extension to the oxygen cycle increased the model's ability to represent the relevant processes and spatial scales. ECO-SELFE validation was achieved based on a set of specific field campaigns performed along the Mira channel. The spatial and temporal patterns observed for the measured variables (chlorophyll *a*, nutrients, dissolved oxygen, salinity, water temperature, currents and water levels) were reproduced by the model with errors smaller or similar to the ones achieved in this type of applications.

The analysis of the spatial and temporal patterns of variability of the water and ecological quality in the Aveiro lagoon at different scales, based on historical data from 1985 to 2010 complemented by the campaigns performed, suggested a combined influence of the climatic variability and anthropogenic interventions. Future scenarios of climate change and anthropogenic interventions simulated revealed a larger influence of climate change when compared with the analysed anthropogenic actions. The most important variations from the reference scenario are predicted for the sea level rise scenarios, followed by the changes in the hydrological regimes scenarios, putting in evidence the main role of circulation (tide and river flow) in establishing the water quality and ecological dynamics in the lagoon. A significant decrease of chlorophyll *a* and nutrients is predicted in the downstream and middle areas of the channel due to sea level rise, while a significant salinity increase is predicted upstream. These changes may promote modifications in the communities' distribution and composition, affecting the food web and promoting a progression further upstream of the marine species. Results also suggest that the identified effects may be more important in shallow estuaries.

CONTENTS

LIST OF FIGURES

LIST OF TABLES

LIST OF SYMBOLS

ρ_u	Uptake rate for nutrients
$\hat{\psi}$	Earth-tidal potential (m)
$\dot{Q}$	Rate of absorption of solar radiation (W m^{-2})
α	Effective earth-elasticity factor (non-dimensional)
ν	Vertical eddy viscosity ($m^2 s^{-1}$)
κ	Vertical eddy viscosity for transport ($m^2 s^{-1}$)
$\eta(x,y,t)$	Free surface elevation (m)
(x,y)	Horizontal Cartesian coordinates (m)
(x_0, y_0, z_0)	Point of maximum concentration in the near field (m)
$(x_{dif}, y_{dif}, z_{dif})$	Diffuser coordinates (m)
$\bar{x}_{25y}$	25-years mean
AirT	Air temperature
AtoDenit	Denitrification
AtoN	Nitrification (mmol N m^{-3})
b	Total source buoyancy flux ($m^3 s^{-3}$)
b_B	Basal specific respiration rate of bacterioplankton (day^{-1})
b_{Pi}	Basal specific respiration rate (day^{-1})
b_{Zl}	Basal specific respiration rate (day^{-1})
C	Generic tracer concentration
CDO	Chemical oxygen demand concentration (mmol O_2 m^{-3})
C_{efec}(x,y)	Final concentration of the tracer predicted by the near field model ([mass] m^{-3})
c_{final}	Final concentration of the ecological variable
Chl a	Chlorophyll *a*
C_{init}	Initial concentration of the tracer in the effluent ([mass] m^{-3})
$c_{initial}$	Initial concentration of the ecological variable
$C_{max}(x_0,y_0,z_0)$	Maximum concentration predicted by the near field model ([mass] m^{-3})
$C_n(x,y,z)$	Concentration of the tracer at (x,y,z) in the near field ([mass] m^{-3})
C_p	Specific heat of water (J $kg^{-1} K^{-1}$)
C_v	Normalized state variable
Denit	Specific denitrification rate (day^{-1})
DO	Dissolved oxygen concentration
DO_{sat}	Dissolved oxygen concentration at saturation (mmol O_2 m^{-3})
DO_w	Increment to the dissolved oxygen saturation value due to the wind stress (mmol O_2 m^{-3})
e_i	Excretion rate (day^{-1})
ELM	Eulerian-Lagragian Method
f	Coriolis factor (s^{-1})
F	Froude number (non-dimensional)
f_B	Oxygen regulating factor (non-dimensional)

F_c	Horizontal diffusion term for tracer transport
F_h	Horizontal diffusion term for heat transport
F_s	Horizontal diffusion term for salt transport
g	Acceleration of gravity (m s^{-2})
g'	Modified acceleration due to gravity (m s^{-2})
GGE_C	Growth efficiency (non-dimensional)
$GGE_C{}^O$	Decrease in growth efficiency under anoxic conditions (non-dimensional)
H	Total water depth at the discharge point (m)
$h(x,y)$	Bathymetric depth (m)
h_e	Thickness of the plume in the near field (m)
i	Phytoplankton groups index
k	Scaling factor (non-dimensional)
K_{reaer}	Reaeration coefficient (m day^{-1})
K_s	Half-saturation constant for the nutrient uptake
K_{s_CDO}	Half-saturation constant for chemical oxygen demand (mmol O_2 m^{-3})
K_{sB_O}	Half-saturation constant for oxygen limitation (mmol O_2 m^{-3})
L	Diffuser length (m)
l	Zooplankton groups index
LD	Limit of detection
m_d	Mass of the tracer from the discharge
m_{int}	Integral of the concentration in the near field ([mass])
N	Buoyancy frequency (s^{-1})
NAO	NAO index
NH_4^+	Ammonium
NO_3^-	Nitrates
NO_x^-	Nitrates + nitrites
p	Given input parameter
$p_a(x,y,t)$	Atmospheric pressure at free-surface (N m^{-2})
PC_i	Phytoplankton carbon concentration of the group i (mmol C m^{-3})
PO_4^{3-}	Phosphates
Q	Wastewater discharge (m^3 s^{-1})
Q_B	Temperature coefficient for bacterioplankton (non-dimensional)
Q_{CDO}	Temperature constant for chemical oxygen demand (non-dimensional)
Q_{Pi}	Temperature coefficient for phytoplankton (non-dimensional)
Q_{Zl}	Temperature coefficient for zooplankton (non-dimensional)
Rain	Rainfall
reaer	Oxygen reaeration
reox	Reoxidation
reox_CDO	Specific reoxidation rate (day^{-1})
respB	Bacterioplankton respiration
$respP_i$	Respiration of the phytoplankton group i
$respZ_l$	Respiration of the zooplankton group l
RFlow	River flow

S	Water salinity
Salt	Salinity
S_{dil}	Minimum dilution in the near field (non-dimensional)
SiO_2	Silicates
SRad	Solar radiation
S_u	Nutrient concentration
t	Time (s)
T	Water temperature (ºC)
TVD	Total Variation Diminishing
U	Current velocity (m s^{-1})
u,v	Horizontal components of the velocity (m s^{-1})
$U_0=(u_{0dif},v_{0dif})$	Horizontal velocity at (x_0,y_0) (m s^{-1})
w	Vertical component of the velocity (m s^{-1})
w_0	Width of the plume in the near field (m)
WindI	Wind intensity
WTemp	Water temperature
x_b	Base value
X_i	Length of the near field (m)
x_{m_25y}	Long-term mean of each month
x_{m_y}	Mean of each month of each year
X_p	Logarithm of the input parameter p
x_p	Input parameter value
x_y	Yearly mean
z	Vertical coordinate (m)
ZC_l	Zooplankton carbon concentration (mmol C m^{-3})
z_m	Height to the top of minimum dilution due to the near field (m)
z_{m_y}	Standardized individual monthly anomaly
z_{mt}	Standardized monthly (*intra-annual*) anomaly
z_y	Standardized inter-annual anomaly
β_{Zl}	Excreted fraction of uptake (non-dimensional)
γ_{Pi}	Fraction of assimilated production (non-dimensional)
ΔX_p	Variation in the parameter p
Δx_p	Difference between the highest and the lowest values for the input parameter p
ΔY	Total influence of the input parameters on the state variable C_v
η_{Zl}	Assimilation efficiency (non-dimensional)
ΛC	Sources and sinks term for tracer transport
ΛCOD	Sources and sinks terms of chemical oxygen demand (mmol O_2 m^{-3})
ΛDO	Sources and sinks terms of dissolved oxygen (mmol O_2 m^{-3})
M	Reference anoxic mineralization rate (mmol O_2 m^{-3} day^{-1})
μ_{r_i}	Realized growth rate of the phytoplankton group i (day^{-1})
μ_{z_l}	Zooplankton growth rate due to food ingestion (day^{-1})
ρ_B	Bacterioplankton uptake
$\rho_{u\_\max}$	Maximum uptake rate for nutrients

σ_{25y}	25-years standard deviation
σ_{m_25y}	Standard deviation of each month over the 25-years period
σ_x, σ_y, σ_z	Standard deviations of the Gauss equation in x, y and z (m)
Ω^O_C	Stoichiometric coefficient to convert carbon to oxygen units (mmol O_2 mmol C^{-1})
Ω^O_N	Stoichiometric coefficient to convert nitrogen units to oxygen units (mmol O_2 mmol N^{-1})
Ω^S_C	Stoichiometric coefficient to convert sulfur to carbon units (mmol S mmol C^{-1})
Ω^S_O	Stoichiometric coefficient to convert sulfur to oxygen units (mmol S mmol O_2^{-1})
μ	Horizontal eddy viscosity ($m^2 s^{-1}$),
ρ	Water density at diffuser level (kg m^{-3})
ρ_0	Reference water density
ρ_{ef}	Effluent density (kg m^{-3})
$\rho_w(x,y,z,t)$	Water density (kg m^{-3})

CHAPTER I
GENERAL INTRODUCTION

SECTION I.1

THESIS OVERVIEW

I.1.1 MOTIVATION AND BACKGROUND

Estuaries are transition zones between the land and the sea and an integral part of the coastal zones, which present unique characteristics due to their location. From an ecological viewpoint, estuaries are among the most productive ecosystems in the world (Linkens, 2010), and harbour unique floral and faunal species. Economically and socially, estuaries support several human activities, such as marine transportation, navigation and harbours, recreational and commercial fishing, and tourism, with about 39 % of the world population living within 100 km from estuaries or coastal zones (World Resources Institute – http://earthtrends.wri.org). In this sense, the estuaries' ecological, economic and social values, and the need for their long-term conservation, have been worldwide recognized.

The structure and dynamics of the estuarine ecosystems is closely linked to the physical and climatic factors (e.g tide, freshwater discharge). An example of this close dependency is the effect of the hydrological regimes in the residence times of the nutrients within the estuary, which in turn influence the phytoplankton biodiversity (Ferreira *et al.*, 2005). So, changes in these drivers are expected to affect the estuarine ecosystems dynamics. There are, however, multiple threats that may alter this natural variability and reduce the estuarine ecosystems health, in particular water and ecological quality.

Climate change is a potential threat for the estuarine water and ecological quality maintenance and a matter of concern worldwide (IPPC, 2007), which should be evaluated when developing long-term management strategies. In particular, the study of climate change impacts on estuarine dynamics is mandatory for an adequate integrated coastal zones management (Gomes *et al.*, 2006; European Science Foundation – Marine Board, 2007) and to promote sustainable adaptation measures (Comissão para as Alterações Climáticas, 2009). Evidences of increases in air temperature, sea level rise and changes in the precipitation and maritime wave regimes grow worldwide (IPCC, 2007). However, although there is some consensus about some of the observed and predicted trends (e.g. air temperature and sea level rise), the extent of these changes remains uncertain (IPCC, 2007). Additionally, uncertainty increases when trends in the hydrological regimes and maritime wave regimes are evaluated (e.g. Miranda *et al.*, 2006). Some of the potential effects of climate change in the ecological dynamics of the estuaries include changes in the species abundance, productivity and composition, in the food

web and in the system economical values, among others (Struyf *et al.*, 2004; Hays *et al.*, 2005; Smith *et al.*, 2008). However, the studies on these issues are recent (e.g. Najjar *et al.*, 2010), and the possible impacts of climate change in estuarine water and ecological quality remain uncertain or poorly known. Moreover, due to the levels of uncertainty associated with the predicted changes in the climate and the interplay between the physical and climate drivers that affect the estuarine ecosystems dynamics, there is an additional level of complexity when evaluating the impacts of climate change in these systems. The system's natural variability should, thus, be taken into account when evaluating the potential impacts of climate change in the estuarine water and ecological dynamics.

Besides climate change, some of the human activities within the estuaries may also represent potential threats to their water and ecological quality (e.g. disposal of domestic, agriculture and industrial effluents, dredging, dam constructions). In particular, increased human activities in estuaries (Rabalais *et al.*, 2009) associated with climate change may increase the vulnerability of these systems. However, the relative role of these distinct drivers and the interactions are extremely difficult to assess. Recent studies suggest distinct effects when evaluating the relative role of climate and anthropogenic pressures in the coastal and estuarine ecosystems dynamics (e.g. Kotta *et al.*, 2009; Grangeré *et al.*, 2012). In this sense, the combined effects of climate change and of the anthropogenic pressures in the ecological quality of estuaries and on eutrophication potential should be evaluated (Ducharne *et al.*, 2007; Kotta *et al.*, 2009; Paerl *et al.*, 2010) and are fundamental for their sustainable management (Paerl, 2006).

Integrated analyses, combining numerical modelling and data studies, are valuable approaches to better understand the complexity of estuarine dynamics and, in particular, to evaluate the effects of climate change and anthropogenic pressures on these systems. Numerical models, which jointly simulate the physical, chemical and biological processes at the relevant spatial and temporal scales, are useful tools, as they allow to reproduce the observed behaviours (Endelvang *et al.*, 2005), to complement the data, and to exploit the ecosystems response to the climatic factors (Megrey *et al.*, 2007) and to the anthropogenic pressures (Grant *et al.*, 2005). Due to the complexity of the processes involved and the interactions between the physical, chemical and biological processes, the use of three-dimensional coupled hydrodynamic and ecological models is essential to adequately represent the ecosystem (Skogen and Moll, 2005). These models allow to consider all the relevant forcings (e.g. tide, river flows, heat exchanges) when evaluating the ecosystem dynamics. In turn, consistent data allow the models' validation at the relevant spatial and temporal scales and provide an alternative mean to investigate the ecosystem evolution, namely the past evolution of water and ecological quality. The concentrations of phytoplankton, nutrients and oxygen are widely used as indicators of surface waters' quality and in the evaluation of the ecosystems health (e.g. Water Framework Directive; Gameiro *et al.*, 2007).

The Aveiro lagoon is an example of an estuarine ecosystem that reflects most of the aspects mentioned above. From the ecological viewpoint it contains one of the largest saltmarshes areas in Europe and harbours ecological relevant species of fauna and flora, while it supports different economical activities (e.g. ports, tourism, aquaculture, small-scale fishing). Some of these anthropogenic pressures have contributed, in the last decades, to the degradation of the lagoon water and ecological quality (Lopes *et al.*, 2005; Lopes and Silva, 2006), although some recent measures have been undertaken to improve the system (e.g. wastewater treatment system – SIMRIA, Sistema Multimunicipal de Saneamento da Ria de Aveiro). Climate change might also affect the lagoon's ecological dynamics and some novel/exotic species of polychaetes have already been identified in the lagoon (Rodrigues *et al.*, 2009a). However the effects of climate change and anthropogenic pressures in the lagoon's ecological dynamics remain poorly understood. Although some numerical modelling studies have been performed (e.g. Dias and Lopes, 2006; Lopes and Silva, 2006), most of the past studies in the Aveiro lagoon rely essentially on physical, chemical and biological data (e.g. water temperature, salinity, chlorophyll *a*) analyses (e.g. Dias *et al.*, 1999; Almeida *et al.*, 2005; Leandro *et al.*, 2006; Lopes *et al.*, 2007a). Some of these studies suggest that the phytoplankton succession depend of the nutrients composition and concentration (Lopes *et al.*, 2007a) and others related it with the salinity and temperature gradients (Resende *et al.*, 2005). Moreover, integrated studies combining the potentialities of numerical modelling and data analyses are still scarce in the Aveiro lagoon, in particular regarding the long-term water quality and ecological dynamics of this estuarine system.

Thus, the combined use of historical data, complemented at the relevant spatial and temporal scales, with a coupled hydrodynamic and ecological model to predict future scenarios constitutes an advantageous methodological approach to study the relative role of the processes controlling the water and ecological quality in the Aveiro lagoon. This comprehensive study allows the extension of the previous knowledge about the relative influence of the climate forcing and of the anthropogenic interventions in the estuarine ecosystems, contributing for the long-term integrated management the Aveiro lagoon and of the estuarine systems, in general.

I.1.2 OBJECTIVES

The aim of this study is to evaluate the effects of climatic factors and anthropogenic pressures in the ecological and water quality of an estuarine system (Ria de Aveiro, Portugal). In particular, this study aims to:

i) contribute towards a better representation of the processes in phytoplankton modelling, through a review of selected parameters used in the evaluation of the phytoplankton

dynamics and in the parameterization of the ecological models, in particular the half-saturation constants for nutrients uptake, and an evaluation of the ecological model sensitivity to the input parameters definition;

ii) improve the state-of-the-art in water quality and ecological modelling based on unstructured grids, particularly adequate for complex geometry coastal systems, through the extension of the three-dimensional numerical model ECO-SELFE (Rodrigues *et al.*, 2009b), which couples the hydrodynamic model SELFE (Zhang and Baptista, 2008) and an ecological model extended from EcoSim 2.0 (Bisset *et al.*, 2004). These improvements intend to increase ECO-SELFE capacities to simulate multi-scale processes, through the coupling to a near field model, and the relevant processes in water quality and ecological modelling, through the addition of the oxygen cycle;

iii) develop a methodology to handle computationally-intensive simulations and validate ECO-SELFE improvements, based on a set of specific field campaigns, performed in the Mira channel of the Aveiro lagoon that account for the relevant scales;

iv) evaluate the evolution of the ecological and water quality in the Aveiro lagoon through the statistical data analyses of a multi-decade, 1985 to 2010, set of atmospheric, hydrological, hydrodynamic, chemical and biological data;

v) evaluate the system response to future scenarios of climate change (e.g. changes in air temperature and precipitation regimes, sea level rise) and anthropogenic pressures (e.g. dredging, wastewater discharges), through the joint use of the numerical model improved and validated in ii and iii) and the data analysis performed in iv).

The approach used to achieve the objectives listed above, combining detailed data analysis and numerical modelling, allows to account for all the relevant forcings (e.g. tide, river flows, solar radiation) to evaluate the scenarios of climate change and anthropogenic pressures, and to integrate them in the scope of the system natural variability.

I.1.3 THESIS ORGANIZATION

This thesis is organized in 6 chapters, including the present one (General Introduction). Some of these chapters correspond to research manuscripts that were already published, submitted or are in preparation to international journals and are listed in section I.1.4.

Besides introducing the thesis and describing its structure, Chapter I covers brief reviews of: i) the estuarine ecosystems and their response to the climatic factors; ii) ecological modelling, in particular, model evolution and state-of-the-art models; and iii) the study area (the Aveiro lagoon).

Chapter II reviews the half-saturation constants for nutrients (nitrogen, phosphorus and silica) uptake by phytoplankton and presents a brief example of application of the review performed.

The model developments, implementation and application in the Ria de Aveiro are presented in Chapter III. This chapter includes 3 sections: i) section III.1 describes the ecological model extension, through the coupling between the near field and the far field models; ii) section III.2 presents the sensitivity analysis to the input parameters of the coupled hydrodynamic and ecological model, applied to the Aveiro lagoon; and iii) section III.3 presents the development and implementation of the oxygen formulation and the extended model validation in the Ria de Aveiro based on the dedicated field campaigns.

Chapter IV presents the 1985 to 2010 statistical data analysis of the physical, chemical and biological variables in the Aveiro lagoon, evaluating the influence of the climatic variability and of the anthropogenic pressures evolution in the lagoon ecological and water quality dynamics. This analysis provides the system's natural variability and sets the conditions for the evaluation of the climate change and anthropogenic actions impacts.

The relative influence of the climate change, including sea level rise, increases in air temperature and changes in the hydrological regimes, and of anthropogenic pressures in the Aveiro lagoon water quality and ecological dynamics is presented in Chapter V.

Finally, the concluding remarks and considerations for future research are presented in Chapter VI.

This thesis also includes 4 appendixes, which complement the discussion presented through the main chapters. Appendix I encloses the set of data collected during the field campaigns. Appendix II describes a preliminary validation of the new formulation for the oxygen cycle in a real system, the Aljezur coastal stream, showing also the applicability of the coupled hydrodynamic and ecological model in other coastal and estuarine systems. Appendix III complements the results presented in Chapter IV, relative to the data analysis of the physical, chemical and biological variables in the Aveiro lagoon between 1985 and 2010. Appendix IV complements the results presented in Chapter V, relative to the influence of climate change and anthropogenic interventions on the Aveiro lagoon dynamics.

I.1.4 DISSEMINATION

Published, submitted or in preparation manuscripts to international journals included in this thesis:

- Chapter III, Section III.2: Rodrigues M, Oliveira A, Costa M, Fortunato AB, Zhang Y. Sensitivity analysis of an ecological model applied to the Ria de Aveiro, *Journal of Coastal Research* 2009, SI56, 448-452;
- Chapter III, Section III.3: Rodrigues M, Oliveira A, Queiroga H, Brotas V. Seasonal and diurnal water quality modelling along a salinity gradient (Mira channel, Aveiro lagoon, Portugal, *Procedia Environmental Sciences* 2012, 899-918;
- Chapter IV, Section IV.1: Rodrigues M, Queiroga H, Oliveira A, Brotas V, Manso MD. Climatic and anthropogenic factors driving water quality variability in the Aveiro lagoon: 1985-2010 data analysis, in preparation to *Sience of the Total Environment*;
- Chapter V, Section V.1: Rodrigues M, Oliveira A, Queiroga H, Brotas V, Fortunato AB. On the role of climate change and anthropogenic pressures in the water quality and ecological dynamics of an estuarine environment (Mira channel, Aveiro lagoon, Portugal), in preparation to *Estuarine, Coastal and Shelf Science*;
- Appendix III: the hydrodynamic model implementation and validation described was partly excerpted from Rodrigues M, Oliveira A, Guerreiro M, Fortunato AB, Menaia J, David LM, Cravo A. Modeling fecal contamination in the Aljezur coastal stream (Portugal), *Ocean Dynamics* 2011, 61(6), 841-856.

Other published or submitted manuscripts to international journals:

- Fortunato AB, Rodrigues M, Dias JM, Oliveira A. Generating inundation maps for a coastal lagoon: a case study in the Ria de Aveiro (Portugal), in review to *Ocean Engineering*.

Conference abstracts, proceedings and communications:

- Rodrigues M, Oliveira A, Costa M, Fortunato AB, Zhang Y. Sensitivity analysis of an ecological model applied to the Ria de Aveiro. Book of Abstracts of the 10th International Coastal Symposium, 2009, 93;
- Rodrigues M, Oliveira A, Queiroga H, Guerreiro M, Fortunato AB, Cravo A, Freitas MC, Menaia J, Dodkins I. Dynamic modeling of dissolved oxygen in the Aljezur coastal stream. Conference Handbook of the International Society for Ecological Modelling 2009 Conference, 2009;
- Rodrigues M, Oliveira A, Guerreiro M, Fortunato AB, Queiroga H. Water and ecological quality in the Aljezur coastal stream (Portugal). Book of Abstracts of the JONSMOD 2010 Conference, 2010;

- Rodrigues M, Oliveira A, Queiroga H, Brotas V, Fortunato AB, Zhang YJ. Modelação ecológica do ecossistema planctónico da Ria de Aveiro. In: Almeida A, Alves FL, Bernardes C, Dias JM, Gomes NCM, Pereira E, Queiroga H, Serôdio J, Vaz N (Eds.), Actas das Jornadas da Ria de Aveiro, 2011, 248-257;
- Rodrigues M, Dias JM, Leandro S, Morgado F, Cunha A, Almeida A, Oliveira A, Queiroga H. Caracterização sinóptica dos gradientes nos canais da Ria de Aveiro. Parte II: oxigénio, clorofila e zonação ecológica. In: Almeida A, Alves FL, Bernardes C, Dias JM, Gomes NCM, Pereira E, Queiroga H, Serôdio J, Vaz N (Eds.), Actas das Jornadas da Ria de Aveiro, 2011, 151-158;
- Dias JM, Rodrigues M, Leandro S, Morgado F, Oliveira A, Queiroga H. Caracterização sinóptica dos gradientes ambientais na Ria de Aveiro. Parte I: salinidade e temperatura, Livro de Actas das Jornadas da Ria de Aveiro. In: Almeida A, Alves FL, Bernardes C, Dias JM, Gomes NCM, Pereira E, Queiroga H, Serôdio J, Vaz N (Eds.), Actas das Jornadas da Ria de Aveiro, 2011,141-150;
- Oliveira A, Rodrigues M, Fortunato AB, Jesus G, Ribeiro NA, Dodet G, Dias JM. Previsão em tempo real da circulação na Ria de Aveiro. In: Almeida A, Alves FL, Bernardes C, Dias JM, Gomes NCM, Pereira E, Queiroga H, Serôdio J, Vaz N (Eds.), Actas das Jornadas da Ria de Aveiro, 2011, 310-315;
- Rodrigues M, Queiroga H, Brotas V, Oliveira A, Manso M. Factors driven phytoplankton variability in the Aveiro lagoon: 1996-2010 data analysis. Abstract of the ICES-NAFO – Symposium on the Variability of the North Atlantic and its Marine Ecosystems during 2000-2009, 2011;
- Rodrigues M, Oliveira A, Queiroga H, Brotas V. Seasonal and diurnal water quality modelling along a salinity gradient (Mira channel, Aveiro lagoon, Portugal. Conference Handbook of the International Society for Ecological Modelling 2011 Conference, 2011;
- Fortunato AB, Rodrigues M, Dias JM, Oliveira A. Modelação da inundação costeira na Ria de Aveiro, Actas do 11º Congresso da Água, 2012.

SECTION I.2

ESTUARIES AND THE ESTUARINE ECOSYSTEMS

Estuaries location, at the land-sea interface, leads to the unique characteristics of these systems. Several definitions have been proposed for *estuary*, mainly due to the large diversity and complexity of areas that constitute the estuarine systems. One of the most commonly used definition for *estuary* was proposed by Pritchard (1967): “An estuary is a semi-enclosed coastal body of water which has a free connection with the open sea and within which sea water is measurably diluted with fresh water derived from land drainage”. Due to the interaction between several factors, such as tide, waves, freshwater discharge and sediments transport, the estuarine systems may have distinct characteristics and morphologies, which are often used in their classification. There are several criteria used in the estuaries classification, such as morphology, stratification, tidal range, freshwater flow, nutrients concentrations (e.g. Cameron and Pritchard, 1963; Hansen and Rattray, 1966; Dyer, 1997; Crouzet *et al.*, 1999), which are complementary of each other.

The estuaries economic and ecological intrinsic values have been recognized worldwide. Overall, about 39 % of the world population lives within 100 km from estuaries or coastal zones (World Resources Institute – http://earthtrends.wri.org) and the human activities developed in these areas are diverse (e.g. marine transportation, navigation and harbours, recreational and commercial fishing, tourism, receiving waters for domestic and industrial effluents). From an ecological viewpoint, estuaries harbour unique species of fauna and flora and the services of their ecosystems are multiple, as coastal protection, biological productivity and diversity maintenance, water purification, recreation, education and research (Barbier *et al.*, 2011).

Estuarine ecosystems are normally characterized by the transition between the marine and the freshwater environment. James (2002) defines an ecosystem as a group of organisms connected to their environment, forming a natural unit of biotic and abiotic components that interact and promote fluxes of materials and energy. In this sense there is a strong interaction between the ecological and the physical processes in estuaries (James, 2002), and the fluxes of materials and energy are usually affected by the light availability, currents and water temperature, among other factors (e.g. Ferreira *et al.*, 2005; Gameiro and Brotas, 2010). These physical forcings interact among each other and vary from estuary to estuary, affecting the transport and dispersion of dissolved and particulate matter (e.g. nutrients), the distribution of the organisms within a specific estuarine system and, consequently, the biological activity (e.g. primary production, fish behaviour). Due to the strong interdependency between processes, the relative importance of these drivers in the estuarine ecosystems dynamics remains a matter of

discussion (Baumert and Petzoldt, 2008). Thus, the understanding of the estuarine ecosystems dynamics must be based on the knowledge of the interaction among the physical, chemical and biological processes.

I.2.1 LOWER TROPHIC LEVELS IN ESTUARIES

Estuaries are one of the most productive ecosystems around the world (McLusky and Elliot, 2004), with mean net primary production of 1500 (200-3500) g (dry matter) m^{-2} $year^{-1}$ (Likens, 2010). The estuarine food web is very complex and recent studies suggested that estuarine food webs could not simply be generalized (Choy *et al.*, 2008): phytoplankton, macroalgae and microphytobenthos are the trophic base supporting consumer production in some estuarine systems, while, in other estuaries, detritus, salt marshes or other producers perform this role. Although there is some controversy in the relative importance of phytoplanktonic productivity in estuaries, with values ranging from 7 to 875 g m^{-2} $year^{-1}$ (Underwood and Kromkamp, 1999), the estuarine primary productivity derives mostly from the photosynthetic activity of both phytoplankton and microphytobenthos in temperate regions (Underwood and Kromkamp, 1999).

Estuarine phytoplankton is composed by several species, but the dominant group is generally diatoms (Lalli and Parsons, 1997). Its composition varies significantly inside the estuary and depends on the transport of species from the rivers and/or from the marine coastal waters, the spatial and temporal variations of the elements that influence the phytoplankton growth (e.g. light and nutrients availability), and the hydrodynamic conditions, such as salinity and vertical mixing (e.g. Underwood and Kromkamp, 1999; Cloern, 2001; Ferreira *et al.*, 2005).

In estuaries factors like turbidity (Cloern, 1987), which may limit light availability in the water column, low residence times, when compared to phytoplankton growth rate (Gameiro and Brotas, 2010), or low nutrient concentrations (Domingues *et al.*, 2011) may limit phytoplankton growth. There are, however, situations of phytoplankton blooms, some of them associated with eutrophication. Ferreira *et al*. (2011) defines *eutrophication* as “the result of import-driven enrichment by nutrients – primarily N and/or P – in a waterbody, which modifies the ’pristine’ seasonal cycle, allowing a greater annual primary production of organic material and potentially leading to accumulation of algal biomass”. Episodes of eutrophication are natural in estuarine ecosystems (Pinckney *et al.*, 2001) but cultural eutrophication (i.e. eutrophication due to human-disturbance) is increasing worldwide due to an increase of nutrients from anthropogenic sources (Cloern, 2001). Eutrophication consequences can be diverse: it may lead to harmful or toxic species blooms (e.g. *Alexandrium*, *Pyrodinium* and *Gymnodinium*), affect the nutrients cycle, leading to a loss of biodiversity and replacement by opportunistic species, promote local hypoxic and anoxic conditions, and influence the food web, among other effects (e.g. Lehtonen *et al.*,

1998; Zimmerman and Canuel, 2000; Cardoso *et al.*, 2004; Burkholder *et al.*, 2007; Smayda, 2008).

Besides the role of physical and chemical processes in limiting the phytoplankton growth and blooms (bottom-up regulation), grazing may also be a limiting process (top-down regulation). The role of grazing in controlling the algal blooms has been a matter of discussion (Harris and Malej, 1986; Tan *et al.*, 2004; Smayda, 2008), as grazing may influence the species dynamics and the food web structure (Bathmann *et al.*, 1990). Tan *et al.* (2004) and Sautour *et al.* (1996) suggested a top-down regulation of phytoplankton in the Pearl River (China) and Gironde (France) estuaries, respectively. In turn, in the Tagus estuary (Portugal), the role of zooplankton in controlling phytoplankton blooms is reduced when compared to physical factors, in particular the light availability in the water column (Brogueira *et al.*, 2007).

I.2.2 ESTUARINE CIRCULATION AND PHYSICAL FACTORS

Hydrodynamics affects directly or indirectly the distribution of the physical, chemical and biological properties in the estuaries. Estuarine circulation derives mainly from the interaction between the freshwater discharged from the rivers and the salt water from tides (Hansen and Rattray, 1966). This interaction is also affected by the morphology and sediment dynamics, wind, waves, anthropogenic interventions and biotic processes (Kjerfve, 1994; Schumann *et al.*, 1999), which lead to patterns of circulation that are often site-specific.

Estuarine systems from temperate regions normally present a seasonal variation of the freshwater discharge associated with the precipitation regimes (Kimmerer, 2002). River flows may transport organisms towards the estuary or promote their transport offshore, and also affect the nutrients and sediments transport (e.g. Kjerfve *et al.*, 1981; Acharyya *et al.*, 2012). Together with the freshwater discharge, tide also controls the currents within the estuary and the transport of organisms, nutrients and sediments (e.g. Kjerfve *et al.*, 1981; Lauria *et al.*, 1999). Residual circulation, which depends on factors such as ebb/flood asymmetry, baroclinic pressure gradients, freshwater discharge and wind stress (e.g. Jay and Smith, 1990a,b), is also important when evaluating the long term net transport in the estuaries (Kjerfve *et al.*, 1981).

Another important concept related with the estuarine circulation is the one of residence time. Although there are several definitions of residence time (e.g., Oliveira and Baptista, 1997), it may be loosely defined as the time required for the renovation of the total volume of water within the estuary and, thus, is affected by the river flows, tide and stratification (Azevedo *et al.*, 2008). As residence time affect the permanence of organisms, nutrients, sediments and other properties in the estuary, it is commonly used to assess the impact of physical processes in the

water quality and ecological dynamics of estuarine ecosystems (Mosen *et al.*, 2002; Delhez, 2005; Oliveira *et al.*, 2007; Oliveira *et al.*, 2010).

The permanent mixing between salt water and freshwater that characterizes the estuaries promotes longitudinal gradients of salinity and water temperature. The salinity and water temperature gradients established within the estuary depend on the interplay between tidal amplitude and freshwater discharge (e.g. Hansen and Rattray, 1966). Besides, the heat exchanges between the water column and atmosphere, which depend on wind stress and shortwave and longwave radiation are also important in establishing water temperature in the water column (Kjerfve, 1994; Pinho, 2000). Several studies have showed that the spatial distribution of organisms within the estuary is affected by the horizontal distribution of salinity and water temperature (e.g. Froneman, 2004; Resende *et al.*, 2005; Qiu *et al.*, 2010; Shen *et al.*, 2011). Salinity tends to be lower upstream, near the river discharge, and larger downstream, promoting longitudinal gradients of species that tend to be characteristic of freshwater environments in the upstream area of the estuaries, and of the marine environment downstream (e.g. Resende *et al.*, 2005). Froneman (2004) relates the increase in the chlorophyll *a* concentration and phytoplankton biomass in the Kasouga estuary (South Africa) with the decrease in the salinity due to larger river flows. Moreover salinity also affects some of the physiological mechanisms of the aquatic species (e.g. Flöder *et al.*, 2010). Like salinity, water temperature also influences the physiological rates of the species, such as the growth, respiration and excretion rates (e.g. Bissinger *et al.*, 2008). Salinity and water temperature may also affect the density of the water and, consequently, influence the stratification of the water column.

Estuarine sediments may also affect the chemical and biological processes, as estuaries are characterized by the presence of large concentrations of sediments in suspension in the water column (Statham, 2012). These sediments affect the turbidity and, consequently, light penetration in the water column, and may limit phytoplankton growth (Cloern, 1987). Sediments resuspension, promoted by the estuarine circulation, can also be a source of nutrients in the water column (e.g. Statham, 2012).

I.2.3 NUTRIENTS

Nutrients, along with light availability in the water column, are the main factors limiting phytoplankton growth in estuaries. The sources of nutrients in estuaries are multiple and include point and diffuse sources from land, and also atmospheric and groundwater sources (Figure I.2.1). Simultaneously these sources can be natural (weathering of bedrock minerals, aerial deposition of dust and salts, natural leaching of organic matter and nutrients from soils,

decaying biological material, and erosion of soil particles) or anthropogenic (e.g. wastewater discharges from domestic and industrial effluents, agriculture) – Crouzet *et al.*, 1999; Statham, 2012.

Nutrients' biogeochemical cycles include all the nutrients transformations through biological, geological and chemical processes. Within estuarine systems nutrients are subjected to several transformations: uptake in the inorganic form by the producer organisms, followed by the release in the organic form (e.g. trough excretion), and then by the mineralization back to the inorganic form.

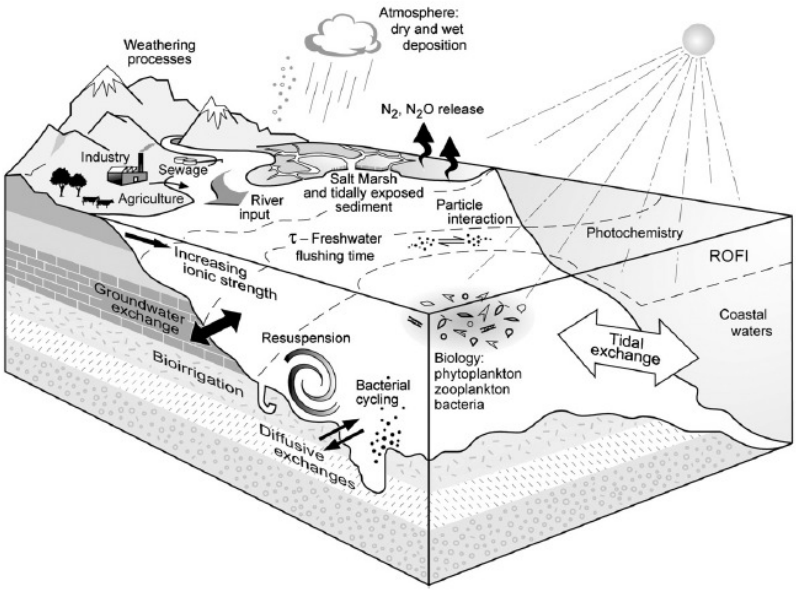

Figure I.2.1. Processes and sources of nutrients (nitrogen, phosphorus and silica) in estuarine systems; ROFI – region of freshwater influence (from Statham, 2012).

Nitrogen and phosphorus are the main nutrients for primary production in marine environments (Underwood e Kromkamp, 1999; Benitez-Nelson, 2000). Usually, nitrogen is considered the limiting nutrient in marine environments, while phosphorus is often the limiting nutrient in freshwater environments (Correll, 1999; Underwood e Kromkamp, 1999). Silicates are also an important nutrient for diatoms, which incorporate silica in their skeletons, and may limit the phytoplankton growth in some ecosystems (e.g. Hutchins and Bruland, 1998; Bruland *et al.*, 2001). Although, in most estuarine ecosystems studies, the analysis relies on the evaluation a single limiting nutrient, this approach may present some weaknesses (Benitez-Nelson, 2000).

The effects of nutrients on the ecosystems dynamics are complex and dependent on several factors. The depletion of one essential nutrient may reduce the primary production or affect the food web. It may also promote a loss of biodiversity or a species replacement by species better

adapted to lower nutrient concentrations. Nutrient enrichment may lead to eutrophication situations as discussed in section I.2.1.

I.2.4 PRESSURES AND THREATS

Due to their nature, estuarine ecosystems present a natural variability dependent on the variation of the several physical and chemical drivers, which should also be considered when evaluating estuarine water quality and ecological dynamics. This natural variability can be altered due to several external pressures. There are multiple threats that may reduce the estuarine ecosystems health, in particular water and ecological quality, and, consequently, affect the estuarine intrinsic values.

Human disturbance associated with their activities within estuaries may reduce the estuaries quality. Human interventions, such as dredging and infrastructures constructions, which influence the estuarine hydrodynamics and sediments dynamics, are one of the threats for estuarine ecosystems. Zhong *et al.* (2010) found that in the Meiliang Bay (China) sediment dredging influenced the mineralization of organic matter and denitrification in the sediments, altering the nitrogen cycle. Nayar *et al.* (2004) found significant copper toxicity to phytoplankton and autotrophic bacteria and related them with intense dredging activity in the Ponggol estuary (Singapore). Renovating coastal structures (e.g. breakwaters, artificial reefs, sea walls) may also potentiate the growth and settlement of opportunistic and invasive species (Science for Environment Policy, 2012). Rocha *et al.* (2002) related the low monthly discharges, modified by the damming system, with the changes in the nutrient ratios and, consequently, in the phytoplankton assemblages and succession in the Guadiana estuary (Portugal). Wastewater discharges, from domestic and/or industrial effluents, constitute another potential threat to the estuarine ecosystems and water quality, as they can change the water balance by altering the quantity of water inflows or change the nutrients balance (Lawrie *et al.*, 2010). Agriculture may also threaten the estuarine ecosystems, providing an additional non-point source of nutrients (Sebastiá *et al.*, 2012). The changes in the nutrients balance may lead to situations of eutrophication with the consequences discussed above. Huang *et al.* (2003) found eutrophication conditions in the Pearl River estuary (China) due to high loadings of nutrients from domestic sewage, industrial wastewater, agriculture and aquacultures. Parker *et al.* (2012) found a decline in the primary production of the Northern San Francisco Bay (USA), which was associated with the secondary treatment of the municipal wastewater treatment plant that discharged mainly ammonium. Another potential threat is the natural resources exploitation and the mechanisms associated with this activity, as they may alter the ecosystems dynamics. Thom *et al.* (1994) evaluated the effects of gravelling to enhance clam production in the Puget Sound (USA), and found that gravel altered benthic assemblage structure, respiration and

nutrient flux rates. Although no significant changes due gravelling were detected in the inorganic nitrogen and dissolved oxygen concentrations, they recommended the need for more detailed studies to evaluate the impacts of gravel as increased nutrient fluxes may stimulate algal growth. In particular, they found a relatively high cover of *Ulva sp.* in some gravelled areas. Increased clam production or invasion may lead to a decrease in primary production (e.g. Jassby *et al.*, 2002).

Besides human disturbance, climate change is also a potential threat to the estuaries health, due to the significant influence of the physical drivers in the bio-chemical processes. Climate change, understood as a significant statistical variation from the mean and/or variability that characterize the climate in a specific location (Santos *et al.*, 2002), are a matter of discussion and concern worldwide. It is currently accepted that climate change is occurring, but the main discussion derives from the role of human activities in changing the natural variability of climate. Expected climate change may induce modifications in air temperature, wind patterns, hydrological regimes and sea level rise (Statham, 2012).

Tide-gauge data analysis indicates a global sea level rise during the 20th century that will continue in the near future (Dias and Taborda, 1992; IPCC, 2007; Lopes *et al.*, 2011). Several studies aimed to evaluate the sea level rise in the Portuguese coast by 2100. Predicted values are: 0.14-0.57 m (Dias and Taborda, 1988), 0.05-0.20 m (Araújo, 2005), 0.47 (0.19-0.75) m (Antunes and Taborda, 2009) and 0.28, 0.35, 0.42 m (Lopes *et al.*, 2011). Recent studies suggest that larger mean sea level rise, of about 1 m, is likely to occur (e.g., Yates *et al.*, 2011, Sano *et al.*, 2011). Although the impacts of sea level rise are site-specific, generically they include: inundation of low-lying coastal areas and erosion of sandy beaches and barrier island coasts, alteration of geomorphological configurations and their associated sediment dynamics; increased tidal prism, with potential changes in the residence times and stratification; landward intrusion of salt water in estuaries and aquifers; displacement of ecosystems and habitats loss; and increased vulnerability of the social infrastructure (from Pethik, 2001; Lopes *et al.*, 2011). Regarding the estuarine ecosystems, sea level rise consequences are mostly associated to the changes in the circulation patterns, and their influence in the transport of organisms, sediments and nutrients, and the habitat loss.

Expected changes in the hydrological regimes are more uncertain than those of air temperature (Miranda *et al.*, 2006). These alterations include changes in the precipitation regimes, and in the intensity and frequency of storms and droughts. For Portugal, precipitation scenarios for 2100 predict a reduction over mainland during spring, summer and autumn: predicted reductions are within the range of 20 to 40% of the present values, and are larger in the southern part of the country (Miranda *et al.*, 2006). In the winter, an increase in precipitation may probably occur (Miranda *et al.*, 2006). Najjar *et al.* (2010) suggest an increase in the planktonic production in the Chesapeake Bay estuary (USA) associated with an increase in the nutrients loading due to

increased precipitation in the winter-spring season. Increased river flows, leading to flow-induced stratification, may also promote shifts in the algal taxonomic composition and alter the food web structure and/or be toxic to higher trophic groups; in particular, several taxa may reduce the zooplankton grazing (Najjar *et al.*, 2010). In turn, prolonged drought may introduce more coastal species within the estuary, which can be invasive and/or toxic (Najjar *et al.*, 2010).

Regarding air temperature, predictions of mean air temperature rise range from 0.6 (0.3-0.9) ºC to 4 (2.4-6.4) ºC (IPCC, 2007). In the Portuguese regions all scenarios predict a significant air temperature increase by 2100: increases in the mean air temperature range from 2 ºC to about 9 C, depending on the scenario and model considered, and increases in the maximum summer air temperature are estimated in 3 ºC in the coastal areas (Miranda *et al.*, 2006). Taking into account the seasonal variation, the maximum air temperature increase is predicted for the summer season (Miranda *et al.*, 2006). Rising temperatures may lead to shifts in algal, plankton and fish abundance, and also affect the oxygen levels (IPCC, 2007). For the Chesapeake Bay estuary (USA), Najjar *et al.* (2010) suggest that higher temperatures will probably promote the acceleration of the nutrients recycling rates, which may stimulate phytoplankton production and lead to a decrease in the dissolved oxygen concentrations. Increasing temperatures may also promote changes in the benthic fauna and modify the nutrients exchanges between the sediments and the water column (Statham, 2012). The growth of macroalgae can be favoured, thereby promoting hypoxic conditions (Najjar *et al.*, 2010). Bottom water hypoxia could also occur associated with lower oxygen solubility due to warming (Najjar *et al.*, 2010). Temperature changes can affect the physiological responses of the species and their phenology, leanding to earlier spring blooms (Kromkamp and Engeland, 2010; Najjar *et al.*, 2010). In particular, photosynthesis and respiration will likely increase with rising temperature (Rabalais *et al.*, 2009). However, this will occur only up to a point, as limiting factors (e.g. light and nutrients) may prevent larger primary production (Rabalais *et al.*, 2009) and the processes will be affected distinctly by temperature. In their studies in the Chesapeake Bay estuary (USA), Lomas *et al.* (2000) found a larger increase of the planktonic respiration with temperature than of photosynthesis.

The interaction between anthropogenic activities, climatic variability and climate change in the estuarine ecosystems is also a matter of concern (Cloern and Jassby, 2010; Paerl *et al.*, 2010). Increased human activities in estuaries (Rabalais *et al.*, 2009) associated with climate change may increase the vulnerability of the estuarine systems, in particular regarding eutrophication (Statham, 2012). Figure I.2.2 summarizes the potential changes in the estuarine systems due to anthropogenic activities and climate change and the complex interactions among them. However, the relative role of these distinct drivers and the interactions among them remains poorly understood. Chust *et al.* (2009) found that, in the Bay of Biscay (Spain), the anthropogenic impacts in the coastal and estuarine habitats overwhelmed the influence of

natural erosive processes and global climate change driving forces between 1954 and 2004. In the Gulf of Riga (Baltic Sea) Kotta *et al.* (2009) found that the zoobenthos communities and herring stock were largely driven by climate, while zooplankton dynamics resulted from the combined effect of anthropogenic and climate drivers. In the Cotentin peninsula (France) ecosystem, Grangeré *et al.* (2012) found that climatic factors act in synergy with anthropogenic factors (i.e. nutrient enrichment) on the west coast of the peninsula, while on the east coast the climatic factors influence was reduced by the anthropogenic factors. In this sense, to understand the relative role of the main pressures and threats in the estuarine ecosystems dynamics and to promote their sustainable development there is a need to integrate both the anthropogenic pressures and the system response to the physical and climate drivers (Paerl, 2006; Ducharne *et al.*, 2007; Kotta *et al.*, 2009).

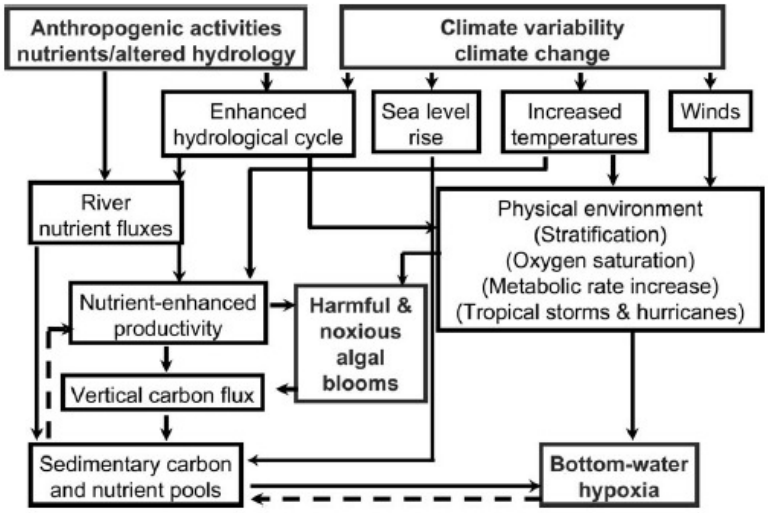

Figure I.2.2. Potential physical and hydrological changes resulting from climate change and their interaction with current and future human activities; the dashed lines represent negative feedback to the system (from Rabalais *et al.*, 2009; Rabalais *et al.* present a case study for the northern Gulf of Mexico, which is strongly influenced by the Mississippi River).

SECTION I.3

ECOLOGICAL MODELLING

Ecological modelling aims to study the processes and interactions within the ecological systems and/or to predict and evaluate their evolution based on future scenarios and management strategies, through the use of mathematical models. However, due to the complexity inherent to the ecosystems dynamics, its translation in a model implies always a simplification of the reality. In this sense, models only consider parts of the ecosystem or simpler systems. In general, ecological models for the marine environment tend to aggregate the species in functional groups (e.g. zooplankton, phytoplankton, bacterioplankton), describing the population dynamics in terms of fluxes of carbon, oxygen and nutrients between these groups and the organic and inorganic matter (James, 2002). The estuarine systems, in particular, are very complex since there are several variables and processes involved, which interactions are strongly non-linear (James, 2002). Thus, the comprehensive study of these systems must rely on a multidisciplinary approach that includes the physical, the chemical and biological processes.

The use of ecological models started in the early seventies, when three main types of models emerged (Jørgensen, 2008; Figure I.3.1): population dynamic models with or without age structure; bio-geo-chemical or bio-energetic dynamic models based on differential equations; and static models, in which the temporal evolution is not simulated. Previously, Streeter and Phelps (1925) and Riley (1946, 1947) developed the first studies on water quality and ecological modelling in the marine environment. The first authors developed the Streeter-Phelps model to simulate the oxygen dynamics in the Ohio River (Streeter and Phelps, 1925). Later, Riley (1946, 1947) investigated and modelled the phytoplankton and zooplankton temporal evolution based on their growth and mortality rates. Ecological models evolved through time, both in terms of complexity and in types of models. Nowadays, the type of ecological models is vast, including also (Jørgensen, 2008; Figure I.3.1): structurally dynamic models, fuzzy models, artificial neural networks, individual-based models and cellular automata. Although there was a significant increase in the ecological models types, the bio-geo-chemical or bio-energetic dynamic models remain the most widely used (Jørgensen, 2008). The approach followed to represent the spatial dynamics and the role of randomness is also used to generically classify the ecological models (Figure I.3.1).

Besides the temporal variation, which allows the simulation of the processes at daily, seasonal and inter-annual scales, the spatial variation is also an important issue in ecological modelling. Spatially and temporally varying models that describe the three-dimensional variation of the processes, the forcing functions and the state variables are the ultimate goal in marine

ecological modelling (Jørgensen, 2008). In these models the adequate representation of the hydrodynamics is fundamental (Pereira *et al.*, 2006; Jørgensen, 2008) and the need for integrated models that consider simultaneously the physical and the ecological processes has been demonstrated in several studies (e.g. Skogen *et al.*, 1995; Mari *et al.*, 2009; Willis, 2011). In the last decades the multidisciplinary modelling has evolved significantly, mostly due to the increase in computational capacity. Wroblewski (1977) developed one of the first approaches to combine a circulation model with an ecological model. In this model, Wroblewsky simulated the phytoplankton, the zooplankton, nitrates, ammonium and particulate organic nitrogen in the Oregon coast. Later, Wroblewsky (1980) related the zooplankton (*Acartia clausi*) distribution and its life stages with the circulation in the Oregon coast. A two dimensional hydrodynamics and water quality model was applied by Portela (1996) in the Tagus estuary (Portugal).

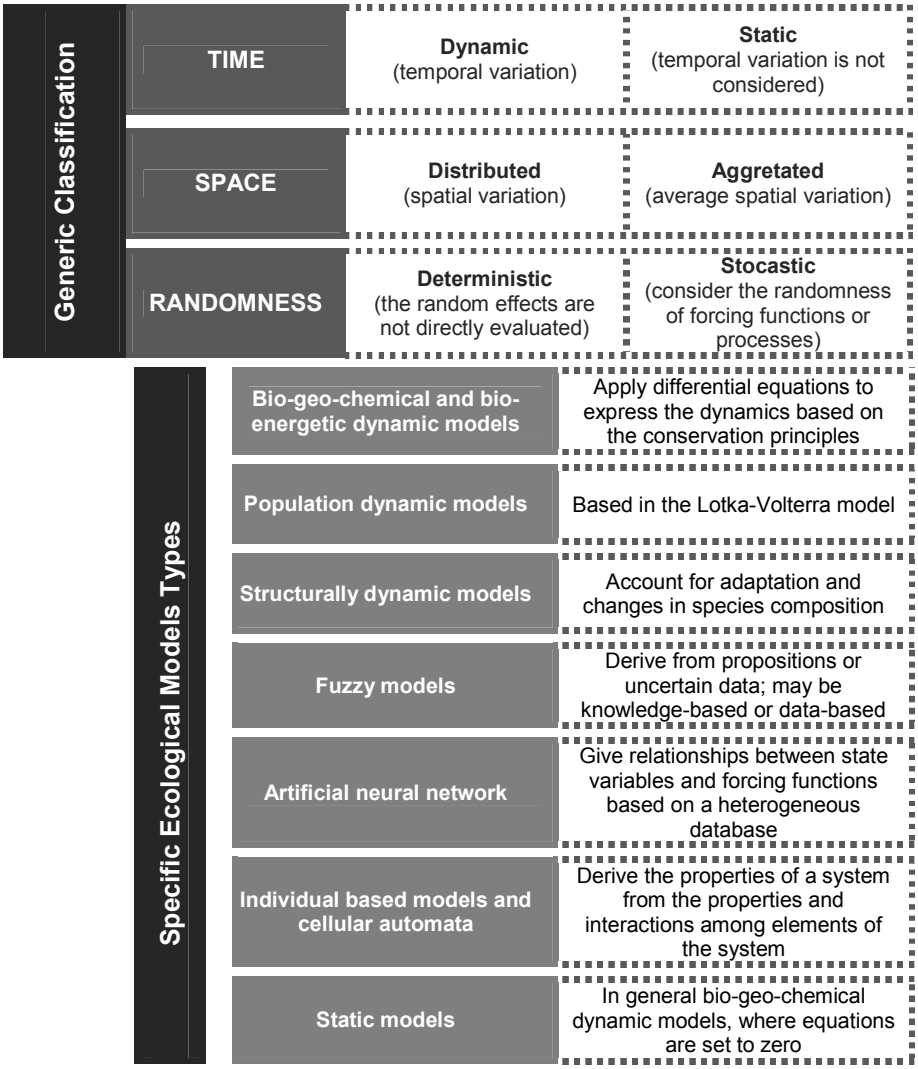

Figure I.3.1. Schematic overview of the main classification and types of ecological models (based on Sá, 2003 and Jørgensen, 2008).

However, the combined use of high-resolution (i.e. considering the relevant processes at the spatial and temporal scales of interest) ecological and hydrodynamic ecological models was possible only recently. Besides the restrictive computational requirements, the inherent difficulties to combine processes that occur at different spatial and temporal scales have also been a limitation for this type of applications (Pereira *et al.*, 2006). Nowadays there are some well-established coupled hydrodynamic and ecological models, which include HEM-3D (Park *et al.*, 2005), PELAGOS (Vichi *et al.*, 2007), COHERENS (Luyten *et al.*, 1999), MOHID (MOHID, 2006), NEMURO (Kishi *et al.*, 2007), ROMS – Regional Ocean Modeling System (Haidvogel *et al.*, 2008), FVCOM – Finite Volume Coastal Ocean Model (http://fvcom.smast.umassd.edu/FVCOM/index.html), ECO-SELFE (Rodrigues *et al.*, 2009b), Delt3D (Deltares, http://www.deltaressystems.com/hydro/product/621497/delft3d-suite/1130952) and MIKE 3 (DHI, http://www.mikebydhi.com/Products/CoastAndSea/MIKE3.aspx), among others.

Ecological models present different levels of complexity (Figure I.3.2). Simpler models, known as NPZ models (nitrogen, phytoplankton and zooplankton; e.g. Franks *et al.*, 1986), simulate the ecosystem based on a dynamics that include only one nutrient cycle and two generic groups that represent the lower trophic levels – the producers (phytoplankton) and the consumers (zooplankton). Examples of applications of these models include: Edwards *et al.* (2000), Franks and Chen (2001) and Swaney *et al.* (2008). Edwards *et al.* (2000) used a two dimensional coupled physical-NPZ model to study the zooplankton dynamics in a coastal upwelling ecosystem. Franks and Chen (2001) studied the George Banks ecosystem dynamics using a three-dimensional coupled physical-NPZ model. More recently, Swaney *et al.* (2008) used a NPZ model to study the estuaries response to nitrogen loadings. The increase in the models complexity is generally associated with the increase in the cycles of nutrients simulated (e.g. Guillaud *et al.*, 2000; Fasham *et al.*, 2006) or a more detailed specification of biological groups represented (e.g. Fasham *et al.*, 1990; Neumman, 2000; Ruzicka *et al.*, 2011). Schrum *et al.* (2006) showed the importance of considering the nitrogen, phosphorus and silica cycles when simulating the zooplankton dynamics in the North Sea. The need to increase the trophic levels simulated, including the higher trophic levels, like the fishes, also contributes to increase the complexity of ecological models. Ito *et al.* (2007) studied the role of climate variability in the growth of Pacific saury using the NEMURO.FISH model (Megrey *et al.*, 2007). Due to the wide range of complexity of the ecological models some of the available coupled physical-ecological models include ecological models with different levels of sophistication (e.g. MOHID, MOHID, 2006; ROMS; SELFE – Semi-implicit Eulerian-Lagragian finite element model, Zhang and Baptista, 2008).

The most adequate degree of sophistication of the ecological models remains a matter of discussion (e.g. Franks, 2002; Raick *et al.*, 2006; Franks, 2009). Wainwright *et al.* (2007) compared a simple NPZ model with a more complex lower trophic model (NEMURO) applied to

the near-shore pelagic zone of the California Current System, concluding that generally the complex model provided a slightly better representation of the ecosystem dynamics when compared with data; however neither model was able to fully capture the dynamics observed. In their studies in the Ligurian Sea (NW Mediterranean Sea), Raick *et al.* (2006) derived simplified models and evaluated their behaviour, showing that a certain degree of sophistication is needed for a realistic simulation of the ecosystem. The main issue related to increasing ecological models complexity is their parameterization. Input parameters of ecological processes are usually uncertain or unknown for a specific application. Thus, increasing the number of processes and state variables represented in the model leads to a larger number of input parameters and, consequently, to a larger uncertainty in the model parameterization. The determination of the relative contribution of each input parameter is essential in ecological modelling applications (Chu *et al.*, 2007). In this sense, sensitivity analyses of the model input parameters are widely used in ecological modelling (e.g. Yoshie *et al.*, 2006; Makler-Pick *et al.*, 2011) providing information about the most significant input parameters and the model uncertainties (Cariboni *et al.*, 2007). In their comparison of ecological models with different levels of complexity, Wainwright *et al.* (2007) found that both models were sensitive to the same parameters (source nitrate concentration, maximum grazing rate, zooplankton Ivlev constant and zooplankton mortality rate).

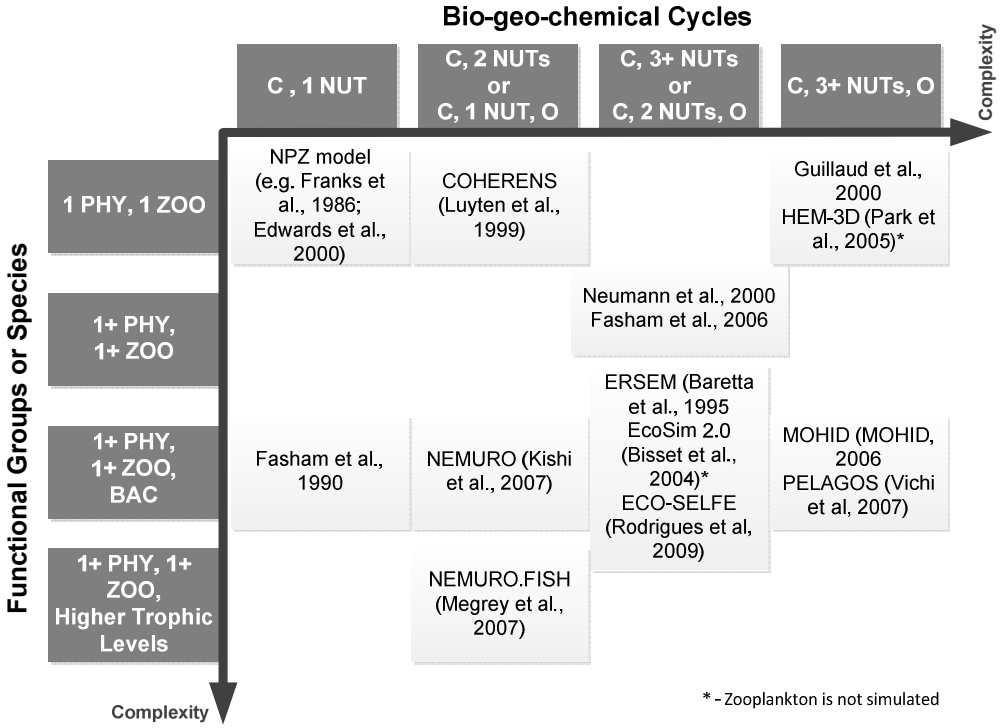

Figure I.3.2. Examples of bio-geo-chemical dynamic ecological models with different levels of complexity (PHY – phytoplankton; ZOO – zooplankton; BAC – bacterioplankton; C – carbon; NUT – inorganic nutrients; O – oxygen; 1+ represents 1 or more; 3+ represents 3 or more).

In order to evaluate the model performance and adequacy to each case, validation and benchmarking are essential in ecological modelling. However, benchmarking exercises are still scarce and improvements should be made to address the adequate data to evaluate the models performance (Franks, 2009). In particular, the water quality models skill assessment and uncertainty definition should be based on a combination of quantitative and qualitative measures (Fitzpatrick, 2009).

In this study, the fully coupled three-dimensional hydrodynamic and ecological model ECO-SELFE (available at http://www.stccmop.org/CORIE/modeling/selfe/) is used. This model is an open-source unstructured grid model providing a better representation of aquatic systems with complex geometries, like the Aveiro lagoon. The ecological model formulation relies on the bio-geo-chemical dynamic models type and was extended from the EcoSim 2.0 (Bisset *et al.*, 2004). In its original formulation, EcoSim 2.0 considers the carbon, nitrogen, phosphorus, silica and iron cycles, allowing the simulation of the following state variables: several phytoplankton functional groups, bacterioplankton, dissolved and particulate organic matter, inorganic nutrients and dissolved inorganic carbon. Rodrigues *et al.* (2008, 2009b) extended this model to simulate the zooplankton dynamics and showed its ability in simulating the Aveiro lagoon ecological dynamics in the lower trophic levels. In the present thesis, ECO-SELFE model is extended to simulate multi-scale processes in water quality (Chapter III, Section III.1) and the oxygen cycle, this last extension being validated against a specific set of data collected for its validation at the spatial and temporal scales of interest (Chapter III, Section III.3).

SECTION I.4

THE RIA DE AVEIRO

The Ria de Aveiro is a coastal lagoon located in the northwest coast of Portugal (40º38'N, 8º45'W). It is 45 km long, from Ovar to Mira, and has a maximum width of 10 km (Figure I.4.1). The lagoon presents unique characteristics from the ecological viewpoint, containing one of the largest saltmarshes in Europe, harbouring permanently several species of fauna and flora and also nesting migratory birds. Simultaneously, it supports several economic activities (e.g. aquaculture, small-scale fishing, tourism, nautical and port activities, salt extraction, industry). Some of these anthropogenic pressures have contributed to the degradation of the Aveiro lagoon ecological quality (e.g. Rebelo, 1992; Abreu *et al*., 2000; Lopes and Silva, 2006) and the need for the lagoon conservation has been addressed in several normative documents (e.g. special area of conservation under the directive 79/409/EEC on the wild birds conservation) and studies (e.g. Morgado *et al*., 2009). Recently, some efforts have been made to reduce some of these atrophic pressures in the lagoon, in particular regarding the treatment and disposal of domestic and industrial effluents (Silva *et al*., 2000). However, the knowledge about the impacts of these measures is still scarce. Ferreira *et al.* (2003) classified the Aveiro lagoon with low overall eutrophic condition (OEC) and low susceptibility index (US-NEEA index), but Lopes *et al.* (2007b) pointed out that the quality status of different areas within the system can vary.

Figure I.4.1. Ria de Aveiro: A) overall view (GoogleEarth image from 2010) and B) inlet detail (aerial photo from 1995).

Morphologically, the Aveiro lagoon spreads over four main channels (Figure I.4.2): in the south, the Mira and Ílhavo channels, which are both narrow and elongated channels, about 25 km and 15 km long, respectively; in the center, the Espinheiro channel, about 17 km long; and in the north, the S. Jacinto channel, which is about 29 km long. The connection to the sea is made through one artificial channel of about 1.3 km, which has evolved through time. The lagoon is very shallow. In the inlet and in the navigation channels, the depths are of about 20 m and 7 m, respectively, and are maintained artificially (through dredging). The main channels, with exception of the Mira channel, have several branches and interconnections, which lead to an increased complexity in the Aveiro lagoon dynamics and geometry (Dias *et al.*, 1999). The Mira channel may be considered a sub-estuarine system of the Aveiro lagoon (Leandro, 2008), which behaves like a tidally and seasonally poikilohaline estuary (i.e., an estuary in which salinity shows considerable fluctuations; Moreira *et al.*, 1993). Thus, this channel was chosen for the development of the field campaigns and coupled hydrodynamic and ecological simulations of the present study, following a similar approach to the one adopted in previous studies (e.g. Moreira *et al.*, 1993; Resende *et al.*, 2005; Leandro, 2008).

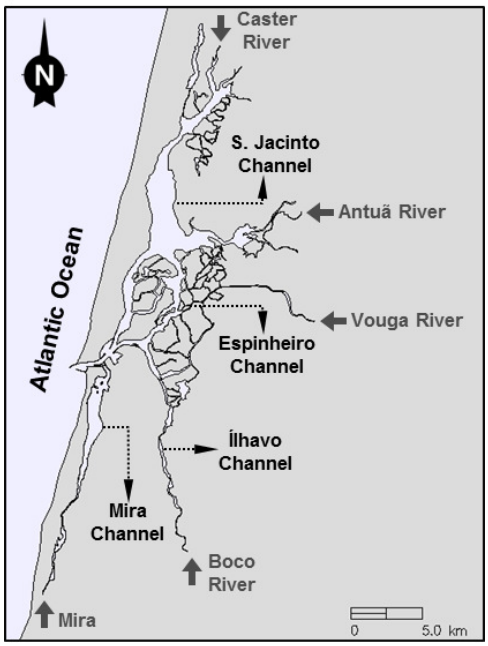

Figure I.4.2. Schematic overview of the Ria de Aveiro.

Tide is the main driver of the circulation in the Aveiro lagoon (Dias *et al.*, 1999) and there are several intertidal areas in the lagoon (saltmarshes and mud flats). The lagoon area is about 83 km^2 at high spring tides, reducing to 66 km^2 at low tide (Dias and Lopes, 2006).Tides are semi-diurnal. The lagoon is mesotidal with mean tidal range of 2 m at the mouth, which reaches its minimum value of 0.6 m during neap tides and its maximum value of 3.2 m in spring tides

(Dias *et al.*, 2000). At the mouth, the mean tidal prism is of about $70x10^6$ m^3 (Dias and Lopes, 2006), with minimum values of 34.9×10^6 m^3 in neap tide and maximum values of 136.7×10^6 m^3 in spring tide (Dias, 2001). In the S. Jacinto, Espinheiro, Mira and Ílhavo channels the tidal prism are about 35, 26, 10 and 14%, respectively, of the tidal prism at the mouth (Dias, 2001). In a recent study to investigate the impacts of the mean sea level rise on the hydrodynamics and morphodynamics of the Aveiro lagoon, Lopes *et al.* (2011) suggested a tidal prism increase in the mouth of about 28% based on the sea level rise scenario of 0.42±0.02 m (scenario A2 SRES – Special Report on Emission Scenarios).

Besides tide, the river flows also influence the physical dynamics in the Aveiro lagoon and, in particular, salinity and water temperature. The estimated mean annual freshwater input during a tidal cycle is relatively small, of about 1.8×10^6 m^3 (Moreira *et al.*, 1993), but may influence significantly the long-term residual transport (Dias *et al.*, 2003).The main sources of freshwater in the lagoon are the rivers Vouga and Antuã, which flow through the Espinheiro channel (Dias *et al.*, 2000; Dias and Lopes, 2006). Some uncertainty remains about the mean flows of these rivers, mainly due to the lack of recent data (Plano de Bacia Hidrográfica do Rio Vouga, 1999; Dias *et al.* (2000) mention values of 29 and 2 $m^3 s^{-1}$ for the rivers Vouga and Antuã, respectively, while Dias and Lopes (2006) refer values of 50 and 5 $m^3 s^{-1}$; in turn, Vaz (2007) found a mean flow of 31.45 $m^3 s^{-1}$ for the Vouga river between September 2003 and August 2004. In the other channels, the freshwater flows are relatively small, but the information is also scarce. The main source of freshwater in the Ílhavo channel is the Boco river, while in the S. Jacinto channel flows the Caster river, among other smaller streams. In the Mira channel, in particular, the freshwater input (flowing from Barrinha de Mira and other small streams) is little known (Dias and Lopes, 2006). In this channel the salinity varies from 0 upstream to 35 downstream, and data collection studies suggest water temperatures varying from about 8 ºC in the winter to 25 ºC in the summer (e.g. Dias *et al.*, 1999; Resende, 2004; Leandro, 2008). Residence times in the lagoon vary from less than 2 days near the mouth to more than 1 week in the upstream areas of the channels (Dias *et al.*, 2001).

The Ria de Aveiro has been widely studied in terms of its physical (e.g. Dias *et al.*, 1999), chemical (e.g., Válega *et al.*, 2008; Pato *et al.*, 2008) and biological (e.g. Moreira *et al.*, 1993; Rodrigues *et al.*, 2011) characteristics. The approach used in these previous studies relied mostly on data collection and analysis. Numerical modelling studies focused mostly on the hydrodynamics (e.g. Dias *et al.*, 2003; Vaz, 2007), although there were some studies on sediments (e.g. Oliveira *et al.*, 2006; Lopes *et al.*, 2006), morphodynamics (e.g. Plecha, 2011), and ecological and water quality (e.g., Lopes *et al.*, 2005; Saraiva, 2005; Trancoso *et al.*, 2005; Lopes and Silva, 2006; Lopes *et al.*, 2008; Rodrigues *et al.*, 2009b). Several of the studies on the water quality and ecological dynamics of the lower trophic level in the Aveiro lagoon aimed at characterizing this dynamics and related it with the main environmental drivers. A few studies

also evaluated the effects of anthropogenic pressures (e.g. dredging) in the biological communities (e.g. Sampaio, 2001).

Cunha *et al.* (1999) studied the oxygen consumption in the Aveiro lagoon, based on a set of data from 1997 and 1998 and suggested that, in the marine zone, the rates of oxygen consumption depend on the tidal circulation. The larger values of planktonic consumption of dissolved oxygen, which ranged from 0.010 to 0.041 mg O_2 l^{-1} h^{-1}, were found in the brackish zone. The main role of tides in the establishment of dissolved oxygen patterns in the Ria de Aveiro was suggested by Lopes and Silva (2006) based on the application of a numerical model. These authors also found that, in the intertidal saltmarshes, re-aeration and flooding and drying processes control the dissolved oxygen concentrations.

Almeida *et al.* (2005) related the bacterioplankton productivity with the primary production and respiration based on a set of data collected along the lagoon in four seasons between 2000 and 2001, showing that the primary production varies from 0.2 to 19.1 g C m^3 d^{-1} and the respiration from 0.1 to 8.2 g C m^3 d^{-1}. Their results suggested that the bacterial productivity patterns (2.7–744.2 mg C m^3 d^{-1}) did not coincide with those of the primary production and respiration, depending on non-phytoplanktonic carbon sources. In particular, they found that the allochthonous substrates leached out by rain controlled the distribution of bacterial activity, and that the salinity decrease during the rainy season negatively affected bacterial productivity (Almeida *et al.*, 2007).

The primary production dynamics in the Aveiro lagoon was studied by Trancoso *et al.* (2005), using a numerical model. These authors concluded that the hydrodynamic conditions may affect the competition among phytoplankton and macroalgae. Lopes *et al.* (2010) also suggested that primary production in the Ria de Aveiro is directly linked to the local conditions, namely the tidal cycle, the water depth and currents, and the solar radiation, applying another numerical model.

Resende *et al.* (2005) studied the phytoplankton ecology along the Mira channel (between 2002 and 2003) showing that the diatoms assemblages composition and distribution depended directly on the salinity spatial gradient and on the water temperature temporal gradient. The nutrients (ammonium and phosphates) role was small relative to these two physical variables. Two different communities were identified: one near the downstream area of the channel and dominated by marine species (e.g. *Auliscus sculptus*, *Chaetoceros densus*, *Surirella comis*) and another dominated by freshwater species and located further upstream (e.g. *Caloneis permagna*, *Cymbella tumida*, *Pinnularia stommatophora*). Cerejo (2006) found near the inlet of the Aveiro lagoon a seasonal succession of phytoplankton species that was dependent of water temperature, intensity and variability of coastal upwelling and nutrients availability, based on data from 2004 to 2005. The role of water temperature in the establishment of the phytoplankton communities near the mouth of the Aveiro lagoon was also shown by Pereira

(2007): dinoflagellates species dominated during the spring and summer months, while diatoms species were associated with lower water temperatures between 2006 and 2007.

Lopes *et al.* (2007a) inferred from silica variation a seasonal succession pattern in phytoplankton assemblages, dominated by diatoms from late autumn to early spring and by chlorophytes during late spring and summer, based on a set of data collected between 2000 and 2001 along the several channels of the Aveiro lagoon. Silicates and nitrates were inversely correlated with salinity, while nitrites, ammonium and phosphates showed a random distribution (Lopes *et al.*, 2007b). Besides the nutrients concentrations in the water column, the phytoplankton seasonal variation in the Aveiro lagoon may also depend on the grazing (Lopes *et al.*, 2007a).

The role of environmental forcings was also studied in the zooplankton community. Leandro (2008) suggested that the spatial zooplankton distribution was affected by the hydrological regimes (data from 2000-2002) and that the relative significance of the hydrological parameters on the copepods abundance varied among the different zones of the Mira channel. Previously, tide and wind speed and direction had also been shown to be important drivers in the vertical migration and recruitment processes of decapod larvae (e.g. Morgado *et al.*, 2003; Queiroga *et al.*, 2006).

Although previous studies in the planktonic dynamics of the Ria de Aveiro are numerous, integrated studies on the water quality and ecological dynamics, in particular in the lower trophic levels, are still uncommon. Previous studies also lack the evaluation of the long-term system evolution. In this sense, in order to develop sustainable management plans for this estuarine system, in particular regarding its water and ecological quality, there is a need to understand its evolution based on long-time series analyses. This analysis allows the evaluation of the system response to the climatic natural variability and also to the undertaken human interventions. Besides the understanding of the past evolution, there is also a need to evaluate possible impacts of both climate change and anthropogenic interventions. This will allow a better understanding of how factors like sea level rise, increased air temperature and variations in the hydrological regimes will affect the Aveiro lagoon water quality and ecological dynamics, and also their relative importance when compared with potential anthropogenic modifications or pressures. An integrated approach which covers different temporal scales, like the one adopted in the present thesis, presents multiple advantages as it allows to: i) evaluate the system long-term evolution and its variability driven both by climatic and anthropogenic factors; ii) validate the hydrodynamic and ecological model at the relevant spatial and temporal scales; and iii) use it to exploit future evolutional scenarios. Thus, this thesis contributes as a tool to support the Aveiro lagoon sustainable development, taking into account the effects of climate change and anthropogenic interventions on its water and ecological quality. It also provides additional

information for the development and implementation of future monitoring programs and management plans, and also for the development of more detailed research studies in this area.

REFERENCES

Abreu SN, Pereira ME, Vale C, Duarte AC. Accumulation of mercury in sea bass from a continental lagoon (Ria de Aveiro, Portugal). *Marine Pollution Bulletin* **2000**, 40, 293-297.

Acharyya T, Sarma VVSS, Sridevi B, Venkataramana V, Bharathi MD, Naidu SA, Kumar BSK, Prasad VR, Bandyopadhyay D, Reddy NPC, Kumar MD. Reduced river discharge intensifies phytoplankton bloom in Godavari estuary, India. *Marine Chemistry* **2012**, 132–133, 15–22.

Almeida MA, Cunha MA, Alcântara F. Relationship of bacterioplankton production with primary production and respiration in a shallow estuarine system (Ria de Aveiro, NW Portugal). *Microbiological Research* **2005**, 160(3), 315-328.

Almeida MA, Cunha MA, Dias JM. Bacterial productivity distribution during a rainy year in an estuarine system. *Microbial Ecology* **2007**, 53(2), 208-220.

Antunes C, Taborda R. Sea level at Cascais tide gauge: data, analysis and results. *Journal of Coastal Research* **2009**, SI 56, 218–222.

Araújo IGB. Sea level variability: examples from the Atlantic Coast of Europe. PhD thesis, University of Southampton, UK, **2005**.

Azevedo IC, Duarte PM, Bordalo AA. Understanding spatial and temporal dynamics of key environmental characteristics in a mesotidal Atlantic estuary (Douro, NW Portugal). *Estuarine, Coastal and Shelf Science* **2008**, 76(3), 620-633.

Barbier EB, Hacker SD, Kennedy C, Koch EW, Stier AC, Silliman BR. The value of estuarine and coastal ecosystem services. *Ecological Monographs* **2011**, 81(2), 169-193.

Baretta JW, Ebenhoh W, Ruardij P. The European Regional Seas Ecosystem Model, a complex marine ecosystem model, *Netherlands Journal of Sea Research* **1995**, 33, 233-246.

Bathmann UV, Noji TT, von Bodugen B. Copepod grazing potential in late winter in the Norwegian Sea - a factor in the control of spring phytoplankton growth? *Marine Ecology Progress Series* **1990**, 60, 225-233.

Baumert HZ, Petzoldt T. The role of temperature, cellular quota and nutrient concentrations for photosynthesis, growth and light–dark acclimation in phytoplankton. *Limnologica - Ecology and Management of Inland Waters* **2008**, 38(3–4), 313-326.

Benitez-Nelson CR. The biogeochemical cycling of phosphorus in marine systems. *Earth-Science Reviews* **2000**, 51, 109-135.

Bisset WP, Debra S, Dye D. Ecological Simulation (EcoSim) 2.0 Technical Description, Tampa, Florida: Florida Environmental Research Institute, **2004**, 25 pp.

Bissinger JE, Montagnes DJS, Sharples J, Atkinson D. Predicting marine phytoplankton maximum growth rates from temperature: improving on the Eppley curve using quantile regression. *Limnology and Oceanography* **2008**, 53 (2), 487-493.

Brogueira MJ, Oliveira MR, Cabeçadas G. Phytoplankton community structure defined by key environmental variables in Tagus estuary, Portugal. *Marine Environmental Research* **2007**, 64(5), 616–628.

Bruland KW, Rue EL, Smith GJ. Iron and macronutrients in California coastal upwelling regimes: implications for diatom blooms. *Limnology and Oceanography* **2001**, 46, 1661-1674.

Burkholder JM, Tomasko DA, Touchette BW. Seagrasses and eutrophication. *Journal of Experimental Marine Biology and Ecology* **2007**, 350(1–2), 46-72.

Cameron WM, Pritchard DW. Estuaries. In: Hill MN (ed.), *The Sea*. John Wiley & Sons, New York, **1963**, 306–324.

Cardoso PG, Pardal MA, Lillebø AI, Ferreira SM, Raffaelli D, Marques JC. Dynamic changes in seagrass assemblages under eutrophication and implications for recovery. *Journal of Experimental Marine Biology and Ecology* **2004**, 302(2), 233-248.

Cariboni J, Gatelli D, Liska R, Saltelli A. The role of sensitivity analysis in ecological modelling. *Ecological Modelling* **2007**, 203, 167-182.

Cerejo M. Contribuição para a monitorização de algas tóxicas na Ria de Aveiro – ciclo anual de sucessão fitoplanctónica e modelização da dispersão de microalgas. MsC Thesis, Universidade de Aveiro, **2006**.

Choy EJ, An S, Kang C. Pathways of organic matter through food webs of diverse habitats in the regulated Nakdong River estuary (Korea). *Estuarine, Coastal and Shelf Science* **2008**, 78(1), 215-226.

Chu PC, Ivanov LM, Margolina TM. On non-linear sensitivity of marine biological models to parameter variations. *Ecological Modelling* **2007**, 206(3–4), 369-382.

Chust G, Borja A, Liria P, Galparsoro I, Marcos M, Caballero A, Castro R. Human impacts overwhelm the effects of sea-level rise on Basque coastal habitats (N Spain) between 1954 and 2004. *Estuarine, Coastal and Shelf Science* **2009**, 84(4), 453-462.

Cloern JE, Jassby AD. Patterns and scales of phytoplankton variability in estuarine-coastal systems. *Estuaries and Coasts* **2010**, 33, 230-241.

Cloern JE. Our evolving conceptual model of the coastal eutrophication problem. *Marine Ecology Progress Series* **2001**, 210, 223-253.

Cloern JE. Turbidity as acontrol on phytoplankton biomass and productivity in estuaries. *Continental Shelf Research* **1987**, 7(11-12), 1367-1381.

Comissão para as Alterações Climáticas. *Proposta de Estratégia Nacional de Adaptação às Alterações Climáticas.* Versão para Consulta Pública. **2009**, 41 pp.

Correll DL. Phosphorus: a rate limiting nutrient in surface waters. *Poultry Science* **1999**, 78, 674-682.

Crouzet P, Leonard J, Nixon S, Rees Y, Parr W, Laffon L, Bøgestrand, Kristessen P, Lallana C, Izzo G, Bokn T, Back J, Lack TJ. *Nutrients in European ecosystems, Environmental Assessment Report nº 4*. European Environmental Agency, **1999** (http://www.eea.europa.eu/publications/ENVIASSRP04).

Cunha MA, Almeida MA, Alcântara F. Compartments of oxygen consuption in a tidal mesotrophic estuary (Ria de Aveiro, Portugal). *Acta Oecologica* **1999**, 20, 227-235.

Delhez EJM. Transient residence and exposure times. *Ocean Science Discussions* **2005**, 2, 247–265.

Dias JA, Taborda R. Evolução recente do nível médio do mar em Portugal. *Anais do Instituto Hidrográfico* **1988**, 9, 83–97.

Dias JA, Taborda R. Tidal gauge data in deducing secular trends of relative sea level and crustal movements in Portugal. *Journal of Coastal Research* **1992**, 8, 655–659.

Dias JM, Lopes JF, Dekeyser I. A numerical system to study the transport properties in the Ria de Aveiro lagoon. *Ocean Dynamics* **2003**, 53, 220-231.

Dias JM, Lopes JF, Dekeyser I. Hydrological characterisation of Ria de Aveiro, Portugal, in early summer. *Oceanologica Acta* **1999**, 22(5), 473-485.

Dias JM, Lopes JF, Dekeyser I. Lagrangian transport of particles in Ria de Aveiro lagoon, Portugal. *Physics and Chemistry of the Earth, Part B: Hydrology, Oceans and Atmosphere* **2001**, 26(9), 721-727.

Dias JM, Lopes JF, Dekeyser I. Tidal propagation in Ria de Aveiro Lagoon, Portugal. *Physics and Chemistry of the Earth, Part B: Hydrology, Oceans and Atmosphere* **2000**, 25(4), 369-374.

Dias JM, Lopes JF. Implementation and assessment of hydrodynamic, salt and heat transport models: the case of Ria de Aveiro lagoon (Portugal). *Environmental Modelling & Software* **2006**, 21(1), 1-15.

Dias, JM. Contribution to the study of the Ria de Aveiro hydrodynamics. PhD Thesis, Universidade de Aveiro, **2001**.

Domingues RB, Anselmo TP, Barbosa AB, Sommer U, Galvão HM. Nutrient limitation of phytoplankton growth in the freshwater tidal zone of a turbid, Mediterranean estuary. *Estuarine, Coastal and Shelf Science* **2011**, 91(2), 282-297.

Ducharne A, Baubion C, Beaudoin N, Benoit M, Billen G, Brisson N, Garnier J, Kieken H, Lebonvallet S, Ledoux E, Mary B, Mignolet C, Poux X, Sauboua E, Schott C, Théry S, Viennot P. Long term prospective of the Seine River system: confronting climatic and direct anthropogenic changes, *Science of the Total Environment* **2007**, 375(1-3), 292-311.

Dyer KR. *Estuaries. A Physical Introduction.* 2nd Edition. John Wiley and Sons, **1997**, 195 pp.

Edwards CA, Batchelder HP, Powell TM. Modeling microzooplankton and macrozooplankton dynamics within a coastal upwelling system. *Journal of Plankton Research* **2000**, 22(9), 1619–1648.

Endelvang K, Kaas H, Erichsen AC, Alvarez-Berastegui D, Bundgaard K, Jorgensen PV. Numerical modelling of phytoplankton biomass in coastal areas. *Journal of Marine Systems* **2005**, 57(1-2), 13-29.

European Science Foundation – Marine Board. *Position Paper 9, Impacts of Climate Change on the European Marine and Coastal Environment, Ecosystems Approach*, **2007**, 84 pp.

Fasham MJR, Ducklow HW, McKelvie SM. A nitrogen-based model of plankton dynamics in the oceanic mixed layer. *Journal of Marine Research* **1990**, 48, 591–639.

Fasham MJR, Flynn KJ, Pondaven P, Anderson TR, Boyd PW. Development of a robust marine ecosystem model to predict the role of iron in biogeochemical cycles: A comparison of results for iron-replete and iron-limited areas, and the SOIREE iron-enrichment experiment. *Deep-Sea Research I* **2006**, 53(2), 333–366.

Ferreira JG, Andersen JH, Borja A, Bricker SB, Camp J, Silva MC, Garcés E, Heiskanen A-S, Humborg C, Ignatiades L, Lancelot C, Menesguen A, Tett P, Hoepffner N, Claussen U. Overview of eutrophication indicators to assess environmental status within the European Marine Strategy Framework Directive. *Estuarine, Coastal and Shelf Science* **2011**, 93(2), 117-131.

Ferreira JG, Simas T, Nobre A, Silva MC, Shifferegger K, Lencart-Silva J. *Identification of sensitive areas and vulnerable zones in transitional and coastal portuguese systems*, INAG, **2003**, 151 pp.

Ferreira JG, Wolff WJ, Simas TC, Bricker SB. Does biodiversity of estuarine phytoplankton depend on hydrology? *Ecological Modelling* **2005**, 187, 513-523.

Fitzpatrick JJ. Assessing skill of estuarine and coastal eutrophication models for water quality managers. *Journal of Marine Systems* **2009**, 76, 195-211.

Flöder S, Jaschinski S, Wells G, Burns CW. Dominance and compensatory growth in phytoplankton communities under salinity stress. *Journal of Experimental Marine Biology and Ecology* **2010**, 395(1–2), 223-231.

Franks PJS, Chen C. A 3-D prognostic numerical model study of the Georges bank ecosystem. Part II: biological-physical model. *Deep-Sea Research II* **2001**, 48, 457-482.

Franks PJS, Wroblewski JS, Flierl GR. Behavior of a simple plankton model with food-level acclimation by herbivores. *Marine Biology* **1986**, 91,121-129.

Franks PJS. NPZ Models of plankton dynamics: their construction, coupling to physics, and application. *Journal of Oceanography* **2002**, 58, 379-387.

Franks PJS. Planktonic ecosystem models: perplexing parameterizations and a failure to fail. *Journal of Plankton Research* **2009**, 31(11), 1299–1306.

Froneman PW. Zooplankton community structure and biomass in a southern African temporarily open/closed estuary. *Estuarine, Coastal and Shelf Science* **2004**, 60(1), 125-132.

Gameiro C, Brotas V. Patterns of phytoplankton variability in the Tagus Estuary. *Estuaries and Coasts* **2010**, 33, 311-323.

Gameiro C, Cartaxana P, Brotas V. Environmental drivers of phytoplankton distribution and composition in Tagus Estuary, Portugal. *Estuarine, Coastal and Shelf Science* **2007**, 75, 21-34.

Gomes FV, Barroco A, Pereira AR, Reis CS, Calado H., Ferreira JG, Freitas MC, Biscoito M. *Bases para a Estratégia Integrada da Zona Costeira Nacional. Versão para discussão pública*, **2006**, 62 pp.

Grangeré K, Lefebvre S, Blin J-L. Spatial and temporal dynamics of biotic and abiotic features of temperate coastal ecosystems as revealed by a combination of ecological indicators. *Estuarine, Coastal and Shelf Science* **2012**, 108, 109-118.

Grant SB, Kim JH, Jones BH, Jenkins SA, Wasyl J, Cudaback C. Surf zone entrainment, along-shore transport and human health implication of pollution from tidal inlets. *Journal of Geophysical Research* **2005**, 110, C10025.

Guillaud J, Andrieux F, Menesguen A. Biogeochemical modelling in the Bay of Seine (France/): an improvement by introducing phosphorus in nutrient cycles. *Journal of Marine Systems* **2000**, 25(3-4),369–386.

Haidvogel DB, Arango H, Budgell WP, Cornuelle BD, Curchitser E, Di Lorenzo E, Fennel K, Geyer WR, Hermann AJ, Lanerolle L, Levin J, McWilliams JC, Miller AJ, Moore AM, Powell TM, Shchepetkin AF, Sherwood CR, Signell RP, Warner JC, Wilkin J. Ocean forecasting in terrain-following coordinates: Formulation and skill assessment of the Regional Ocean Modeling System. *Journal of Computational Physics* **2008**, 227(7), 3595-3624.

Hansen DV, Rattray M. New dimensions in estuarine classification. *Limnology and Oceanography* **1966**, 11, 319–326.

Harris RP, Malej A. Diel patterns of ammonium excretion and grazing rhythms in *Calanus helgolandicus* in surface stratified waters. *Marine Ecology Progress Series* **1986**, 31, 75-85.

Hays GC, Richardson AJ, Robinson C. Climate change and marine plankton. *Trends in Ecology and Evolution* **2005**, 20(6), 337-334.

Huang XP, Huang LM, Yue WZ. The characteristics of nutrients and eutrophication in the Pearl River estuary, South China. *Marine Pollution Bulletin* **2003**, 47(1-6), 30–36.

Hutchins DA, Bruland KW. Iron-limited diatom growth and Si:N uptake ratios in a coastal upwelling regime. *Nature* **1998**, 393, 561-564.

Intergovernmental Panel on Climate Change (IPCC). Climate Change 2007: The Physical Science Basis. UNEP and WMO, 2007 (http://www.ipcc.ch/SPM2feb07.pdf).

Ito S-I, Megrey BA, Kishi MJ, Mukai D, Kurita Y, Ueno Y, Yamanaka Y. On the interannual variability of the growth of Pacific saury (Cololabis saira): A simple 3-box model using NEMURO.FISH. *Ecological Modelling* **2007**, 202, 174–183.

James ID. Modelling pollution dispersion, the ecosystem and water quality in coastal waters: a review. *Environmental Modelling & Software* **2002**, 17(4), 363-385.

Jassby AD, Cloern JE, Cole BE. Annual primary production: patterns and mechanisms of change in a nutrient-rich tidal ecosystem. *Limnology and Oceanography* **2002**, 47(3), 698-712.

Jay DA, Smith JD. Residual circulation in shallow estuaries. 1. Highly stratified, narrow estuaries. *Journal of Geophysical Research* **1990a**, 95(C1), 711-731.

Jay DA, Smith JD. Residual circulation in shallow estuaries. 2. Weakly stratified and partially mixed, narrow estuaries. *Journal of Geophysical Research* **1990b**, 95(C1), 733-748.

Jørgensen SE. Overview of the model types available for development of ecological models. *Ecological Modelling* **2008**, 215, 3-9.

Kimmerer WJ. Effects of freshwater flow on abundance of estuarine organisms: physical effects or trophic linkages? *Marine Ecology Progress Series* **2002**, 243, 39-55.

Kishi MJ, Kashiwai M, Ware DM, Megrey BA, Eslinger DL, Werner FE, Noguchi-Aita M, Azumaya T, Fujii M, Hashimoto S, Huang D, Iizumi H, Ishida Y, Kang S, Kantakov GA, Kim H, Komatsu K, Navrotsky VV, Smith SL, Tadokoro K, Tsuda A, Yamamura O, Yamanaka Y, Yokouchi K, Yoshie N, Zhang J, Zuenko YI, Zvalinsky ZI. NEMURO – a lower trophic level model for the North Pacific marine ecosystem. *Ecological Modelling* **2007**, 202, 12-25.

Kjerfve B, Stevenson LH, Proehl JA, Chrxanowski TH, Kitchens WM. Estimation of material fluxes in an estuarine cross section: A critical analysis of spatial measurement density and errors. *Limnology and Oceanography* **1981**, 26(2), 325-335.

Kjerfve B. Coastal lagoon processes. In: Kjerve B (ed.), *Coastal Lagoon Processes*. *Elsevier Oceanographic Series* **1994**, 60, 1–8.

Kotta I, Simm M, Põllupüü M. Separate and interactive effects of eutrophication and climate variables on the ecosystems elements of the Gulf of Riga. *Estuarine, Coastal and Shelf Science* **2009**, 84, 509-518.

Kromkamp JC, Engeland TV. Changes in phytoplankton biomass in the Western Scheldt estuary during the period 1978-2006. *Estuaries and Coasts* **2010**, 33, 270-285.

Lalli CM, Parsons TR. *Biological Oceanography: an introduction*, The Open University, **1997**, 314 pp.

Lauria ML, Purdie DA, Sharples J. Contrasting phytoplankton distributions controlled by tidal turbulence in an estuary. *Journal of Marine Systems* **1999**, 21(1–4), 189-197.

Lawrie RA, Stretch DD, Perissinotto R. The effects of wastewater discharges on the functioning of a small temporarily open/closed estuary. *Estuarine, Coastal and Shelf Science* **2010**, 87(2), 237-245.

Leandro SM, Tiselius P, Queiroga H. Growth and development of nauplii and copepodites of the estuarine copepod *Acartia tonsa* from southern Europe (Ria de Aveiro, Portugal) under saturating food conditions. *Marine Biology* **2006**, 150(1), 121-129.

Leandro SM. Forçamento ambiental na abundância e produção de zooplâncton num gradiente estuarino. PhD Thesis, Universidade de Aveiro, **2008**.

Lehtonen H, Urho I, Kjellman J. Responses of ruffe (*Gymnocephalus cernuus* (L.)) abundance to eutrophication. *Journal of Great Lakes Research* **1998**, 24(2), 1998, 285-292.

Likens GE. *Plankton of Inland Waters*, Encyclopedia of Inland Waters, Elsevier, **2010**.

Lomas MW, Giibert PM, Kwoshiah F, Smith EM. Microbial processes and temperature in Chesapeake Bay: current relationships and potential impacts of regional warming. *Global Change Biology* **2002**, 8, 51-70,

Lopes CB, Lillebø AI, Dias JM, Pereira E, Vale C, Duarte AC. Nutrient dynamics and seasonal succession of phytoplankton assemblages in a Southern European Estuary: Ria de Aveiro, Portugal. *Estuarine, Coastal and Shelf Science* **2007a**, 71(3-4), 480-490.

Lopes CB, Pereira ME, Vale C, Lillebø AI, Pardal MA, Duarte AC. Assessment of spatial environmental quality status in Ria de Aveiro. *Scientia Marina* **2007b**, 71(2), 293-304.

Lopes CL, Silva PA, Dias JM, Rocha A, Picado A, Plecha S, Fortunato AB. Local sea level change scenarios for the end of the 21st century and potential physical impacts in the lower Ria de Aveiro (Portugal). *Continental Shelf Research* **2011**, 31(14), 1515-1526.

Lopes JF, Almeida MA, Cunha MA. Modelling the ecological patterns of a temperate lagoon in a very wet spring season. *Ecological Modelling* **2010**, 221(19), 2302-2322.

Lopes JF, Dias JM, Cardoso AC, Silva CIV. The water quality of the Ria de Aveiro lagoon, Portugal: From the observations to the implementation of a numerical model. *Marine Environmental Research* **2005**, 60(5), 594-628.

Lopes JF, Silva C. Temporal and spatial distribution of the dissolved oxygen in the Ria de Aveiro lagoon. *Ecological Modelling* **2006**, 197, 67-88.

Lopes JF, Silva CI, Cardoso AC. Validation of a water quality model for the Ria de Aveiro lagoon, Portugal. *Environmental Modelling & Software* **2008**, 23, 479-494.

Lopes JP, Dias JM, Dekeyser I. Numerical modelling of cohesive sediments transport in the Ria de Aveiro lagoon, Portugal. *Journal of Hydrology* **2006**, 316(1-4), 176-198.

Luyten PJ, Jones JE, Proctor R, Tabor A, Tett P, Wild-Allen K. *COHERENS – A coupled hydrodynamical-ecological model for regional and shelf seas: User Documentation*. MUMM Report, Management Unit of the Mathematical Models of the north Sea, Belgium, **1999**, 911 pp.

Makler-Pick V, Gal G, Gorfine M, Hipsey MR, Carmel Y. Sensitivity analysis for complex ecological models – A new approach. *Environmental Modelling & Software* **2011**, 26(2), 124-134.

Mari L, Biotto C, Decoene A, Bonaventura L. A coupled ecological–hydrodynamic model for the spatial distribution of sessile aquatic species in thermally forced basins. *Ecological Modelling* **2009**, 220(18), 2310-2324.

McLusky DS, Elliott M. *The Estuarine Ecosystem – Ecology, Threats and Management*, Third Edition, Oxford University Press, **2004**, 214 pp.

Megrey BA, Kenneth AR, Ito S, Hay DE, Werner FE, Yamanaka Y, Aita MN. North Pacific basin-scale differences in lower and higher trophic level marine ecosystem responses to climate

impacts using a nutrient-phytoplankton-zooplankton model coupled to a fish bioenergetics model. *Ecological Modelling* **2007**, 202, 196-210.

Miranda PMA, Valente MA, Tomé AR, Trigo R, Coelho MFES, Azevedo EB. *O clima de Portugal nos séculos XX e XXI. Alterações Climáticas em Portugal Cenários. Impactos e Medidas de Adaptação Projecto SIAM II*. Gradiva. Lisboa, **2006**, 169–208.

MOHID. *Water Quality Manual*. MARETEC, Instituto Superior Técnico, Universidade Técnica de Lisboa, **2006**.

Monsen NE, Cloern JE, Lucas LV, Monismith SG. A comment on the use of flushing time, residence time, and age as transport time scales. *Limnology and Oceanography* **2002**, 47(5), 1545-1553.

Moreira MH, Queiroga H, Machado MM, Cunha MR. Environmental gradients in a southern europe estuarine system: Ria de Aveiro, Portugal. Implications for soft bottom macrofauna colonization. *Netherlands Journal of Aquatic Ecology* **1993**, 27, 465-482.

Morgado F, Queiroga H, Melo F, Sorbe J. Zooplankton abundance in a coastal station off the Ria de Aveiro inlet (north-west Portugal): relations with tidal and day/night cycles. *Acta Oecologica* **2003**, 24(1), S175-S181.

Morgado R, Nobre M, Ribeiro A, Puga J, Luís A. A Importância do salgado para a gestão da avifauna limícola invernante na Ria de Aveiro (Portugal). *Revista da Gestão Costeira Integrada* **2009**, 9(3), 79-93.

Najjar RG, Pyke CR, Adams MB, Breitburg D, Hershner C, Kemp M, Howarth R, Mulholland MR, Paolisso M, Secor D, Sellner K, Wardrop D, Wood R. Potential climate-change impacts on the Chesapeake Bay. *Estuarine, Coastal and Shelf Science* **2010**, 86(1), 1-20.

Nayar S, Goh BPL, Chou LM. Environmental impact of heavy metals from dredged and resuspended sediments on phytoplankton and bacteria assessed in in situ mesocosms. *Ecotoxicology and Environmental Safety* **2004**, 59(3), 349-369.

Neumman T. Towards a 3D-ecosystem model of the Baltic Sea. *Journal of Marine Systems* **2000**, 25(3-4), 405-419.

Oliveira A, Baptista AM. Diagnostic modeling of residence times in estuaries. *Water Resources Research* **1997**, 33(8), 1935–1946.

Oliveira A, Fortunato AB, Dias JM. Numerical modeling of the Aveiro inlet dynamics. *Coastal Engineering* **2006**, 3282-3294.

Oliveira A, Fortunato AB, Guerreiro M, Bertin X, Bruneau N, Rodrigues M, Taborda R, Andrade C, Silva AM, Antunes C, Freire P, Pedro LS, Dodet G, Loureiro C, Mendes A. Effect of inlet morphology and wave action on pollutant pathways and sediment dynamics in a coastal

stream. Estuarine and Coastal Modeling - Proceedings of the Eleventh International Conference, Ed. Malcolm L. Spaulding, ASCE, **2010**, 601-620.

Oliveira A, Fortunato AB, Rodrigues M, Azevedo A. Integration of physical and water quality models. *La Houille Blanche* **2007**, 4, 40-46.

Paerl HW. Assessing and managing nutrient-enhanced eutrophication in estuarine and coastal waters: Interactive effects of human and climatic perturbations. *Ecological Engineering* **2006**, 26(1), 40-54.

Paerl HW, Rossignol KL, Hall SN, Peierls BL, Wetz MS. Phytoplankton community indicators of short- and long-term ecological change in the anthropogenically and climatically impacted Neuse River estuary, North Carolina, USA. *Estuaries and Coasts* **2010**, 33, 485-497.

Park K, Jung H, Kim H, Ahn S. Three-dimensional hydrodynamic-eutrophication model (HEM-3D): application to Kwang-Yang Bay, Korea. *Marine Environmental Research* **2005**, 60(2), 171-193.

Parker AE, Dugdale RC, Wilkerson FP. Elevated ammonium concentrations from wastewater discharge depress primary productivity in the Sacramento River and the Northern San Francisco Estuary. *Marine Pollution Bulletin* **2012**, 64(3), 574-586.

Pato P, Lopes C, Válega M, Lillebø AI, Dias JM, Pereira E, Duarte AC. Mercury fluxes between an impacted coastal lagoon and the Atlantic Ocean, *Estuarine, Coastal and Shelf Science* **2008**, 76, 787-796.

Pereira A, Duarte P, Norro A. Different modelling tools of aquatic ecosystems: A proposal for a unified approach. *Ecological Informatics* **2006**, 1(4), 407-421.

Pereira C. Ecologia do fitoplâncton costeiro. MsC Thesis, Universidade de Aveiro, **2007**.

Pethick J. Coastal management and sea-level rise. *CATENA* **2001**, 42(2–4), 307-322.

Pinckney JL, Paerl HW, Tester P, Richardson TL. The role of nutrient loading and eutrophication in estuarine ecology. *Environmental Health Perspectives* **2001**, 109(5), 699–706.

Pinho JLS. Aplicação de modelação matemática ao estudo da hidrodinâmica e da qualidade da água em zonas costeiras. PhD Thesis, Universidade do Minho, **2000**.

Plano de Bacia Hidrográfica do Rio Vouga. *Anexo 10, Qualidade dos Meios Hídricos*. Consórcio: Ambio, CHIRON, Agri.Pro, Drena, HCL, FBO Consultores, **1999**, 160 pp.

Plecha S. Contribuição para o estudo da morfodinâmica da embocadura da Ria de Aveiro. PhD Thesis, Universidade de Aveiro, **2011**.

Portela LI. Modelação matemática de processos hidrodinâmicos e de qualidade da água no estuário do Tejo. PhD Thesis, Instituto Superior Técnico, Universidade Técnica de Lisboa, **1996**.

Pritchard DW. What is an estuary: a physical viewpoint. In: Lauff, G.H. (Ed.), Estuaries. American Association of Advancement of Science, Washington, **1967**, 83, 3–5.

Qiu D, Huang L, Zhang J, Lin S. Phytoplankton dynamics in and near the highly eutrophic Pearl River Estuary, South China Sea. *Continental Shelf Research* **2010**, 30(2), 177–186.

Queiroga H, Almeida MJ, Alpuim T, Flores AAV, Francisco S, Gonzalez-Gordillo JI, Miranda AI, Silva I, Paula J. Wind and tide control of megalopal supply to estuarine crab populations on the Portuguese west coast. *Marine Ecology Progress Series* **2006***,* 307, *21-36.*

Rabalais NN, Turner RE, Díaz RJ, Justić D. Global change and eutrophication of coastal waters. *ICES Journal of Marine Science* **2009**, 66, 1528-1537.

Raick C, Soetaert K, Grégoire M. Model complexity and performance: How far can we simplify? *Progress in Oceanography* **2006**, 70, 27–57.

Rebelo, JE. The ichthyofauna and abiotic hydrological environment of the Ria de Aveiro, Portugal. *Estuaries and Coasts* **1992**, 15(3), 403-413.

Resende P, Azeiteiro U, Pereira MJ. Diatom ecological preferences in a shallow temperate estuary (Ria de Aveiro, Western Portugal). *Hydrobiologia* **2005**, 544, *77-88.*

Resende P. Ecologia do fitoplâncton em meio estuarino – canal de Mira, Ria de Aveiro. MsC Thesis, Faculdade de Ciências e Tecnologia, Universidade de Coimbra, **2004**.

Riley GA. A theoretical analysis of the zooplankton population on Georges Bank. *Journal of Marine Research* **1947**, 6, 104-113.

Riley GA. Factors controlling phytoplankton populations on Georges Bank. *Journal of Marine Research* **1946**, 6, 54–72.

Rocha C, Galvão H, Barbosa A. Role of transient silicon limitation in the development of cyanobacteria blooms in the Guadiana estuary, south-western Iberia. *Marine Ecology Progress Series* **2002**, 228, 35-45.

Rodrigues AM, Pires A, Mendo S, Quintino V. *Diopatra neapolitana* and *Diopatra marocensis* from the Portuguese coast: Morphological and genetic comparison. *Estuarine, Coastal and Shelf Science* **2009a**, 85(4), 609-617.

Rodrigues AM, Quintino V, Sampaio L, Freitas R, Neves R. Benthic biodiversity patterns in Ria de Aveiro, Western Portugal: Environmental-biological relationships. *Estuarine, Coastal and Shelf Science* **2011**, 95(2-3), Issues 2–3, 338-348.

Rodrigues M, Oliveira A, Queiroga H, Fortunato AB, Zhang YJ. Three-dimensional modeling of the lower trophic levels in the Ria de Aveiro. *Ecological Modelling* **2009b**, 220(9-10), 1274-1290.

Rodrigues M, Oliveira A, Queiroga H, Zhang YJ, Fortunato AB, Baptista AM. Integrating a circulation model and an ecological model to simulate the dynamics of zooplankton. In: Spaulding M, editors. Estuarine and Coastal Modeling Conference Book, Proceedings of the Tenth International Conference, New York: ASCE, **2008**, p. 427-446.

Ruzicka JJ, Wainwright TC, Peterson WT. A simple plankton model for the Oregon upwelling ecosystem: Sensitivity and validation against time-series ocean data. *Ecological Modelling* **2011**, 222, 1222–1235.

Sá CBP. Calibração automática de modelos ecológicos baseados em equações diferenciais ordinárias utilizando algoritmos genéricos. PhD Thesis, Universidade Federal do Rio de Janeiro, **2003**.

Sampaio L. Processo sucessional de recolonização dos fundos dragados da Ria de Aveiro após o desassoreamento: comunidades macrobentónicas. MsC Thesis, Universidade de Aveiro, **2001**, 87pp.

Sano M, Golshani A, Splinter KD, Strauss D, Thurston W, Tomlinson R. A detailed assessment of vulnerability to climate change in the Gold Coast, Australia. *Journal of Coastal Research* **2011**, SI 64, 245-249.

Santos FD, Forbes K, Moita R. *Climate Change in Portugal. Scenarios, Impacts and Adaptation Measures – SIAM Project*. Gradiva, Lisbon, Portugal, **2002**.

Saraiva S. Modelação ecológica da Ria de Aveiro: o papel das macroalgas. MsC Thesis, Instituto Superior Técnico, Universidade Técnica de Lisboa, **2005**.

Sautour B, Artigas F, Herbland A, Laborde P. Zooplankton grazing impact in the plume of dilution of the Gironde estuary (France) prior to the spring bloom. *Journal of Plankton Research* **1996**, 18(5), 835-853.

Schrum C, Alekseeva I, John MS. Development of a coupled physical–biological ecosystem model ECOSMO: Part I: Model description and validation for the North. *Journal of Marine Systems* **2006**, 61(1–2), 79-99.

Schumann E, Largier J, Slinger J. Estuarine hydrodynamics. Ed.: Allanson BR, Baird D, *Estuaries of South Africa*, Cambridge University Press, **1999**, 27-52.

Science for Environment Policy: European Commission DG Environment News Alert Service. Ed. SCU, The University of the West of England, Bristol, **2012**.

Sebastiá M-T, Rodilla M, Sanchis J-A, Altur V, Gadea I, Falco S. Influence of nutrient inputs from a wetland dominated by agriculture on the phytoplankton community in a shallow harbour at the Spanish Mediterranean coast. *Agriculture, Ecosystems & Environment* **2012**, 152, 10-20.

Shen P-P, Li G, Huang L-M, Zhang J-L, Tan Y-H. Spatio-temporal variability of phytoplankton assemblages in the Pearl River estuary, with special reference to the influence of turbidity and temperature. *Continental Shelf Research* **2011**, 31(16), 1672-1681.

Silva JF, Duck RW, Oliveira F, Rodrigues M. Utilização da água e saneamento na área do Baixo Vouga: impactos na Ria de Aveiro. Actas do II Congresso Ibérico de Planeamento e Gestão de Água, **2000**, 9 pp.

Skogen MD, Moll A. Importance of ocean circulation in ecological modeling: An example from the North Sea. *Journal of Marine Systems* **2005**, 57(3-4), 289-300.

Skogen MD, Svendsen E, Berntsen J, Aksnes D, Ulvestad KB. Modelling the primary production in the North Sea using a coupled three-dimensional physical-chemical-biological ocean model. *Estuarine, Coastal and Shelf Science* **1995**, 41, 545-565.

Smayda TJ. Complexity in the eutrophication–harmful algal bloom relationship, with comment on the importance of grazing. *Harmful Algae* **2008**, 8(1), 140-151.

Smith W, Steinberg D, Bronk D, Tang K. Marine plankton food webs and climate change. Virginia Institute of Marine Science, **2008**.

Statham PJ. Nutrients in estuaries — An overview and the potential impacts of climate change. *Science of Total Environment* **2012**, 434, 213-227.

Streeter HW, Phelps EB. A study of pollution and natural purification of the Ohio. *Public Health Bulletin* **1925**, 146, 175.

Struyf E, Van Damme S, Meire P. Possible effects of climate change on estuarine nutrient fluxes: a case study in the highly nutrified Schelde estuary (Belgium, The Netherlands). *Estuarine, Coastal and Shelf Science* **2004**, 60(4), 649-661.

Swaney DP, Scavia D, Howarth RW, Marino RM. Estuarine classification and response to nitrogen loading: Insights from simple ecological models. *Estuarine, Coastal and Shelf Science* **2008**, 77, 253-263.

Tan Y, Huang L, Chen Q, Huang X. Seasonal variation in zooplankton composition and grazing impact on phytoplankton standing stock in the Pearl River Estuary, China. *Continental Shelf Research* **2004**, 24, 1949-1968.

Thom RM, Parkwell TL, Niyogi DK, Shreffler DK. Effects of graveling on the primary productivity, respiration and nutrient flux of two estuarine tidal flats. *Marine Biology* **1994**, 118(2), 329-341.

Trancoso AR, Saraiva S, Fernandes L, Pina P, Leitão P, Neves R. Modelling macroalgae using a 3D hydrodynamic-ecological model in a shallow, temperate estuary. *Ecological Modelling* **2005**, 187, 232–246.

Underwood GJC, Kromkamp J. Primary production by phytoplankton and microphytobenthos in estuaries. *Advances in Ecological Research* **1999**, 29, 93-153.

Válega M, Lillebø AI, Pereira ME, Duarte AC, Pardal MA. Long-term effects of mercury in a salt marsh: Hysteresis in the distribution of vegetation following recovery from contamination. *Chemosphere* **2008**, 71, 765-772.

Vaz N. Estudo dos processos de transporte de calor e de sal no Canal do Espinheiro (Ria de Aveiro). PhD Thesis, Universidade de Aveiro, **2007**.

Vichi M, Pinardi N, Masina S. A generalized model of pelagic biogeochemistry for the global ocean ecosystem. Part I: Theory. *Journal of Marine Systems* **2007**, 64, 89-109.

Wainwright TC, Feinberg LR, Hooff RC, Peterson WT. A comparison of two lower trophic models for the California Current System. *Ecological Modelling* **2007**, 202, 120–131.

Willis J. Modelling swimming aquatic animals in hydrodynamic models. *Ecological Modelling* **2011**, 222(23-24), 3869-3887.

World Resources Institute. http://earthtrends.wri.org, consulted in March 2012.

Wroblewski JS. A model of phytoplankton plume formation during variable Oregon upwelling. *Journal of Marine Research* **1977**, 35, 357-394.

Wroblewski JS. A simulation of the distribution of *Acartia clausi* during Oregon upwelling, August 1973. *Journal of Plankton Research* **1980**, 2, 43-68.

Yates ML, le Cozannet G, Lenôtre N. Quantifying errors in long-term coastal erosion and inundation hazard assessments. *Journal of Coastal Research* **2011**, SI64, 260-264.

Yoshie N, Yamanaka Y, Rose KA, Eslinger DL, Ware DM, Kishi MJ. Parameter sensitivity study of the NEMURO lower trophic level marine ecosystem model. *Ecological Modelling* **2007**, 202, 26-37.

Zhang Y, Baptista AM. SELFE: A semi-implicit Eulerian-Lagrangian finite-element model for cross-scale ocean circulation. *Ocean Modeling* **2008**, 21(3-4), 71-96.

Zhong J, Fan C, Zhang L, Hall E, Ding S, Li B, Liu G. Significance of dredging on sediment denitrification in Meiliang Bay, China: A year long simulation study. *Journal of Environmental Sciences* **2010**, 22(1), 68-75.

Zimmerman AR, Canuel EA. A geochemical record of eutrophication and anoxia in Chesapeake Bay sediments: anthropogenic influence on organic matter composition. *Marine Chemistry* **2000**, 69(1–2), 117-137.

CHAPTER II

ROBUST ECOLOGICAL MODELLING: HALF-SATURATION CONSTANTS REVIEW AND SENSITIVITY ANALYSIS FOR A SITE APPLICATION

SECTION II.1

HALF-SATURATION CONSTANTS FOR NUTRIENTS UPTAKE: A REVIEW AND SENSITIVITY ANALYSIS FOR ECOLOGICAL MODELLING

ABSTRACT

Half-saturation constants for nutrients uptake are widely used to assess ecosystems dynamics, both in data analysis and numerical modelling studies. In ecological modelling, in particular, the specification of the input parameters is one of the main sources of uncertainty and may affect their robustness. Thus, defining the range of variation of these parameters and their influence in the final results is of major concern to optimize the efforts of quantifying the most important parameters. A review of half-saturation constants for nutrients uptake by phytoplankton is performed here, based on values published in the literature. Nutrients considered in the present review include: nitrogen, phosphorus and silica. For nitrogen uptake half-saturation constant values ranged from about 0.01 μM to a maximum value of 33.6 μM. Maximum values of half-saturation constant reported for nitrogen uptake by diatoms are of about 10 μM. Half-saturation constants for nutrients uptake by phytoplankton tend to be smaller in regions were nutrients concentrations are lower. Half-saturation constant for phosphorus uptake ranged from 0.02 μM to 7.0 μM. For silica uptake values ranged from 0.2 to 88.7 μM, although most common values fall in a narrow range. The applicability of the review performed was demonstrated through a sensitivity analysis to ECO-SELFE, a coupled hydrodynamic and ecological model, applied to a coastal lagoon. Results evidenced the lower sensitivity of the modelled phytoplankton concentrations, even within a wider range of variation of the half-saturation constants for nutrients uptake by diatoms. The review allowed for a synthesis of the current knowledge on the ranges of these important parameters, which is of relevance for phytoplankton dynamics studies and for the setting up of ecological models in general.

KEYWORDS

Uptake, Nitrogen, Phosphorus, Silica, Phytoplankton

II.1.1 INTRODUCTION

The role of nutrients in phytoplankton productivity, community structure and distribution is widely discussed. Dugdale (1967) was one of the first authors to examine the role of nutrients uptake in the growth of phytoplankton. Since then, the mechanisms and kinetics of nutrients uptake by phytoplankton were the subject of several studies and some formulations were proposed to describe these processes (e.g. Walsh and Dugdale, 1971; Frost and Franze, 1992; Yajnik and Sharada, 2003). The most common formulation to describe the kinetics of nutrients uptake is a Michaelis-Menten type equation:

$$\rho_u = \rho_{u\_\max} \frac{S_u}{S_u + K_s} \qquad \text{(II.1.1)}$$

where ρ_u is the uptake rate, $\rho_{u\_\max}$ is the maximum uptake rate, S_u is the nutrient concentration and K_s is the half-saturation constant for the nutrient uptake.

The half-saturation constant (K_s) corresponds to the nutrient concentration when $\rho_u = \rho_{u\_\max}/2$. This parameter is widely used to assess phytoplankton response to nutrients concentration in the system (e.g. Gameiro *et al.*, 2007) or in ecological models parameterization (e.g. Cloern, 1999; Sharada *et al.*, 2005; Kishi *et al.*, 2007; Rodrigues *et al.*, 2009b). K_s is difficult to measure, especially in field conditions, and has a large statistical uncertainty associated, since the uptake rates vary with time and may be influenced by the nutrients supply and other environmental factors (Dortch, 1990). However, many studies aimed at evaluating K_s for different species of phytoplankton (e.g. Eppley *et al.*, 1969; Sommer, 1986; Lomas and Glibert, 2000). These studies led to values of K_s in the literature that often vary over several orders of magnitude. Thus, the aim of this review is to compile the values of K_s available in the literature. This compilation, although systematic, does not intend to be exhaustive and is mainly focused in the estuarine and marine environments. Yet, some values for freshwater species are also presented. The K_s values are presented for nitrogen, phosphorus and silica uptake. These nutrients were chosen since nitrogen and phosphorus are the main nutrients for primary production in estuarine and marine environments (Underwood e Kromkamp, 1999; Benitez-Nelson, 2000) and silica is also an important nutrient for diatoms (e.g. Paasche, 1973b).

In order to provide an example of the range of applicability of this review, a sensitivity analysis of the influence of the half-saturation constants on the results of an ecological model is presented. The definition of the input parameters is, at the same time, of key relevance and of major difficulty in ecological modelling, as most of the times these parameters are unknown for a given location. Thus, input parameters definition is an important source of uncertainty in this type of models, and the determination of the relative contribution of each input parameter is

essential in ecological modelling (Cariboni *et al.*, 2007; Chu *et al.*, 2007). In this sense, sensitivity analyses of the model input parameters are widely used (e.g. Makler-Pick *et al.*, 2011). The sensitivity analysis presented here is performed on ECO-SELFE model (Rodrigues *et al.*, 2009b), a three-dimensional, unstructured grid hydrodynamic and ecological model, applied to the Aveiro lagoon. This analysis is based on former applications (Chapter III, Section III.2, Rodrigues *et al*., 2009a).

In the next sections the values of K_s are presented for each of the nutrients reviewed: nitrogen (section II.1.2), phosphorus (section II.1.3) and silica (section II.1.4). The application of the reviewed half-saturation constants for phytoplankton uptake on a sensitivity analysis of an ecological model is presented in section II.1.5. Section II.1.6 presents the main conclusions of the review.

II.1.2 NITROGEN

Table II.1.1 summarizes the values of K_s for ammonium uptake by phytoplankton. Studies based on natural phytoplankton communities present values that range from 0.01 μM (oligotrophic waters; MacIsaac and Dugdale, 1969) to 9.83±2.63 μM, which was determined in the Choptank River (USA) during a *Prorocentrum minimum* bloom (Fan *et al.*, 2003). In the absence of blooms the largest value was observed in the Neuse estuary (USA, 4.91±0.48; Fan *et al.*, 2003). The maximum value of K_s for ammonium uptake was observed for *Gymnodinium catenatum* (33.6 μM; Hiroshima bay, Japan; Yamamoto *et al.*, 2004b). For dinoflagellates the minimum value was registered for *Alexadrium catenella* (0.2 μM; Thau lagoon, France; Collos *et al.*, 2007). Regarding diatoms, K_s values range from 0.3±0.3 μM (*Chaetoceros gracilis*; Eppley *et al.*, 1969) to 9.3±1.5 μM (*Rhizosolenia robusta*; Eppley *et al.*, 1969), which are within the range of variation proposed by Sarthou *et al.* (2005) of 0.02-10.2 μM for nitrogen uptake by diatoms. Other species of phytoplankton present K_s values for ammonium uptake that are within the ranges mentioned above.

Table II.1.1. Half-saturation constants for ammonium uptake by phytoplankton.

Species or Class	Region or Zone	K_s (μM)	Comments	Source
General				
Natural phytoplankton community	Eutrophic coastal areas	0.5-2.0	-	Lalli and Parsons, 1997
	Eutrophic oceanic waters	2.0-10.0	-	Lalli and Parsons, 1997
	Subartic Pacific Ocean (eutrophic)	1.3	-	MacIsaac and Dugdale, 1969
	Oligotrophic waters	0.01-0.1	-	Lalli and Parsons, 1997

Table II.1.1 (Cont.). Half-saturation constants for ammonium uptake by phytoplankton.

Species or Class	Region or Zone	K_s (μM)	Comments	Source
General				
Natural phytoplankton community	Tropical Pacific Ocean (oligotrophic)	0.1	-	MacIsaac and Dugdale, 1969
		0.55	-	MacIsaac and Dugdale, 1969
		0.62	-	MacIsaac and Dugdale, 1969
	North Pacific Ocean	0.15	-	Eppley *et al.*, 1973
	Pacific Ocean	0.41 (±0.09)	K_s+S	Kanda *et al.*, 1985
		0.16 (±0.02)	K_s+S	Kanda *et al.*, 1985
		0.07 (±0.02)	K_s+S	Kanda *et al.*, 1985
		0.15 (±0.01)	K_s+S	Kanda *et al.*, 1985
		0.32 (±0.06)	K_s+S	Kanda *et al.*, 1985
		0.10 (±0.05)	K_s+S	Kanda *et al.*, 1985
		0.05 (±0.01)	K_s+S	Kanda *et al.*, 1985
		0.05 (±0.00)	K_s+S	Kanda *et al.*, 1985
		0.13 (±0.05)	K_s+S	Kanda *et al.*, 1985
		0.09 (±0.02)	K_s+S	Kanda *et al.*, 1985
		0.07 (±0.02)	K_s+S	Kanda *et al.*, 1985
		0.12 (±0.01)	K_s+S	Kanda *et al.*, 1985
		0.09 (±0.01)	K_s+S	Kanda *et al.*, 1985
		0.05 (±0.02)	K_s+S	Kanda *et al.*, 1985
		0.11 (±0.02)	K_s+S	Kanda *et al.*, 1985
		0.12 (±0.01)	K_s+S	Kanda *et al.*, 1985
		0.10 (±0.01)	K_s+S	Kanda *et al.*, 1985
		0.07 (±0.01)	K_s+S	Kanda *et al.*, 1985
	Central North Pacific Gyre	0.06	Coastal	Sahlsten, 1987
		0.03	Oceanic	Sahlsten, 1987
	North Atlantic Ocean	0.030 (0.011-0.083)	Oceanic; K_s+S	Harrison *et al.*, 1996
		0.025 (0.013-0.041)	Oceanic; K_s+S	Harrison *et al.*, 1996
		0.198 (0.047-0.412)	Neritic; K_s+S	Harrison *et al.*, 1996
		0.052 (0.028-0.092)	Neritic; K_s+S	Harrison *et al.*, 1996
	Canary Basin	0.040 (0.018-0.071)	K_s+S	Harrison *et al.*, 1996
	Southern Benguela (South Africa)	0.10	-	Probyn, 1985
	Lake Calado (Brazil)	0.3-5	-	Fisher *et al.*, 1988b
	Arabian Peninsula	0.47	-	McCarthy *et al.*, 1999
	Black Sea	0.26	μM kg^{-1}; Spring 1998	McCarthy *et al.*, 2007
		0.61	μM kg^{-1}; Autumn 1999	McCarthy *et al.*, 2007
		0.13	μM kg^{-1}; Spring 2001	McCarthy *et al.*, 2007

Table II.1.1 (Cont.). Half-saturation constants for ammonium uptake by phytoplankton.

Species or Class	Region or Zone	K_s (μM)	Comments	Source
General				
Natural phytoplankton community	Eagle Moutain Lake Texas (USA)	4.15 (±2.58)	DIN[1]	Sterner and Grover, 1998
		1.74 (±0.59)	DIN[1]	Sterner and Grover, 1998
		1.33 (±0.43)	DIN[1]	Sterner and Grover, 1998
		2.48 (±1.29)	DIN[1]	Sterner and Grover, 1998
		12.29 (±5.68)	DIN[1]	Sterner and Grover, 1998
		7.5 (±2.99)	DIN[1]	Sterner and Grover, 1998
		5.86 (±1.85)	DIN[1]	Sterner and Grover, 1998
		7.79 (±0.56)	DIN[1]	Sterner and Grover, 1998
		14.36 (±5.28)	DIN[1]	Sterner and Grover, 1998
	Choptank River (USA)	9.83 (±2.63)	*Prorocentrum minimum* bloom	Fan *et al.*, 2003
		4.07 (±4.27)	*Prorocentrum minimum* bloom	Fan *et al.*, 2003
		5.09 (±2.23)	*Prorocentrum minimum* bloom	Fan *et al.*, 2003
		2.38 (±0.27)	*Prorocentrum minimum* bloom	Fan *et al.*, 2003
	Neuse Estuary (USA)	4.91 (±0.48)	-	Fan *et al.*, 2003
	Barents Sea (Norway)	1.3 (±0.3)	$[NO_3^-]_{ambient} \geq 1$ μM	Kristiansen *et al.*, 1994
		0.1 (±0.0)	$[NO_3^-]_{ambient} < 1$ μM	Kristiansen *et al.*, 1994
	Toolik Lake (Artic)	0.05-0.49	-	Whalen and Alexander, 1986
	Greenland Sea (Artic)	2.24 (±0.60)	-	Muggli and Smith, 1993
	Eastern Canadian Artic	0.17	-	Smith and Harrison, 2001
	Barrow Strait (Canada)	1.60 (±0.25)	-	Harrison *et al.*, 1990
	Western Ross Sea (Antarctica)	0.124 (±0.025)	-	Cochlan and Bronk, 2001
		0.040 (±0.010)	Corrected value (isotope-dilution correction)	Cochlan and Bronk, 2001
		1.597 (±0.163)	-	Cochlan and Bronk, 2001
		0.333 (±0.098)	Corrected value (isotope-dilution correction)	Cochlan and Bronk, 2001
		0.193 (±0.027)	-	Cochlan and Bronk, 2001

Table II.1.1 (Cont.). Half-saturation constants for ammonium uptake by phytoplankton.

Species or Class	Region or Zone	K_s (μM)	Comments	Source
General				
Natural phytoplankton community	Western Ross Sea (Antarctica)	0.284 (±0.025)	-	Cochlan and Bronk, 2001
		0.131 (±0.032)	Corrected value (isotope-dilution correction)	Cochlan and Bronk, 2001
		0.861 (±0.141)	-	Cochlan and Bronk, 2001
		0.378 (±0.093)	-	Cochlan and Bronk, 2001
		0.378 (±0.051)	-	Cochlan and Bronk, 2001
		0.152 (±0.043)	Corrected value (isotope-dilution correction)	Cochlan and Bronk, 2001
	Western New Zealand	0.5	-	Chang *et al.*, 1995 *in* Kudela *et al.*, 2008b
	Southern California (USA)	0.586 (±0.627)	*Lingulodinium polyedrum* bloom	Kudela and Cochlan, 2000
	Monterey Bay (USA)	2.05 (±0.58)	*Akashiwo sanguinea* bloom	Kudela *et al.*, 2008a
		2.37 (±0.22)	-	Kudela *et al.*, 2008a
	Lake Kinneret (Israel)	1.1	-	Berman *et al.*, 1984
	Chesapeake Bay, Delaware Bay, Hudson River Estuary (USA)	2	DIN	Fisher *et al.*, 1988a
Diatoms				
Asterionella japonica	Culture	1.5, 0.6 (±1.2, ±0.8)	-	Eppley *et al.*, 1969
Chaetoceros debilis	Culture	0.5	-	Conway and Harrison, 1977
Chaetoceros gracilis	Culture	0.5, 0.3 (±0.5, ±0.3)	-	Eppley *et al.*, 1969
Coscinodiscus lineatus	Culture (clone FCRG 12)	2.8, 1.2 (±2.6, ±1.0)	-	Eppley *et al.*, 1969
Coscinodiscus wailesii	Culture (Cos. R.)	4.3, 5.5 (±5.4, ±2.0)	-	Eppley *et al.*, 1969
Thalassiosira pseudonana (Cyclotella nana)	Culture (clone 13-1)	0.4 (±0.3)	-	Eppley *et al.*, 1969
Ditylum brightwellii	Culture	1.1 (±0.6)	-	Eppley *et al.*, 1969
Leptocylindrus danicus	Culture (clone FCRG 11)	3.4, 0.9, 0.5 (±1.4, ±0.2, ±0.4)	-	Eppley *et al.*, 1969
Pseudo-nitzschia australis	Culture (AU-03184-5D)	5.37 (±0.32)	-	Cochlan *et al.*, 2008
Rhizosolenia robusta	Culture (clone FCRG 13)	5.6, 9.3 (±2.0, ±1.5)	-	Eppley *et al.*, 1969
Rhizosolenia stolterfothii	Culture (clone FCRG 3)	0.5, 0.5 (±0.9, ±0.4)	-	Eppley *et al.*, 1969
Skeletonema costatum	Culture (clone Skel.)	3.6, 0.8, 0.8 (±0.8, ±0.7, ±0.5)	-	Eppley *et al.*, 1969
	Culture	0.44	-	Conway *et al.*, 1976

Table II.1.1 (Cont.). Half-saturation constants for ammonium uptake by phytoplankton.

Species or Class	Region or Zone	K_s (μM)	Comments	Source
Diatoms				
Skeletonema costatum	Culture	0.5	-	Conway and Harrison, 1977
Thalassiosira gravida	Culture	0.5	-	Conway and Harrison, 1977
Thalassiosira pseudonana	Culture (clone 3H)	0.45-1.15	Without NO_3^- added	Yin *et al.*, 1998
		0.35-1.85	With NO_3^- added	Yin *et al.*, 1998
Dinoflagellates				
Alexandrium catenella	Culture (Thau Lagoon, France)	0.2-20	4-year period	Collos *et al.*, 2007
	Culture (Thau Lagoon, France)	0.5-6.2	3-day interval	Collos *et al.*, 2007
	Thau Lagoon (France)	8.4 (±1.7)	In the field	Collos *et al.*, 2004
	Culture (Thau Lagoon, France)	2.0 (±0.6)	-	Collos *et al.*, 2004
Alexandrium tamarense	Culture	1.95	-	MacIsaac *et al.*, 1979 *in* Yamamoto, 2004
	Culture (Hiroshima Bay, Japan)	0.12	NH_4^+ enriched	Leong and Taguchi, 2004
Dissodinium lunula	Culture (clone T-37)	3.8 (±5.1)	-	Bhovichitra and Swift, 1977
Gonyaulax polyedra	Culture (clone FCRG 8)	5.7, 5.3 (±0.6, ±1.1)	-	Eppley *et al.*, 1969
Gymnodinium catenatum	Culture (Hiroshima Bay, Japan)	33.6	-	Yamamoto *et al.*, 2004b
Gymnodinium splendens	Culture (clone Gy.)	1.1 (±1.0)	-	Eppley *et al.*, 1969
Prorocentrum minimum	Culture (Chesapeake Bay, USA)	5.18 (±1.46)	NO_3^- grown culture	Fan *et al.*, 2003
		23.3 (±11.1)	NH_4^+ grown culture	Fan *et al.*, 2003
		0.23 (±0.68)	Urea grown culture	Fan *et al.*, 2003
Pyrocystis fusiformis	Culture (clone 4)	1.4 (±1.1)	-	Bhovichitra and Swift, 1977
Pyrocystis noctiluca	Culture (clone 7)	4.4 (±2.2)	-	Bhovichitra and Swift, 1977
Chlorophytes				
Dunaliella tertiolecta	Culture (clone Dun.)	0.1 (±0.6)	-	Eppley *et al.*, 1969
Micromonas pusilla	Culture	0.40	-	Cochlan and Harrison, 1991
Prasinomonas capsulatus	Culture (CCMP 1617)	1.036 (0.813-1.322)	NH_4^+ limited	Timmermans *et al.*, 2005
Chrysophytes				
Monochrysis lutheri	Culture (clone Mono.)	0.5 (±0.4)	-	Eppley *et al.*, 1969
Coccolithophorids				
Coccolithus huxleyi	Culture (clone BT-6)	0.1 (±0.7)	-	Eppley *et al.*, 1969

Table II.1.1 (Cont.). Half-saturation constants for ammonium uptake by phytoplankton.

Species or Class	Region or Zone	K_s (μM)	Comments	Source
Coccolithophorids				
Coccolithus huxleyi	Culture (clone F-5)	0.2 (±0.9)	-	Eppley *et al.*, 1969
Emiliania huxleyi	Culture (strain L, NIOZ)	~0.2 (~0.1-0.4)	-	Page *et al.*, 1999
Cyanobacteria				
Nodularia spumigena	Culture (Baltic Sea)	0.22	-	Sörensson and Sahlsten, 1987
Synechococcus sp.	Culture (CCMP 839)	2.635 (1.314-5.286)	NH_4^+ limited	Timmermans *et al.*, 2005
Raphidophytes				
Chattonella subsalsa	Culture (Delaware Inland Bays, USA)	1.46 (±0.010)	-	Zhang *et al.*, 2006
Heterosigma akashiwo	East coast of USA	2	-	Tomas, 1979
	Culture (Delaware Inland Bays, USA)	0.27 (±0.003)	-	Zhang *et al.*, 2006
	Culture (CCMP1912)	2.23 (0.81)	-	Herndon and Cochlan, 2007
		1.17 (0.23)	-	Herndon and Cochlan, 2007
		1.44 (0.35)	-	Herndon and Cochlan, 2007
Others				
Pelagomonas calceolata	Culture (CCMP 1756)	1.037 (0.681-1.580)	NH_4^+ limited	Timmermans *et al.*, 2005

[1] Values for DIN are presented in both Table II.1.1 and Table II.1.2.

Values of K_s for nitrate uptake are presented in Table II.1.2. For natural phytoplankton community studies the maximum K_s is of 28.3±7.2 μM and was observed during a *Peridinium* bloom in Lake Kinneret (Israel; Berman *et al.*, 1984). In estuarine, coastal and oceanic waters the maximum values are significantly lower and are within the range of those observed for K_s for ammonium uptake. Diatoms present values ranging from 0.007 μM (*Asterionella formosa*; Yellowstone National Park, USA; Interlandi, 2002) to 7.60 μM (*Gymnodinium catenatum*; Hiroshima Bay, Japan; Yamamoto *et al.*, 2004b), while for dinoflagellates these values range from 0.32 μM (*Ceratium fusus*; Sagami Bay, Japan; Baek *et al.*, 2004) to 10.3±7.2 μM (*Gonyaulax polyedra*; Eppley *et al.*, 1969).

Generally, K_s for nitrogen uptake is larger in eutrophic areas than in oligotrophic areas. Eutrophic estuarine and coastal waters also present larger K_s for nitrogen uptake than eutrophic oceanic waters. MacIsaac and Dugdale (1969) suggested that the smaller K_s values observed in regions where nutrients concentrations are lower may indicate a better adaptation to low concentration of nutrients of the phytoplankton populations of these regions. Figure II.1.1

summarizes the range of variation of K_s for nitrogen uptake by phytoplankton natural communities in oceanic waters.

Table II.1.2. Half-saturation constants for nitrate uptake by phytoplankton.

Species	Region or Zone	K_s (μM)	Comments	Source
General				
Natural phytoplankton community	-	1.0	$[NO_3^-] > 1\mu M$	Kudela and Chavez, 2000
	-	0.1	$[NO_3^-] < 1\mu M$	Kudela and Chavez, 2000
	Coastal waters	0.5-1	-	Garside, 1985
	Eutrophic coastal areas	2.0-10.0	-	Lalli and Parsons, 1997
	Eutrophic oceanic waters	0.5-2.0	-	Lalli and Parsons, 1997
	Subartic Pacific Ocean (eutrophic)	4.21	-	MacIsaac and Dugdale, 1969
	Tropical Pacific Ocean (eutrophic)	0.98	-	MacIsaac and Dugdale, 1969
	Oligotrophic waters	0.01-0.1	-	Lalli and Parsons, 1997
	Oligotrophic open ocean	<0.1	-	Garside, 1985
	Tropical Pacific Ocean (oligotrophic)	0.04	-	MacIsaac and Dugdale, 1969
		0.21	-	MacIsaac and Dugdale, 1969
		0.01	-	MacIsaac and Dugdale, 1969
		0.03	-	MacIsaac and Dugdale, 1969
		0.14	-	MacIsaac and Dugdale, 1969
	Pacific Ocean	0.79 (±0.32)	K_s+S	Kanda *et al.*, 1985
		0.66 (±0.32)	K_s+S	Kanda *et al.*, 1985
		4.57 (±0.01)	K_s+S	Kanda *et al.*, 1985
		3.00 (±0.18)	K_s+S	Kanda *et al.*, 1985
		1.67 (±0.14)	K_s+S	Kanda *et al.*, 1985
		2.29 (±0.24)	K_s+S	Kanda *et al.*, 1985
		0.78 (±0.04)	K_s+S	Kanda *et al.*, 1985
		0.12 (±0.08)	K_s+S	Kanda *et al.*, 1985
		0.08 (±0.03)	K_s+S	Kanda *et al.*, 1985
		0.09 (±0.01)	K_s+S	Kanda *et al.*, 1985
		0.12 (±0.04)	K_s+S	Kanda *et al.*, 1985
		0.00 (±0.04)	K_s+S	Kanda *et al.*, 1985
		0.12 (±0.08)	K_s+S	Kanda *et al.*, 1985
		0.07 (±0.07)	K_s+S	Kanda *et al.*, 1985
		0.02 (±0.09)	K_s+S	Kanda *et al.*, 1985
		0.06 (±0.05)	K_s+S	Kanda *et al.*, 1985
		0.10 (±0.02)	K_s+S	Kanda *et al.*, 1985

Table II.1.2 (Cont.). Half-saturation constants for nitrate uptake by phytoplankton.

Species	Region or Zone	K_s (μM)	Comments	Source
General				
Natural phytoplankton community	Pacific Ocean	0.13 (±0.10)	K_s+S	Kanda *et al.*, 1985
		0.02 (±0.05)	K_s+S	Kanda *et al.*, 1985
	Central North Pacific Gyre	0.03	-	Sahlsten, 1987
	North Atlantic Ocean	0.190 (0.009-1.319)	-	Harrison *et al.*, 1996
		0.017 (0.001-0.069)	Oceanic	Harrison *et al.*, 1996
		0.029 (0.010-0.059)	Oceanic	Harrison *et al.*, 1996
		0.361 (0.139-0.942)	Neritic	Harrison *et al.*, 1996
		0.022 (0.020-0.25)	Neritic	Harrison *et al.*, 1996
	Gulf of Main	0.086 (0.057-0.157)	-	Harrison *et al.*, 1996
	Canary Basin	0.027 (0.010-0.039)	-	Harrison *et al.*, 1996
	Atlantic Ocean	0.09422	-	Painter *et al.*, 2008
		0.08043	-	Painter *et al.*, 2008
		0.13343	-	Painter *et al.*, 2008
		0.09899	All data	Painter et al., 2008
	Monterey Bay (USA)	1.22	-	Kudela and Dugdale, 2000
		4.14	-	Kudela and Dugadale, 2000
		1.01	*Cochlodinium* bloom	Kudela *et al.*, 2008b
	Oregon coast (USA)	1.26	-	Dickson and Wheeler, 1995
	Eastern Agulhas Bank (South Africa)	2.02 (±0.73)	-	Probyn *et al.*, 1995
	Southern Benguela (South Africa)	0.93	-	Probyn, 1985
	Lake Calado (Brazil)	0.3-5	-	Fisher *et al.*, 1988a
	Arabian Peninsula	1.7	-	McCarthy *et al.*, 1999
	Black Sea	0.31	μM kg^{-1}; Spring 1998	McCarthy *et al.*, 2007
		1.03	μM kg^{-1}; Autumn 1999	McCarthy *et al.*, 2007
		0.33	μM kg^{-1}; Spring 2001	McCarthy *et al.*, 2007
	Eagle Moutain Lake Texas (USA)	4.15 (±2.58)	DIN[1]	Sterner and Grover, 1998
		1.74 (±0.59)	DIN[1]	Sterner and Grover, 1998
		1.33 (±0.43)	DIN[1]	Sterner and Grover, 1998
		2.48 (±1.29)	DIN[1]	Sterner and Grover, 1998
		12.29 (±5.68)	DIN[1]	Sterner and Grover, 1998
		7.5 (±2.99)	DIN[1]	Sterner and Grover, 1998

Table II.1.2 (Cont.). Half-saturation constants for nitrate uptake by phytoplankton.

Species	Region or Zone	K_s (μM)	Comments	Source
General				
Natural phytoplankton community	Eagle Moutain Lake Texas (USA)	5.86 (±1.85)	DIN[1]	Sterner and Grover, 1998
		7.79 (±0.56)	DIN[1]	Sterner and Grover, 1998
		14.36 (±5.28)	DIN[1]	Sterner and Grover, 1998
	Choptank River (USA)	1.36 (±0.22)	*Prorocentrum minimum* bloom	Fan *et al.*, 2003
		4.6 (±0.44)	*Prorocentrum minimum* bloom	Fan *et al.*, 2003
		7.12 (±5.54)	*Prorocentrum minimum* bloom	Fan *et al.*, 2003
		1.8 (±1.39)	*Prorocentrum minimum* bloom	Fan *et al.*, 2003
	Neuse Estuary (USA)	0.54 (±0.08)	-	Fan *et al.*, 2003
	Barents Sea (Norway)	1.8 (±1.1)	$[NO_3^-]_{ambient} \geq 1$ □M	Kristiansen *et al.*, 1994
		0.2 (±0.1)	$[NO_3^-]_{ambient} < 1$ □M	Kristiansen *et al.*, 1994
	Toolik Lake (Artic)	0.05-0.30		Whalen and Alexander, 1986
	Greenland Sea (Artic)	2.24 (±0.60)	-	Muggli and Smith, 1993
		0.29 (±0.10)	-	Muggli and Smith, 1993
	Eastern Canadian Artic	0.87	-	Smith and Harrison, 2001
	Barrow Strait (Canada)	< 4	-	Harrison *et al.*, 1990
	Western New Zealand	1.1	-	Chang *et al.*, 1995 *in* Kudela *et al.*, 2008b
	Southern California (USA)	0.467 (±0.18)	*Lingulodinium polyedrum* bloom	Kudela and Cochlan, 2000
	Lake Kinneret (Israel)	28.9 (±7.2)	*Peridinium* bloom ; $[NH_4^+]<1$ μM	Berman *et al.*, 1984
	Chesapeake Bay, Delaware Bay, Hudson River Estuary (USA)	2	DIN	Fisher *et al.*, 1988a
Diatoms				
General	-	0.5-5.0	-	Lalli and Parsons, 1997
Asterionella formosa	Culture (Yellowstone National Park, USA)	0.007	-	Interlandi, 2002
		0.042	Cu added	Interlandi, 2002
Asterionella japonica	Culture	0.7, 1.3 (±0.3, ±0.5)	-	Eppley *et al.*, 1969
Bellerochia sp.	Culture (Great South Bay)	6.87 (±1.38)	-	Carpenter and Guillard, 1971 *in* Valiela, 1995
	Culture (Off Sutinam)	0.12 (±0.08)	-	Carpenter and Guillard, 1971 *in* Valiela, 1995
	Culture (Sargasso Sea)	0.25 (±0.18)	-	Carpenter and Guillard, 1971 *in* Valiela, 1995

Table II.1.2 (Cont.). Half-saturation constants for nitrate uptake by phytoplankton.

Species	Region or Zone	K_s (μM)	Comments	Source
Diatoms				
Bidulphia sinensis	Culture	0.74 (±0.92)	-	Qasim *et al.*, 1973
Chaetoceros sp.	Culture (Chesapeake Bay, USA)	3.1 (±0.8)	-	Lomas and Glibert, 2000
Chaetoceros gracilis	Culture	0.3, 0.1 (±0.5, ±0.2)	-	Eppley *et al.*, 1969
Chaetoceros neglectum	Culture (Drake Passage, Antartic)	1.4	-	Sommer, 1986
Corethron criophilum	Culture (Drake Passage, Antartic)	0.3	-	Sommer, 1986
Coscinodiscus lineatus	Culture (clone FCRG 12)	2.4, 2.8 (±0.5, ±0.6)	-	Eppley *et al.*, 1969
Coscinodiscus wailesii	Culture (clone Cos. R.)	2.1, 5.1 (±0.3, ±1.8)	-	Eppley *et al.*, 1969
Thalassiosira pseudonana (*Cyclotella nana*)	Culture (clone 13-1)	0.3, 0.7 (±0.4, ±0.5)	-	Eppley *et al.*, 1969
	Culture (clone 13-1; Sargasso Sea)	0.38 (±0.17)	-	Carpenter and Guillard, 1971 *in* Valiela, 1995
	Culture (clone 3H; Moriches Bay)	1.87 (±0.48)	-	Carpenter and Guillard, 1971 *in* Valiela, 1995
	Culture (clone 7-15; Edge of shelf)	1.19 (±0.44)	-	Carpenter and Guillard, 1971 *in* Valiela, 1995
Ditylum brightwellii	Culture	0.6 (±1.7)	-	Eppley *et al.*, 1969
Eucampia zodiacus	Culture (Seto Inland Sea, Japan)	0.76	At 9 ºC	Nishikawa and Hori, 2004; Nishikawa *et al.*, 2007
		2.59	At 9 ºC	Nishikawa *et al.*, 2009
		0.86	At 20 ºC	Nishikawa and Hori, 2004; Nishikawa *et al.*, 2007
		2.92	At 20 ºC	Nishikawa *et al.*, 2009
Fragilaria cotonensis	Culture (Yellowstone National Park, USA)	0.053	-	Interlandi, 2002
		0.110	Cu added	Interlandi, 2002
Fragilaria pinnata	Culture (clone 13-3)	0.62 (±0.17)	-	Carpenter and Guillard, 1971 *in* Valiela, 1995
	Culture (clone 0-12)	1.64 (±0.59)	-	Carpenter and Guillard, 1971 *in* Valiela, 1995
Gymnodinium catenatum	Culture (Hiroshima Bay, Japan)	7.60	-	Yamamoto *et al.*, 2004b
Leptocylindrus danicus	Culture (clone FCRG 11)	1.3, 1.2 (±0.5, ±0.1)	-	Eppley *et al.*, 1969
Nitzschia cylindrus	Culture (Drake Passage, Antartic)	4.2	-	Sommer, 1986
Nitzschia kerguelensis	Culture (Drake Passage, Antartic)	0.8	-	Sommer, 1986
Pseudo-nitzschia australis	Culture (AU-03184-5D)	2.82 (±0.32)	-	Cochlan *et al.*, 2008
Rhizosolenia robusta	Culture (clone FCRG 13)	3.5, 2.5 (±1.0, ±1.0)	-	Eppley *et al.*, 1969

Table II.1.2 (Cont.). Half-saturation constants for nitrate uptake by phytoplankton.

Species	Region or Zone	K_s (μM)	Comments	Source
Diatoms				
Rhizosolenia stolterfothii	Culture (clone FCRG 3)	1.7 (±0.4)	-	Eppley *et al.*, 1969
Thalassiosira pseudonana	Culture (clone 13-1)	5.0	-	Perry, 1976
Thalassiosira subtilis	Culture (Drake Passage, Antartic)	0.0.9	-	Sommer, 1986
Thalassiosira weissflogii	Culture (Fryxel et Hasle)	2.8 (±0.3)	-	Lomas and Glibert, 2000
Skeletonema costatum	Culture (clone Skel.)	0.5, 0.4 (±0.4, ±0.1)	-	Eppley *et al.*, 1969
	Culture (Cleve)	0.4 (±0.1)	-	Lomas and Glibert, 2000
Dinoflagellates				
Akashiwo sanguinea	Monterey Bay (USA)	1.00 (±0.22)	-	Kudela *et al.*, 2008a
Alexandrium catenella	Thau Lagoon, France	4.6 (±1.1)	In the field	Collos *et al.*, 2004
	Culture (Thau Lagoon, France)	0.6-28.1	-	Collos *et al.*, 2004
Alexandrium minutum	Culture (Greek coastal waters)	1.18		Ignatiades *et al.*, 2007
Alexandrium tamarense	Culture (Hiroshima Bay, Japan)	1.31	NO_3^- enriched	Leong and Taguchi, 2004
Ceratium furca	Culture (Sagami Bay, Japan)	0.49	-	Baek *et al.*, 2008
	Culture	0.44 (±2.49)	-	Qasim *et al.*, 1973
Ceratium fusus	Culture (Sagami Bay, Japan)	0.32	-	Baek *et al.*, 2008
Cochlodinium polykrikoides	Culture	2.10	-	Kim *et al.*, 2001 *in* Kudela *et al.*, 2008b
Dissodinium lunula	Culture (clone T-37)	1.7 (±2.0)	-	Bhovichitra and Swift, 1977
Gonyaulax polyedra	Culture (clone FCRG 8)	8.6, 10.3 (-, ±2.4)	-	Eppley *et al.*, 1969
Gymnodinium splendens	Culture (clone Gy.)	3.8 (±0.9)	-	Eppley *et al.*, 1969
Pavlova lutheri	Culture (Butcher)	22.7 (±7.4)	-	Lomas and Glibert, 2000
Prorocentrum minimum	Culture (Chesapeake Bay, USA)	5.0 (±0.6)	-	Lomas and Glibert, 2000
		5.18 (±1.46)	NO_3^- grown culture	Fan *et al.*, 2003
		23.3 (±11.1)	NH_4^+ grown culture	Fan *et al.*, 2003
		0.23 (±0.68)	Urea grown culture	Fan *et al.*, 2003
Pyrocystis fusiformis	Culture (clone 4)	3 (±6)	-	Bhovichitra and Swift, 1977
Pyrocystis noctiluca	Culture (clone 7)	5 (±4)	-	Bhovichitra and Swift, 1977
Chlorophytes				
Ankistrodesmus falcatus	Culture (Yellowstone National Park, USA)	0.001		Interlandi, 2002
		0.001	Cu added	Interlandi, 2002

Table II.1.2 (Cont.). Half-saturation constants for nitrate uptake by phytoplankton.

Species	Region or Zone	K_s (μM)	Comments	Source
Chlorophytes				
Dunaliella tertiolecta	Culture (clone Dun.)	1.4 (±1.1)	-	Eppley *et al.*, 1969
	Culture (Butcher)	11.1 (±3.6)	-	Lomas and Glibert, 2000
Micromonas pusilla	-	0.47	-	Cochlan and Harrison, 1991
Scenedesmus sp.	Culture	8.421±1.570	N limited culture	Rhee, 1978
		5.607±0.350	N limited culture	Rhee, 1978
		3.343±0.479	N limited culture	Rhee, 1978
		2.914±0.286	N limited culture	Rhee, 1978
Chrysophytes				
Isochrysis galbana	Culture (clone Iso.)	0.1, 0.1 (±0.2, 0.2)	-	Eppley *et al.*, 1969
Monochrysis lutheri	Culture (clone Mono.)	0.6 (±0.3)	-	Eppley *et al.*, 1969
Coccolithophorids				
Coccolithus huxleyi	Culture (clone BT-6)	0.1 (±0.3)	-	Eppley *et al.*, 1969
Coccolithus huxleyi	Culture (clone F-5)	0.1 (±1.6)	-	Eppley *et al.*, 1969
Emiliania huxleyi	Culture (strain L, NIOZ)	~0.1-0.4	-	Page *et al.*, 1999
Cyanobacteria				
Nodularia spumigena	Culture (Baltic Sea)	0.02	-	Sörensson and Sahlsten, 1987
Raphidophytes				
Chatonella antiqua	Culture (clone Ho-1)	2.81 (±0.26)	In light	Nakamura and Watanabe, 1983a,b
	Culture (clone Ho-1)	3.14 (±0.26)	In dark	Nakamura and Watanabe, 1983a,b
Chattonella subsalsa	Culture (Delaware Inland Bays, USA)	8.98 (±0.02)	-	Zhang *et al.*, 2006
Heterosigma akashiwo	East coast of USA	2	-	Tomas, 1979
	Culture (Delaware Inland Bays, USA)	0.28 (±0.04)	-	Zhang *et al.*, 2006
	Culture (CCMP1912)	1.68 (0.48)	-	Herndon and Cochlan, 2007
		1.35 (0.31)	-	Herndon and Cochlan, 2007
		1.47 (0.25)	-	Herndon and Cochlan, 2007
Others				
Blue-green coccoid alga	Culture (Yellowstone National Park, USA)	0.048	-	Interlandi, 2002
		0.019	Cu added	Interlandi, 2002

[1] Values for DIN are presented at both Table II.1.1 and Table II.1.2.

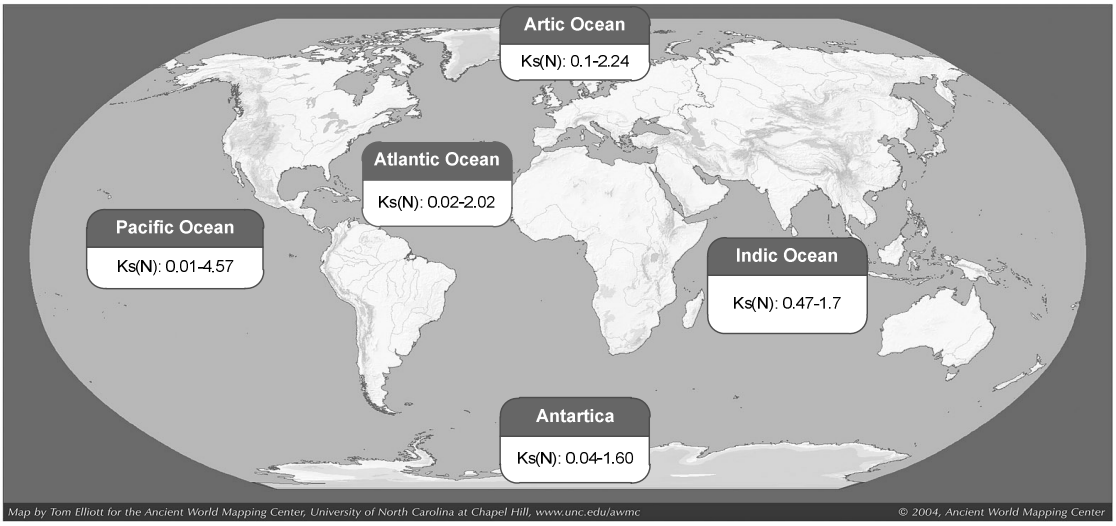

Figure II.1.1. Range of variation of half-saturation constants for nitrogen (ammonium and nitrates) uptake (μM) for natural phytoplankton communities in the ocean.

II.1.3 PHOSPHORUS

K_s for phosphorus uptake ranges from 0.02 μM (general phytoplankton community; Lalli and Parsons, 1997) to 7.0 μM (*Thalassiosira pseudonana*; Perry, 1976) – Table II.1.3. Diatoms and dinoflagellates, in particular, present K_s values for phosphorus uptake that fall inside this range of variation. Collos *et al.* (2008) presents a compilation of K_s for soluble reactive phosphorus, where they suggest that cyanobacteria appear to be well adapted to low concentrations of phosphorus in the environment (see Table II.1.4). The values presented in Table II.1.3 also suggest lower values of K_s for phosphorus uptake by cyanobacteria, in particular *Synechococcus sp.* (Timmermans *et al.*, 2005).

Table II.1.3. Half-saturation constants for phosphorus uptake by phytoplankton.

Species	Region or Zone	K_s (μM)	Comments	Source
General				
	Oligotrophic to eutrophic waters	0.02-0.5	-	Lalli and Parsons, 1997
	Eastern Mediterranean	0.170	K_s+S, Size fraction of particulate P>5 μm	Kress *et al.*, 2005
		0.045	K_s+S, Size fraction of particulate P: 5-1 μm	Kress *et al.*, 2005
		0.027	K_s+S, Size fraction of particulate P: 1-0.2 μm	Kress *et al.*, 2005

Table II.1.3 (Cont.). Half-saturation constants for phosphorus uptake by phytoplankton.

Species	Region or Zone	K_s (μM)	Comments	Source
General				
	Ebrié Lagoon (West Africa)	2.99	-	Lemasson *et al.*, 1980
		2.59	-	Lemasson *et al.*, 1980
		2.61	-	Lemasson *et al.*, 1980
		0.12	-	Lemasson *et al.*, 1980
		0.37	-	Lemasson *et al.*, 1980
		4.17	-	Lemasson *et al.*, 1980
		2.37	-	Lemasson *et al.*, 1980
		0.25	-	Lemasson *et al.*, 1980
		0.20	-	Lemasson *et al.*, 1980
		0.25	-	Lemasson *et al.*, 1980
		0.46	-	Lemasson *et al.*, 1980
		3.32	-	Lemasson *et al.*, 1980
		1.44	-	Lemasson *et al.*, 1980
		3.15	-	Lemasson *et al.*, 1980
		0.12	-	Lemasson *et al.*, 1980
		0.62	-	Lemasson *et al.*, 1980
	Eagle Moutain Lake Texas (USA)	0.33 (±0.1)	-	Sterner and Grover, 1998
	Chesapeake Bay, Delaware Bay, Hudson River Estuary (USA)	0.5		Fisher *et al.*, 1988a
Diatoms				
Asterionella formosa	Culture (FraAf)	2.8	-	Tilman and Kilham, 1976
	Culture	0.70 (±0.55)	-	Holm and Armstrog, 1981
Biddulphia sinensis	Culture	0.17 (±3.22)	-	Qasim *et al.*, 1973
Cyclotella meneghiniana	Culture (CyOc2)	0.8	-	Tilman and Kilham, 1976
Eucampia zodiacus	Culture (Seto Inland Sea, Japan)	0.29	At 9 ºC	Nishikawa and Hori, 2004; Nishikawa *et al.*, 2007
		1.83	At 9 ºC	Nishikawa *et al.*, 2009
		0.31	At 20 ºC	Nishikawa and Hori, 2004; Nishikawa *et al.*, 2007
		4.85	At 20 ºC	Nishikawa *et al.*, 2009
Phaeodactylum tricornutum	-	0.34	-	Harvey, 1963 *in* Dugdale, 1969
Skeletonema costatum	-	0.68	-	Tarutani and Yamamoto, 1994 *in* Yamamoto and Tarutani, 1999

Table II.1.3 (Cont.). Half-saturation constants for phosphorus uptake by phytoplankton.

Species	Region or Zone	K_s (μM)	Comments	Source
Diatoms				
Thalassiosira pseudonana	Culture (clone 3H)	7.0	-	Perry, 1976
	Culture (clone 3H)	5.8	-	Perry, 1976
	Culture (clone 13-1)	7.0	-	Perry, 1976
	Culture (clone 66-A)	6.0	-	Perry, 1976
		7.0	-	Perry, 1976
Thalassiosira weissflogii	-	1.72	-	Fushs, 1972 *in* Baek *et al.*, 2008
Dinoflagellates				
Alexandrium andersoni	Culture (EF12)	0.74	-	Frangópulos *et al.*, 2004
Alexandrium minutum	Culture (AL1V)	1.16	-	Frangópulos *et al.*, 2004
	Culture (MDQ1096)	1.68	-	Frangópulos *et al.*, 2004
	Culture (EF04)	1.0	-	Frangópulos *et al.*, 2004
	Culture (Greek coastal waters)	0.12		Ignatiades *et al.*, 2007
Alexandrium tamarense	-	0.4	-	Cembella *et al.*, 1984 *in* Baek *et al.*, 2008
	Culture (clone ATHS92)	2.6	-	Yamamoto and Tarutani, 1999
Ceratium furca	Sagami Bay (Japan)	0.05	-	Baek *et al.*, 2008
	Culture	0.15 (±0.93)	-	Qasim *et al.*, 1973
Ceratium fusus	Sagami Bay (Japan)	0.03	-	Baek *et al.*, 2008
Gymnodinium catenatum	Culture (Hiroshima Bay, Japan)	3.40	-	Yamamoto *et al.*, 2004b
Peridinium sp.	North Brunswick (USA)	6.3	-	Lehman, 1976
Prorocentrum minimum		1.96	-	Cembella *et al.*, 1984 *in* Baek *et al.*, 2008
Chlorophytes				
Chlamydomonas reinhardtii	Culture	0.59	-	Kennedy and Sangren *in* Reynolds, 2006
Chlorella pyrenoidosa	Culture	0.68	-	Nyholm, 1977 *in* Reynolds, 2006
Eudorina elegans	Culture	0.53	-	Kennedy and Sangren *in* Reynolds, 2006
Prasinomonas capsulatus	Culture (CCMP 1617)	0.094 (0.0374-0.231)	PO_4^{3-} limited	Timmermans *et al.*, 2005
Scenedesmus sp.	Culture	0.6	-	Rhee, 1973
Scenedesmus quadricauda	Culture	1.2-4.0	-	Nalewajko and Lean, 1978 *in* Reynolds, 2006
Volvox aureus	Culture	1.62	-	Kennedy and Sangren *in* Reynolds, 2006
Chrysophytes				
Dynobryon cylindricum	Culture (North Brunswick, USA)	0.72	-	Lehman, 1976

Table II.1.3 (Cont.). Half-saturation constants for phosphorus uptake by phytoplankton.

Species	Region or Zone	K_s (μM)	Comments	Source
Chrysophytes				
Dynobryon divergens	Culture (Mirror Lake, USA)	0.27	-	Lehman, 1976
Dynobryon sociale var. *americanum*	Culture (North Brunswick, USA)	0.39	-	Lehman, 1976
Cyanobacteria				
Anabaena flos-aquae	Culture	1.8-2.5	-	Nalewajko and Lean, 1978 *in* Reynolds, 2006
Microcystis aeruginosa	Culture	1.23 (±0.56)	-	Holm and Armstrong, 1981
Planktothrix agardhii	Culture	0.2-0.3	-	van Liere, 1979, Ahlgren, 1977, 1978 *in* Reynolds, 2006
Synechococcus sp.	Culture (CCMP 839)	0.014 (0.0003-0.79)	PO_4^{3-} limited	Timmermans *et al.*, 2005
Raphidophytes				
Chatonella antiqua	Culture (clone Ho-1)	1.76 (±0.22)	In light	Nakamura and Watanabe, 1983a,b
	Culture (clone Ho-1)	2.04 (±0.33)	In dark	Nakamura and Watanabe, 1983a,b
Chattonella subsalsa	Culture (Delaware Inland Bays, USA)	0.84 (±0.08)	-	Zhang *et al.*, 2006
Heterosigma akashiwo	East coast of USA	1.0-1.98	-	Tomas, 1979
	Culture (Delaware Inland Bays, USA)	0.19 (±0.001)	-	Zhang *et al.*, 2006

Table II.1.4. Half-saturation constants for soluble reactive phosphorus uptake by unicellular algae (compilation from Collos *et al.*, 2009)

Class	Conditions	K_s (μM)
Chlorophyceace	All	2.5
	P deficient	2.6
Cyanophyceace	All	0.7
	P deficient	0.7
Diatomophycea	All	1.3
	P deficient	1.3
Dinophyceae	All	1.8
	P deficient	2.4
Euglenophyceae	All	4.6
Prymnesiophyceae	All	1.3
Raphidophyceae	All	1.7

II.1.4 SILICA

For natural phytoplankton assemblages of the Pacific Ocean, Nelson *et al.* (2001) present values for silica uptake that range from <1 to >50 μM (Table II.1.5). Most common maximum values observed in Table II.1.5 are of about 5-7 μM. For diatoms, Sarthou *et al.* (2005) present values that range from 0.2-22 μM (average value of 3.9 μM). A larger value of K_s for silica uptake, 88.7 μM, was found by Sommer (1986) for a culture of *Nitzschia kerguelensis* (Drake Passage, Antartic). One of the lower values observed was of 0.022 μM (*Thalassiosira nordenskiöldii*; Paasche *et al.*, 1975). Martin-Jézéquel *et al.* (2000) also review the silica metabolism in diatoms presenting values for K_s that range from 0.2 μM (*Thalassiosira gravida*) to 62 μM (*Nitzschia alba*).

Table II.1.5. Half-saturation constants for silica uptake by phytoplankton.

Species	Region or Zone	K (μM)	Comments	Source
General				
Natural phytoplankton assemblages	Monterey Bay (USA)	4.20	-	White and Dugdale, 1997
	Gulf of California (USA)	2.53	-	Azam and Chisholm, 1976
		1.59	-	
	Gulf of Lion (NW Mediterranean Sea)	3.46	July 2000	Leblanc *et al.*, 2003
		4.97	September 2000	Leblanc *et al.*, 2003
	Pacific Ocean (southern sector)	~4	Without substrate limitation	Franck *et al.*, 2000
		~12-18	With substrate limitation	
		<1 - >50	-	Nelson *et al.*, 2001
	Ross Sea (Antarctic)	1.11 (±0.90)	Diatom bloom	Nelson and Tréguer, 1992
		2.37 (±0.61)	Diatom bloom	Nelson and Tréguer, 1992
		4.58 (±1.42)	Diatom bloom	Nelson and Tréguer, 1992
	Oslofjord (Norway)	1.7-11.5	*Thalassiosira nordenskioeldii* dominated	Kristiansen *et al.*, 2000
	Chesapeake Bay, Delaware Bay, Hudson River Estuary (USA)	5		Fisher *et al.*, 1988a
Diatoms				
General	Culture (Antartic Ocean, Indian Sector)	12-22	-	Jacques, 1983

Table II.1.5 (Cont.). Half-saturation constants for silica uptake by phytoplankton.

Species	Region or Zone	K (μM)	Comments	Source
Diatoms				
General	Peruvian coast	1.8		Goering *et al.*, 1973
		2.93	-	Goering *et al.*, 1973
Diatom dominated	Bay of Brest (France)	1.6 (±0.2)	Si added = 0.1 $\mu M.d^{-1}$	Fouillaron *et al.*, 2007
		3.3 (±0.3)	Si added = 1 $\mu M.d^{-1}$	Fouillaron *et al.*, 2007
		5.6 (±0.9)	Si added = 2 $\mu M.d^{-1}$	Fouillaron *et al.*, 2007
		1.3-2.1	-	Ragueneau *et al.*, 2002
Asterionella formosa	Culture (clone FraAf)	7.7	-	Tilman and Kilham, 1976
	Culture (clone AfOH2)	1.93	K_s+S	Kilham, 1975
	Culture (clone L262)	1.09	K_s+S	Kilham, 1975
Chaetoceros debilis	Culture	2.2	-	Conway and Harrison, 1977
Chaetoceros neglectum	Culture (Drake Passage, Antartic)	21.7	-	Sommer, 1986
Corethron criophilum	Culture (Drake Passage, Antartic)	60.1	-	Sommer, 1986
Cyclotella meneghiniana	Culture (clone CyOc2)	7.5	-	Tilman and Kilham, 1976
Ditylum brighwellii	-	2.59 (±1.66)	-	Paasche, 1973b
	-	4.50 (±1.21)	-	Paasche, 1973b
	-	2.35 (±0.40)	-	Paasche, 1973b
	-	3.23 (±0.79)	-	Paasche, 1973b
	-	1.85 (±0.76)	-	Paasche, 1973b
	-	3.24 (±0.68)	-	Paasche, 1973b
Eucampia zodiacus	Culture (Seto Inland Sea, Japan)	0.91	At 9 ºC	Nishikawa and Hori, 2004; Nishikawa *et al.*, 2007
		0.88	At 20 ºC	Nishikawa and Hori, 2004; Nishikawa *et al.*, 2007
Licmorpha sp.	Culture	3.52 (±1.06)	-	Paasche, 1973b
	Culture	2.06 (±0.54)	-	Paasche, 1973b
	Culture	1.53 (±0.56)	-	Paasche, 1973b
	Culture	3.19 (±0.74)	-	Paasche, 1973b
Nitzschia cylindrus	Culture (Drake Passage, Antartic)	8.4	-	Sommer, 1986
Nitzschia kerguelensis	Culture (Drake Passage, Antartic)	88.7	-	Sommer, 1986
Skeletonema costatum	Culture	0.80 (±0.26)	-	Paasche, 1973b
	Culture	1.11 (±0.44)	-	Paasche, 1973b

Table II.1.5 (Cont.). Half-saturation constants for silica uptake by phytoplankton.

Species	Region or Zone	K (μM)	Comments	Source
Diatoms				
Skeletonema costatum	Culture	0.42 (±0.28)	-	Paasche, 1973b
	Culture	0.94 (±0.20)	-	Paasche, 1973b
	Culture	0.71 (±0.26)	-	Paasche, 1973b
	Culture	0.7	-	Conway et al., 1976
	Culture	1.3	-	(Conway *et al.*, 1976; Conway and Harrison, 1977)
Thalassiosira decipiens	Culture	2.97 (±1.24)	-	Paasche, 1973b
	Culture	3.02 (±1.13)	-	Paasche, 1973b
	Culture	5.65 (±1.56)	-	Paasche, 1973b
	Culture	3.69 (±1.30)	-	Paasche, 1973b
	Culture	2.52 (±1.03)	-	Paasche, 1973b
	Culture	2.38 (±1.19)	-	Paasche, 1973b
Thalassiosira gravida	Culture	0.3	-	Conway and Harrison, 1977
Thalassiosira nordenskiöldii	Culture	0.088	-	Paasche *et al.*, 1975
		0.022	-	Paasche *et al.*, 1975
Thalassiosira pseudonana	Culture (clone 3H)	0.83 (±0.26)	-	Paasche, 1973a
	Culture (clone 3H)	1.36 (±0.24)	-	Paasche, 1973a
	Culture (clone 3H)	0.48 (±0.72)	$[Si]_0$=0.70 μM	Paasche, 1973a
	Culture (clone 3H)	1.24 (±0.22)	$[Si]_0$=0.70 μM	Paasche, 1973a
	Culture (clone 3H)	0.98	-	Guillard *et al.*, 1973
	Culture	1.00 (±0.41)	-	Paasche, 1973b
	Culture	1.80 (±0.39)	-	Paasche, 1973b
	Culture	1.07 (±0.31)	-	Paasche, 1973b
	Culture	1.40 (±0.55)	-	Paasche, 1973b
	Culture	0.91 (±0.07)	-	Paasche, 1973b
	Culture	2.13 (±0.42)	-	Paasche, 1973b
	Culture (clone 13-1)	0.19	-	Guillard *et al.*, 1973
Thalassiosira subtilis	Culture (Drake Passage, Antartic)	5.7	-	Sommer, 1986
Thalassiothrix antarctica	Culture	4.2	-	Sommer, 1991

II.1.5 SENSITIVITY ANALYSIS OF AN ECOLOGICAL MODEL TO THE SPECIFICATION OF THE HALF-SATURATION CONSTANTS

The sensitivity analysis performed here aimed to exemplify one of the applications of the review presented in the previous sections. The sensitivity of ECO-SELFE applied in the Aveiro lagoon

to the half-saturation constants for nutrients uptake definition was evaluated, in particular with respect to phytoplankton concentration. This sensitivity analysis also intended to complement the analysis presented by Rodrigues *et al.* (2009a; Chapter III, Section III.2).

ECO-SELFE (available at www.stccmop.org/CORIE/modeling/selfe/) is a fully coupled three-dimensional hydrodynamic and ecological model. The model couples the hydrodynamic model SELFE (Zhang and Baptista, 2008) and an ecological model extended from Bisset *et al.* (2004). SELFE is an unstructured grid model, which solves the three-dimensional shallow-waters equations for the free-surface elevation, water velocity, salinity and water temperature. The ecological model includes the cycles of carbon, nitrogen, phosphorus, silica and iron. The model can simulate several zooplankton and phytoplankton groups, bacterioplankton, dissolved and particulate organic matter, inorganic nutrients and dissolved inorganic carbon. Regarding the nutrients uptake by phytoplankton, ECO-SELFE considers a Michaelis-Menten function for all nutrients (Bisset *et al.*, 2004). Further description of the model can be found in Zhang and Baptista (2008), Bisset *et al.* (2004) and Rodrigues *et al.* (2009b).

The model was applied to the Ria de Aveiro, based on a previously validated application (Rodrigues *et al.*, 2009b). Ria de Aveiro is a shallow temperate coastal lagoon located on the Northwest (NW) coast of Portugal, about 45 km long and 10 km wide (Figure II.1.2). The lagoon is connected to the ocean by an artificial inlet and spreads over four main branches: the Mira, Ílhavo, Espinheiro and S. Jacinto channels. The circulation in the lagoon is mainly driven by tide, with semi-diurnal tides at the mouth, and the major sources of freshwater are the rivers Vouga and Antuã (Dias *et al.,* 2000). Smaller sources of freshwater also flow into the lagoon.
The methodology adopted here derives from the one described by Rodrigues *et al.*, 2009a (Chapter III, Section III.2). A similar model setup was used. The simulations were performed for a period of 30 days, using a time-step of 90 s. The domain was discretized with a horizontal grid of about 21000 nodes and a vertical grid with 7 *S* levels. Six open boundaries (one oceanic and five riverine) were considered. At the ocean boundary the model was forced by tidal elevations, while at the riverine boundaries constant river flows were forced. Salinity and temperature were set constant at all boundaries. The range of variation considered for the half-saturation constants for nutrients uptake is presented in Table II.1.6. For each simulation one value was varied, while all the others remain constant. The analysis was performed for the average values of phytoplankton concentration in each branch of the lagoon and a group of virtual stations (SA stations) located along the lagoon was also used to analyse the results (Figure II.1.2), as described by Rodrigues *et al.* (2009a; Chapter III, Section III.2).

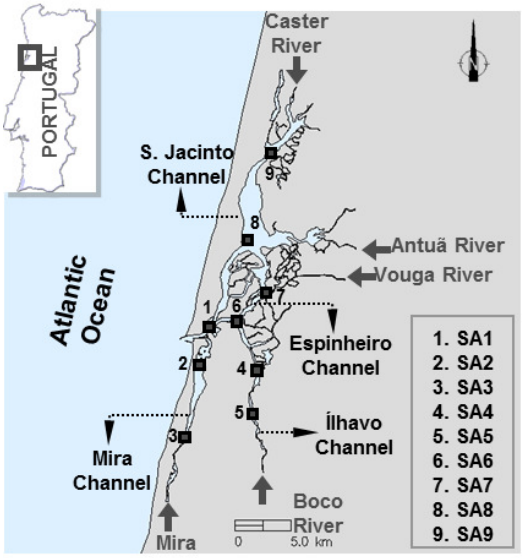

Figure II.1.2. General overview of the Ria de Aveiro and location of the stations used in the sensitivity analysis (SA stations) – from Rodrigues *et al.* (2009a).

Table II.1.6. Half-saturation constants for nutrients uptake considered in the sensitivity analysis (based on the range of variation reviewed for diatoms).

	Simulation		
	A	B[1]	C
K_s NH_4^+ (μM)	0.207	0.414	10.0
K_s NO_3^- (μM)	0.412	0.824	10.0
K_s PO_4^{3-} (μM)	0.0257	0.0515	0.5
K_s SiO_2 (μM)	0.912	1.824	5.0

[1]Simulation B corresponds to the base values used in the sensitivity analysis presented by Rodrigues *et al.* (2009a).

Figures II.1.3 to II.1.6 present the average variation of phytoplankton concentration in each one of the branches of the Aveiro lagoon. Results show that, on branch scale, there is no considerable influence of the half-saturation constants for nutrients uptake in the phytoplankton concentration for the range of variation tested. These results are similar to the ones observed at most of the SA stations. In some stations, namely stations SA3 and SA9, some small differences on phytoplankton concentrations, on the order of 5-10%, occur when the half-saturation constants for ammonium and phosphate are changed within the range of variation considered. At station SA9, in particular (Figure II.1.7), results show that the larger values of ammonium and phosphate half-saturation constants for uptake (10 μM and 0.5 μM, respectively) lead to smaller concentrations of phytoplankton when compared with simulations A and B. However the differences observed are relatively small, of about 0.1-0.2 mg C l^{-1}. At this station, the variation of the half-saturation constants for ammonium and phosphate uptake is

more influent on the concentrations of ammonium and phosphate (Figure II.1.8). These results complement the analysis performed by Rodrigues *et al.* (2009a; Chapter III, Section III.2) and suggest that, although there is some influence of the half-saturation constants for nutrients uptake in the application of ECO-SELFE in the Ria de Aveiro, it is relatively small even within a larger range of variation, in particular regarding phytoplankton concentrations.

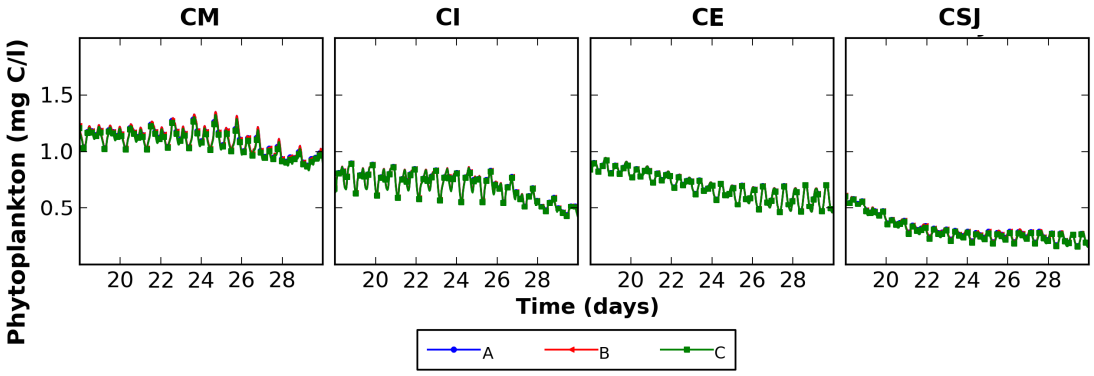

Figure II.1.3. Influence of half-saturation constant for ammonium uptake (A – K_s NH_4^+ = 0.207 μM; B – K_s NH_4^+ = 0.414 μM; C – K_s NH_4^+ = 10 μM) on phytoplankton concentration along the branches of the Ria de Aveiro (CM – Mira channel; CI – Ílhavo channel; CE – Espinheiro channel; CSJ – S. Jacinto channel;.

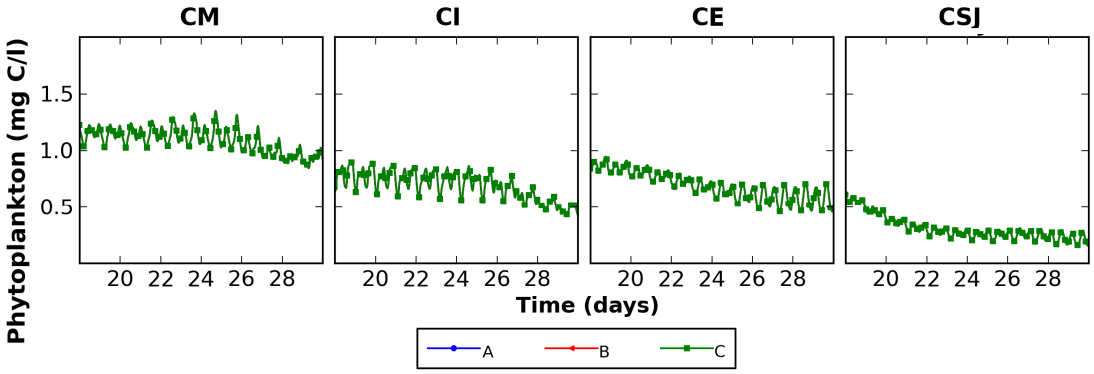

Figure II.1.4. Influence of half-saturation constant for nitrate uptake (A – K_s NO_3^- = 0.412 μM; B – K_s NO_3^- = 0.824 μM; C – K_s NO_3^- = 10 μM) on phytoplankton concentration along the branches of the Ria de Aveiro (CM – Mira channel; CI – Ílhavo channel; CE – Espinheiro channel; CSJ – S. Jacinto channel).

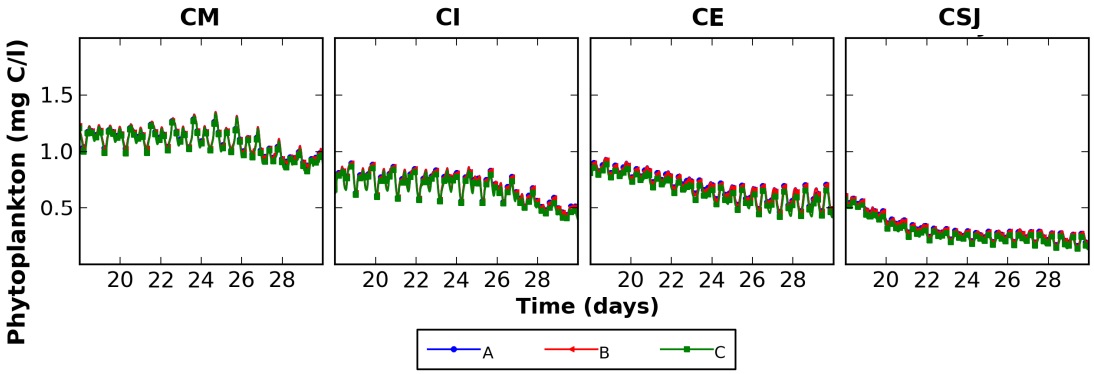

Figure II.1.5. Influence of half-saturation constant for phosphate uptake (A – $K_s\ PO_4^{3-}$ = 0.0257 μM; B – $K_s\ PO_4^{3-}$ = 0.0515 μM; C – $K_s\ PO_4^{3-}$ = 0.5 μM) on phytoplankton concentration along the branches of the Ria de Aveiro (CM – Mira channel; CI – Ílhavo channel; CE – Espinheiro channel; CSJ – S. Jacinto channel).

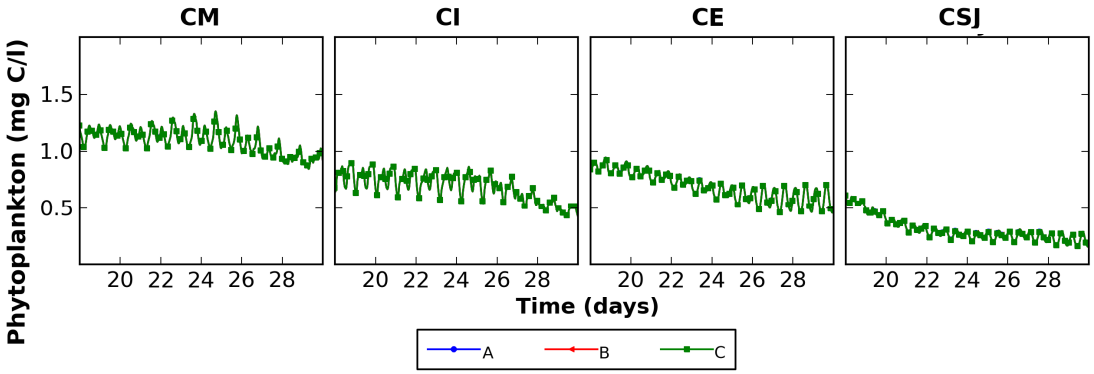

Figure II.1.6. Influence of half-saturation constant for silicate uptake (A – $K_s\ SiO_2$ = 0.912 μM; B – $K_s\ SiO_2$ = 1.824 μM; C – $K_s\ SiO_2$ = 5 μM) on phytoplankton concentration along the branches of the Ria de Aveiro (CM – Mira channel; CI – Ílhavo channel; CE – Espinheiro channel; CSJ – S. Jacinto channel).

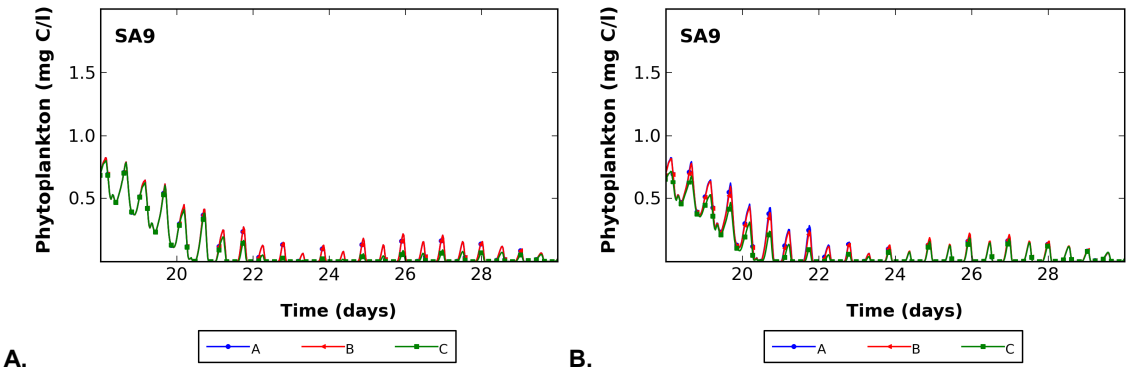

Figure II.1.7. Phytoplankton concentration in station SA9: A) half-saturation constant for ammonium uptake variation (A – $K_s\ NH_4^+$ = 0.207 μM; B – $K_s\ NH_4^+$ = 0.414 μM; C – $K_s\ NH_4^+$ = 10 μM) and B) half-saturation constant for phosphate uptake variation (A – $K_s\ PO_4^{3-}$ = 0.0257 μM; B – $K_s\ PO_4^{3-}$ = 0.0515 μM; C – $K_s\ PO_4^{3-}$ = 0.5 μM).

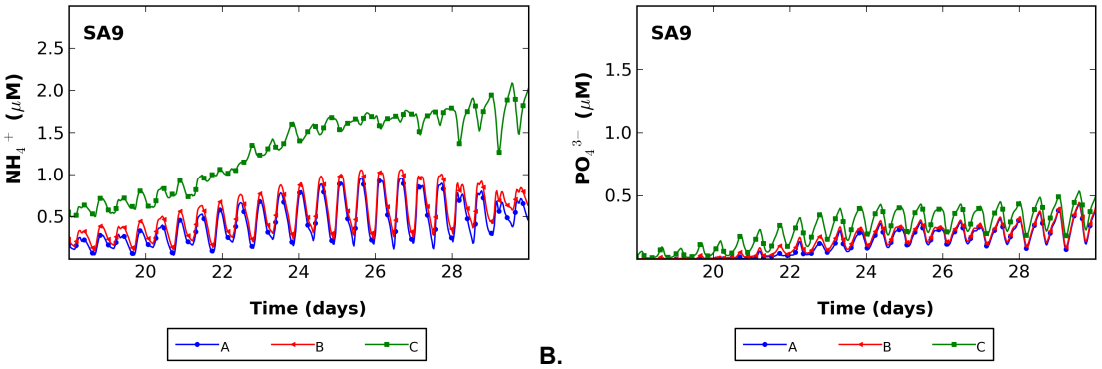

A. **B.**

Figure II.1.8. A) Half-saturation constant for ammonium uptake (A – K_s NH_4^+ = 0.207 μM; B – K_s NH_4^+ = 0.414 μM; C – K_s NH_4^+ = 10 μM) influence in ammonium concentration at station SA9 and B) Half-saturation constant for phosphate uptake (A – K_s PO_4^{3-} = 0.0257 μM; B – K_s PO_4^{3-} = 0.0515 μM; C – K_s PO_4^{3-} = 0.5 μM) influence in phosphate concentration at station SA9.

II.1.6 SUMMARY

A review on K_s for nutrients uptake by phytoplankton was presented contributing as a support tool for studies on phytoplankton and ecosystems dynamics. In ecological modelling, in particular, defining the range of variation of the input parameters and their relative influence on the model results is of major relevance, as this is one of the main sources of uncertainty in these applications.

For nitrogen uptake by phytoplankton, K_s values found in the literature ranged from about 0.01 μM (oligotrophic waters) to a maximum value of 33.6 μM (*Gymnodinium catenatum*). For diatoms, maximum values found of K_s for nitrogen uptake were of about 10 μM. Overall, K_s for nitrogen uptake tends to be smaller in zones where nutrients concentrations are lower, which may indicate a better adaptation of the phytoplankton populations of these regions.

Regarding phosphorus uptake by phytoplankton, K_s ranged from 0.02 μM (general phytoplankton community) to 7.0 μM (*Thalassiosira pseudonana*). Some of the lower values of K_s reported are associated with cyanobacteria, in particular *Synechococcus sp.*

For silica uptake, K_s values found in the literature ranged from 0.2 to 88.7 μM, although few observations reported values larger than 8 μM. Some of the lower values of K_s were observed for *Thalassiosira sp.*, while some of the larger values were found for *Nitzschia sp.*

The usefulness of the review performed was illustrated through a sensitivity analysis to ECO-SELFE, a coupled hydrodynamic and ecological model, applied to the Aveiro lagoon. Results evidenced the small influence of these input parameters on the modelled phytoplankton

concentrations, even within a wider range of variation than that presented in Rodrigues *et al.* (2009a) – Chapter III, Section III.2.

II.1.7 REFERENCES

Azam F, Chisholm SW. Silicic acid uptake and incorporation by natural marine phytoplankton populations. *Limnology and Oceanography* **1976**, 21(3), 427-435.

Baek SH, Shimode S, Han M, Kikuchi T. Growth of dinoflagellates, *Ceratium furca* and *Ceratium fusus* in Sagami Bay, Japan: The role of nutrients. *Harmful Algae* **2008**, 7, 729-739.

Benitez-Nelson CR. The biogeochemical cycling of phosphorus in marine systems. *Earth-Science Reviews* **2000**, 51, 109-135.

Berman T, Sherr BF, Sherr E, Wynne D, McCarthy, JJ. The characteristics of ammonium and nitrate uptake by phytoplankton in Lake Kinneret. *Limnology and Oceanography* **1984**, 29(2), 287-297.

Bhovichitra M, Swift E. Light and dark uptake of nitrate and ammonium by large oceanic dinoflagellates: *Pyrocystis noctiluca*, *Pyrocystis fusiformis*, and *Dissodinium lunula*. *Limnology and Oceanography* **1977**, 22(1), 73-83.

Bisset WP, Debra S, Dye D. Ecological Simulation (EcoSim) 2.0 Technical Description, Tampa, Florida: Florida Environmental Research Institute, **2004**, 25pp.

Cariboni J, Gatelli D, Liska R, Saltelli A. The role of sensitivity analysis in ecological modelling. *Ecological Modelling* **2007**, 203, 167-182.

Chu PC, Ivanov LM, Margolina TM. On non-linear sensitivity of marine biological models to parameter variations. *Ecological Modelling* **2007**, 206(3–4), 369-382.

Cloern JE. The relative importance of light and nutrient limitation of phytoplankton growth: a simple index of coastal ecosystem sensitivity to nutrient enrichment. *Aquatic Ecology* **1999**, 33, 3-16.

Cochlan WP, Bronk DA. Nitrogen uptake kinetics in the Ross Sea, Antarctica. *Deep-Sea Research II* **2001**, 48, 4127-4153.

Cochlan WP, Harrison PJ. Kinetics of nitrogen (nitrate, ammonium and urea) uptake by the picoflagellate *Micromonas pusilla* (Prasinophyceae). *Journal of Experimental Marine Biology and Ecology* **1991**, 153(2), 129-141.

Cochlan WP, Herndon J, Kudela, RM. Inorganic and organic nitrogen uptake by the toxigenic diatom *Pseudo-nitzschia australis* (Bacillariophyceae), *Harmful Algae* **2008**, 8(1), 111-118.

Collos Y, Bec B, Jauzein C, Abadie E, Laugier T, Lautier J, Pastoureaud A, Souchu P, Vaquer A. Oligotrophication and emergence of picocyanobacteria and a toxic dinoflagellate in Thau lagoon, southern France. *Journal of Sea Research* **2009**, 61(1-2), 68-75.

Collos Y, Gagne C, Laabir M, Vaquer A, Cecchi P, Souchu P. Nitrogenous nutrition of *Alexandrium catenella* (Dinophyceae) in cultures and in Thau lagoon, southern France. *Journal of Phycology* **2004**, 40, 96-103.

Collos Y, Vaquer A, Laabir M, Abadie E, Laugier T, Pastoureaud A, Souchu P. Contribution of several nitrogen sources to growth of *Alexandrium catenella* during blooms in Thau lagoon, southern France. *Harmful Algae* **2007**, 6(6), 781-789.

Conway HL, Harrison PJ, Davis CO. Marine diatoms grown in chemostats under silicate or ammonium limitation. II. Transient response of *Skeletonema costatum* to a single addition of the limiting nutrient. *Marine Biology* **1976**, 35(2), 187–199.

Conway HL, Harrison PJ. Marine diatoms grown in chemostats under silicate or ammonium limitation. IV. Transient response of *Chaetoceros debilis*, *Skeletonema costatum* and *Thalassiosira gravida* to a single addition of the limiting nutrient. *Marine Biology* **1977**, 43(1), 33–43.

Dias JM, Lopes JF, Dekeyser I. Tidal propagation in Ria de Aveiro Lagoon, Portugal. *Physics and Chemistry of the Earth, Part B: Hydrology, Oceans and Atmosphere* **2000**, 25(4), 369-374.

Dickson ML, Wheeler PA. Nitrate uptake rates in a coastal upwelling regime: A comparison of PN-specific, absolute, and Chl *a*-specific rates, *Limnology and Oceanography* **1995**, 40(3), 533-543.

Dortch Q. The interaction between ammonium and nitrate uptake in phytoplankton. *Marine Ecology Progress Series* **1990**, 61, 183-201.

Dugdale RC. Nutrient limitation in the sea: dynamics, identification, and significance. *Limnology and Oceanography* **1967**, 12(4), 685-695.

Eppley RW, Renger EH, Venricl EL, Mullin MM. A study of plankton dynamics and nutrient cycling in the central gyre of the North Pacific Ocean *Limnology and Oceanography* **1973**, 18(4), 534-551.

Eppley RW, Rogers JN, McCarthy JJ. Half-saturation constants for uptake of nitrate and ammonium by marine phytoplankton. *Limnology and Oceanography* **1969**, 14, 912-920.

Fan C, Glibert PM, Burkholder JM. Characterization of the affinity for nitrogen, uptake kinetics, and environmental relationships for *Prorocentrum minimum* in natural blooms and laboratory cultures. *Harmful Algae* **2003**, 2(4), 283-299.

Fisher TR, Harding Jr. LW, Stanley DW, Ward LG. Phytoplankton, nutrients, and turbidity in the Chesapeake, Delaware, and Hudson estuaries. *Estuarine, Coastal and Shelf Science* **1988a**, 27(1), 61–93.

Fisher TR, Morrisey KM, Carlson PR, Alves LF, Melack JM. Nitrate and ammonium uptake by plankton in an Amazon River floodplain lake. *Journal of Plankton Research* **1988b**, 10(1), 7-29.

Fouillaron P, Claquin P, L'Helguen S, Huonnic P, Martin-Jézéquel V, Masson A, Longphuirt SN, Pondaven P, Thouzeau G, Leynaert A. Response of a phytoplankton community to increased nutrient inputs: a mesocosm experiment in the Bay of Brest (France). *Journal of Experimental Marine Biology and Ecology* **2007**, 351(1-2), 188-198.

Franck VM, Brzezinski MA, Coale KH, Nelson DM. Iron and silicic acid concentrations regulate Si uptake north and south of the Polar Frontal Zone in the Pacific Sector of the Southern Ocean. *Deep-Sea Research II* **2000**, 47(15-16), 3315-3338.

Frangópulos M, Guisande C, deBlas E, Maneiro I. Toxin production and competitive abilities under phosphorus limitation of *Alexandrium* species. *Harmful Algae* **2004**, 3(2), 131–139.

Frost B W, Franzen NC. Grazing and iron limitation in the control of phytoplankton stock and nutrient concentration; a chemostat analog of the Pacific equatorial upwelling zone. *Marine Ecology Progress Series* **1992**, 83, 291-303.

Gameiro C, Cartaxana P, Brotas V. Environmental drivers of phytoplankton distribution and composition in Tagus Estuary, Portugal. *Estuarine, Coastal and Shelf Science* **2007**, 75(1-2), 21-34.

Garside C. The vertical distribution of nitrate in open ocean surface water. *Deep-Sea Research Part A. Oceanographic Research Papers* **1985**, 32(6), 723-732.

Goering JJ, Nelson DM, Carter JA. Silicic acid uptake by natural populations of marine phytoplankton. *Deep-Sea Research and Oceanographic Abstracts* **1973**, 20(9), 777–789.

Guillard RRL, Kilharn P, Jackson TA. Kinetics of silicon-limited growth in the marine diatom *Thalassiosira pseudonana* Hasle and Heimdal (=*Cyclotella nana* Hustedt). *Journal of Phycology* **1973**, 9(3), 23-237.

Harrison WG, Cota GF, Smith REH. Nitrogen utilization in ice algal communities of Barrow Strait, Northwest Territories, Canada. *Marine Ecology Progress Series* **1990**, 67, 275-283.

Harrison WG, Harris LR, Irwin BD. The kinetics of nitrogen utilization in the oceanic mixed layer: nitrate and ammonium interactions at nanomolar concentrations. *Limnology and Oceanography* **1996**, 41(1), 16-32.

Herndon J, Cochlan W. Nitrogen utilization by the raphidophyte *Heterosigma akashiwo*: growth and uptake kinetics in laboratory cultures. *Harmful Algae* **2007**, 6(2), 260-270.

Holm NP, Armstrong D. Role of nutrient limitation and competition in controlling the populations of *Asterionella formosa* and *Microcystis aeruginosa* in semicontinuous culture. *Limnology and Oceanography* **1981**, 26(4), 622-634.

Ignatiades L, Gotsis-Skretas O, Metaxatos A. Field and culture studies on the ecophysiology of the toxic dinoflagellate *Alexandrium minutum* (Halim) present in Greek coastal waters. *Harmful Algae* **2007**, 6(2), 153–165.

Interlandi SJ. Nutrient-toxicant interactions in natural and constructed phytoplankton communities: results of experiments in semi-continuous and batch culture. *Aquatic Toxicology* **2002**, 61(1-2), 35-51.

Jacques G. Some ecophysiological aspects of the antartic phytoplankton. *Polar Biology* **1983**, 2, 27-33.

Kanda J, Saino T, Hattori A. Nitrogen uptake by natural populations of phytoplankton and primary production in the Pacific Ocean: Regional variability of uptake capacity. *Limnology and Oceanography* **1985**, 30(5), 987-999.

Kilham SS. Kinetics of silicon-limited growth in the freshwater diatom *Asterionella formosa*. *Journal of Phycology* **1975**, 11(4), 396-399.

Kishi MJ, Kashiwai M, Ware DM, Megrey BA, Eslinger DL, Werner FE, Noguchi-Aita M, Azumaya T, Fujii M, Hashimoto S, Huang D, Iizumi H, Ishida Y, Kang S, Kantakov GA, Kim H, Komatsu K, Navrotsky VV, Smith SL, Tadokoro K, Tsuda A, Yamamura O, Yamanaka Y, Yokouchi K, Yoshie N, Zhang J, Zuenko YI, Zvalinsky ZI. NEMURO – a lower trophic level model for the North Pacific marine ecosystem. *Ecological Modelling* **2007**, 202, 12-25.

Kress N, Thingstad TF, Pitta P, Psarra S, Tanaka T, Zohary T, Groom S, Herut B, Mantoura FR, Polychronaki T, Rassoulzadegan F, Spyres G. Effect of P and N addition to oligotrophic Eastern Mediterranean waters influenced by near-shore waters: A microcosm experiment. *Deep-Sea Research II* **2005**, 52(22-23), 3054-3073.

Kristiansen S, Farbrot T, Naustvoll L. Production of biogenic silica by spring diatoms. *Limnology and Oceanography* **2000**, 45(2), 472-478.

Kristiansen S, Farbrot T, Wheeler PA. Nitrogen cycling in the Barents Sea – Seasonal dynamics of new and regenerated production. *Limnology and Oceanography* **1994**, 39(7), 1630-1642.

Kudela RM, Chavez FP. Modeling the impact of the 1992 El Niño on new production in Monterey Bay, California. *Deep-Sea Research II* **2000**, 47(5-6), 1055-1076.

Kudela RM, Cochlan W. Nitrogen and carbon uptake kinetics and the influence of irradiance for a red tide bloom off southern California. *Aquatic Microbial Ecology* **2000**, 21(1), 31-47.

Kudela RM, Dugdale RC. Nutrient regulation of phytoplankton productivity in Monterey Bay, California. *Deep-Sea Research II* **2000**, 47(5-6), 1023-1053.

Kudela RM, Lane JQ, Cochlan W. The potential role of anthropogenically derived nitrogen in the growth of harmful algae in California, USA. *Harmful Algae* **2008a**, 8(1), 103-110.

Kudela RM, Ryan JP, Blakely MD, Lane JQ, Peterson TD. Linking the physiology and the ecology of *Cochlodinium* to better understand harmful algal bloom events: A comparative approach. *Harmful Algae* **2008b**, 7(3), 278-272.

Lalli CM, Parsons TR. *Biological Oceanography. An Introduction*, Second Edition, The Open University, **1997**, 314 pp.

Leblanc K, Quéguiner B, Garcia N, Rimmelin P, Raimbault P. Silicon cycle in the NW Mediterranean Sea: seasonal study of a coastal oligotrophic site. *Oceanologica Acta* **2003**, 26(4), 339-355.

Lehman JT. Ecological and nutritional studies on *Dinobryon* Ehrenb.: seasonal periodicity and the phosphate toxicity problem. *Limnology and Oceanography* **1976**, 21(5), 646-658.

Lemasson L, Pagès J, Cremoux J. Inorganic phosphate uptake in a brackish tropical lagoon. *Estuarine and Coastal Marine Science* **1980**, 11(5), 547-561.

Leong SCY, Taguchi S. Response of the dinoflagellate *Alexandrium tamarense* to a range of nitrogen sources and concentrations: growth rate, chemical carbon and nitrogen, and pigments. *Hydrobiologia* **2004**, 515(1-3), 215–224.

Lomas MW, Glibert PM. Comparisons of nitrate uptake, storage and reduction in marine diatoms and flagellates. *Journal of Phycology* **2000**, 36(5), 903-913.

MacIsaac JJ, Dugdale RC. The kinetics of nitrate and ammonia uptake by natural populations of marine phytoplankton. *Deep-Sea Research and Oceanographic Abstracts* **1969**, 16(1), 45-57.

Makler-Pick V, Gal G, Gorfine M, Hipsey MR, Carmel Y. Sensitivity analysis for complex ecological models – A new approach. *Environmental Modelling & Software* **2011**, 26(2), 124-134.

Martin-Jézéquel V, Hildebrand M, Brzezinski MA. Silicon metabolism in diatoms: implications for growth. *Journal of Phycology* **2000**, 36(5), 821-840.

McCarthy JJ, Garside C, Nevins JL. Nitrogen dynamics during the Arabian Sea Northeast Monsoon. *Deep-Sea Research II* **1999**, 46(8-9), 1623-1664.

McCarthy JJ, Yilmaz A, Coban-Yildiz Y, Nevis JL. Nitrogen cycling in the offshore waters of the Black Sea. *Estuarine, Coastal and Shelf Science* **2007**, 74(3), 493-514.

Muggli DL, Smith WO. Regulation of nitrate and ammonium uptake in the Greenland Sea. *Marine Biology* **1993**, 115(2), 199-208.

Nakamura Y, Watanabe M. Growth characteristics of *Chattonella antiqua*, Part 2. Effects of nutrients on growth. *Journal of the Oceanographical Society of Japan* **1983a**, 39(4), 151-155.

Nakamura Y, Watanabe M. Nitrate and phosphate uptake kinetics of *Chattonella antique* grown in light/dark cycles. *Journal of Oceanographical Society of Japan* **1983b**, 39(4), 167-170.

Nelson DM, Bzerzinski MA, Sigmon DE, Franck VM. A seasonal progression of Si limitation in the Pacific sector of the Southern Ocean. *Deep-Sea Research II* **2001**, 48(19-20), 3973-3995.

Nelson DM, Tréguer P. Role of silicon as a limiting nutrient to Antarctic diatoms: evidence from kinetic studies in the Ross Sea ice-edge zone. *Marine Ecology Progress Series* **1992**, 80(2-3), 255-264.

Nishikawa T, Hori Y, Tanida K, Imai I. Population dynamics of the harmful diatom *Eucampia zodiacus* Ehrenberg causing bleachings of *Porphyra thalli* in aquaculture in Harima-Nada, the Seto Inland Sea, Japan. *Harmful Algae* **2007**, 6(6), 763-773.

Nishikawa T, Hori Y. Effects of nitrogen, phosphorus and silicon on the growth of the diatom *Eucampia zodiacus* Ehrenberg causing *Porphyra* bleaching from Harima-Nada, the Seto Inland Sea, Japan. *Nippon Suisan Gakk* **2004**, 66 (6), 993-998 (in Japanese, with English abstract and figures).

Nishikawa T, Tarutani K, Yamamoto T. Nitrate and phosphate uptake kinetics of the harmful diatom *Eucampia zodiacus* Ehrenberg, a causative organism in the bleaching of aquacultured *Porphyra thalli*. *Harmful Algae* **2009**, 8(3), 513-517.

Paasche E. Growth of the plankton diatom *Thalassiosira nordenskioeldii* Cleve at low silicate conditions. *Journal of Experimental Marine Biology and Ecology* **1975**, 18(2), 173-183.

Paasche E. Silicon and the ecology of marine plankton diatoms. I. *Thalassiosira pseudonana* (*Cyclotella nana*) grown in a chemostat with silicate as limiting nutrient. *Marine Biology* **1973a**, 19(2), 117-126.

Paasche E. Silicon and the ecology of marine plankton diatoms. II. Silicate-uptake kinetics in five diatoms species. *Marine Biology* **1973b**, 19(3), 262-269.

Page S, Hipkin CR, Flynn KJ. Interactions between nitrate and ammonium in *Emiliania huxleyi. Journal of Experimental Marine Biology and Ecology* **1999**, 236(2), 307-319.

Painter SC, Sanders R, Waldron HN, Lucas MI, Woodward EMS, Chamberlain K. Nitrate uptake along repeat meridional transects of the Atlantic Ocean. *Journal of Marine Systems* **2008**, 74(1-2), 227-240.

Parsons TR, Takahashi M. *Biological Oceanographic Processes*, Pergamon Press, United Kingdom, **1973**, 186 pp.

Perry MJ. Phosphate utilization by an oceanic diatom in phosphorus-limited chemostat culture and in oligotrophic waters at the central North Pacific. *Limnology and Oceanography* **1976**, 21(1), 88-107.

Probyn TA, Mitchell-Innes BA, Searson S. Primary productivity and nitrogen uptake in the subsurface chlorophyll maximum on the Eastern Agulhas Bank, *Continental Shelf Research* **1995**, 15(15), 1903-1920.

Probyn TA. Nitrogen uptake by size-fractionated phytoplankton populations in the southern Benguela upwelling system. *Marine Ecology Progress Series* **1985**, 22, 249-258.

Qasim SZ, Bhattathiri PM, Devassy VP. Growth kinetics and nutrient requirements of two tropical marine phytoplankters. *Marine Biology* **1973**, 21(4), 299–304.

Ragueneau O, Chauvaud L, Leynaert A, Thouzeau G, Paulet Y-M, Bonnet S, Lorrain A, Grall J, Corvaisier R, Le Hir M, Jean F, Clavier J. Direct evidence of biologically active coastal silicate pump: ecological implications. *Limnology and Oceanography* **2002**, 47(6), 1849–1854.

Reynolds C. Ecology of phytoplankton, Cambridge University Press, United Kingdom, **2006**, 535 pp.

Rhee G. Effects of N:P atomic ratios and nitrate limitation on algal growth, cell composition, and nitrate uptake, *Limnology and Oceanography* **1978**, 23(1), 10-25.

Rhee, G. A continuous culture study of phosphate uptake, growth rate and polyphosphate in *Scenedesmus* sp. *Journal of Phycology* **1973**, 9(4), 495-506.

Rodrigues M, Oliveira A, Costa M, Fortunato AB, Zhang YJ. Sensitivity analysis of an ecological model applied to the Ria de Aveiro. *Journal of Coastal Research* **2009a**, SI56, 448-452.

Rodrigues M, Oliveira A, Queiroga H, Fortunato AB, Zhang YJ. Three-dimensional modeling of the lower trophic levels in the Ria de Aveiro. *Ecological Modelling* **2009b**, 220(9-10), 1274-1290.

Sahlsten E. Nitrogenous nutrition in the euphotic zone of the Central North Pacific Gyre. *Marine Biology* **1987**, 96(3), 433-439.

Sandgren CD. Chysophyte growth and perennation strategies. In: Sandgren CD, *Growth and reproductive strategies of freshwater phytoplankton*, Cambridge University Press, USA, **1988**, 442 pp.

Sarthou G, Timmermans KR, Blain S, Tréguer P. Growth physiology and fate of diatoms in the ocean: a review. *Journal of Sea Research* **2005**, 53(1-2), 25-42.

Sharada MK, Yajnik KS, Swathi PS. Evaluation of six relations of the kinetics of uptake by phytoplankton in multi-nutrient environment using JGOFS experimental results. *Deep-Sea Research II* **2005**, 52, 1892-1909.

Smith WO, Harrison WG. New production in polar regions: The role of environmental controls, *Deep-Sea Research Part A. Oceanographic Research Papers* **1991**, 38(12), 1463-1479.

Sommer U. Comparative nutrient status and competitive interactions of two Antarctic diatoms (*Corethron criophilum* and *Thalassiothrix antarctica*), *Journal of Plankton Research* **1991**, 13, 61–75.

Sommer U. Nitrate- and silicate-competition among antartic phytoplankton, *Marine Biology* **1986**, 91(3), 345-351.

Sörensson F, Sahlsten E. Nitrogen dynamics of a cyanobacteria bloom in the Baltic Sea: new versus regenerated production. *Marine Ecology Progress Series* **1987**, 37, 277-284.

Sterner RW, Grover JP. Algal growth in warm temperate reservoirs: kinetic examination of nitrogen, temperature, light, and other nutrients. *Water Research* **1998**, 32(12), 3539-3548.

Tilman D, Kilham SS. Phosphate and silicate growth and uptake kinetics of the diatoms *Asterionella formosa* and *Cyclotella meneghiniana* in batch and semi-continuous culture. *Journal of Phycology* **1976**, 12(4), 375-383.

Timmermans KR, van der Wagt B, Veldhuis MJW, Maatman A, de Baar HJW. Physiological responses of three species of marine pico-plankton to ammonium, phosphate, iron and light limitation. *Journal of Sea Research* **2005**, 53(1-2), 109-120.

Tomas CR. *Olisthodiscus luteus* (Chrysophyceae). III. Uptake and utilization of nitrogen and phosphorus, *Journal of Phycology* **1979**, 15(1), 5–12.

Valiela I. *Marine Ecological Processes*, 2nd edition, Springer, USA, **1995**, 686 pp.

Walsh JJ, Dugdale RC. A simulation model of the nitrogen flow in the Peruvian upwelling system. *Invéstigacion Pesquera* **1971**, 35, 309-330.

Whalen SC, Alexander V. Seasonal inorganic carbon and nitrogen transport by phytoplankton in an Artic lake. *Canadian Journal of Fisheries and Aquatic Science* **1986**, 43(6), 1177-1186.

White KK, Dugdale RC. Silicate and nitrate uptake in the Monterey Bay upwelling system. *Continental Shelf Research* **1997**, 17(5), 455-472.

Yajnik KS, Sharada MK. Ammonium inhibition of nitrate uptake by phytoplankton: A new relation based on similarity and hyperbolicity. *Current Science* **2003**, 85 (8), 1180-1189.

Yamamoto T, Inokuchi Y, Sugiyama T. Biogeochemical cycles during the species succession from *Skeletonema costatum* to *Alexandrium tamarense* in northern Hiroshima Bay. *Journal of Marine Systems* **2004a**, 52(1-4), 15-32.

Yamamoto T, Oh SJ, Kataoka Y. Growth and uptake kinetics for nitrate, ammonium and phosphate by toxic dinoflagellate *Gymnodinium catenatum* isolated from Hiroshima Bay, Japan. *Fisheries Science* **2004b**, 70(1), 108-115.

Yamamoto T, Tarutani K. Growth and phosphate uptake kinetics of the toxic dinoflagellate *Alexandrium tamarense* from Hiroshima Bay. *Phycological Research* **1999**, 47(1), 27-32.

Yin K, Harrison PJ, Dortch Q. Lack of ammonium inhibition of nitrate uptake for a diatom grown under low light conditions. *Journal of Experimental Marine Biology and Ecology* **1998**, 228(1), 151-165.

Zhang Y, Baptista AM. SELFE: A semi-implicit Eulerian-Lagrangian finite-element model for cross-scale ocean circulation. *Ocean Modeling* **2008**, 21(3-4), 71-96.

Zhang Y, Fu F, Whereat E, Coyne KJ, Hutchins DA. Bottom-up controls on a mixed-species HAB assemblage: A comparison of sympatric *Chattonella subsalsa* and *Heterosigma akashiwo* (Raphidophyceae) isolates from Delaware Inland Bays, USA. *Harmful Algae* **2006**, 5(3), 310-320.

CHAPTER III

COUPLED HYDRODYNAMIC-ECOLOGICAL MODEL IMPROVEMENTS, IMPLEMENTATION AND APPLICATION IN THE AVEIRO LAGOON

SECTION III.1

MULTI-SCALE WATER QUALITY MODELLING: COUPLING A FAR FIELD AND A NEAR FIELD MODEL[III.1.1]

ABSTRACT

A hybrid coupling approach was used to couple the RSB model (near field model) to the three-dimensional model SELFE (far field model), allowing the detailed simulation of local discharges within SELFE. The coupling was done assuming a three-dimensional Gaussian distribution of the tracer in the far field based on the characteristics of the plume predicted by the near field model. The two models were fully coupled, running simultaneously. A set of synthetic tests were performed to evaluate the model response to different characteristics of the ambient (ambient current velocity and stratification) and of the discharge (number of diffusers and duration of the discharge). Results show the ability of the model to represent the plume in the near field with mass errors generally smaller than 1%. The coupled model is also able to represent adequately the plume characteristics as a result of the different environment conditions. This extension of the model SELFE represents an additional capability in the application of this model in a wide range of environmental studies, namely the ones related to the impact of local discharges in the water quality of receiving water bodies.

KEYWORDS

SELFE hydrodynamic model, Near field model, Three-dimensional, Tracer discharges

[III.1.1] The coupled model is used to simulate an emergency discharge of domestic effluents in Chapter V.

III.1.1 INTRODUCTION

Water quality and ecological modelling studies deal with processes that occur at a wide range of spatial and temporal scales. In particular, local discharges (e.g. outfalls discharges) can be affected by small scale processes (centimetres to meters) and can be transported and have impacts away from their source (meters to kilometres).

The initial mixing zone, referred to as *near field*, is defined as the region over which the discharge momentum and the buoyancy significantly influence local flow patterns (Adams *et al.*, 1986). In the near field, the turbulent mixing is caused by shear on lateral boundaries of the individual effluent plumes, which is a process with a time scale of seconds to minutes and a space scale of centimetres to meters (Zhang and Adams, 1999). After the initial mixing and establishment of the plume in the near field, local ambient currents and turbulence promote the plume advection and diffusion in the *far field*, where spatial and temporal scales are significantly larger.

Thus, due to the range of scales involved, the detailed simulation of the processes occurring at the near field and at the far field scales with a single model is difficult (Zhang and Adams, 1999; Roberts *et al.*, 2010). Difficulties are mostly related with the domain discretization and the associated computational times, which often leads to the development and application of separate models to simulate the processes occurring in each one of these regions.

Several models are available for the simulation of initial mixing zone conditions, which can be classified into three major categories: length scale models, entrainment models and computational fluid dynamics models (CFD) (Roberts *et al.*, 2010). Among these models are: RSB (Roberts *et al.*, 1989a,b), UM3 (available in Visual Plumes, Frick *et al.*, 2001; Frick, 2004), CORMIX-GI (Jirka *et al.*, 1991; Donneker and Jirka, 2007) and VISJET (Lee and Chu, 2003). As for the near field, the models available to simulate the far field are vast. Examples include: POM – Princeton Ocean Model (Mellor, 2002), ROMS – Regional Ocean Modeling System (Haidvogel *et al.*, 2008), ADCIRC (Luettich *et al.*, 1991) and SELFE - Semi-implicit Eulerian-Lagrangian Finite-element model (Zhang and Baptista, 2008).

The coupling between near and far field models has been addressed in several studies where different approaches were followed. Coupling can vary from one-way coupling, where local currents predicted by the far field model are used to determine the near field initial mixing but no interaction from the near field is considered in the far field (e.g. RPS MetOcean, 2010), to two-way coupling (i.e. dynamic coupling) where the link between the near and far field models is established at grid cell level (e.g. Distributed Entrainment Sink Approach from Choi and Lee (2007)). Hybrid coupling approaches have also been used (e.g. Suh, 2001; Kim *et al.*, 2002; Bleninger and Jirka, 2004), and are particularly useful for predicting pollutants impacts (Roberts

et al., 2010). In hybrid coupling, the time-varying ambient currents and stratification predicted by the far field model are used to simulate the near field plume characteristics, which in turn are inputted in the far field model at the predicted grid cells. However, in most of these hybrid approaches the models run independently, since running the models simultaneously is more complex and computationally more expensive. Besides these coupling approaches, several authors have also investigated the use of far field models to predict the near field plume characteristics (e.g. Blumberg *et al.*, 1996; Zhang and Adams, 1999).

The aim of this study is to improve the three-dimensional hydrodynamic model SELFE through the coupling of a near field model, which will allow the simulation of any given tracer from local outfall discharges within a single model. This coupling will contribute to improve SELFE flexibility, in particular to simulate the ecological and water quality in multi-scale applications. The model development is described in section III.1.2 and some synthetic validation tests are presented in section III.1.3. Section III.1.4 summarizes the main conclusions.

III.1.2 MODEL DESCRIPTION

The new model couples the model SELFE (available at www.stccmop.org/CORIE/modeling/selfe/), used to represent the far field circulation and tracers' transport, and a near field model based on the RSB model (Roberts *et al.*, 1989a,b; Economopoulou and Economopoulos, 2001). The two models are coupled using an hybrid approach in which the near field model is established based on the ambient characteristics simulated by the far field model (local currents velocity and ambient density) and provides the input conditions for the far field model. Plume characteristics determined by the near field model (length, width, thickness, trap height and dilution) are inputted at the grid cells of the far field model, taking into consideration the ambient concentrations of the tracer in the far field. The two models are fully coupled running simultaneously at each time step. A brief description of SELFE is presented in section III.1.2.1 and the near field model is described in detail in section III.1.2.2.

III.1.2.1 Far Field Model – SELFE

SELFE is an unstructured grid model developed for the baroclinic flow simulation from rivers to oceans, which computes the free-surface elevation and the three-dimensional fields of velocity, salinity and temperature. The hydrostatic version of the model solves the three-dimensional shallow-water equations, with the hydrostatic and Boussinesq approximations, and the transport equations for salt and heat:

$$\frac{\partial u}{\partial x}+\frac{\partial v}{\partial y}+\frac{\partial w}{\partial z}=0 \tag{III.1.1}$$

$$\frac{\partial \eta}{\partial t}+\frac{\partial}{\partial x}\int_{-h}^{\eta} u\,dz+\frac{\partial}{\partial y}\int_{-h}^{\eta} v\,dz=0 \tag{III.1.2}$$

$$\begin{aligned}\frac{\partial u}{\partial t}+u\frac{\partial u}{\partial x}+v\frac{\partial u}{\partial y}+w\frac{\partial u}{\partial z}=fv-\frac{\partial}{\partial x}\left[g(\eta-\alpha\hat{\psi})+\frac{p_a}{\rho_0}\right]-\frac{g}{\rho_0}\int_{z}^{\eta}\frac{\partial \rho_w}{\partial x}dz+\\+\frac{\partial}{\partial x}\left(\mu\frac{\partial u}{\partial x}\right)+\frac{\partial}{\partial y}\left(\mu\frac{\partial u}{\partial y}\right)+\frac{\partial}{\partial z}\left(\nu\frac{\partial u}{\partial z}\right)\end{aligned} \tag{III.1.3}$$

$$\begin{aligned}\frac{\partial v}{\partial t}+u\frac{\partial v}{\partial x}+v\frac{\partial v}{\partial y}+w\frac{\partial v}{\partial z}=-fu-\frac{\partial}{\partial y}\left[g(\eta-\alpha\hat{\psi})+\frac{p_a}{\rho_0}\right]-\frac{g}{\rho_0}\int_{z}^{\eta}\frac{\partial \rho_w}{\partial y}dz+\\+\frac{\partial}{\partial x}\left(\mu\frac{\partial v}{\partial x}\right)+\frac{\partial}{\partial y}\left(\mu\frac{\partial v}{\partial y}\right)+\frac{\partial}{\partial z}\left(\nu\frac{\partial v}{\partial z}\right)\end{aligned} \tag{III.1.4}$$

$$\frac{\partial S}{\partial t}+u\frac{\partial S}{\partial x}+v\frac{\partial S}{\partial y}+w\frac{\partial S}{\partial z}=\frac{\partial}{\partial z}\left(\kappa\frac{\partial S}{\partial z}\right)+F_s \tag{III.1.5}$$

$$\frac{\partial T}{\partial t}+u\frac{\partial T}{\partial x}+v\frac{\partial T}{\partial y}+z\frac{\partial T}{\partial z}=\frac{\partial}{\partial z}\left(\kappa\frac{\partial T}{\partial z}\right)+\frac{\dot{Q}}{\rho_0 C_p}+F_h \tag{III.1.6}$$

where u and v are the horizontal components of the velocity (m s^{-1}), w is the vertical component of the velocity (m s^{-1}), (x,y) are the horizontal Cartesian coordinates (m), z is the vertical coordinate (m), t is the time (s), $\eta(x,y,t)$ is the free surface elevation (m), $h(x,y)$ is the bathymetric depth (m), f is the Coriolis factor (s^{-1}), g is the acceleration of gravity (m s^{-2}), $\hat{\psi}$ is the earth-tidal potential (m), α is the effective earth-elasticity factor (non-dimensional), $\rho_w(x,y,z,t)$ is the water density (kg m^{-3}), ρ_0 is the reference water density, $p_a(x,y,t)$ is the atmospheric pressure at free-surface (N m^{-2}), S is the water salinity, T is the water temperature (ºC), μ is the horizontal eddy viscosity ($m^2 s^{-1}$), ν is the vertical eddy viscosity ($m^2 s^{-1}$), κ is the vertical eddy viscosity for transport ($m^2 s^{-1}$), F_h and F_s represent the horizontal diffusion for heat and salt transport, C_p is the specific heat of water (J $kg^{-1} K^{-1}$) and $\dot{Q}$ is the rate of absorption of solar radiation (W m^{-2}).

The model also includes a user-defined transport module which allows the simulation of any given tracer, besides salinity and temperature:

$$\frac{\partial C}{\partial t}+u\frac{\partial C}{\partial x}+v\frac{\partial C}{\partial y}+w\frac{\partial C}{\partial z}=\frac{\partial}{\partial z}\left(\kappa\frac{\partial C}{\partial z}\right)+F_c+\Lambda C \tag{III.1.7}$$

where C is a generic tracer, F_c represents the horizontal diffusion for the tracer and ΛC is the sources and sinks term. Through this module several models have been coupled to SELFE, including an ecological model – ECO-SELFE (Rodrigues *et al.*, 2009; Chapter III, Section III.3,

Rodrigues *et al.*, 2012), a fecal contamination model (Rodrigues *et al.*, 2011), a morphodynamic model (Pinto *et al.*, in review) and an oil spill model (Azevedo, 2010).

The differential system of equations (1.1-1.6) is closed with a state equation describing the water density as a function of salinity and temperature, the definition of the tidal potential and of the Coriolis factor, the turbulence closure equations, and appropriate initial and boundary conditions.

Numerically, the differential system of equations is solved with finite-elements and finite-volumes schemes. Semi-implicit schemes are applied to all equations, which improves stability and efficiency. The advection in the momentum equation is solved with an Eulerian-Lagragian method (ELM). The advective terms in the transport equations (1.5-1.7) can be solved with ELM, upwind or Total Variation Diminishing (TVD) schemes. Horizontally the domain is discretized with unstructured grids. For the vertical domain hybrid coordinates are used (*S* coordinates and *Z* coordinates), providing higher flexibility in the bathymetric representation (Figure III.1.1). A more detailed description of the model can be found in Zhang and Baptista (2008).

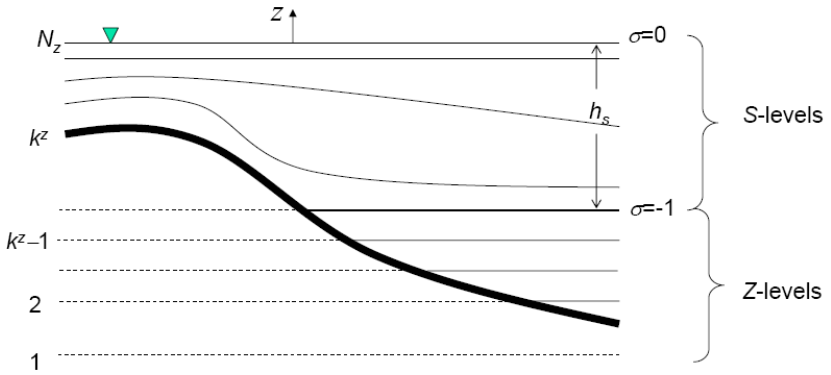

Figure III.1.1. Vertical grid schematic representation: *S* levels are always on top of *Z* levels; N_z is the free-surface and h_s is the depth of transition between *S* and *Z* levels (from Zhang and Baptista, 2008).

III.1.2.2 Near Field Model

The near field model implemented within SELFE is based on the RSB model (Roberts *et al.*, 1989a,b), for multi-port diffusers. The concentration of the tracer in the near field is assumed to follow a three-dimensional Gaussian distribution:

$$C_n(x,y,z) = \frac{m_d}{2\pi\sigma_x\sigma_y\sigma_z}\exp\left(-\frac{(x-x_0)^2}{2\sigma_x{}^2}-\frac{(y-y_0)^2}{2\sigma_y{}^2}-\frac{(z-z_0)^2}{2\sigma_z{}^2}\right) \qquad \text{(III.1.8)}$$

where $C_n(x,y,z)$ is the concentration of the tracer at (x,y,z) due to the near field model alone ([mass] m^{-3}), m_d is the mass of the tracer from the discharge, σ_x, σ_y and σ_z are the standard deviations in x, y and z (m), and x_0, y_0 and z_0 define the point of maximum concentration (m).

The point of maximum concentration (x_0, $y_{0,}$ z_0) is calculated by the following relations:

$$x_0 = x_{dif} + X_i \frac{u_{0dif}}{|U_0|} \quad \text{(III.1.9)}$$

$$y_0 = y_{dif} + X_i \frac{v_{0dif}}{|U_0|} \quad \text{(III.1.10)}$$

$$z_0 = z_{dif} + z_m \quad \text{(III.1.11)}$$

where x_{dif}, y_{dif} and z_{dif} are the diffuser coordinates, X_i is the length of the near field (m), z_m is the height to the top of minimum dilution (m), and U_0=(u_{0dif},v_{0dif}) is the horizontal velocity at (x_0,y_0) (Figure III.1.2 and Figure III.1.3). For U_0=0 m s^{-1}, (x_0,y_0)=(x_{dif}, y_{dif}). In well-mixed environmental conditions, the plume is retained at the surface of the water column (Figure III.1.4).

The standard deviations of the Gauss distribution, taking into account that x is defined in the along flow direction and y is perpendicular to U_0, are defined as:

$$\sigma_x = kX_i \quad \text{(III.1.12)}$$

$$\sigma_y = kw_0 \quad \text{(III.1.13)}$$

$$\sigma_z = kh_e \quad \text{(III.1.14)}$$

where w_0 is the width of the plume in the near field (m), h_e is the thickness of the plume in the near field (m) and k is a scaling factor (non-dimensional). The factor k was introduced herein to determine the relationship between the empirically-determined characteristic dimensions of the plume, X_i, w_0 and h_e, and standard deviations of the Gaussian representation of the plume. The value of k is based on equation III.1.8 at the point of maximum concentration determined:

$$k = \sqrt[3]{\frac{m_d}{2\pi X_i w_0 h_e C_{\max}(x_0, y_0, z_0)}} \quad \text{(III.1.15)}$$

and $C_{max}(x_0,y_0,z_0)$ is defined as:

$$C_{\max}(x_0, y_0, z_0) = \frac{C_{init}}{S_{dil}} \quad \text{(III.1.16)}$$

where S_{dil} is the minimum dilution in the near field (non-dimensional) and C_{init} is the initial concentration of the tracer in the effluent ([mass] m^{-3}).

The derivations of equation III.1.8 and III.1.15 use some simplifying assumptions, such as an infinite domain, constant depth and uniform flow. Since these hypotheses are seldom strictly

valid in practice, the use of equation III.1.8 alone can lead to mass errors. The concentration determined by equation III.1.8 should therefore be corrected to enforce mass conservation. This correction is performed by multiplying equation III.1.8 by the ratio between the known mass discharged (m_d) by the domain integral of the concentration given by equation III.1.8:

$$C_{efec}(x_0, y_0, z_0) = C(x, y, z)\frac{m_d}{m_{\text{int}}} \qquad \text{(III.1.17)}$$

where C_{efec}(x,y) is the final concentration of the tracer in ([mass] m^{-3}) and m_{int} is the integral of the concentration, both in the near field. The tracer concentration in the near field is added to concentration in the far field.

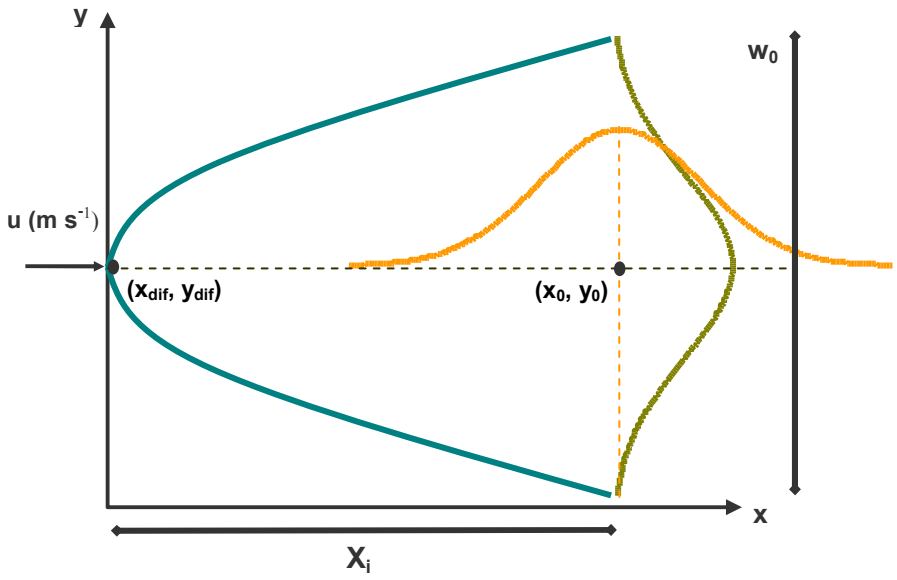

Figure III.1.2. Near field solution scheme (plan view): plume (blue line), tracer concentration distribution along the x-axis (orange line) and tracer concentration distribution along the y-axis (green line).

The parameters X_i, w_0, z_m, h_e and S_{dil} are determined based on the equations presented in Table III.1.1 derived by Roberts *et al.* (Roberts, 1979; Roberts *et al.*, 1989a,b; Confederación Hidrográfica del Norte, 1995; Roberts, 1996; Economopoulou e Economopoulos, 2001) for both linearly stratified and well-mixed ambients, and for currents at various angles relative to the diffuser (0º, 45 and 90º). The equations for linearly stratified ambient were determined for diffusers with T-shaped risers (ports perpendicular to the diffuser axis in both directions), negligible port spacing, negligible jet momentum flux and linear variation of ambient density with water height (Economopoulou and Economopoulos, 2001). The RSB model assumes different relations based on fixed current directions (90º, 45º and 0º). For intermediate directions, a linear interpolation is assumed between each two directions (0º and 45º; 45º and 90º). In the near

field, both the horizontal and vertical grid must have an adequate resolution to solve the dimensions of the plume, and unstructured grids are particularly flexible for this type of implementations.

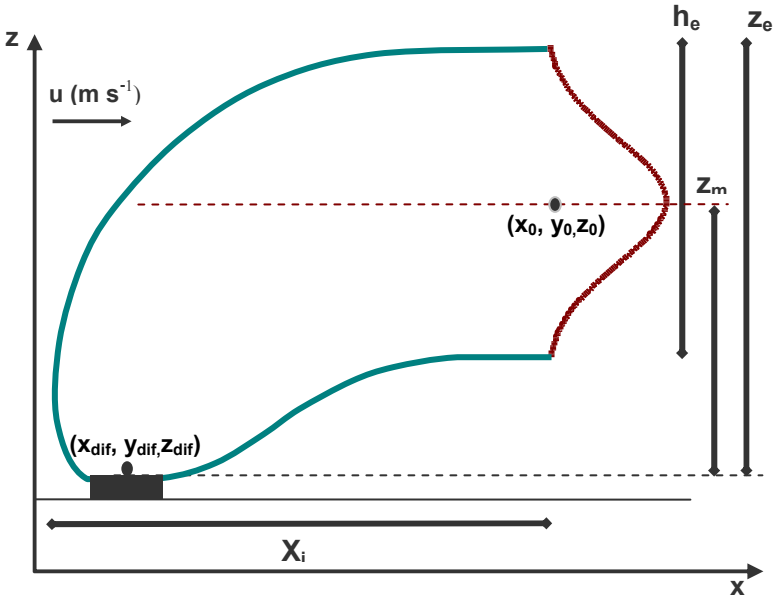

Figure III.1.3. Near field solution scheme (side view) for the linearly stratified ambient: plume (blue line) and tracer concentration distribution along the z-axis (red line).

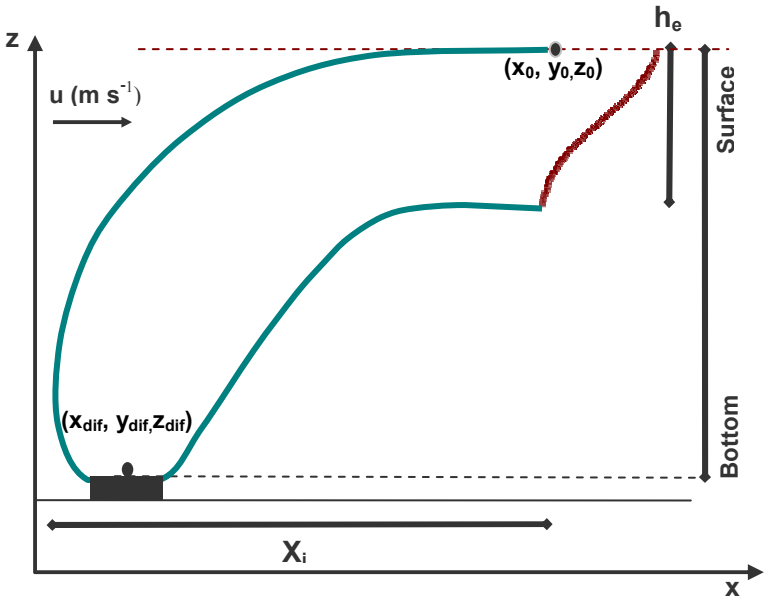

Figure III.1.4. Near field solution scheme (side view) for the well-mixed ambient: plume (blue line) and tracer concentration distribution along the z-axis (red line).

Table III.1.1. Near field formulations (Roberts, 1979; Roberts *et al.*, 1989a,b; Confederación Hidrográfica del Norte, 1995; Roberts, 1996; Economopoulou e Economopoulos, 2001).

	Linearly Stratified Ambient[1,2,3,4,5]	Well-mixed Ambient[1,2,3,4,5]
Length	$X_i = 8.5\frac{U}{N}$; 90º, 45º and 0º	$X_i = H(0.566F + 3.389)$, 90º, 45º and 0º
Width of the plume	$w_0 = 1.5L$, 90º and 45º $w_0 = 0.70X_iF^{-1/3}$, 0º	
Height to top of the plume	$z_e = 2.6\frac{b^{1/3}}{N}$; F=0 $z_e = 2.74\frac{b^{1/3}}{N}$; 0.1≤F ≤1 $z_e = 2.5\frac{b^{1/3}}{N}F^{-1/6}$; 90º, 45º; 1<F≤100 $z_e = 2.59\frac{b^{1/3}}{N}F^{-0,0447}$; 0º; 1<F≤100	-
Thickness of the plume	$h_e = 1.8\frac{b^{1/3}}{N}$; F=0 $h_e = (0.365F^{-1/6} + 1.82)\frac{b^{1/3}}{N}$; 0.1≤F≤1 $h_e = (1.85F^{-1/6} + 0.306)\frac{b^{1/3}}{N}$; 90º, 45º; F>1 $h_e = (0.447F^{-1/6} + 1.69)\frac{b^{1/3}}{N}$; 0º; F>1	$h_e = 0.08H$
Height to minimum dilution	$z_m = 1.7\frac{b^{1/3}}{N}$; F=0 $z_m = 1.7\frac{b^{1/3}}{N}F^{-0.0483}$; 90º, 45º; 0.1≤F≤1 $z_m = 1.6621\frac{b^{1/3}}{N}F^{-0.2577}$; 90º, 45º; 1<F<5 $z_m = 1.5\frac{b^{1/3}}{N}F^{-1/6}$; 90º, 45º; F≥5 $z_m = 1.9\frac{b^{1/3}}{N}$; 0º; 0.1≤F≤10 $z_m = 2.4642\frac{b^{1/3}}{N}F^{-0.0938}$; 0º; F>10	-

Table III.1.1 (Cont.). Near field formulations (Roberts, 1979; Roberts *et al.*, 1989a,b; Confederación Hidrográfica del Norte, 1995; Roberts, 1996; Economopoulou e Economopoulos, 2001).

	Linearly Stratified Ambient[1,2,3,4,5]	Unstratified Ambient[1,2,3,4,5]
Minimum Initial Dilution		$S_{dil} = \frac{U.H}{Q/L} 0.58$, 90º, 0.1≤F≤100
	$S_{dil} = \frac{b^{2/3}}{QN/L}(2.19F^{1/6} - 0.52)$, 90º	$S_{dil} = \frac{U.H}{Q/L}(0.3653F^{-0.185})$, 45º, 0.1≤F≤1
	$S_{dil} = \frac{b^{2/3}}{QN/L}(1.3214F^{0.2014})$, 45º	$S_{dil} = \frac{U.H}{Q/L}(0.3715 - 0.005\ln F)$, 45º, 1<F≤100
	$S_{dil} = \frac{b^{2/3}}{QN/L}(1.15F^{0.1345})$, 0º	$S_{dil} = \frac{U.H}{Q/L}(0.314F^{-0.2495})$, 0º, 0.1≤F≤20
		$S_{dil} = \frac{U.H}{Q/L}(0.188 - 0.0128\ln F)$, 0º, 20<F≤100

[1] Q is the wastewater discharge in $m^3 s^{-1}$; L is the diffuser length in m; H is the total water depth at the discharge point in m; U is the current velocity in $m s^{-1}$; ρ is the density of ambient water at port level in $kg m^{-3}$; ρ_{ef} is the effluent density at port level in $kg m^{-3}$.

[2] Total source buoyancy flux per unit of diffuser length (b in $m^3 s^{-3}$) is defined as: $b = g'Q/L$.

[3] Buoyancy frequency (N in s^{-1}) is defined as: $N = \left(\frac{g}{\rho}\frac{d\rho}{dz}\right)^{1/2}$.

[4] Froude number (F) is defined as: $F = U^3 / b$.

[5] Modified acceleration due to gravity (g' in $m s^{-2}$) is defined as: $g' = g\frac{\rho - \rho_{ef}}{\rho}$.

III.1.3 SYNTHETIC TESTS

Two synthetic tests were performed to validate the implementation of the coupled model. Test 1 aimed at validating the model in different environment conditions, while Test 2 evaluated different discharge characteristics. These synthetic tests were adapted from the ones presented in Zhang and Adams (1999) and Azevedo (2010). For all the simulations performed the mass conservation was evaluated, comparing the initial mass imposed at the discharge with the mass in the domain.

III.1.3.1 Test 1 – Environmental Conditions

Simulations were performed with a square horizontal grid of 20 x 20 km and a uniform spatial resolution of 100 m. The domain depth was of 70 m, which was discretized with a vertical grid of 10 equally spaced S levels. Simulations were performed for 2 days with a time step of 180 s. Horizontal and vertical viscosity and diffusivity were set equal to 0 $m^2 s^{-1}$, as the main goal of these synthetic tests were to validate the implementation of the coupled model. The drag coefficient was set equal to 0 to establish a uniform current velocity throughout the water

column. However, some additional tests were performed considering a drag coefficient of 0.002, in order to evaluate a more realistic vertical profile of current velocities. Salinity was set equal to 35. The discharge was initiated at the end of the first day, after the establishment of the hydrodynamic conditions, and was imposed near the bottom in the center of the domain (x=10 km; y= 10 km). Diffuser length was set equal to 1034 m. A constant flow of 3.4 $m^3 s^{-1}$ with a density of 1000 kg m^{-3} and a concentration of 1634 [mass] m^{-3} of a generic tracer was considered. The transport of this tracer was simulated considering only advection and diffusion (i.e. the sources and sinks term of the tracer was set equal to zero). The environmental conditions tested included the velocity and the vertical temperature gradient. Three current velocities and two water temperature gradients (2 ºC and 0.5 ºC), which lead to plumes with different characteristics in the near field, were simulated. Table III.1.2 summarizes the simulations, regarding the environmental conditions.

Table III.1.2. Synthesis of the simulations performed for the environment conditions (Test 1).

	Velocity (m s^{-1})	Vertical Temperature Difference (ºC)
Simulation 1.A (S1.A)	0	2 (N^2 = 7.7x10^5 s^{-2})
Simulation 1.B (S1.B)	0.06	2 (N^2 = 7.7x10^5 s^{-2})
Simulation 1.C (S1.C)	0.12	2 (N^2 = 7.7x10^5 s^{-2})
Simulation 1.D (S1.D)	0.06	0.5 (N^2 = 1.9x10^5 s^{-2})

The comparison between the input mass and the mass in the domain shows that the mass is conserved while it the remains inside the domain (Figure III.1.5). Differences between input mass and simulated mass are smaller than 1% in day 2 for simulations S1.A, S1.B and S1.D. In simulation S1.C a decrease of the mass simulated is observed from day 1.4 due to the plume reaching the boundary (i.e. due to the larger velocity imposed in this simulation, part of the tracer mass is advected outside of the domain).

Environmental conditions affected significantly the behaviour of the plume (Figure III.1.6 and Figure III.1.7). Current velocity, in particular, influenced the extension of the plume in the domain and the tracer concentration. For u=0.0 m s^{-1} the plume remains in the area near the discharge leading to larger concentrations along the water column. Trap heights predicted for the currents velocities of 0.06 m s^{-1} and 0.12 m s^{-1} are of about 19 m and 15 m, respectively. The thickness of the plume is slightly affected by the current velocity, varying from 21 m, for the current velocity of 0.12 m s^{-1}, to 24 m, when the current velocity is lower. These results are in accordance to the ones presented by Zhang and Adams (1999). Regarding the tracer's concentration, the lower current velocity (0.06 m s^{-1}) leads to a thicker area of larger concentrations in the middle of the plume (Figure III.1.6), which is a similar pattern to the one described by Zhang and Adams (1999). Considering a more realistic vertical profile of current

velocities alters significantly the shape of the plume along the channel (Figure III.1.8), although its characteristics in the near field remain similar. The shape of the plume predicted for these conditions is more realistic and similar to the one presented by Zhang and Adams (1999). The stratification of the water column (represented by the temperature gradient) had a larger influence in the rise of the plume, in the trap height predicted by the near field model and in the plume thickness. For the same local velocity (u=0.6 m s^{-1}) the trap height is of about 20 m for ΔT=2 ºC (N^2=7.7x10^{-5} s^{-2}) and of about 39 m for ΔT=0.5 ºC (N^2=1.9x10^{-5} s^{-2}), evidencing larger trap heights when the stratification is lower. These traps heights predicted by the model are in accordance with the results of Zhang and Adams (1999), which are of about 19 m (N^2= 7.7x10^{-5} s^{-2}) and 36 m (N^2=1.9x10^{-5} s^{-2}), respectively. Globally, results show the ability of the coupled model to represent the plume predicted by near field model in the far field model for different environment conditions.

III.1.3.2 Test 2 – Discharge Characteristics

Numerical setup was similar to the one adopted in Test 1, with exception of the domain depth that was set equal to 10 m. Boundary conditions were set to establish uniform current velocity of 0.15 m s^{-1}, constant water temperature of 15ºC and constant salinity of 35, leading to an well-established ambient. The discharge was initiated at the end of the first day, allowing for the establishment of the hydrodynamic conditions. Three discharge conditions were evaluated (Table III.1.3). As for Test 1 a generic tracer was simulated, with a concentration of 2778 [mass] m^{-3} and no decaying.

Table III.1.3. Synthesis of the simulations performed for the discharges characteristics (Test 2).

	Number of Discharges	Type of Discharge
Simulation 2.A (S2.A)	1	Continuous
Simulation 2.B (S2.B)	2	Continuous
Simulation 2.C (S2.C)	1	Instantaneous

Mass conservation results are similar to those obtained in Test 1. A good mass conservation was achieved (differences smaller than 1% for S2.A and S2.B) during the period in which all the mass of the tracer remained inside the domain (Figure III.1.9). The model was also able to accurately represent several sources of discharges (Figure III.1.10). The instantaneous discharge is represented in Figure III.1.10 and Figure III.1.11. The mass error for this simulation was smaller 0.1% (results not shown). In these simulations, the plume remained near the surface since the stratification is equal to zero. The mixing of the plume in the water column due to advection and diffusion was observed from day 1 to day 2. Throughout the water column the expected tailing

effect was also observed. This test showed the ability of the model for simulating different discharge conditions and also for simulating discharges in well-mixed environments.

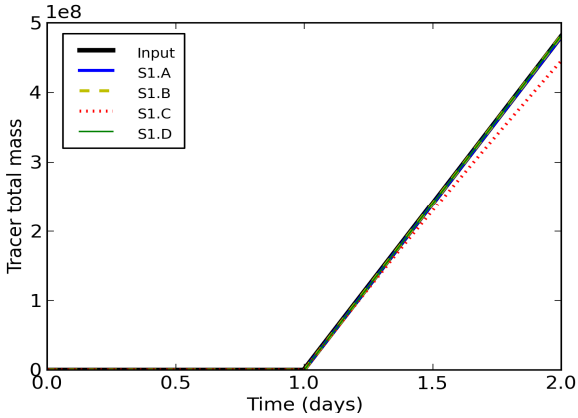

Figure III.1.5. Comparison between the initial mass imposed at the discharge and the total mass in the domain for the different environmental conditions (Test 1).

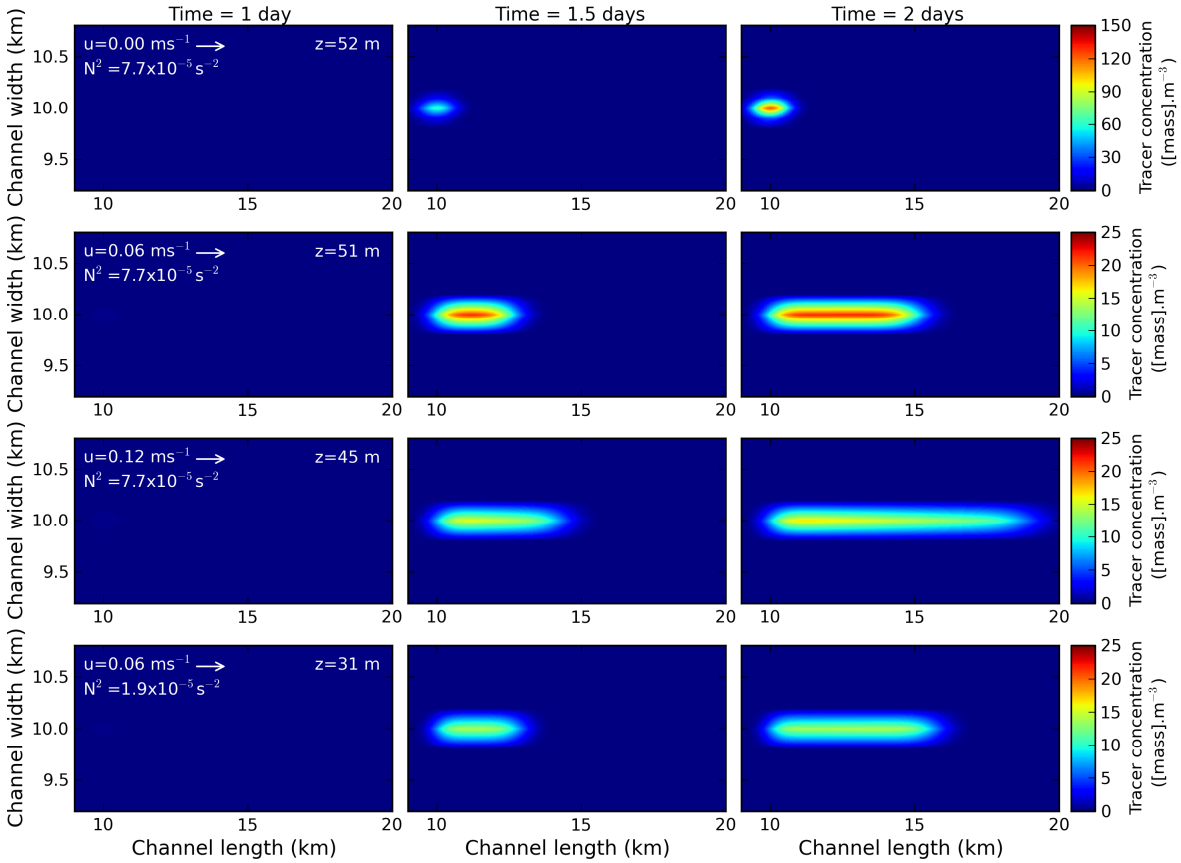

Figure III.1.6. Top view of the plume evolution for the different environment conditions (Test 1). Results are presented at the depth of maximum concentration.

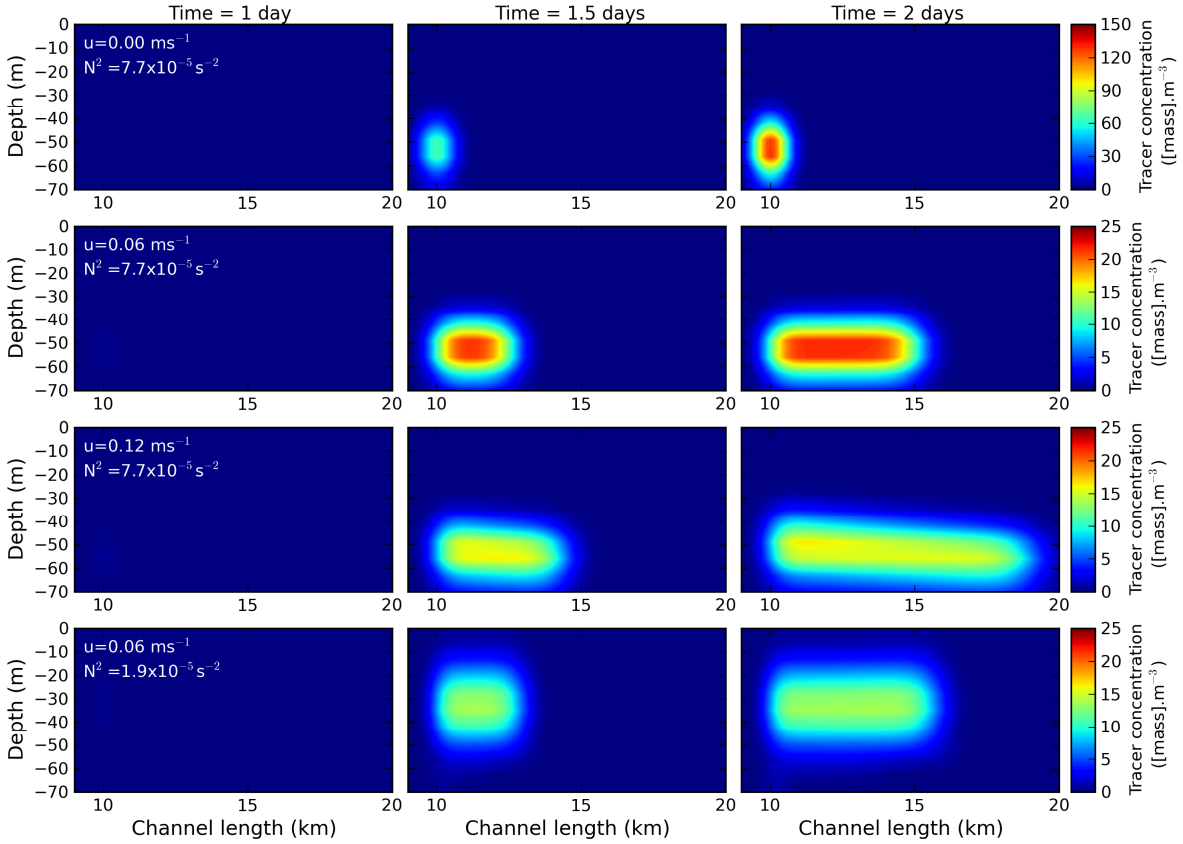

Figure III.1.7. Top to bottom, vertical section view of the plume evolution for the different environment conditions (Test 1). Results are presented in the center of the plume (y= 10 km).

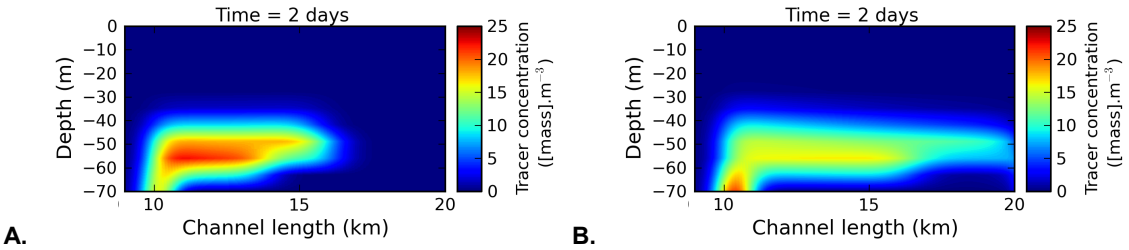

Figure III.1.8. Top to bottom, vertical section view of the plume after 2 days considering a drag coefficient of 0.002 for: A) current velocity of 0.06 m s^{-1} and B) current velocity of 0.12 m s^{-1}. Results are presented in the center of the plume (y= 10 km).

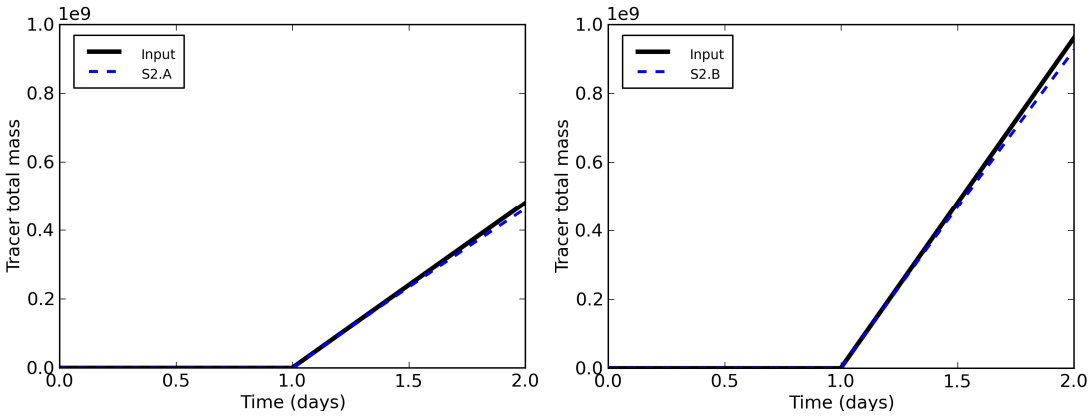

Figure III.1.9. Comparison between the initial mass imposed at the discharge and the total mass in the domain for the different environment conditions (Test 2).

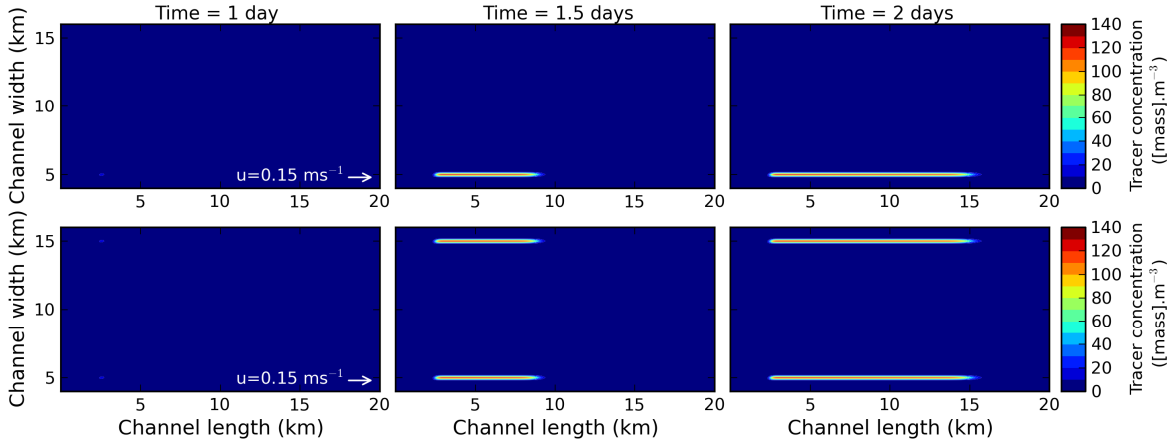

Figure III.1.10. Top view of the plume evolution for one and two discharges (Test 2, S2.A and S2.B). Results are presented at the surface.

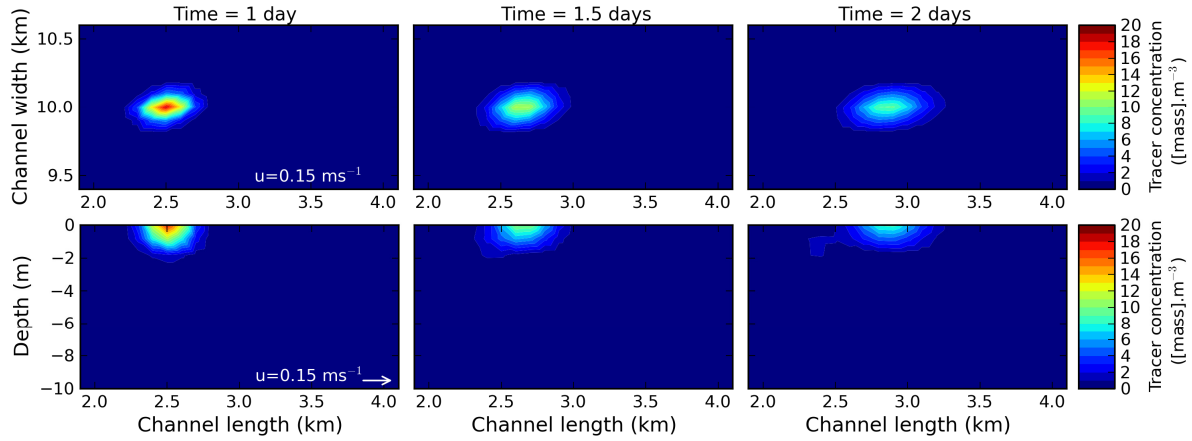

Figure III.1.11. Top (hotizontal) and top to bottom (vertical section) view of the plume evolution for the instantaneous discharge (Test 2, S2.C). Results are presented at the surface and in the center of the plume (y= 10 km).

III.1.4 SUMMARY

A near field model based on RSB model (Roberts *et al.*, 1989a,b) was coupled to the three-dimensional model SELFE (far field model), allowing the simulation of small scale, localized discharges for any generic tracer. The two models run simultaneously, so that the far field model provides the ambient conditions (current velocity and density) for the near field model, which in turn provides the initial conditions for the tracer in the far field model. The plume defined by the near field model is provided to the far field model following a three-dimensional Gaussian equation and taking into account the ambient concentration of the tracer.

A set of synthetic tests were performed for different environment and discharge conditions. Results showed the validity of the implementation performed. The coupled model is able to represent the plume with mass errors smaller than 1%. The model also responds to the different environment conditions as expected.

This recent extension of the SELFE model will increase its flexibility in future applications (e.g. simulation of wastewater outfall discharges).

III.1.5 REFERENCES

Adams EE, Kossik R, Baptista AM. Source representation in a numerical transport model, *Proceedings of the VI International Conference on Finite Elements in Water Resources*, LNEC: Lisbon, **1986**, 589-597.

Azevedo A. *Sistema integrado de modelação para apoio à prevenção e mitigação de acidentes de hidrocarbonetos em estuários e orla costeira*. PhD Thesis, University of Lisbon, **2010**.

Bleninger T, Jirka, G H. Near- and far-field model coupling methodology for wastewater discharges. Environmental hydraulics and sustainable water management, JHW Lee and KM Lam eds., Taylor & Francis, London, **2004**, 447–453.

Blumberg AF, Ji Z-G, Ziegler CK. Modeling outfall plume behaviour using far field circulation model, *Journal of Hydraulic Engineering* **1996**, 122(11), 610-616.

Choi KW, Lee JHW. Distributed entrainment sink approach for modelling mixing and transport in the intermediate field. *Journal of Hydraulic Engineering* **2007**, 113(7), 804-815.

Confederación Hidrográfica del Norte (1995). *Metodología de Estudio de los Saniamentos Litorales*, Edición Base, Oviedo, **1995**.

Doneker RL, Jirka GH.CORMIX User Manual: A hydrodynamic mixing zone model and decision support system for pollutant discharges into durface daters, EPA-823-K-07-001, **2007**.

Economopoulou MA, Economopoulos AP. Graphical sizing and analysis of ocean outfalls with buoyant plumes. *Journal of Environmental Engineering* **2001**, 127(1), 3-12.

Frick WE, Roberts PJW, Davis LR, Keyes J, Baumgartner DJ, George KP. *Dilution models for effluent discharges (Visual Plumes),* 4th Edition, Environmental Research Division, NERL, ORD, US Environmental Protection Agency, 2001.

Frick WE. Visual Plumes mixing zone modeling software. *Environmental Modelling & Software* **2004**, 19(7-8), 645-654.

Haidvogel DB, Arango H, Budgell WP, Cornuelle BD, Curchitser E, Di Lorenzo E, Fennel K, Geyer WR, Hermann AJ, Lanerolle L, Levin J, McWilliams JC, Miller AJ, Moore AM, Powell TM, Shchepetkin AF, Sherwood CR, Signell RP, Warner JC, Wilkin J. Ocean forecasting in terrain-following coordinates: Formulation and skill assessment of the Regional Ocean Modeling System. *Journal of Computational Physics* **2008**, 227(7), 3595-3624.

Jirka GH, Doneker RL, Barnwell TO. CORMIX: A comprehensive expert system for mixing zone analysis of aqueous pollutant discharges. *Water Science and Technology* **1991**, 24(6), 267-274.

Kim YD, Seo IW, Kang S W, Oh BC. Jet integral particle tracking hybrid model for single buoyant jets. *Journal of Hydraulic Engineering* **2002**, 128(8), 753–760.

Lee, JHW, Chu VH. Turbulent jets and plumes – A Lagrangian approach, Kluwer Academic Publishers, USA, **2003**.

Luettich RA, Westerink JJ, Sheffner NW. *ADCIRC: An Advanced Three-Dimensional Model for Shelves, Coasts and Estuaries. Report 1: Theory and Methodology of ADCIRC-2DDI and ADCIRC-3DL*. Department of the Army, US Army Corps of Engineers, **1991**.

Mellor GL. Mellor, Users' Guide for a Three-Dimensional, Prim-Itive Equation, Numerical Ocean Model (July 2002 version). Program in Atmospheric and Oceanic Sciences, Princeton University, **2002**, 42pp.

Pinto L, Fortunato AB, Zhang Y, Oliveira A, Sancho FEP. Development and validation of a three-dimensional morphodynamic modelling system for non-cohesive sediment. *Ocean Modelling*, in review.

Roberts PJW, Salas HJ, Reiff FM, Libhaber M, Labbe A, Thomson JC. *Marine Wastewater Outfalls and Treatment Systems*. IWA Publishing, UK, **2010**.

Roberts PJW, Snyder WH, Baumgartner DJ. Ocean outfalls. I: Submerged wastefield formation. *Journal of Hydraulic Engineering* **1989a**, 115(1), 1-25.

Roberts PJW, Snyder WH, Baumgartner DJ. Ocean outfalls. II: Spatial evolution of submerged wastefield. *Journal of Hydraulic Engineering* **1989b**, 115(1), 26-48.

Roberts PJW. Sea Outfalls, Environmental Hydraulics, Singh VP and Hager WH eds., Water Science and Techonology Lybrary, Kluwer Academic Publishers, The Netherlands, **1996**.

Roberts, PJW. Line plume and ocean outfall dispersion. *Journal of Hydraulics Division* **1979**, 105(4), 313-331.

Rodrigues M, Oliveira A, Guerreiro M, Fortunato AB, Menaia J, David LM, Cravo A. Modeling fecal contamination in the Aljezur coastal stream (Portugal), *Ocean Dynamics* **2011**, 61(6), 841-856.

Rodrigues M, Oliveira A, Queiroga H, Brotas V. Seasonal and diurnal water quality modelling along a salinity gradient (Mira channel, Aveiro lagoon, Portugal. *Procedia Environmental Sciences* **2012**, 899-918.

Rodrigues M, Oliveira A, Queiroga H, Fortunato AB, Zhang YJ. Three-dimensional modeling of the lower trophic levels in the Ria de Aveiro. *Ecological Modelling* **2009**, 220(9-10), 1274-1290.

RPS MetOcean. Hydrodynamic modelling program for the proposed Gunns Pulp Mill, Report no. 2: coupling near and far-field models, **2010**.

Suh SW. A hybrid near-field/far-field thermal discharge model for coastal areas. *Marine Pollution Bulletin* **2001**, 43(7-12), 225-233.

Zhang X.-Y., Adams EE. Prediction of near field plume characteristics using far field circulation model. *Journal of Hydraulic Engineering* **1999**, 125(3), 233-241.

Zhang Y, Baptista AM. SELFE: A semi-implicit Eulerian-Lagrangian finite-element model for cross-scale ocean circulation. *Ocean Modeling* **2008**, 21(3-4), 71-96.

SECTION III.2

SENSITIVITY ANALYSIS OF AN ECOLOGICAL MODEL APPLIED TO THE RIA DE AVEIRO[III.2.1]

ABSTRACT

Ecological models can be useful tools for understanding the dynamics of the estuarine and coastal ecosystems. However, the application of these models in real systems requires the specification of many empirical input parameters, which are in general difficult to quantify for a specific site. This study presents a sensitivity analysis on the input parameters of the model ECO-SELFE applied to the Ria de Aveiro. ECO-SELFE is a three-dimensional, unstructured grid, fully-coupled hydrodynamic-ecological model. The sensitivity analysis is based on a previous analysis using the zero-dimensional ecological model, where one parameter was varied with the others being held constant. Results show that phytoplankton growth rate and zooplankton excretion and mortality rates are the parameters that influence the results the most. The degree of influence of these parameters depends on the local concentrations of zooplankton and phytoplankton. These two ecological variables are also most affected by the variations in the input parameters.

KEYWORDS

Ecological Models, Input Parameters, Sensitivity Analysis, Coastal Lagoon

[III.2.1] Published in: *Journal of Coastal Research* 2009, SI56, 448-452.

III.2.1 INTRODUCTION

Ecological models are very useful tools for estuarine and coastal management. Duly validated, these models can be used to help understand processes, to diagnose the status of the system and to predict its evolution, or to evaluate management scenarios.

The first ecological models were very simple (e.g. Riley, 1946). Commonly, these models considered only one phytoplankton group and one single nutrient for phytoplankton growth. The increase of the computational power contributed significantly for the growing complexity in ecological modelling and, presently, several complex three-dimensional ecological models are available, like NEMURO (Kishi *et al.*, 2007), and ECO-SELFE (Rodrigues *et al.*, 2008; Rodrigues *et al.*, 2009).

Snowling and Kramer (2001) verified that the sensitivity of the ecological models increased with their complexity, due to the structure of the interactions between parameters and variables, and the larger number of degrees of freedom. The higher complexity of the models entails a larger number of processes represented and, consequently, more input parameters are needed to establish the model. These parameters are often poorly known for a specific site. Thus, one of the major difficulties associated with the use of complex ecological models is the definition of the input parameters.

Sensitivity analyses, which allow the estimation of the change in the model solution due to the change in the input parameters, have an important role in the implementation of ecological models. Several questions can be addressed by sensitivity analyses, as highlighted by Cariboni *et al.* (2007):

> *Which are the input factors that influence the outputs the most?*
>
> *If the uncertainty of one input factor could be eliminated, which one should be chosen to minimize the variance of the output?*
>
> *Are there some input factors whose effect on the output is so low that they can be confidently fixed anywhere in their ranges of variation?*

Several methods are available to perform sensitivity analyses (e.g. Hamby, 1994). These methods can be *quantitative* or *qualitative* (Cariboni *et al.*, 2007). They can also be *local*, when the effect of the variation of a single factor is evaluated, or *global*, otherwise (Cariboni *et al.*, 2007), and have been widely applied to different ecological models (e.g. Yoshie *et al.*, 2008)

The aim of this paper is to perform a sensitivity analysis on the input parameters of ECO-SELFE. Previous studies with the zero-dimensional version of the model showed the importance of some parameters, namely those related to phytoplankton growth and zooplankton dynamics (Rodrigues *et al.*, 2008). Here, the sensitivity analysis is performed to the three-

dimensional model applied to a real system, the Ria de Aveiro, where ECO-SELFE was previously validated (Rodrigues *et al.*, 2009).

III.2.2 METHODOLOGY

III.2.2.1 Study Area

The Ria de Aveiro is a shallow temperate coastal lagoon located on the Northwest (NW) coast of Portugal (40º38'N, 8º45'W). This lagoon is the habitat of several species of flora and fauna, and plays an important ecological role.

The lagoon is about 45 km long and 10 km wide (Figure III.2.1), and has an average depth of about 1 m (Dias *et al.*, 2000). It is connected to the ocean by an artificial tidal inlet about 20 m deep. This channel connects to the four main branches of the lagoon, through which the main sources of freshwater are supplied to the lagoon: the Mira, Ílhavo, Espinheiro and S. Jacinto channels (Figure III.2.1). The major sources of freshwater to the lagoon are the rivers Vouga and Antuã (Dias *et al.,* 2000). Smaller sources of freshwater also flow into the system, namely the rivers Boco, Caster and several small others in the Mira channel. Tides at the mouth of the lagoon are semi-diurnal, with a mean tidal range of about 2 m (Dias *et al.,* 2000).

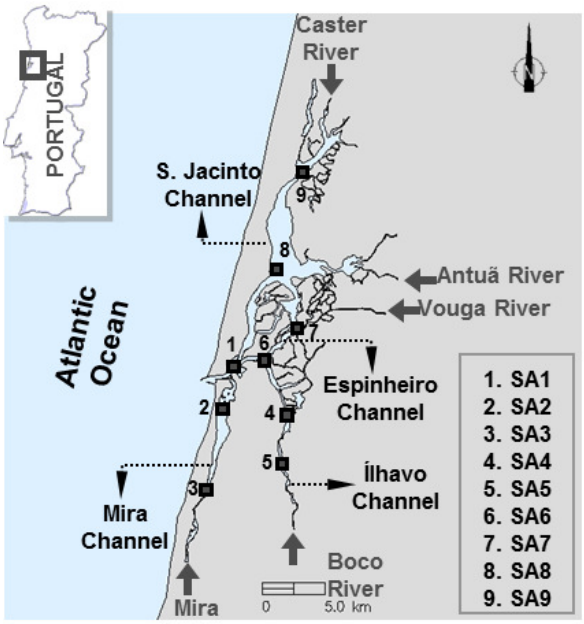

Figure III.2.1. General overview of the Ria de Aveiro and stations used in the sensitivity analysis (SA stations).

III.2.2.2 Model Description

ECO-SELFE (Rodrigues *et al.*, 2008), couples the three-dimensional hydrodynamic model, SELFE (Zhang and Baptista, 2008, available at www.stccmop.org/CORIE/modeling/selfe/) and an ecological model. SELFE is an unstructured grid model, which solves the three-dimensional shallow-waters equations for the free-surface elevation, the water velocity, the salinity and the temperature. This model includes a user-defined transport module, allowing the solution of the transport equation for any user-defined tracer:

$$\frac{\partial C}{\partial t}+u\frac{\partial C}{\partial x}+v\frac{\partial C}{\partial y}+w\frac{\partial C}{\partial z}=\frac{\partial}{\partial z}\left(\kappa\frac{\partial C}{\partial z}\right)+F_c+\Lambda C \qquad \text{(III.2.1)}$$

where C is a generic tracer, (u,v,w) is the velocity, κ is the vertical eddy diffusivity, Fc is the horizontal diffusion and ΛC are the sources and sinks. The two models are coupled through the sources and sinks terms, calculated by the ecological model.

The ecological model was extended from model EcoSim 2.0 (Bisset *et al.*, 2004, available at www.myroms.org/) to account for the simulation of several groups of zooplankton (Rodrigues *et al.*, 2008). The model includes the cycles of carbon, nitrogen, phosphorus, silica and iron. Besides zooplankton, the model can simulate several phytoplankton groups, bacterioplankton, dissolved and particulate organic matter, inorganic nutrients and dissolved inorganic carbon (Figure III.2.2).

The coupled model is based on a finite-element/finite-volume numerical scheme. The domain is discretized horizontally with unstructured triangular grids and vertically with hybrid coordinates (*S* coordinates and *Z* coordinates), allowing for high flexibility in both vertical and horizontal directions.

The parallel version of the coupled model (version v2.0f) was used in this study, which allowed a significant improvement of the computational times. To improve computational efficiency, the optimal number of processors was previously evaluated. For this application this optimum number is about 20-24 processors (Figure III.2.3).

III.2.2.3 Model Setup

The simulations were performed with a horizontal grid of about 21000 nodes (Figure III.2.4) and a vertical grid with 7 *S* levels. Six open boundaries (one oceanic and five riverine) were considered. At the ocean boundary the model was forced by tidal elevations from the regional model of Fortunato *et al.* (2002). Salinity and temperature at the ocean boundary were set as 36 and 15 ºC, respectively. At the river boundaries, the flows used were: 31.3 $m^3 s^{-1}$ (Vouga), 10.3 $m^3 s^{-1}$ (Antuã), 8.5 $m^3 s^{-1}$ (Caster), 4.5 $m^3 s^{-1}$ (Boco) and 4.5 $m^3 s^{-1}$ (Mira). At these

boundaries, salinity was set to 0 and temperature was set to: 14.0 ºC (Vouga), 15.4 ºC (Antuã), 18.3 ºC (Caster), 17 ºC (Boco) and 15.5 ºC (Mira). The simulations were done for a period of 30 days, using a time-step of 90 s and a warm-up period of 2 days.

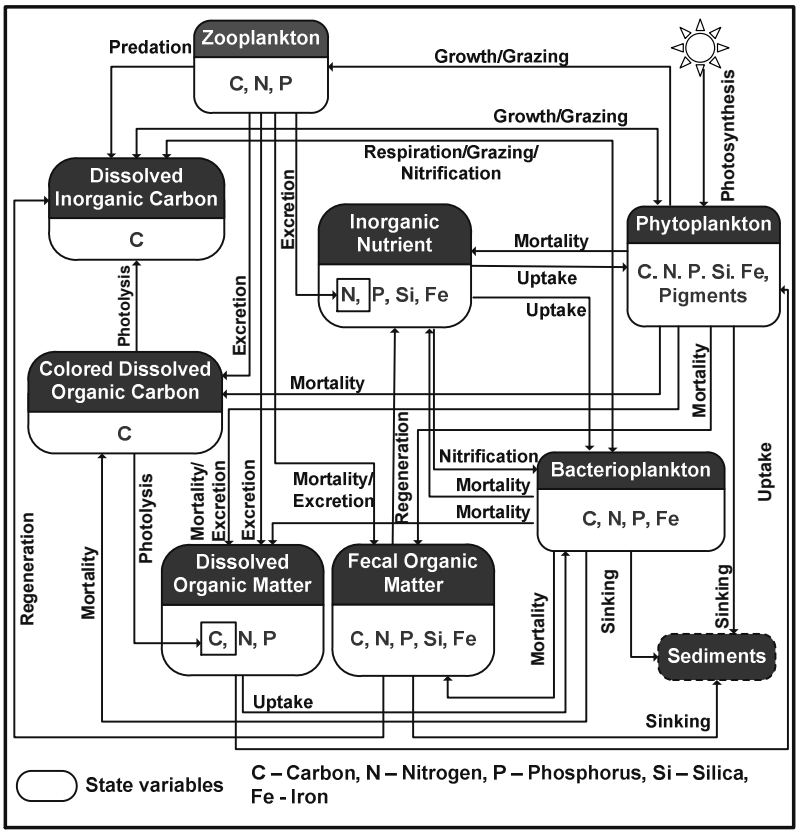

Figure III.2.2. Sources and sinks of the ecological model.

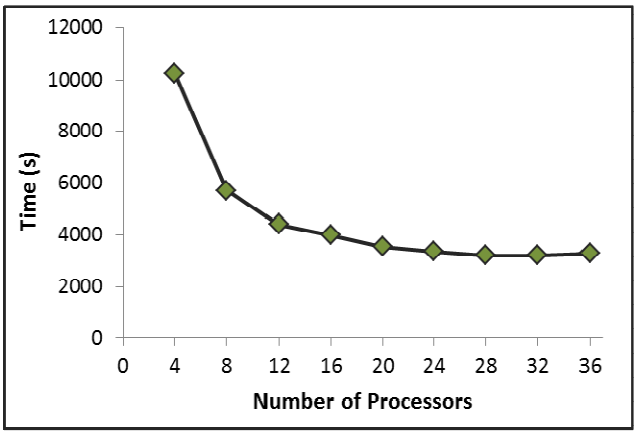

Figure III.2.3. Computational times (time needed to perform the simulation) vs. number of processors in the MEDUSA cluster (for SELFE).

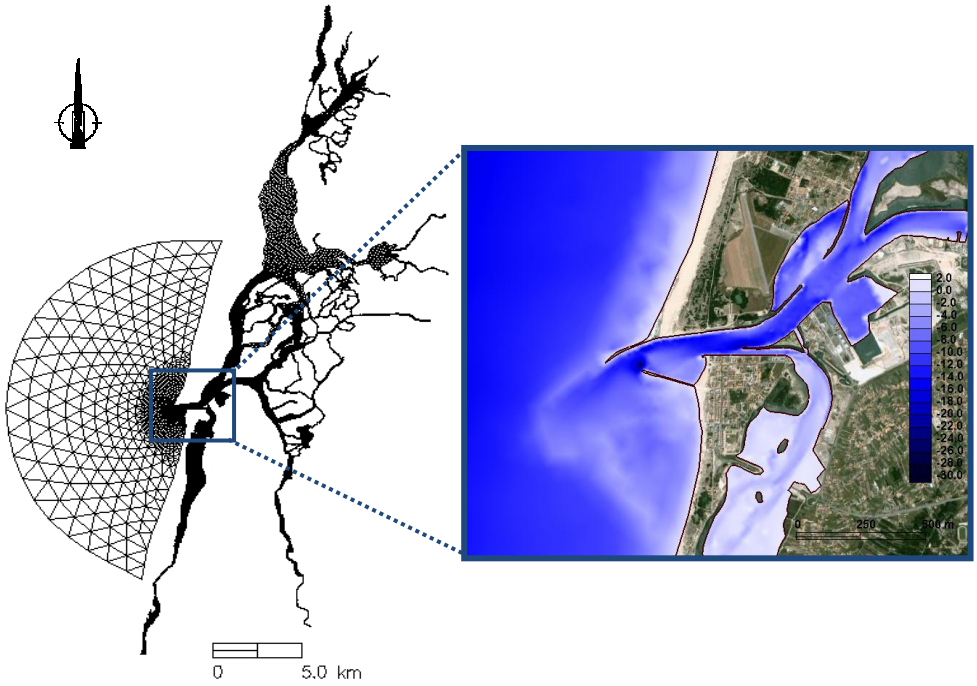

Figure III.2.4. Horizontal grid and detail of the inlet bathymetry (meters, relative to mean sea level).

III.2.2.4 Input Parameters Influence Analysis

The sensitivity analysis was performed for 20 input parameters, selected based on the results of the sensitivity analysis performed previously. Based on the previous approach (Rodrigues *et al.*, 2008) most parameters were changed in a range of -50% and +100% from a base value (generating 3 different values for each parameter), while the other parameters remained constant[III.2.2]. However, this range was unrealistic for some parameters. Hence, base temperature for phytoplankton growth was changed between 20 ºC and 30 ºC and the proportions of material released to organic and inorganic pools were changed such that their sum is always 1. The availability of prey to predator was changed between 0.5 and 1. The base values are listed in Table III.2.1.

The analysis was performed for the average values of the ecological tracers in each branch and in the whole lagoon. A group of hypothetical stations (SA stations) located along the lagoon was also used to analyse the results (Figure III.2.1). The analysis was performed with the results of the last 15 days of simulation.

[III.2.2] Based on the review for half-saturation constants for nutrients uptake presented in Chapter II, Section II.1 some additional tests to these parameters were performed and are presented in that chapter.

Table III.2.1. Sensitivity analysis: input parameters and base values.

Parameter[1]	Value
1. Half-saturation for NO_3 uptake (mmol NO_3 m^{-3})	0.824
2. Half-saturation for NH_4 uptake (mmol NH_4 m^{-3})	0.414
3. Half-saturation for SiO_2 uptake (mmol SiO m^{-3})	1.82
4. Half-saturation for PO_4 uptake (mmol PO_4 m^{-3})	0.0515
5. Maximum phytoplankton growth rate (day^{-1})	3.7
6. Base temperature for exponential growth (ºC)	27
7. Phytoplankton temperature factor ($ºC^{-1}$)	0.0633
8. Fraction of dissolved organic matter released by phytoplankton (n.d.)	0.333
9. Fraction of particulate organic matter released by phytoplankton (n.d.)	0.333
10. Inorganic matter released by phytoplankton (n.d.)	0.333
11. Phytoplankton excretion rate (day^{-1})	0.005
12. Phytoplankton natural mortality rate (day^{-1})	0.01
13. Fraction of dissolved organic matter released by zooplankton (n.d.)	0.333
14. Fraction of particulate organic matter released by zooplankton(n.d.)	0.333
15. Fraction of inorganic matter released by zooplankton (n.d.)	0.333
16. Availability of prey to predator (n.d.)	1
17. Half-saturation for zooplankton's food ingestion (mmol C m^{-3})	1.04
18. Assimilation efficiency of zooplankton's predators	0.5
19. Zooplankton excretion rate (day^{-1})	0.05
20. Zooplankton mortality rate (day^{-1})	0.046

[1]n.d. – non-dimensional

The influence of an individual parameter was calculated based on the rate of variation $\partial C_v/\partial X_p$, where C_v is the normalized state variable and X_p is the input value of the parameter p (see Table III.2.1). These values were normalized as:

$$C_v = \frac{c_{final} - c_{initial}}{c_{initial}} \quad \text{(III.2.2)}$$

$$X_p = \ln x_p \quad \text{(III.2.3)}$$

where $c_{initial}$ and c_{final} are, respectively, the initial and the final concentrations of the ecological variable, and x_p is the input parameter value used in the sensitivity analysis.

The total influence of the input parameters in the results of each state variable (ΔY) was evaluated as:

$$\Delta Y = \sum_p \frac{\partial C_v}{\partial X_p} \Delta X_p \quad \text{(III.2.4)}$$

where ΔY is the total influence of the input parameters on the state variable C_v and ΔX_p is the variation in the parameter p given by:

$$\Delta X_p = \frac{\Delta x_p}{x_b} \tag{III.2.5}$$

where Δx_p is the difference between the highest and the lowest values for the input parameter p, and x_b is the base value.

III.2.3 RESULTS AND DISCUSSION

Phytoplankton concentration is mostly influenced by the parameters that control its growth rate and the ones related to zooplankton excretion and mortality rates. This behaviour occurs throughout the lagoon (Figure III.2.5), but not uniformly.

Phytoplankton growth rate parameters are more influent in the Mira and Ílhavo channels and zooplankton loss parameters are more influent in the Espinheiro and S. Jacinto channels.

A more detailed analysis shows that zooplankton mortality rate is the input parameter which influences phytoplankton concentration the most in all SA stations, with the exception of stations SA3 and SA5 located in the Mira and Ílhavo channels, respectively (Figure III.2.6). At these two stations, phytoplankton concentration depends mostly on base temperature for growth and on phytoplankton maximum growth rate. Zooplankton concentrations in SA3 and SA5 are smaller (about 0.06 mg C l^{-1}) than in the other SA stations (about three times larger on average) and phytoplankton concentration is of the same order of magnitude (about 1 mg C l^{-1} on average). Since phytoplankton mortality depends on zooplankton biomass, these results suggest that the magnitude of the influence of the phytoplankton growth rate and zooplankton loss parameters depends on the local concentrations of these two ecological variables. Consequently, for higher zooplankton concentrations, zooplankton mortality and excretion rates affect phytoplankton concentrations more. For smaller zooplankton concentrations, the most influent parameters in phytoplankton concentrations are related to its growth rate.

Because the Espinheiro and S. Jacinto channels occupy a large fraction of the lagoon area, the influence of zooplankton loss parameters in phytoplankton concentrations is dominant when considering the Ria de Aveiro as a whole (Figure III.2.7). These results are consistent with those observed for zooplankton, which is mostly affected by its excretion and mortality rates (Figure III.2.5 and Figure III.2.7). Zooplankton and phytoplankton are the ecological variables most affected by the inputs parameters (Table III.2.2).

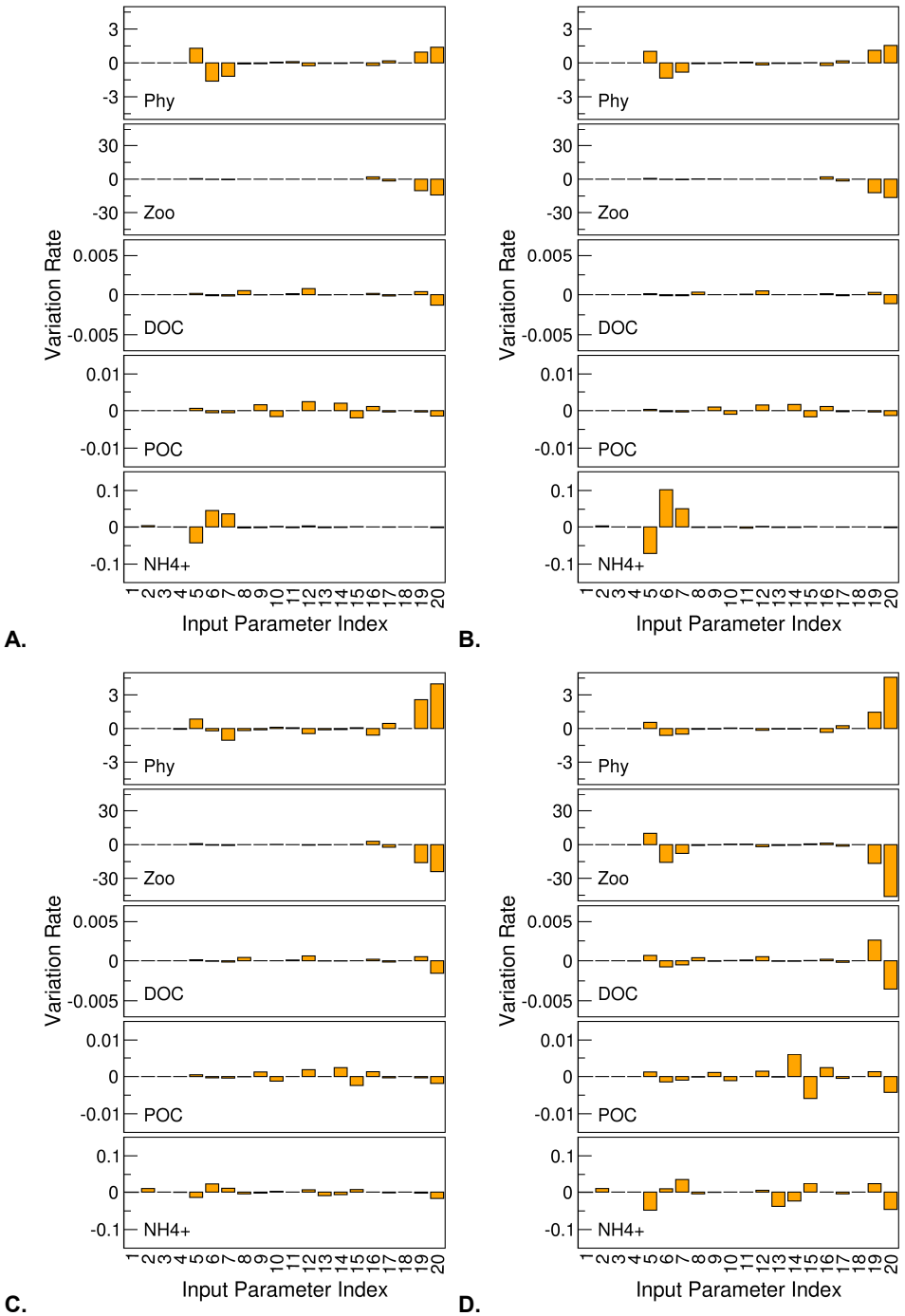

Figure III.2.5. Influence of the input parameters in: A) Mira channel, B) Ílhavo channel, C) Espinheiro channel and D) S. Jacinto channel (Phy: Phytoplankton; Zoo: Zooplankton; DOC: Dissolved Organic Carbon; POC: Particulate Organic Carbon; NH4+: Ammonium).

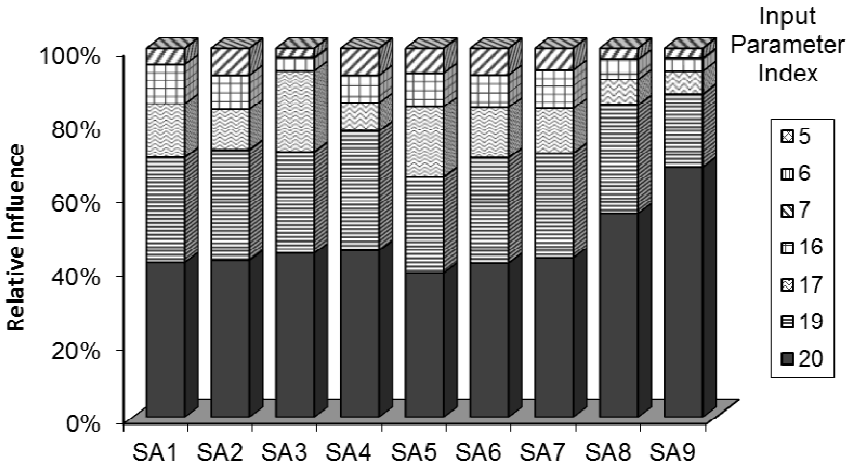

Figure III.2.6. Relative influence of the top-five most influential input parameter of phytoplankton concentration in each SA station.

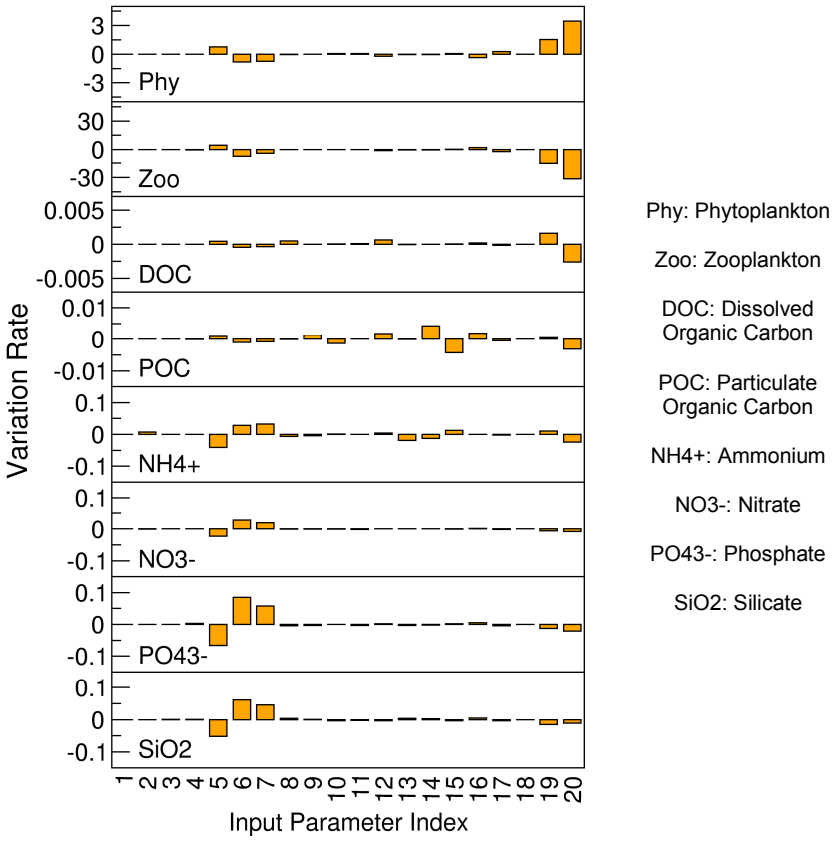

Figure III.2.7. Influence of the input parameters in the Ria de Aveiro.

Ammonium concentrations are mostly influenced by phytoplankton growth parameters in the Mira and Ílhavo channels (Figure III.2.5A and III.2.5B). In the S. Jacinto channel, where

zooplankton concentrations are larger, zooplankton loss terms also influence significantly ammonium (Figure III.2.5D). In the Ria domain, the other nutrients are also influenced by phytoplankton growth terms (Figure III.2.7), which shows the dependence between phytoplankton and nutrients concentrations, since phytoplankton growth depends on nutrient availability.

Dissolved organic carbon (DOC) and particulate organic carbon (POC) are, together with nutrients, the variables less affected by the input parameters (Table III.2.2). These two ecological variables are slightly affected by the parameters related to zooplankton and phytoplankton mortality rates (Figure III.2.5 and Figure III.2.7). POC is also influenced by the fractions of material released by zooplankton, which are the ones that affect this variable in the S. Jacinto channel the most (Figure III.2.5D).

Table III.2.2. Total influence (ΔY) of the input parameters in the ecological variables (RA: Ria de Aveiro; CM: Mira channel; CI: Ílhavo channel; CE: Espinheiro channel; CSJ: S. Jacinto channel)

Variable	ΔY				
	RA	CM	CI	CE	CSJ
Phytoplankton	0.37	0.15	0.19	0.47	0.45
Zooplankton	-3.8	-2.0	-2.3	-3.3	-5.2
DOC	-1.6×10^{-5}	-1.3×10^{-5}	-9.8×10^{-6}	-1.7×10^{-5}	-2.4×10^{-5}
POC	-1.4×10^{-4}	-6.7×10^{-6}	-5.7×10^{-5}	-8.5×10^{-5}	-2.1×10^{-4}
Ammonium	-2.0×10^{-3}	5.7×10^{-4}	2.4×10^{-4}	-8.6×10^{-4}	-3.8×10^{-3}
Nitrate	-9.4×10^{-4}	3.2×10^{-5}	-3.1×10^{-4}	-3.2×10^{-4}	-2.0×10^{-3}
Phosphate	-2.4×10^{-3}	3.2×10^{-4}	-4.8×10^{-4}	-4.1×10^{-4}	-7.4×10^{-3}
Silicate	-1.7×10^{-3}	3.0×10^{-4}	-	-1.8×10^{-4}	-4.1×10^{-3}

As environmental conditions vary seasonally, for some of the most influent parameters, some additional tests were performed for environmental conditions characteristic of summer periods, where river flows are lower and boundary temperatures are higher. In these simulations, the flows and the temperatures considered at the boundaries were: 3.92 $m^3 s^{-1}$ and 19.2 ºC (Vouga), 1.3 $m^3 s^{-1}$ and 19.9 ºC (Antuã), 1.1 $m^3 s^{-1}$ and 22.6ºC (Caster), 0.6 $m^3 s^{-1}$ and 20.4 ºC (Boco) and 0.6 $m^3 s^{-1}$ and 22.4 ºC (Mira). Averaging over the whole Ria, the results show that zooplankton mortality rate has a higher influence on phytoplankton concentration than phytoplankton maximum growth rate, for both types of river flows (Figure III.2.8). They also highlight the effect that zooplankton concentrations have on the magnitude of the influence of these parameters: during lower river flows periods, local concentrations of zooplankton are higher, which decreases the influence of phytoplankton maximum growth rate (Figure III.2.8A) and increases the influence of zooplankton mortality rate (Figure III.2.8B).

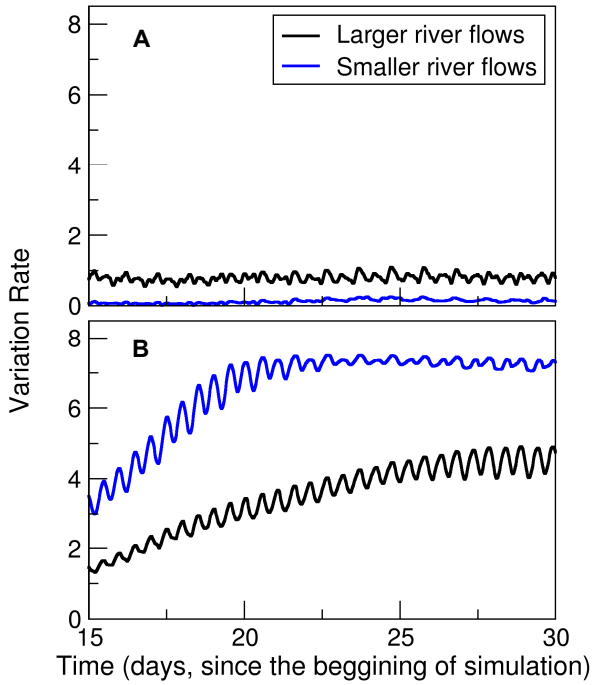

Figure III.2.8. Effects of the variation of A) phytoplankton maximum growth rate and B) zooplankton mortality rate in phytoplankton concentration for different environmental conditions, averaging over the whole Ria de Aveiro

III.2.4 CONCLUSIONS

This study highlighted the most influent parameters when implementing sophisticated ecological models in a real system. The parameters related to phytoplankton growth and zooplankton losses (mortality and excretion rates) are the ones that influence the results the most. These findings are similar to those achieved with the sensitivity analysis of the zero-dimensional ecological model (Rodrigues *et al.*, 2008). However, the three-dimensional model sensitivity analysis also evidenced that the influence of these parameters on phytoplankton concentration depends on the local concentrations of zooplankton. These results suggest that the simple model can be used in this type of analyses, providing that different phytoplankton and zooplankton concentrations are evaluated.

Similar studies with other ecological models also showed the larger influence of zooplankton and phytoplankton parameters on the final results of the models (e.g. Yoshie *et al.*, 2007). In particular, the larger influence of zooplankton mortality found here agrees with the findings of Steele and Henderson (1992), which showed that the definition of this parameter can have a larger influence on the ecological models' dynamics. Thus, when implementing these models in

real systems, phytoplankton and zooplankton parameters should be as accurate as possible, using site-specific data whenever it is available.

Future exploitation of the model sensitivity should account for the simultaneous variation of the input parameters, to evaluate their combined influence and, in particular, the feedback of the phytoplankton growth and zooplankton loss parameters on phytoplankton and zooplankton concentrations.

III.2.5 REFERENCES

Bisset WP, Debra S, Dye D. *Ecological Simulation (EcoSim) 2.0 Technical Description*, Tampa, Florida: Florida Environmental Research Institute, **2004**, 25pp.

Cariboni J, Gatelli D, Liska R, Saltelli A. The role of sensitivity analysis in ecological modelling. *Ecological Modelling* **2007**, 203, 167-182.

Dias JM, Lopes JF, Dekeyser I. Tidal propagation in Ria de Aveiro lagoon, Portugal. *Physics and Chemistry of the Earth* **2000**, 25, 369-374.

Fortunato AB, Pinto LL, Oliveira A, Ferreira JS. Tidally-generated shelf waves off the western Iberian coast. *Continental Shelf Research* **2002**, 22(14), 1935-1950.

Hamby DM. A review of techniques for parameter sensitivity analysis of environmental models. *Environmental Monitoring and Assessment* **1994**, 32(2), 135-154.

Kishi MJ, Kashiwai M, Ware DM, Megrey BA, Eslinger DL, Werner FE, Noguchi-Aita M, Azumaya T, Fujii M, Hashimoto S, Huang D, Iizumi H, Ishida Y, Kang S, Kantakov GA, Kim H, Komatsu K, Navrotsky VV, Smith SL, Tadokoro K, Tsuda A, Yamamura O, Yamanaka Y, Yokouchi K, Yoshie N, Zhang J, Zuenko YI, Zvalinsky ZI. NEMURO – a lower trophic level model for the North Pacific marine ecosystem. *Ecological Modelling* **2007**, 202, 12-25.

Rodrigues M, Oliveira A, Queiroga H, Fortunato AB, Zhang YJ. Three-dimensional modeling of the lower trophic levels in the Ria de Aveiro. *Ecological Modelling* **2009**, 220(9-10), 1274-1290.

Rodrigues M, Oliveira A, Queiroga H, Zhang YJ, Fortunato AB, Baptista AM. Integrating a circulation model and an ecological model to simulate the dynamics of zooplankton. In: Estuarine and Coastal Modeling Conference Book, Proceedings of the Tenth International Conference, Ed.: Malcom Spaulding, N.Y. ASCE **2008**, 427-446.

Snowling SD, Kramer JR. Evaluating modelling uncertainty for model selection. *Ecological Modelling* **2001**, 138, 17-30.

Steele JH, Henderson EW. The role of predation in plankton models. *Journal of Plankton Research* **1992**, 14, 157-172.

Yoshie N, Yamanaka Y, Rose KA, Eslinger DL, Ware DM, Kishi MJ. Parameter sensitivity study of the NEMURO lower trophic level marine ecosystem model. *Ecological Modelling* **2007**, 202, 26-37.

Zhang Y, Baptista AM. SELFE: A semi-implicit Eulerian-Lagrangian finite-element model for cross-scale ocean circulation. *Ocean Modeling* **2008**, 21(3-4), 71-96.

SECTION III.3

SEASONAL AND DIURNAL WATER QUALITY AND ECOLOGICAL DYNAMICS ALONG A SALINITY GRADIENT (MIRA CHANNEL, AVEIRO LAGOON, PORTUGAL)[III.3.1]

ABSTRACT

The patterns of water quality and ecological dynamics in estuaries vary at different time scales. Characterizing this variability at short (diurnal and seasonal) time scales is a pre-requisite to investigate the effects of long-term climate change. Seasonal scales depend mostly on the natural climatic variability, while diurnal scales are generally associated with the tidal cycle and wind events. In order to study the role of these superimposed scales in the Aveiro lagoon, an integrated approach, which combines data acquisition and numerical modelling, was followed. The analysis was conducted with the three-dimensional, fully coupled hydrodynamic and ecological numerical model, ECO-SELFE, extended to account for the oxygen cycle. For data acquisition three field campaigns were performed along a salinity gradient (Mira channel), covering different seasonal situations: March 2009, September 2009 and January 2010. These campaigns, each lasting 24 hours, included the measurement of physical, chemical and biological parameters (river flow, water levels, currents velocities, water temperature, salinity, dissolved oxygen, nutrients and chlorophyll *a*). Results show the ability of the model to represent both the spatial and temporal patterns observed for the different variables. Chlorophyll *a* and nutrients tend to present larger concentrations upstream than downstream, with the largest values observed in spring. The distribution patterns are significantly influenced by the tidal dynamics.

KEYWORDS

Chlorophyll *a*, Dissolved Oxygen, Nutrients, Tide

[III.3.1] Published in: *Procedia Environmental Sciences 2012*, 899-918.

III.3.1 INTRODUCTION

Ecological models are very useful tools for estuarine and coastal management. Duly validated, these models can be used to help understand processes, to diagnose the status of the system and to predict its evolution, or to evaluate management scenarios.

The complex dynamics of estuarine ecosystems depends on the interaction between several factors, being influenced by both natural forcings and anthropogenic activities. Among the natural forcings the combined effect of ocean tides and river flows is one of the main drivers of the estuarine dynamics. Estuaries also present attractive resources for human activities and are subject to different pressures, which may contribute to significant changes on their ecological quality and dynamics (e.g wastewater discharges, river flow regulation, sand extraction and other dredging activities).

The Aveiro lagoon is a coastal ecosystem located in the Northwest coast of Portugal (Figure III.3.1), valuable both at ecological and economical levels. It holds several habitats and anthropic activities (e.g tourism, port, fisheries/bivalve collection). In the last decades the Aveiro lagoon faced several issues that contributed to the degradation of its water quality (Lopes *et al.*, 2005). Some management measures were undertaken recently to improve the lagoon ecological quality (e.g. reduction of the nutrients loads discharged to the lagoon).

The interplay between the several drivers of the estuarine dynamics affects the time scales of the ecological processes, which vary from hours to years. Seasonal scales depend mostly on the natural climatic variability (e.g. seasonal variation in river flows and in the air temperature), while diurnal scales are generally associated with the tidal cycle and wind events. Besides seasonal and diurnal scales, long-term trends in estuarine ecological dynamics are also a matter of concern nowadays, in particular, those associated with climate change (Gameiro and Brotas, 2010).

Several possible impacts of climate change are identified for estuaries. Sea level rise, increases in air temperature and changes in regime flows predicted for 2100 (IPCC, 2007) may affect the forcing regimes of estuaries and, thus, their ecological dynamics. These impacts can affect the species abundance, productivity and composition, the food web and the system economical values, among others (Hays *et al.*, 2005; Smith *et al.*, 2008). However, to fully understand the role of these superimposed time scales and how climate change will affect the estuarine ecological dynamics, their possible impacts should be evaluated in the scope of the systems natural variability.

Integrated analyses, combining numerical modelling and data studies, are useful tools to understand estuaries dynamics. Numerical models, duly validated, are attractive to study the ecosystem for periods when data is unavailable, and also to predict scenarios (Grant *et al.*,

2005). In the last decade, due to the increase in the computational resources, water quality and ecological models have evolved significantly. Several models are now well established, e.g.: EcoSim 2.0 (Bisset *et al.*, 2004), ERSEM (Baretta-Bekker and Baretta, 1997) and NEMURO (Kishi *et al.*, 2007). In the Aveiro lagoon most of the past studies were based only on data measurements, and the studies of the water quality and ecological dynamics of the lagoon supported by numerical models are still scarce (e.g. Trancoso *et al.*, 2005; Lopes *et al.*, 2006; Lopes *et al.*, 2008; Rodrigues *et al.*, 2009b). Most of these studies are based on structured grids, leading to a coarse representation of the complex geometry of this ecosystem, and have not addressed all relevant time and spatial scales.

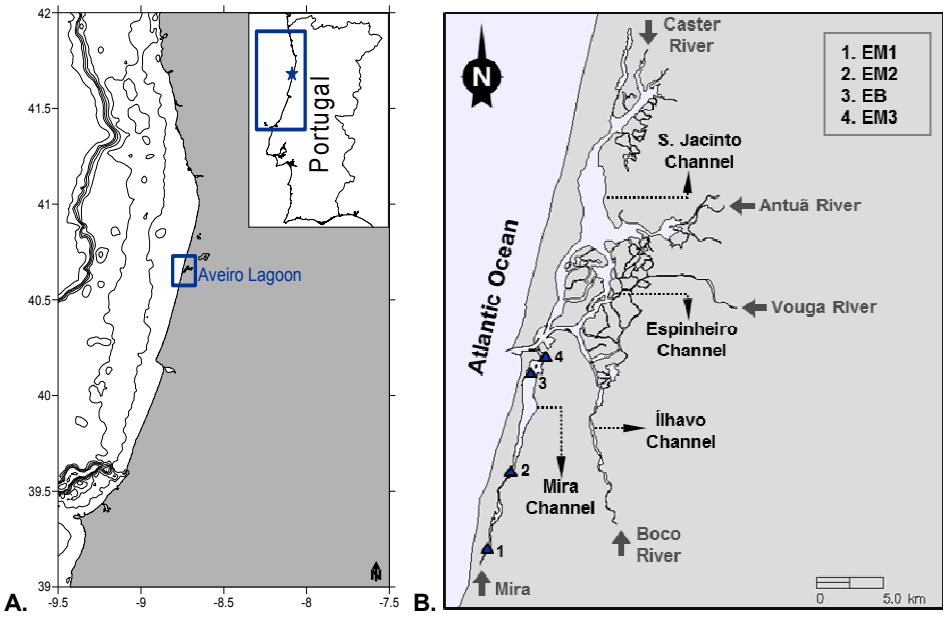

Figure III.3.1. Location of the: A) Aveiro lagoon and B) sampling stations along the Mira channel.

Thus, the main goal of this study is to investigate the combined impacts of climate change and anthropogenic pressures in the water quality and ecological dynamics of the Aveiro lagoon. A first step to achieve this goal is the extension the ecological model ECO-SELFE (Rodrigues *et al.*, 2009b) to simulate the oxygen cycle and its validation along a salinity gradient in the Aveiro lagoon for different temporal scales, which is presented in this paper. The combined analysis of data and model results will also allow a better understanding of the ecological/water quality processes occurring in this system and contribute to improve the knowledge of the system natural variability. Thus, the methodological approach used aimed to analyse the ecological dynamics of the lower trophic levels in the Aveiro lagoon along a salinity gradient, and, simultaneously, to validate the new developments of the model for different temporal and spatial scales. A set of specific field campaigns were established covering a one-year period. Model

simulations were performed using a two-step approach to optimize the computational times, since the hydrodynamic model is about 2-3 times faster than the coupled hydrodynamic-ecological model. Thus, validation was performed first for the hydrodynamic model and then for the coupled model.

III.3.2 STUDY AREA

The Aveiro lagoon is about 45 km long and 10 km wide, covering an area that, during spring tides, varies from 66 km^2 at low tide to 83 km^2 at high tide (Dias and Lopes, 2006). The lagoon is separated from the sea by a sandbar and connects to it through an artificial inlet. From this inlet the lagoon spreads in four main branches: Mira, S. Jacinto, Ílhavo and Espinheiro channels (Figure III.3.1B). These four main channels have several narrow channels and interconnections enhancing the complexity of this system. The exception is the Mira channel which behaves as a sub-estuarine system, and for this reason was chosen to the development of this study. The lagoon is very shallow with mean depths of 1 m (Dias *et al.*, 2000) and maximum depths of about 20 m in the artificial channel near the inlet. Tides at the mouth are semi-diurnal ranging from 0.6 m in neap tides to 3.2 m in spring tides, and have a mean tidal range of 2 m (Dias *et al.*, 2000). The tidal prism in the mouth is of about $70x10^6$ m^3 in spring tides, 10% of which flows to the Mira channel (Dias *et al.*, 2000). Freshwater flows into the lagoon from the upstream areas of the four main channels. The main sources of freshwater are the rivers Vouga and Antuã (Dias and Lopes, 2006; Dias *et al.*, 2000), but some uncertainty remains about the flows in the lagoon. Annual average flows found in the literature vary from 29-50 $m^3 s^{-1}$ for the Vouga river, and from 2-5 $m^3 s^{-1}$ for the Antuã river (Dias and Lopes, 2006; Dias *et al.*, 2000). In the other channels the river flows are lower, but there is a significant lack of data. In the Mira channel, in particular, the freshwater flow is poorly known (Dias and Lopes, 2006). Residence times in the lagoon, defined as Dias *et al.* (2001), vary from less than 2 days near the mouth to more than 1 week in the upstream areas of the channels. More detailed descriptions of the lagoon can be found in Dias *et al.* (2000) and references therein.

III.3.3 DESCRIPTION OF THE FIELD CAMPAIGNS[III.3.2]

Three field campaigns were performed in the Mira channel on: March 29-31, 2009, September 15-17, 2009, and January 27-29, 2010. Samplings of physical, chemical and biological parameters were collected at four stations (Figure III.3.1B). Additionally, the main rivers flowing

[III.3.2] Appendix I presents the full data collected during the field campaigns and some photos of the sampling stations.

into the lagoon were also sampled: Poço da Cruz (Mira), Ouca (Boco), Angeja (Vouga), Estarreja (Antuã) and Ribeira-Ovar (Caster), to provide boundary conditions for the model.

At the stations along the Mira channel, measurements were performed during a 24 hour period and started on the second day of the campaign. The exception was station EM3 (Navio-Museu) where measurements of water levels started in the first day of the campaigns and lasted for 42 hours periods with 10 minute intervals (pressure gauge – LevelTroll 500). Water levels and current velocities (electromagnetic current meter) were measured with 1 hour intervals at station EB (Costa Nova). At stations EM2 (Vagueira) and EM3 (Areão) water levels were measured with 3 hours intervals using graduate rulers. In-situ measurements of salinity, water temperature and dissolved oxygen were done at all stations using multiparametric probes (YSI 556 and STD Anderaa). At station EB, a CTD with a fluorimeter was also used (NXIC CTD). Water samples were collected at all stations. For chlorophyll *a* analysis, filtration of 0.5 l triplicate samples through Whatman GF/C filters was done. Sampling was performed at 2 levels in the water column (surface and bottom), with 3 hours intervals at EM stations. At station EB the sampling interval was lower (1 hour for in-situ measurements and 2 hours for water sampling) and was done at 3 levels (surface, mid-depth and bottom). At the rivers, flows were measured, water samples were collected and in-situ measurements of salinity, water temperature and dissolved oxygen were performed.

Water samples for the determination of chlorophyll *a* and nutrients concentrations were analysed in laboratory. Chlorophyll *a* was determined espectrophotometrically after extraction with 90% acetone (following Lorezen (1967)). Ammonium (NH_4^+) was quantified following the indophenol blue method (Koroleff, 1969). Nitrates + nitrites (NO^{3-}+NO^{2-}), phosphates (PO_4^{3-}) and silicates (SiO_2) analyses were performed in an autoanalyser (FIAstar 5000 Analyzer). Nitrates (including nitrites) were determined by the sulfanilic acid method after reduction of nitrates to nitrites in a cadmium column (Grasshoff, 1976). Phosphates were determined by the molibdate blue method of Murphy and Riley (1962). Silicates were determined by reaction with molibdate, and then reduced to form a heteropoly blue complex (Famming and Pilson, 1973).

III.3.4 MODEL DESCRIPTION AND IMPLEMENTATION IN THE AVEIRO LAGOON[III.3.3]

III.3.4.1 Physical and Numerical Formulation

ECO-SELFE couples the hydrodynamic model SELFE (Zhang and Baptista, 2008; parallel version 3.1c, available at www.stccmop.org/CORIE/modeling/selfe/) and an ecological model.

[III.3.3] Appendix II presents a preliminary validation of the formulation for the oxygen cycle in a small coastal stream.

SELFE is an unstructured grid model that simulates the baroclinic circulation across river-to-ocean scales. The model solves the shallow water equations and computes the free surface elevation and the three-dimensional fields of velocity, salinity and temperature. The model has a user-defined transport module that allows the simulation of any given tracer:

$$\frac{\partial C}{\partial t} + u\frac{\partial C}{\partial x} + v\frac{\partial C}{\partial y} + w\frac{\partial C}{\partial z} = \frac{\partial}{\partial z}\left(\kappa\frac{\partial C}{\partial z}\right) + F_c + \Lambda C \qquad \text{(III.3.1)}$$

where C is a given tracer concentration, (u,v,w) is the velocity (m s^{-1}), κ is the vertical eddy diffusivity (m^2 s^{-1}), F_c represents the horizontal diffusion term and ΛC is the sources and sinks term. The two models are coupled through the last term of Equation III.3.1.

The ecological model formulation is derived from EcoSim 2.0 – Ecological Simulation (Bisset *et al.*, 2004). In its base formulation EcoSim2.0 allows the simulation of several ecological tracers (phytoplankton, bacterioplankton, dissolved and particulate organic matter, inorganic nutrients and dissolved inorganic carbon) for the carbon, nitrogen, phosphorus, silica and iron cycles. In previous works this model was extended to simulate zooplankton tracers (Rodrigues *et al.*, 2008). In the present study the model was extended to simulate the oxygen cycle due to its relevance in evaluating the ecological status of water bodies (e.g. Water Framework Directive). Thus, besides the ecological tracers of the EcoSim 2.0, ECO-SELFE also simulates several groups of zooplankton, dissolved oxygen and chemical oxygen demand. Figure III.3.2 presents the source and sink terms of the ecological model and section III.3.4.2 describes the recently implemented oxygen cycle.

Numerically ECO-SELFE uses a finite elements/finite volumes scheme. The domain is discretized horizontally with unstructured grids and vertically with hybrid *SZ* coordinates. Salinity and temperature advection can be solved with Eulerian-Lagragian Methods (ELM), upwind or TVD schemes. For ecological tracers only upwind and TVD schemes are available.

More detailed descriptions of the model formulation can be found in Bisset *et al.* (2004), Rodrigues *et al.* (2008), Zhang and Baptista (2008) and Rodrigues *et al.* (2009b).

III.3.4.2 Oxygen Cycle

3.4.2.1 DISSOLVED OXYGEN

Dissolved oxygen (DO) is mainly defined as proposed by Vichi *et al.* (2007), considering an additional term relative to re-aeration (physical exchanges with the atmosphere). The changes in the DO concentration result from the gains due to the gross primary production and re-aeration (imposed only at the surface boundary), and the losses from phytoplankton, zooplankton and bacterioplankton respiration, the nitrification and the pelagic chemical reactions:

$$\Lambda DO = \Omega^{O}_{C}\sum_{i}\left(\mu_{r\_i}PC_i - respP_i\right) - \Omega^{O}_{C}\sum_{l} respZ_l - \Omega^{O}_{C} f_B respB - \Omega^{O}_{N} AtoN - \frac{1}{\Omega^{S}_{O}} COD \qquad \text{(III.3.2)}$$

where ΛDO are the sources and sinks terms of DO (mmol O_2 m^{-3}), Ω^{O}_{C} is the stoichiometric coefficient to convert carbon to oxygen units (mmol O_2 mmol C^{-1}), i is the phytoplankton groups index, μ_{r_i} is the realized growth rate of the phytoplankton group i (day^{-1}), PC_i is the phytoplankton carbon concentration of the group i (mmol C m^{-3}), $respP_i$ is the respiration of the phytoplankton group i, f_B is the oxygen regulating factor (non-dimensional, nd.), $respB$ is the bacterioplankton respiration, l is the zooplankton groups index, $respZ_l$ is the respiration of the zooplankton group l, $reaer$ is the reaeration, Ω^{O}_{N} is the stoichiometric coefficient to convert nitrogen units to oxygen units (mmol O_2 mmol N^{-1}), $AtoN$ is the nitrification (mmol N m^{-3}), Ω^{S}_{O} is the stoichiometric coefficient to convert sulfur to oxygen units (mmol S mmol O_2^{-1}) and CDO is the chemical oxygen demand concentration (mmol O_2 m^{-3}).

Phytoplankton respiration ($respP$) is defined as Vichi *et al.* (2007):

$$respP_i = b_{Pi} Q_{Pi}^{\frac{T-10}{10}} PC_i + \gamma_{Pi}\left(\mu_{r\_i}PC_i - e_i PC_i\right) \qquad \text{(III.3.3)}$$

where b_{Pi} is the basal specific respiration rate (day^{-1}), Q_{Pi} is a temperature coefficient for phytoplankton (nd.), T is the water temperature (ºC), γ_{Pi} is the fraction of assimilated production (nd.) and e_i the excretion rate (day^{-1}). The realized growth rate is defined as the minimum growth based on light or nutrient availability (Bisset *et al.*, 2004).

Zooplankton respiration ($respZ$) is defined as Vichi *et al.* (2007):

$$respZ_l = b_{Zl} Q_{Zl}^{\frac{T-10}{10}} ZC_l + (1-\beta_{Zl})(1-\eta_{Zl})\mu_{z\_l} ZC_l \qquad \text{(III.3.4)}$$

where b_{Zl} is the basal specific respiration rate (day^{-1}), Q_{Zl} is a temperature coefficient for zooplankton (nd.), ZC_l is the zooplankton carbon concentration (mmol C m^{-3}), β_{Zl} is the excreted fraction of uptake (nd.), η_{Zl} is the assimilation efficiency (nd.) and μ_{z_l} is the zooplankton growth rate due to food ingestion (day^{-1}). The zooplankton growth rate due to food ingestion is calculated following Rodrigues *et al.* (2008). The excreted fraction is defined as the ratio between the zooplankton growth and excretion rates (day^{-1}).

Bacterioplankton respiration ($respB$) is defined as Vichi *et al.* (2007):

$$respB = b_B Q_B BC + (1 - GGE_C + GGE^{O}_{C}(1-f_B))\rho_B \qquad \text{(III.3.5)}$$

where b_B is the basal specific respiration rate of bacterioplankton (day^{-1}), Q_B is a temperature coefficient for bacterioplankton (nd.), GGE_C is the growth efficiency (nd.), GGE_C^{O} is the decrease in growth efficiency under anoxic conditions (nd.) and ρ_B is the bacterioplankton

uptake. The bacterioplankton uptake is the defined as the minimum uptake from the available resources (Bisset *et al.*, 2004). The oxygen regulating factor is calculated as Vichi *et al.* (2007):

$$f_B = \frac{DO^3}{DO^3 + K_{sB\_O}} \tag{III.3.6}$$

where K_{sB_O} is the half-saturation constant for oxygen limitation (mmol O_2 m^{-3}).

The oxygen reaeration (reaer) is imposed only at the surface boundary and is calculated as proposed by Hull *et al.* (2008):

$$reaer = K_{reaer}(DO_{sat} + DO_w - DO) \tag{III.3.7}$$

where K_{reaer} is the reaeration coefficient (m day^{-1}), DO_{sat} is the oxygen concentration at saturation (mmol O_2 m^{-3}), DO_w is the increment to the saturation value due to the wind stress (mmol O_2 m^{-3}) and DO is the actual oxygen concentration. The use of DO_w is optional and user-defined. Two alternative formulations are available for K_{reaer}: Thomman and Muller (1987) and Wanninkhof (1992). DO_{sat} is given by Weiss (1970) and DO_w is given by Hull *et al.* (2008).

3.4.2.2 CHEMICAL OXYGEN DEMAND

The chemical oxygen demand (COD) represents the reduced elements that can be oxidized by inorganic means, implying the oxygen consumption. A similar approach to the one adopted by Vichi *et al.* (2007), where this variable is mostly regarded as sulfur (S), was chosen. The reduced elements are produced as a result of bacterial anoxic respiration and are used for the denitrification processes:

$$\Lambda COD = \Omega_C^S \Omega_C^O (1 - f_B) respB - \Omega_C^S \Omega_C^O \, AtoDenit - reox \tag{III.3.8}$$

where *AtoDenit* is the denitrification, *reox* is the reoxidation, Ω^S_C is the stoichiometric coefficient to convert sulfur to carbon units (mmol S mmol C^{-1}) and the first term represents the metabolic formation of reduction equivalents (Vichi *et al.*, 2007).

Denitrification and reoxidation are calculated as proposed by Vichi *et al.* (2007):

$$AtoDenit = Denit\left[\frac{1}{\mathrm{M}}\Omega_C^O(1 - f_B) respB\right] NO_3 \tag{III.3.9}$$

$$reox = reox\_COD \; Q_{COD}^{\frac{T-10}{10}} \frac{DO}{DO + K_{S\_COD}} COD \tag{III.3.10}$$

where *Denit* is the specific denitrification rate (day^{-1}), *M* is the reference anoxic mineralization rate (mmol O_2 m^{-3} day^{-1}), *reox_CDO* is the specific reoxidation rate (day^{-1}), Q_{COd} is the a

temperature constant for CDO (nd.) and K_{s_COD} is the half-saturation constant for COD (mmol O_2 m^{-3}).

Changes in the ecological model implied also changes on other tracers formulations, namely phytoplankton, zooplankton, bacterioplankton, nitrates and dissolved inorganic carbon.

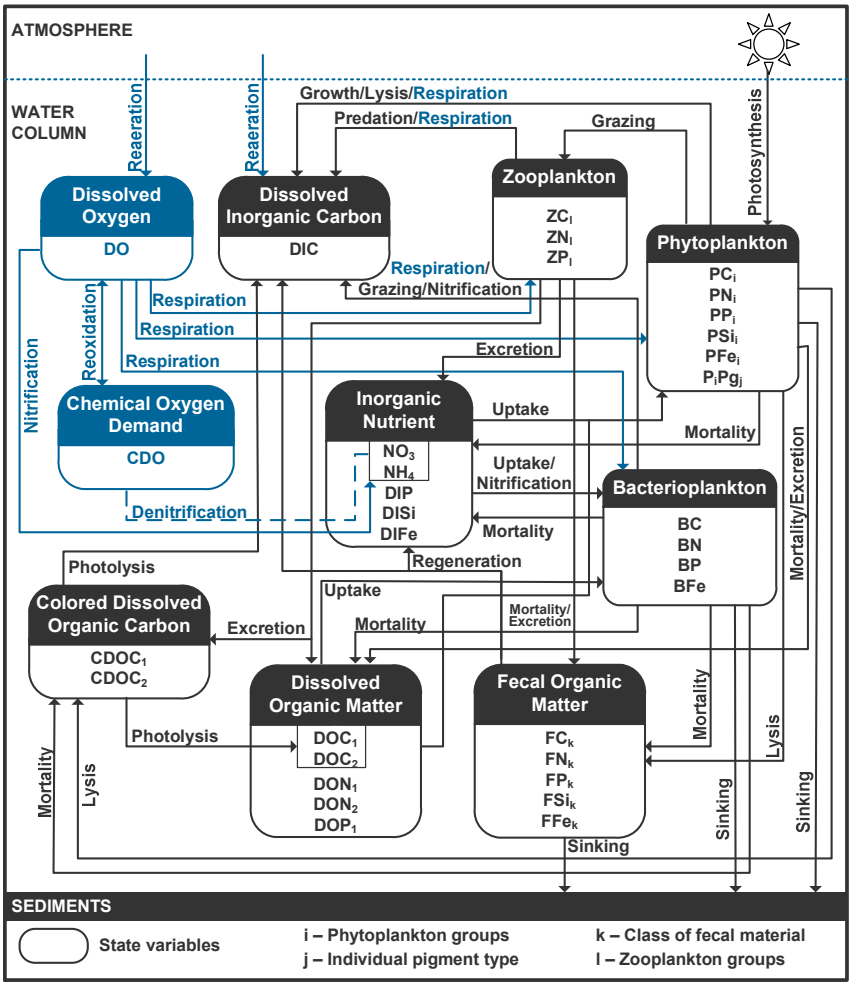

Figure III.3.2. Source and sink terms of the ecological (black lines represent the previous variables of the model and blue lines represent the new variables for the oxygen cycle). C – Carbon, N – Nitrogen, P – Phosphorus, Si – Silica, Fe – Iron.

III.3.4.3 Model Setup

The model setup was derived from Rodrigues *et al.* (2009b). The grid was refined and the bathymetry near the mouth was updated, based on 2008 data. For hydrodynamic simulations the horizontal domain was discretized in a grid with 31000 nodes, with a resolution varying from 1.5 km in the coastal area to 2 m in the narrow channels (Figure III.3.3A). Vertically, 7 equally spaced *S* levels were used. A spatially varying bottom roughness from 0.07 cm in the coastal

area to 0.02 cm upstream (Dias and Lopes, 2006) was considered. For turbulence closure, the Generic Length Scale KKL model with Kantha & Clayson's stability function was used. Simulations were performed for 1 year (March 2009 to February 2010) with a warm-up period of 2 days and a time step of 30 seconds.

Six open boundaries were considered. The oceanic boundary was forced with 14 tidal constituents (Z0, MSF, M2, S2, N2, K2, O1, K1, P1, Q1, M4, MN4, MS4 e M6) from the regional model of Fortunato *et al.* (2002). Riverine boundaries (Vouga, Antuã, Boco and Caster and Mira) were forced with monthly varying flows. For the periods of the campaigns measured values were used, while for the rest of the period historical data was used, using an approach similar to the one described in Rodrigues *et al.* (2009b). For the Mira channel freshwater flow was set to 0.7 $m^3 s^{-1}$, 0.1 $m^3 s^{-1}$ and 3.5 $m^3 s^{-1}$ for March, September and January, respectively.

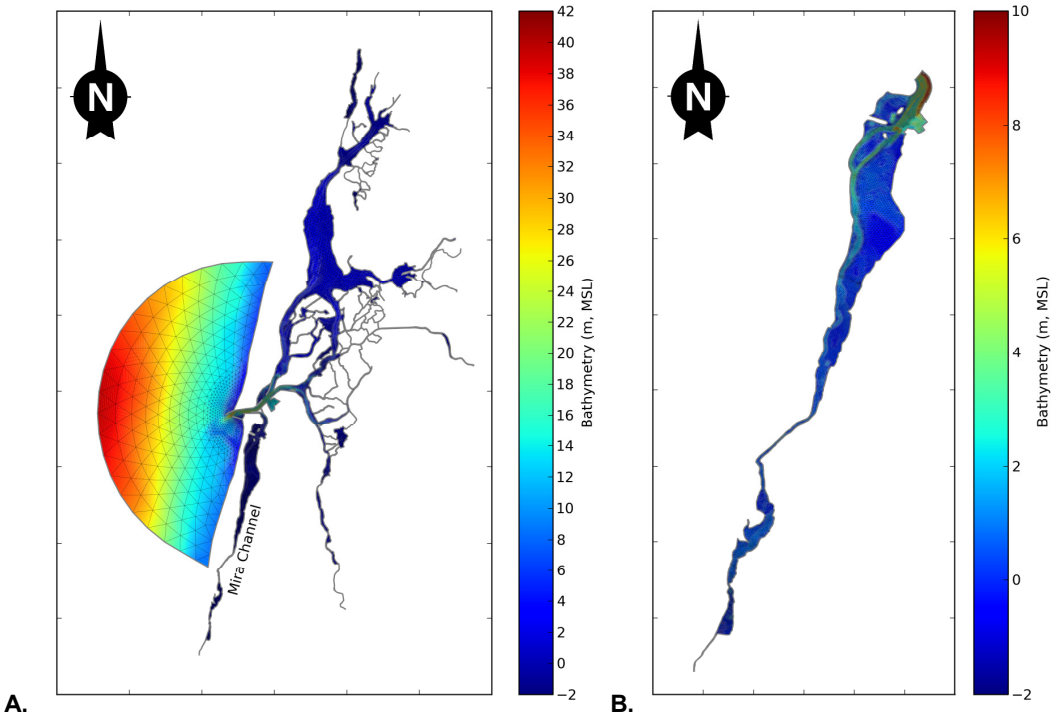

Figure III.3.3. Horizontal grid and bathymetry (meters, relative to mean sea level): A) Aveiro lagoon and B) Mira channel.

Initial conditions of salinity and temperature were set spatially varying. At the oceanic boundary salinity was forced constant (36) and temperature was forced with data from Leixões buoy (http://www.hidrografico.pt/). At river boundaries salinity and temperature were forced using a similar approach to the described for the river flows.

Surface heat exchanges between water and atmosphere were simulated with Zheng *et al.* (1998). Atmospheric forcing was obtained from the University of Aveiro meteorological station and from the NCEP Reanalysis Data (http://www.esrl.noaa.gov/psd/).

Ecological tracers along the Mira channel were simulated using an horizontal grid of about 12000 nodes (Figure III.3.3B). At the downstream boundary the three-dimensional forcing for water levels, velocity, salinity and temperature was obtained from the hydrodynamic model. At the upstream boundary the forcing used was the one described for the hydrodynamic model. Initial conditions were set similar to the approach used in Rodrigues *et al.* (2009b). Monthly varying boundary conditions were used. For the variables measured during the field campaigns, values were established based on values of station EM3 and Poço da Cruz; historical data from the S. Tomé station (http://snirh.pt) were used for the other periods. For the other variables a similar criteria to the one described by Rodrigues *et al.* (2009b) was used. Input parameters of the ecological model were set as proposed by Rodrigues *et al.* (2009b). Since the model was updated to simulate the oxygen cycle, the input parameters the ecological processes added to the model are presented (Table III.3.1). A sensitivity of the model results to basal phytoplankton respiration (b_{Pi}) and increase in the oxygen saturation concentration due to wind (DO_w) was performed. A sensitivity analyses to other parameters had been performed previously Rodrigues *et al.* (2009a) – Chapter III, Section III.2.

Table III.3.1. Input parameters – oxygen cycle (Vichi *et al.*, 2007; Fujii *et al.*, 2007).

b_{Pi} (day^{-1})	Q_{Pi} (-)	γ_{Pi} (-)	b_{Zl} (day^{-1})	Q_{Zl} (-)	η_{Zl} (-)	b_B (day^{-1})	Q_B (-)	GGE_C^O (-)	K_{sB_O} ($mmol\ O_2\ m^{-3}$)
0.01; 0.044	2.0	0.1	0.02	3.0	0.6	0.01	2.95	0.2	30.0

i = 1 (diatoms); l = 1 (copepods)

b_{Pi} – phytoplankton basal specific respiration rate; Q_{Pi} - temperature coefficient for phytoplankton; γ_{Pi} – fraction of assimilated production; b_{Zl} – zooplankton basal specific respiration rate; Qz_l – temperature coefficient for zooplankton; η_{Zl} – assimilation efficiency; b_B – bacterioplankton basal specific respiration rate; Q_B – temperature coefficient for bacterioplankton; GGE_C^O – decrease in growth efficiency under anoxic conditions; K_{sB_O} – half-saturation constant for oxygen limitation

III.3.5 RESULTS AND DISCUSSION

III.3.5.1 Hydrodynamics

Water levels at station EM3 show the ability of the model to represent adequately tide both in terms of phase and amplitude (Figure III.3.4A). Differences between data and model are generally smaller than 5-10 cm with mean absolute errors (MAE) of about 10 cm. From the downstream station to the upstream station tide has a delay of about 1-2 hours (results not shown). For currents velocity a good agreement between data and the model is also observed,

with MAE of about 0.2 m s^{-1} (Figure III.3.4B). Current velocity at station EB vary from 0.5 m s^{-1} during the ebb to 1 m s^{-1} during the flood. The differences observed may be due to changes in bathymetry along the channel, since the bathymetry available for this channel (from 1987/88) is not contemporary of the campaigns.

A longitudinal gradient of salinity is observed along the channel, varying from 36 downstream to almost 0 upstream during the wet season (Figures III.3.5 and III.3.6). During the tidal cycle salinity variations are observed along the channel: during flood, salinity increases upstream, while it decreases during ebb downstream. The larger salinity variations are observed at station EM2. Seasonally larger amplitudes are observed during the wet periods, when the river flows are larger. During winter, salinities near the downstream area of the channel (station EB and EM3) can reach values smaller than 20. During the dry season, salinity variations in the tidal cycle are smaller and increase in the upstream station (EM1) to values of about 20. No significant stratification is observed along the channel (results not shown). The model is able to represent both the tidal and the seasonal variations of salinity along the Mira channel with differences generally smaller than 2.5.

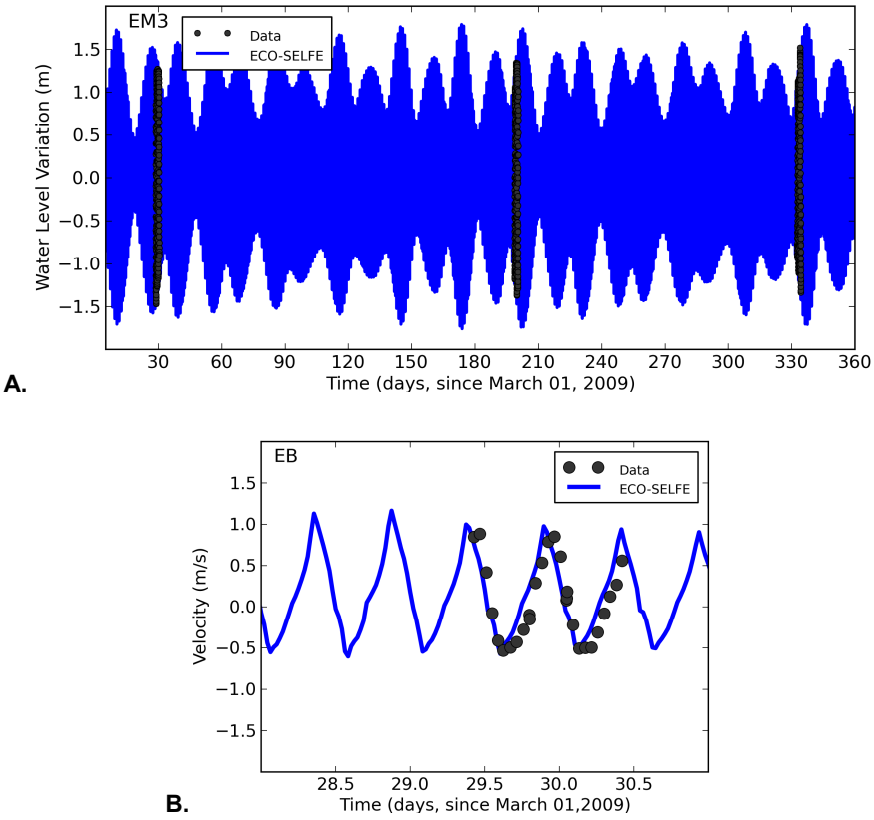

Figure III.3.4. Comparison between data and model results: A) water level variation at station EM3 and B) velocity at station EB (positive values represent flood).

Water temperature also presents variations at both spatial and temporal scales (diurnal and seasonal). During the day, an increase of temperature is observed, which is more significant in the shallower areas located upstream in the channel (Figure III.3.5). At the seasonal scale, water temperature varies from values of 20-30 ºC in the summer and decreases to 5-10 ºC in the winter. The model is also able to reproduce the temperature patterns observed, with differences smaller than 1 C.

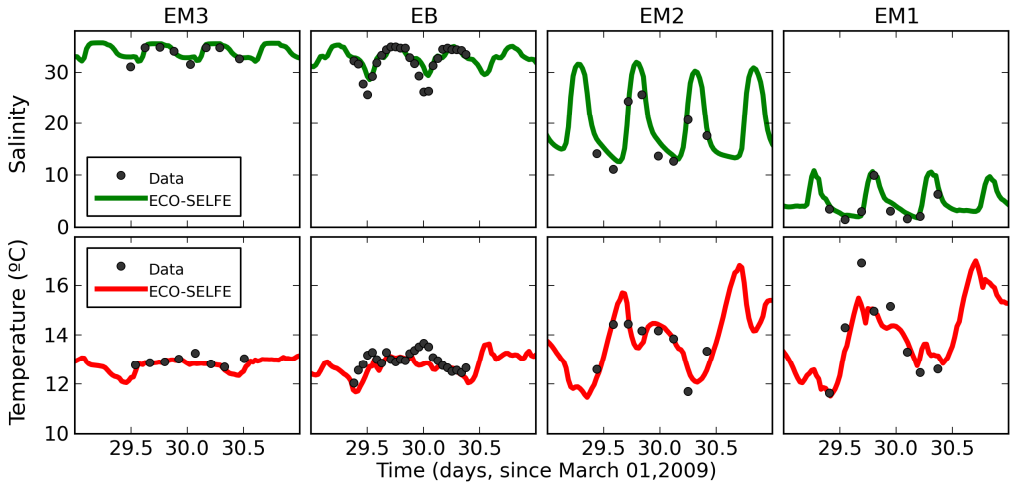

Figure III.3.5. Diurnal variation (March 29-30, 2009) of salinity and water temperature at surface along Mira channel.

III.3.5.2 Diurnal Variability of Ecological Tracers

Results for the diurnal variability of ecological tracers on March 2009 are presented in Figure III.3.7.

Chlorophyll *a* presents a longitudinal gradient along the channel, decreasing from upstream (5-15 $\mu g\ l^{-1}$) to downstream (<2 $\mu g\ l^{-1}$). The model is able to represent this gradient, in particular for the phytoplankton basal specific respiration rate of 0.045 day^{-1}. During the night (day 30) an increase of the chlorophyll *a* concentrations is observed downstream, which is related with the tidal cycle and the transport during the ebb of the upstream water masses that present larger concentrations.

Dissolved oxygen longitudinal and diurnal variations are relatively smaller, with exception of the EM1 station (Areão) where a decrease of 3-4 mg l^{-1} is observed during the night. The model is able to represent the main patterns observed with differences smaller than 1 mg l^{-1}. At the EM1 station previous studies showed a similar pattern in the dissolved oxygen diurnal variation, which was explained by the photosynthetic and respiration dynamics of the vegetation that covers the channel bed (Cunha and Moreira, 1995). Thus, the differences observed between

the data and the model in this station may derive from the fact that only the lower trophic levels dynamics is represented by the model. The effect of the increase in oxygen saturation concentration due to the wind is observed only in this tracer and is more significant in the shallower areas of the lagoon (stations EM2 and EM1).

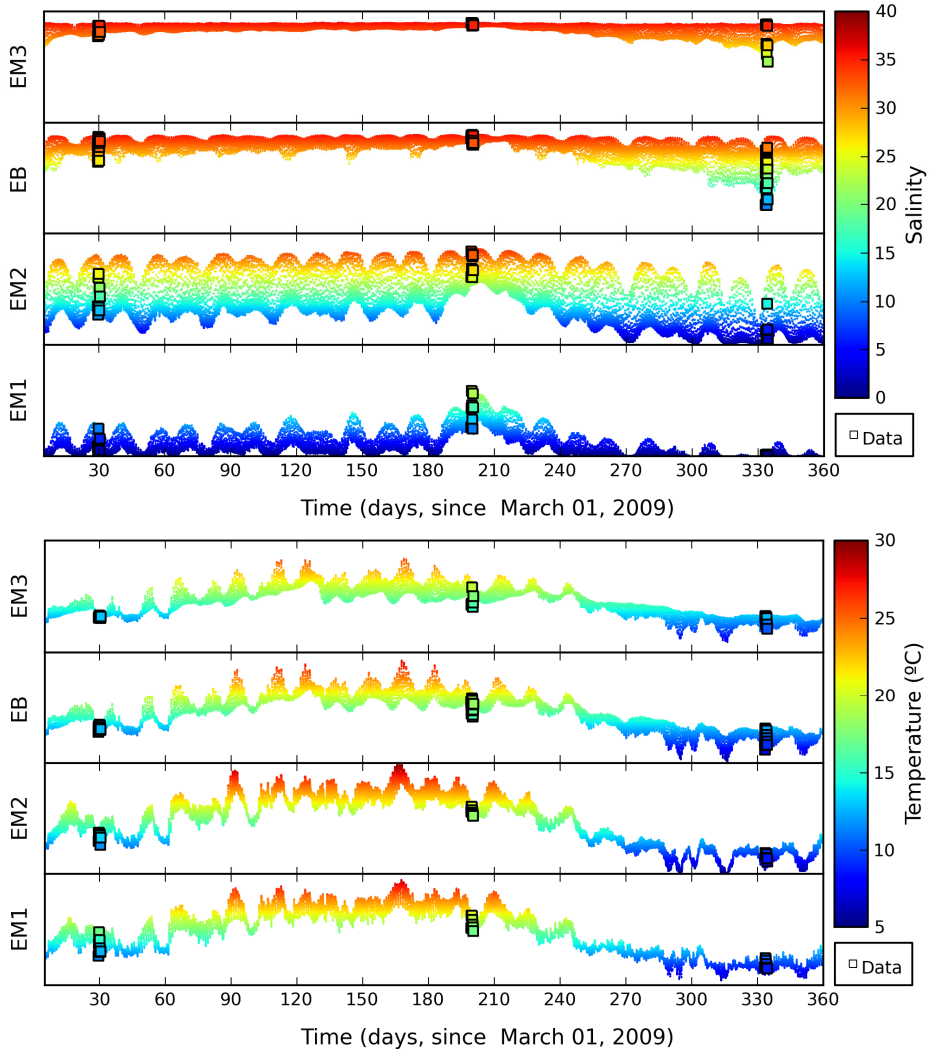

Figure III.3.6. Seasonal variation from March/2009 to February/2010 of salinity and water temperature at surface along the Mira channel.

Nutrients also present a longitudinal gradient, similarly to chlorophyll *a*. During this period (March 2009) larger concentrations are observed upstream with exception of the phosphates. This longitudinal gradient promotes changes in the concentrations of the nutrients along the tidal cycle, which are related to the flood and the ebb. The model is able to represent this dynamics. Nutrients concentrations revealed a small sensitivity to the two parameters evaluated. The exception is the ammonium concentration upstream, for which the results show

the significant relation between the phytoplankton growth and the ammonium consumption. Phosphates and silicates (since diatoms are the phytoplankton group simulated) present smaller differences.

Globally, results show the ability of the model to represent the ecological dynamics in the Mira channel during small time scales. Since the parameterization of the ecological processes is one of the main sources of uncertainty in this application, differences observed between data and model results may derive from it. Previous studies in the Aveiro lagoon suggested the importance of using adequate parameterization when establishing ecological models (Rodrigues *et al.*, 2009a,b) which was reinforced in the present study for the two parameters evaluated. The establishment of the boundary conditions and of the atmospheric forcing (in particular, solar radiation, air temperature and wind), and the existence of other point or diffuse sources of nutrients (e.g. agricultural fields), may also be additional sources of errors.

III.3.5.3 Seasonal Variability of Ecological Tracers

Figure III.3.8 presents the results for the seasonal variation of the ecological tracers between March 2009 and February 2010. Mean values and range (minimum and maximum) of the ecological variables measured during each field campaign and a comparison with model results for the same periods are presented in Table III.3.2.

Chlorophyll *a* showed a seasonal pattern, in particular, at the upstream stations (EM1 and EM2). At station EM3, concentrations remained bellow 1 $\mu g\ l^{-1}$ almost during the entire year. At the upstream stations larger concentrations were observed in Spring (March 2009), where chlorophyll a ranged from 0.9 $\mu g\ l^{-1}$ to 18.9 $\mu g\ l^{-1}$ (mean values of 10.3 $\mu g\ l^{-1}$ and 4.0 $\mu g\ l^{-1}$ at station EM1 and EM2, respectively). At station EM1 chlorophyll *a* concentrations reached values of 6.0 $\mu g\ l^{-1}$ (2.6-10.0 $\mu g\ l^{-1}$) on January 2010, which are larger than the ones observed on September 2009. Larger concentrations of chlorophyll *a* had already been observed by Leandro (2008) during winter in the upstream end of Mira channel. Vertically, differences in the water column were usually smaller than 0.5-1.0 $\mu g\ l^{-1}$; some exceptions were observed at station EM1 on March 2009 and at station EM3 on September 2009 (results not shown). The model is able to represent the main patterns observed in the seasonal variation of chlorophyll *a* along the channel with mean differences generally smaller than 1-2 $\mu g\ l^{-1}$. The differences observed between the data and the model results may be related with the sources of errors identified previously (section III.3.5.2), in particular those related to the boundary conditions, the atmospheric forcing and the uncertainty in the parameterization. Lopes *et al.* (2007) identified a seasonal succession of phytoplankton in the Aveiro lagoon dominated by diatoms from late autumn until early spring, and by chlorophytes during late spring and summer. Since only one group of phytoplankton is considered in the simulations, this may also explain some of the

differences observed. However increasing the number of phytoplankton groups would increase the uncertainty in the parameterization of the ecological model.

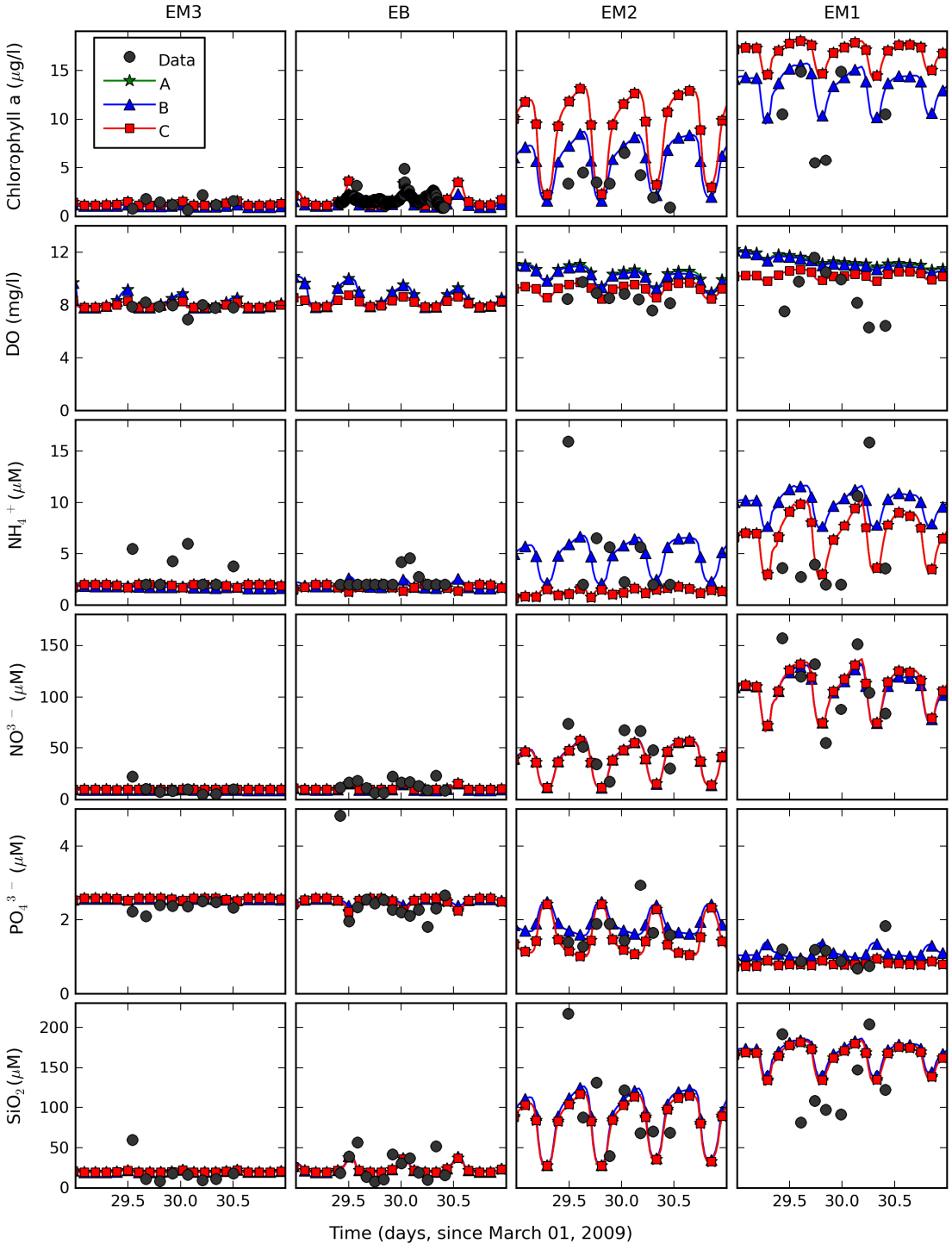

Figure III.3.7. Comparison between data and ECO-SELFE results for the ecological tracers: daily variability on March 2009. Legend: A – b_P =0.01 day^{-1}; DO_w = variable; B - b_P =0.05 day^{-1}; DO_w = variable; C= b_P =0.01 day^{-1}; DO_w = 0 mmol O_2 m^{-3}.

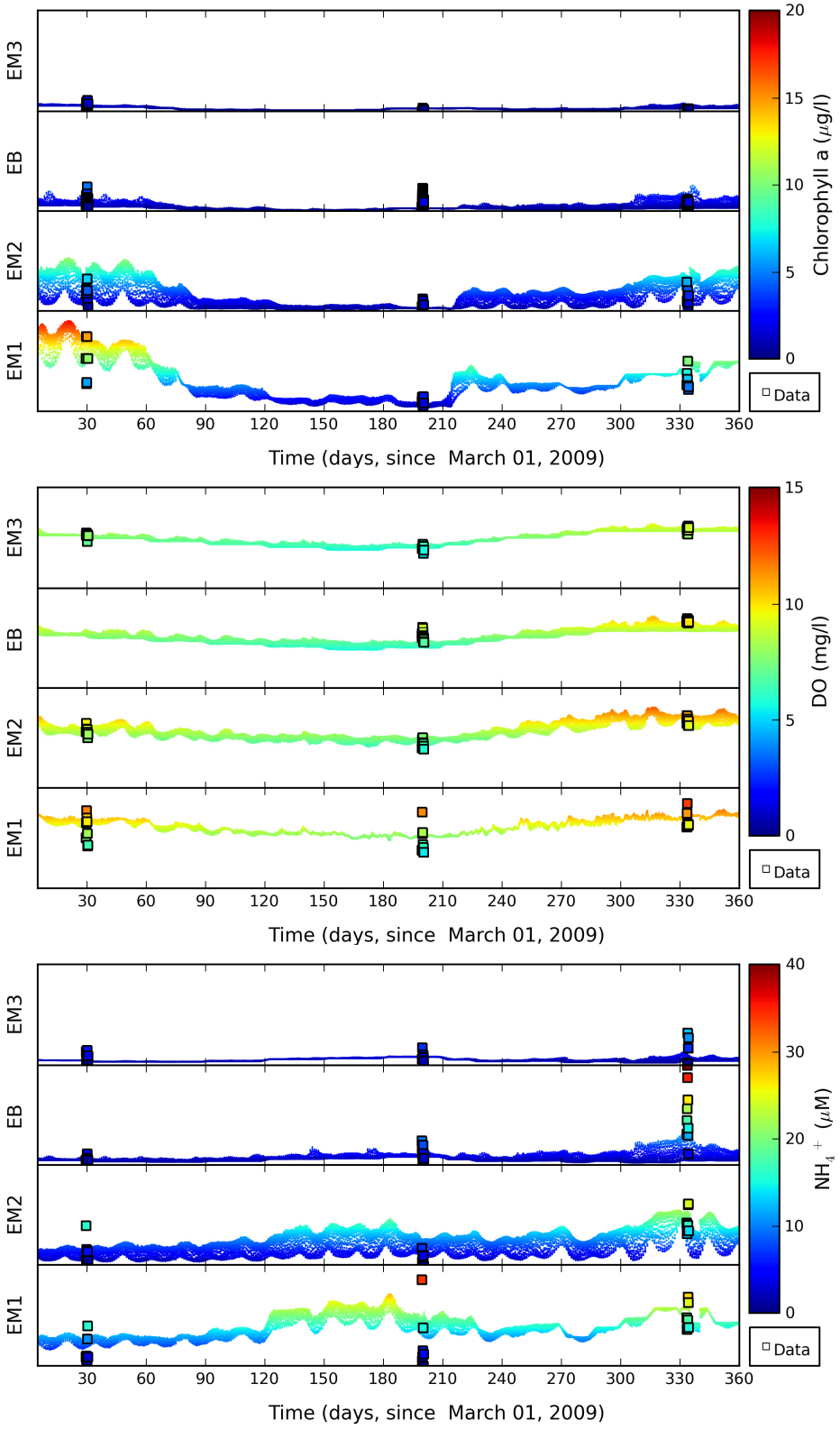

Figure III.3.8. Seasonal variation from March/2009 to February/2010 of the ecological tracers at surface along the Mira channel (NH_4^+ – Ammonium; NO_3^- – Nitrates; PO_4^{3-} – Phosphates; SiO_2 – Silicates).

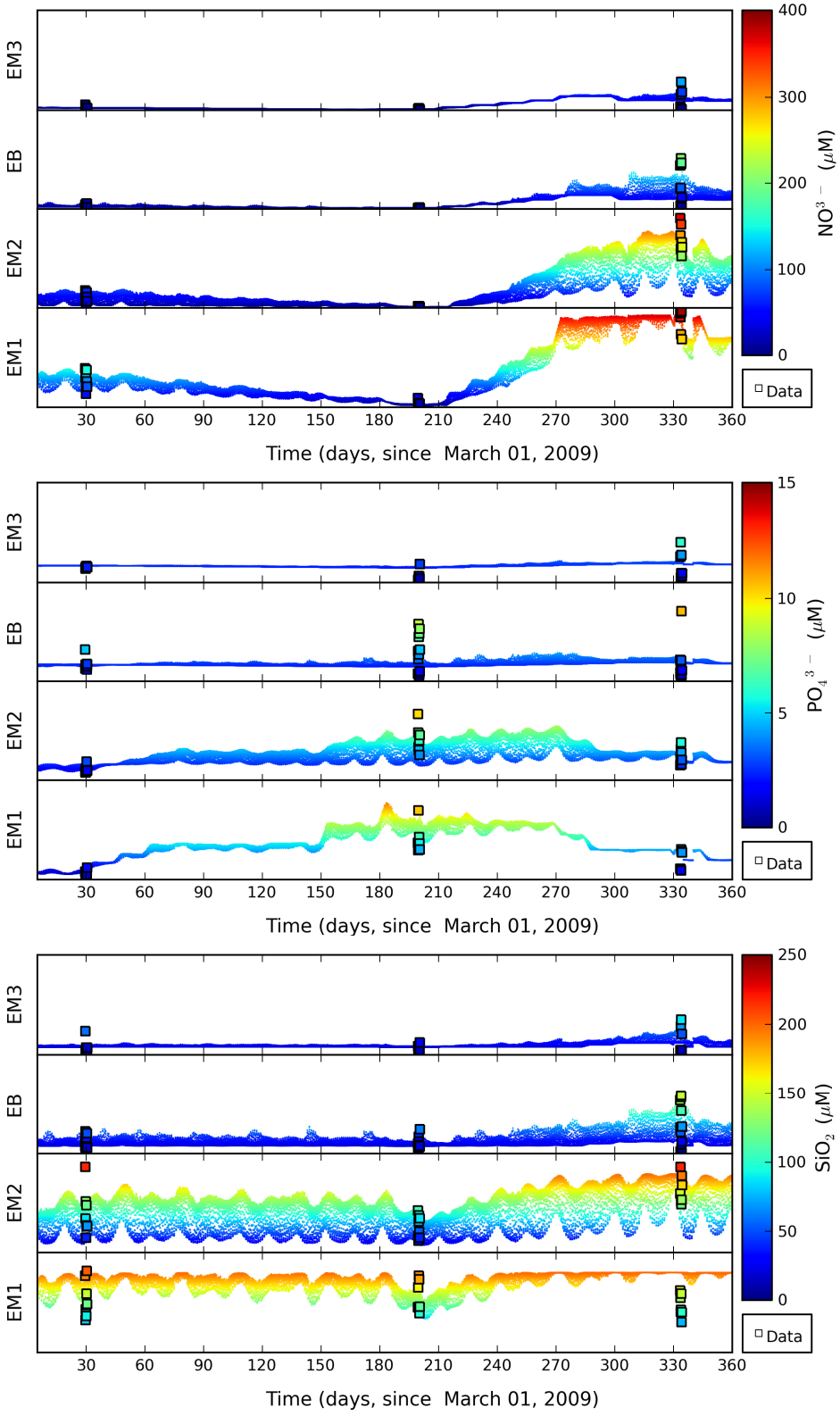

Figure III.3.8 (cont.). Seasonal variation from March/2009 to February/2010 of the ecological tracers at surface along the Mira channel (NH_4^+ – Ammonium; NO_3^- – Nitrates; PO_4^{3-} – Phosphates; SiO_2 – Silicates).

Table III.3.2. Range of variation (in parenthesis) and mean values of the ecological tracers during each campaign: comparison between data and model results.

Station	Date	Chlorophyll *a* (μg l^{-1})		Dissolved Oxygen (mg l^{-1}))		NH_4^+ (μM)		NO_3^- (μM)		PO_4^{3-} (μM)		SiO_2 (μM)	
		Data	ES	Data	ES	Data	ES	Data	ES	Data	ES	Data	ES
EM3	M09	1.1 (0.1-2.2)	1.1 (1.0-1.2)	7.8 (6.9-8.3)	7.8 (7.6-8.3)	3.1 (<LD-10.2)	1.7 (1.7-1.9)	9.9 (4.8-22.1)	9.3 (9.0-9.6)	2.6 (2.1-5.4)	2.5 (2.5-2.6)	19.5 (8.6-59.4)	20.3 (19.7-22.6)
	S09	0.6 (<LD-2.8)	0.6 (0.5-0.6)	6.0 (5.2-6.8)	6.2 (6.0-6.9)	3.3 (<LD -6.9)	3.3 (3.3-3.3)	5.1 (1.6-9.1)	5.0 (4.5-5.1)	2.2 (0.4-9.0)	2.2 (2.2-2.3)	18.9 (11.4-31.1)	19.3 (19.0-20.5)
	J10	0.5 (0.1-0.8)	0.8 (0.6-1.4)	8.6 (8.0-9.2)	8.6 (8.5-9.2)	4.2 (<LD - 12.7)	2.3 (1.8-4.4)	40.5 (5.1-113.6)	43.6 (39.6-60.0)	2.9 (0.4-6.0)	2.9 (2.9-3.1)	32.7 (5.3-88.0)	34.8 (30.0-54.6)
EB	M09	1.7 (0.8-4.5)	1.3 (1.0-2.5)	-	8.1 (7.6-8.8)	1.5 (<LD -4.9)	1.9 (1.7-2.7)	13.8 (5.9-33.2)	10.4 (9.0-16.8)	2.4 (1.8-4.8)	2.5 (2.3-2.6)	41.4 (7.9-150.8)	24.2 (19.7-42.9)
	S09	1.6 (0.4-4.9)	0.6 (0.5-0.6)	7.7 (6.5-9.2)	6.6 (6.0-7.2)	5.1 (<LD - 31.9)	3.4 (3.3-3.8)	4.3 (1.4-7.8)	4.7 (4.2-5.1)	2.7 (0.2-8.8)	2.3 (2.2-2.6)	31.6 (12.7-63.7)	20.7 (19.0-26.0)
	J10	0.9 (0.3-2.4)	1.5 (0.6-3.9)	10.1 (8.3-10.5)	9.1 (8.5-10.3)	21.3 (<LD - 49.4)	4.7 (1.8-11.9)	104.6 (8.4-259.0)	66.0 (39.6-149.4)	2.4 (0.7-10.7)	3.1 (2.9-3.6)	100.8 (1.8-284.5)	56.1 (30.1-118.0)
EM2	M09	4.0 (0.9-6.7)	5.8 (1.5-8.8)	8.5 (7.5-9.8)	9.1 (8.4-9.6)	4.9 (<LD - 15.9)	4.8 (2.0-6.7)	46.7 (17.1-107.9)	39.0 (11.2-59.6)	1.7 (1.3-2.9)	1.9 (1.6-2.5)	95.9 (29.9-221.3)	88.6 (27.2-126.0)
	S09	1.3 (0.4-2.6)	0.5 (0.5-0.6)	6.8 (5.9-7.7)	7.5 (6.9-7.9)	2.8 (<LD -9.7)	7.1 (3.4-10.6)	8.4 (2.7-14.6)	5.0 (4.2-5.9)	6.1 (3.8-10.1)	4.1 (2.3-5.7)	70.4 (31.8-107.6)	56.7 (21.5-88.4)
	J10	3.0 (0.5-5.9)	5.7 (1.8-7.1)	10.2 (9.4-10.9)	10.9 (9.3-11.4)	16.8 (11.2-25.7	17.2 (5.5-21.5)	276.8 (179.3-364.0)	228.7 (71.0-300.6)	3.3 (1.5-5.8)	4.0 (3.1-4.4)	166.5 (96.1-262.9)	162.4 (63.9-197.1)
EM1	M09	10.3 (0.9-18.9)	13.4 (9.8-15.7)	8.8 (6.3-11.6)	10.1 (9.6-10.6)	4.3 (<LD-15.8)	9.9 (7.3-11.7)	107.1 (42.2-169.4)	105.9 (69.4-131.6)	1.1 (0.7-1.8)	1.3 (1.0-1.5)	126.6 (71.9-223.9)	167.1 (135.6-186.5)
	S09	2.4 (0.8-4.8)	1.1 (0.6-1.8)	7.4 (5.3-11.4)	8.2 (7.9-8.4)	5.7 (<LD - 34.1)	16.2 (11.4-20.9)	14.3 (8.0-37.4)	9.2 (6.2-12.9)	5.6 (4.5-10.4)	7.8 (6.0-9.4)	126.8 (94.7-191.9)	126.9 (94.5-155.8)
	J10	6.0 (2.6-10.0)	7.4 (7.2-7.4)	9.9 (9.0-12.7)	10.3 (10.0-10.8)	19.7 (14.4-27.2)	22.7 (21.9-23.0)	346.9 (274.3-386.3)	358.1 (321.2-369.2)	3.3 (1.4-6.7)	4.5 (4.4-4.5)	122.5 (76.2-192.0)	199.6 (198.4-199.8)

M09 – March 2009; S09 – September 2009; J10 – January 2010

ES – ECO-SELFE; LD – limit of detection

NH_4^+ – Ammonium; NO_3^- – Nitrates; PO_4^{3-} – Phosphates; SiO_2 – Silicates

Phosphates mean variation ranged from 1 μM (station EM1, March 2009) to 6 μM (station EM2, September 2009). Mean values of phosphate remained almost constant during the year at stations EM3 and EB (2-3 μM), while at stations EM1 and EM2 a seasonal variation, with larger concentrations on September 2009, was observed. On September 2009 larger concentrations of phosphates were also observed at the surface samples of the station EB, which may be related to sediments ressuspension. During this period the model is not able to represent the vertical variation observed, since the exchanges between the sediments and the water column are not implemented in the model. As for ammonium, the model also lacks the representation of some occasional larger concentrations. In terms of mean variation the differences between the data and the model results are generally smaller than 1-2 μM.

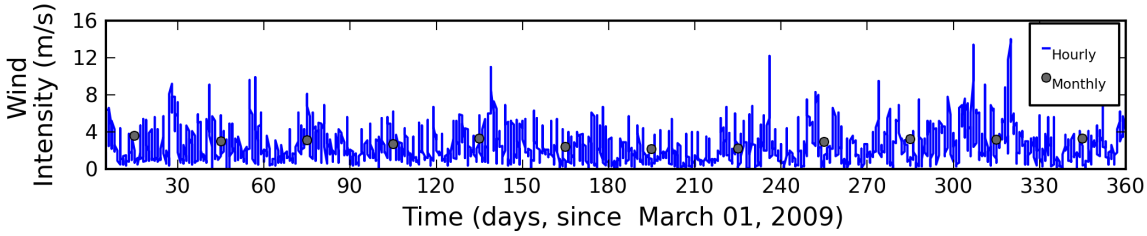

Figure III.3.9. Wind intensity from March 2009 to February 2010: hourly and mean monthly values.

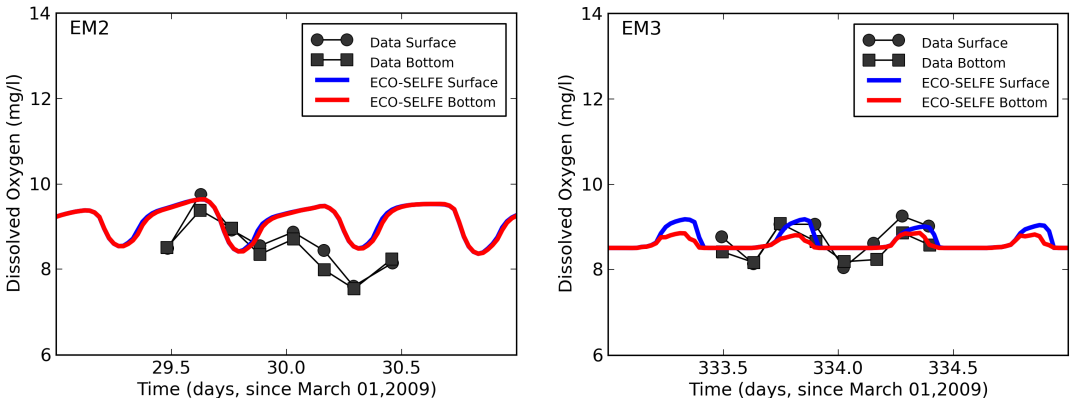

Figure III.3.10. Vertical variation (surface and bottom) of dissolved oxygen at station EM2 (March 2009) and station EM3 (January 2010).

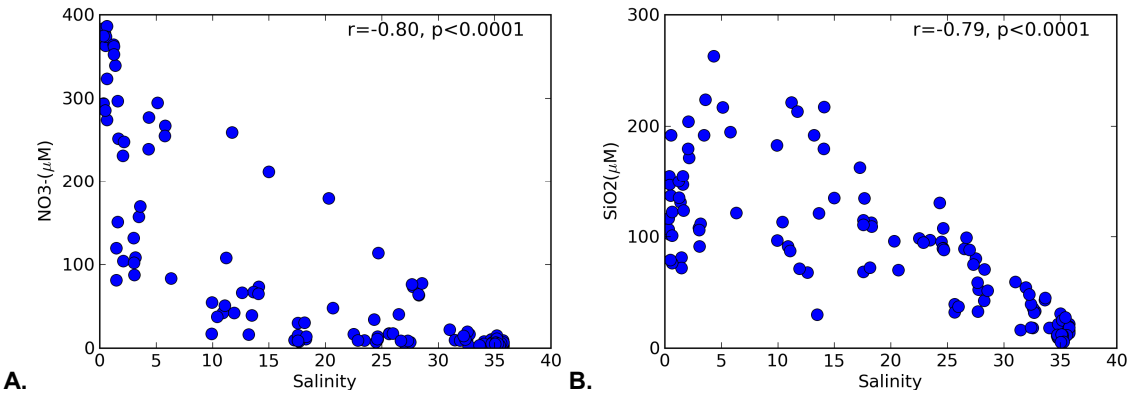

Figure III.3.11. Correlation between salinity and: A) nitrates and B) silicates concentrations (r – Pearson correlation coefficient; values are presented only for stations EM1, EM2 and EM3).

Silicates presented larger concentrations during the winter (January 2011), except at station EM1 where mean concentrations remained approximately constants (about 125 μM). As nitrates, silicates are also inversely correlated with the salinity (Figure III.3.11B), as their main sources are precipitation and flood events (Lopes *et al.*, 2007). However, at station EM2 during

winter (January 2010) the diurnal variation observed was not related with the tide, but probably was due to sediment resuspension. Overall the model represents the several patterns observed for this variable. The main differences observed may derive from the aspects mentioned above for the other nutrients.

III.3.6 CONCLUSIONS

ECO-SELFE, a fully coupled hydrodynamic and ecological model, was extended for the oxygen cycle simulation and validated at diurnal and seasonal time scales along the Mira channel in the Aveiro lagoon. Validation was performed against a set of data collected specifically for this effect, contributing the combined analysis of the data and model results to an improvement on the knowledge of this system variability.

Results showed that the coupled model is able to represent the main patterns of the physical, chemical and ecological processes along the channel, for the different time scales evaluated. The differences observed are, generally, smaller or similar to the ones achieved in this type of modelling applications (e.g. Lopes *et al.*, 2008; Fitzpatrick, 2009). The diurnal variability observed is mostly associated with the tide. Freshwater from upstream (usually with larger concentrations of chlorophyll *a* and nutrients) is transported downstream during the ebb. Seasonally the variations are associated with the river flow and the variation of the concentrations at the boundaries, and also with the atmospheric variations.

The main differences observed between the data and the model results may derive from three main factors. First, the parameterization of the ecological processes, which is simultaneously one of the most important steps and one of the main sources of uncertainty in the application of this type of models. Second, the sources flowing to the system and, in particular, the uncertainty in the establishment of the boundary conditions, since a continuous monitoring strategy does not exist in this system. The existence of additional, unknown point or diffuse sources that are not considered in the model may also explain the differences observed. Third, the existence of other processes that are not implemented in the model, namely the resuspension of the sediments, and may contribute to changes in the concentrations observed in the water column.

Results also showed the importance of establishing adequate monitoring campaigns with periodicity and spatial coverage that allow the validation of ecological models at the scales of interest.

Globally, ECO-SELFE extension and validation showed its utility and applicability as a tool to support the management of the estuarine ecosystems and, in particular, to study the impacts of climate change and anthropogenic pressures in the water quality and ecological dynamics of the Aveiro lagoon.

III.3.7 REFERENCES

Baretta-Bekker JG, Baretta JW. European Regional Seas Ecosystem Model (ERSEM II). *Journal of Sea Research* **1997**, 38, 169-438.

Bisset WP, Debra S, Dye D. Ecological Simulation (EcoSim) 2.0 Technical Description, Tampa, Florida: Florida Environmental Research Institute, **2004**, 25 pp.

Cunha MR, Moreira MH. Macrobenthos of potamogetonand myriophyllumbeds in the upper reaches of canal de Mira (Ria de Aveiro, NW Portugal): community structure and environmental factors. *Netherlands Journal of Aquatic Ecology* **1995**, 29(3-4), 377-390.

Dias JM, Lopes JF, Dekeyser I. Lagrangian transport of particles in Ria de Aveiro lagoon, Portugal. *Physics and Chemistry of the Earth, Part B: Hydrology, Oceans and Atmosphere* **2001**, 26(9), 721-727.

Dias JM, Lopes JF, Dekeyser I. Tidal propagation in Ria de Aveiro lagoon, Portugal. *Physics and Chemistry of the Earth* **2000**, 25, 369-374.

Dias JM, Lopes JF. Implementation and assessment of hydrodynamic, salt and heat transport models: the case of Ria de Aveiro lagoon (Portugal). *Environmental Modelling & Software* **2006**, 21, 1-15.

Famming JC, Pilson MEQ. On the spectrophotometric determination of dissolved silica in natural waters. *Analytical Chemistry* **1973**, 45, 136-140.

Fitzpatrick JJ. Assessing skill of estuarine and coastal eutrophication models for water quality managers. *Journal of Marine Systems* **2009**, 76, 195-211.

Fortunato AB, Pinto LL, Oliveira A, Ferreira JS. Tidally-generated shelf waves off the western Iberian coast. *Continental Shelf Research* **2002**, 22(14), 1935-1950.

Fujii M, Yamanaka Y, Nojiri Y, Kishi MJ, Chai F. Comparison of seasonal characteristics in biogeochesmitry among the subartic North Pacific stations described with a NEMURO-based ecosystem model. *Ecological Modelling* **2007**, 202, 52-67.

Gameiro C, Brotas V. Patterns of phytoplankton variability in Tagus Estuary (Portugal). *Estuaries and Coasts Special Issue: Phytoplankton in Coastal Ecosystems* **2010**, 33, 311-323.

Grant SB, Kim JH, Jones BH, Jenkins SA, Wasyl J, Cudaback C. Surf zone entrainment, along-shore transport and human health implication of pollution from tidal inlets. *Journal Geophysical Research* **2005**, 110(C10025), 1-20.

Grasshoff K. *Methods of seawater analysis*, Verlag, NY: Chimie, **1976**.

Hays GC, Richardson AJ, Robinson C. Climate change and marine plankton. *Trends in Ecology and Evolution* **2005**, 20(6), 337-334.

Hull V, Parrella L, Falcucci M. Modelling dissolved oxygen in coastal lagoons. *Ecological Modelling* **2008**, 211, 468-480.

Intergovernamental Panel on Climate Change. Climate Change 2007: The Physical Science Basis. UNEP and WMO, **2007** (http://www.ipcc.ch/SPM2feb07.pdf).

Kishi MJ, Kashiwai M, Ware DM, Megrey BA, Eslinger DL, Werner FE, Noguchi-Aita M, Azumaya T, Fujii M, Hashimoto S, Huang D, Iizumi H, Ishida Y, Kang S, Kantakov GA, Kim H, Komatsu K, Navrotsky VV, Smith SL, Tadokoro K, Tsuda A, Yamamura O, Yamanaka Y, Yokouchi K, Yoshie N, Zhang J, Zuenko YI, Zvalinsky ZI. NEMURO – a lower trophic level model for the North Pacific marine ecosystem. *Ecological Modelling* **2007**, 202, 12-25.

Koroleff F. Direct determination of ammonia in natural water as indophenol blue. ICES, Pap. C.M. **1969**/C:9, revised 1970, 19-22.

Leandro SM. Forçamento ambiental na abundância e produção de zooplâncton num gradiente estuarino. PhD Thesis, Universidade de Aveiro, **2008**.

Lopes CB, Lillebo AI, Dias JM, Pereira E, Vale C, Duarte AC. Nutrient dynamics and seasonal succession of phytoplankton assemblages in a southern european estuary: Ria de Aveiro, Portugal. *Estuarine Coastal and Shelf Science* **2007**, 71, 480-490.

Lopes JF, Dias JM, Cardoso AC, Silva CIV. The water quality of the Ria de Aveiro lagoon, Portugal: From the observations to the implementation of a numerical model. *Marine Environmental Research* **2005**, 60, 594-628.

Lopes JF, Dias JM, Dekeyser I. Numerical modelling of cohesive sediments transport in the Ria de Aveiro lagoon. *Journal of Hydrology* **2006**, 319(1-4), 176-198.

Lopes JF, Silva CI, Cardoso AC. Validation of a water quality model for the Ria de Aveiro lagoon, Portugal. *Environmental Modelling & Software* **2008**, 23, 479-494.

Lorezen CJ. Determination of chlorophyll and phaeopigments: spectrophotometric equations. *Limnology and Oceanography* **1967**, 12(2), 343–346.

Murphy J, Riley JP. A modified single solution method for the determination of phosphate in natural waters. *Chimie Acta* **1962**, 27, 301-318.

Rodrigues M, Oliveira A, Costa M, Fortunato AB, Zhang YJ. Sensitivity analysis of an ecological model applied to the Ria de Aveiro. *Journal of Coastal Research* **2009a**, SI56, 448-452.

Rodrigues M, Oliveira A, Queiroga H, Fortunato AB, Zhang YJ. Three-dimensional modeling of the lower trophic levels in the Ria de Aveiro. *Ecological Modelling* **2009b**, 220(9-10), 1274-1290.

Rodrigues M, Oliveira A, Queiroga H, Zhang YJ, Fortunato AB, Baptista AM. Integrating a circulation model and an ecological model to simulate the dynamics of zooplankton. In: Estuarine and Coastal Modeling Conference Book, Proceedings of the Tenth International Conference, Ed.: Spaulding M, NY, ASCE, **2008**, 427-446.

Smith W, Steinberg D, Bronk D, Tang K. Marine plankton food webs and climate change. Virginia Institute of Marine Science, **2008**.

Thomann, RV, Mueller JA. Principles of surface water quality modeling and control. New York: Harper and Row Publishing, **1987**.

Trancoso AR, Saraiva S, Fernandes L, Pina P, Leitão P, Neves R. Modelling macroalgae using a 3D hydrodynamic-ecological model in a shallow, temperate estuary. *Ecological Modelling* **2005**, 187, 232–246.

Vichi M, Pinardi N, Masina S. A generalized model of pelagic biogeochemistry for the global ocean ecosystem. Part I: Theory. *Journal of Marine Systems* **2007**, 64, 89-109.

Wanninkhof R. Relationship between wind speed and gas exchange over the ocean. *Journal of Geophysical Research* **1992**, 97(C5), 7373-7382.

Weiss RF. The solubility of nitrogen, oxygen and argon in water and seawater. *Deep Sea Research* **1970**, 17, 721-735.

Zeng X, Zhao M, Dickinson RE. Intercomparison of bulk aerodynamic algorithms for the computation of sea surface fluxes using TOGA COARE and TAO data. *Journal of Climate* **1998**, 11, 2628-2644.

Zhang Y, Baptista AM. SELFE: A semi-implicit Eulerian-Lagrangian finite-element model for cross-scale ocean circulation. *Ocean Modeling* **2008**, 21(3-4), 71-96.

CHAPTER IV

ANALYSIS OF LONG-TERM EFFECTS OF CLIMATIC VARIABILITY AND OF ANTHROPOGENIC PRESSURES ON THE WATER QUALITY AND ECOLOGICAL DYNAMICS OF THE AVEIRO LAGOON

SECTION IV.1

CLIMATIC AND ANTHROPOGENIC FACTORS DRIVING WATER QUALITY VARIABILITY IN THE AVEIRO LAGOON: 1985-2010 DATA ANALYSIS[IV.1.1]

ABSTRACT

The Aveiro lagoon is a very important system from both economic and ecological viewpoints. Understanding the natural variability of this coastal ecosystem is of major concern for the establishment of appropriate management strategies. It increases the knowledge of the system dynamics and, at the same time, allows the distinction between the natural fluctuations and the ones that are caused by anthropogenic interventions and long-term climatic variability. In the present study the factors controlling seasonal, inter-annual and long-term variability of the water quality in the Aveiro lagoon were analysed. The statistical analysis was based on a set of climatic, hydrological and water quality data from the period between 1985 and 2010. Seasonal variations were mostly associated with the seasonal variation of the main climatic and hydrological forcings. In the upstream area of the lagoon, chlorophyll *a* inter-annual variations were mostly driven by climatic variability. A recovery of the system from hypoxia conditions after the adoption of secondary treatment for industrial effluents on 1992 occurred in this area of the lagoon. In the downstream area of the lagoon, chlorophyll *a* presented a downward trend between 1985 and 2010 and lower concentrations after 2000. These lower concentrations were probably associated with lower concentrations of silicates that occurred after 2000, and may derive from some anthropogenic modifications that occurred in the lagoon. Results showed that the seasonal, inter-annual and long-term trends observed in the Aveiro lagoon depend on the influence of both anthropogenic and climate forcings, evidencing the need to combine these different drivers when evaluating and developing management strategies for estuarine ecosystems.

KEYWORDS

Long-term variability, Chlorophyll *a*, Dissolved Oxygen, Nutrients, Estuaries

[IV.1.1] In preparation to: *Science of the Total Environment*.

IV.1.1 INTRODUCTION

Estuaries unique characteristics and intrinsic value have been recognized worldwide, as they harbour invaluable habitats and provide multiple economic and ecosystem services: coastal protection, erosion control, maintenance of fisheries, biological productivity and diversity maintenance, water purification, tourism, recreation, education and research, among others (Barbier *et al.*, 2011). The Aveiro lagoon, located in the northwest coast of Portugal (Figure IV.1.1), contains one of the largest saltmarshes and saltpans in Europe, harbouring several ecologically relevant species of flora and fauna, in particular migratory birds. The lagoon is classified as a special area of conservation under the directive 79/409/EEC on the wild birds conservation. As many other coastal lagoons and estuaries, due to its privileged location at the interface sea-land, it also supports a population of 350 000 habitants (Polis Litoral – Ria de Aveiro, 2010) and several human activities, which include: aquaculture, artisan fishing, tourism, nautical and port facilities, salt collection and industries.

This large diversity of services and activities developed in estuaries causes, in many cases, threats and pressures over their ecosystems, which may lead to a loss of ecological health and, consequently, to the degradation of their quality. One of these threats is the nutrients enrichment (e.g. due to domestic and industrial wastewater discharges) that may potentiate eutrophication. Although periodical episodes of eutrophication are natural in estuarine ecosystems (Pickney *et al.*, 2001), cultural eutrophication (i.e. eutrophication due to human disturbance) is increasing worldwide (Cloern, 2001). Eutrophication consequences are various: loss of biodiversity and replacement by opportunistic species, harmful and toxic algae blooms, local hypoxic and anoxic conditions, and loss of fisheries stocks, among others (e.g. Lehtonen *et al.*, 1998; Zimmerman and Canuel, 2000; Paerl *et al.*, 2003; Cardoso *et al.*, 2004; Burkholder *et al.*, 2007; Smayda, 2008). The Aveiro lagoon, in particular, was classified with moderate low overall eutrophic condition (Ferreira *et al.*, 2003), but the quality status of different areas within the system can vary (Lopes *et al.*, 2007b). The untreated or poorly treated industrial and domestic effluents that were discharged directly into the lagoon until recently were one of the pressures that contributed to a degradation of its quality (e.g. Rebelo, 1992). In the past years some efforts have been made to reduce this pressure in the Aveiro lagoon and an integrated wastewater treatment and disposal system was constructed (Sistema Municipal de Saneamento da Ria de Aveiro – SIMRIA), which discharges most of the treated domestic and industrial effluents in the Atlantic ocean. However, the information about how these measures affected the lagoon water quality and ecological dynamics is still scarce.

The need to protect the estuarine water masses and ecosystems has been addressed in several normative documents (e.g. Water Framework Directive) and numerous studies aimed at evaluating their quality based on a set of indicators (e.g. Scanes *et al.*, 2007). Among these

indicators, chlorophyll *a*, dissolved oxygen and inorganic nutrients are widely used (e.g. Boyer *et al.*, 2009; Gameiro and Brotas, 2010).

Estuarine ecosystems present a natural variability dependent on several physical-chemical characteristics, which should also be investigated when evaluating the estuarine water quality. Hydrodynamics and morphology combined with the freshwater runoff affect the residence times, the water column stratification, the sediments in the water column, the light penetration and the nutrients availability (e.g. Pickney *et al.*, 2001; Gameiro *et al.*, 2007) in temporal scales that vary from daily to seasonal. Water temperature, influenced by heat exchanges with the atmosphere, and vertical mixing, influenced by wind and tides, may also affect the dynamics of estuarine ecosystems (e.g. Yin *et al.*, 2004; Queiroga *et al.*, 2006). However the relative importance of these several drivers in the estuarine ecosystems dynamics, and, in particular, in the lower trophic levels, is not consensual and is still a matter of discussion (Baumert and Petzoldt, 2008). Besides, the actual concern about climate change, which may induce modifications in air temperature, wind patterns, hydrological regimes and mean sea level, enhances the need to deeply understand the system response to these forcings (Statham, 2012).

In the Aveiro lagoon several studies aimed at characterizing the water quality and ecological dynamics, and to establish and evaluate the relationships between these dynamics and the main climatic and/or hydrological forcings (e.g. Cunha *et al.*, 1999; Almeida *et al.*, 2005; Resende *et al.*, 2005; Lopes *et al.*, 2007a,b) or, to a smaller extent, the anthropogenic pressures (Sampaio, 2001). Between 2002 and 2003, Resende *et al.* (2005) studied the phytoplankton ecology along one of the channels of the Aveiro lagoon and suggested that the main drivers of the diatoms assemblages composition and distribution were the salinity longitudinal gradient and the water temperature temporal gradient, while the nutrients (ammonium and phosphates) role was relatively reduced when compared with these physical variables. Lopes *et al.* (2007a) inferred, based on a data set collected between 2000 and 2001 along the several channels of the Aveiro lagoon, a seasonal succession pattern in phytoplankton assemblages in the Aveiro lagoon, which depended on the nutrients concentrations in the water column and also on grazing. Although these past studies contributed significantly for the knowledge about the Aveiro lagoon dynamics, and, in particular, the one related with the lower trophic levels, they were severely limited by the short duration of the datasets.

In this sense, in order to fully understand the role of the main drivers in the ecosystem dynamics and to develop sustainable management strategies, there is a need to integrate both the anthropogenic pressures and the system response to the physical drivers (Kotta *et al.*, 2009), which can be achieved through long-term comprehensive studies (Gameiro *et al.*, 2007) that allow the understanding of the system natural variability. These long-term integrated studies about the estuarine water quality are still scarce. In the Portuguese estuarine systems, these

studies are limited to the Tagus (Gameiro *et al.*, 2007; Gameiro and Brotas, 2010), the Douro (Azevedo *et al.*, 2008) and the Guadiana estuaries (Barbosa *et al.*, 2010).

Thus, this study aims to: i) evaluate the seasonal, inter-annual and spatial dynamics of the chlorophyll *a*, dissolved oxygen and nutrients dynamics in the Aveiro lagoon over a period of 25 years (1985-2010) and ii) to evaluate this dynamics in the scope of the climate variability and the anthropogenic interventions in the lagoon, in order to contribute to the knowledge about the system's natural variability, the impacts of the management measures undertaken in the past years and, ultimately, to provide information that allow the future development of sustainable strategies for the management of the Aveiro lagoon.

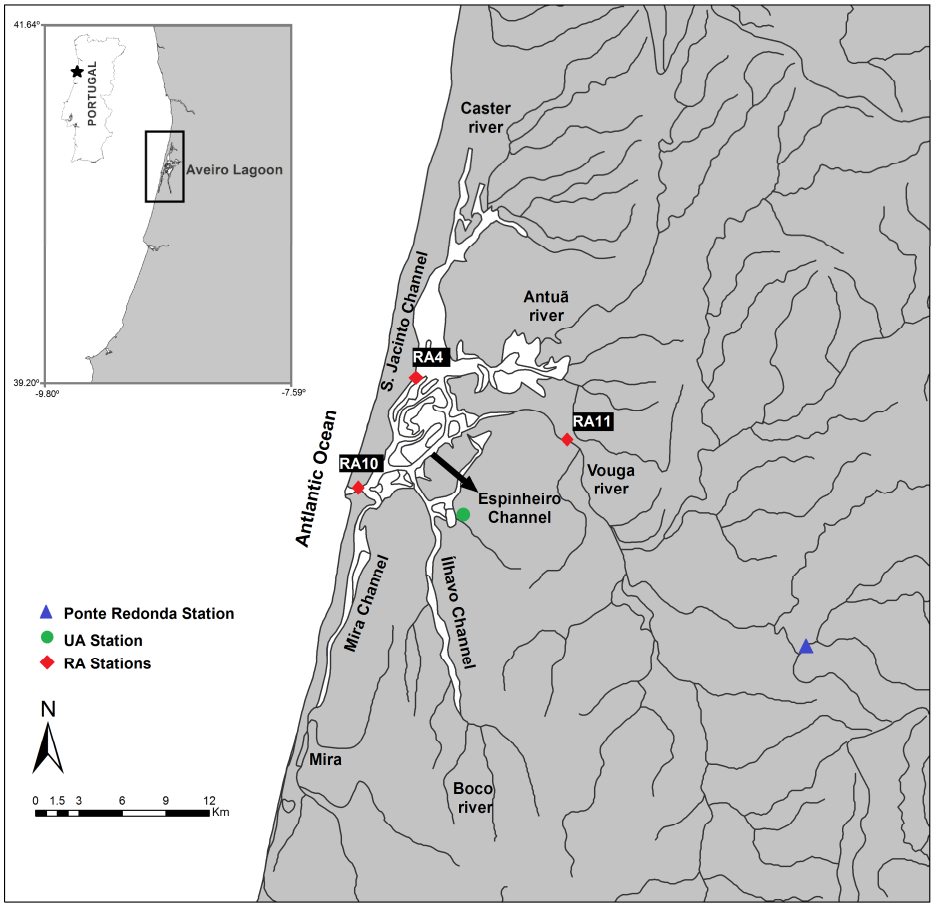

Figure IV.1.1. Schematic overview of the Aveiro lagoon and location of the water quality stations (RA stations), University of Aveiro meteorological station (UA station) and Ponte Redonda hydrometric station.

IV.1.2 METHODOLOGY

IV.1.2.1 Study Area

The Ria de Aveiro is a coastal lagoon located in the northwest coast of Portugal (40º38'N, 8º45'W), about 45 km long, from Ovar to Mira, and up to 10 km wide. It spreads over four main channels (Mira, Ílhavo, Espinheiro and S. Jacinto channels), with several branches, and connects to the sea through one artificial channel of about 1.3 km (Figure IV.1.1). The lagoon is very shallow with exception of the navigation channels, where the depths range from 7 to 20 m and are maintained artificially. The circulation in the lagoon is mainly driven by tide (Dias *et al.*, 1999) and its area varies from 66 km^2 at low tide to 83 km^2 at high spring tide (Dias and Lopes, 2006). The lagoon is mesotidal and tides are semi-diurnal. The tidal range at the inlet mouth varies between 0.6 and 3.2 m, with an average of 2 m (Dias *et al.*, 2000). The mean tidal prism is of about $70x10^6$ m^3 (Dias and Lopes, 2006). Comparatively to tide, the annual mean freshwater input during a tidal cycle is relatively small, of about 1.8×10^6 m^3 (Moreira *et al.*, 1993). The main sources of freshwater in the lagoon are the rivers Vouga and Antuã, which flow through the Espinheiro channel (Dias *et al.*, 2000). Some uncertainty remains about the mean flows of these rivers, mainly due to the lack of recent data.

IV.1.2.2 Data Description

The datasets used in this study included atmospheric, hydrological and water quality variables and come from different sources.

Atmospheric data were obtained from the University of Aveiro meteorological station, including daily values of air temperature, total solar radiation, rainfall and wind intensity from January 1st, 1985 to December 31st, 2010 (monthly values are presented in Figure IV.1.2).

For the river flow, data from the Ponte Redonda station were used – available at the SNIRH database (http://snirh.pt). This station only covers part (ca. 10%) of the water catchment area of the Vouga river (approximately 2350 km^2). However, the data available for the Angeja station, which covers the whole water catchment area of the Vouga river, are limited in time, and the Ponte Redonda station is the only with data available throughout the period in analysis. Preliminary evaluation showed that the water levels at the two stations have a significant positive correlation, with Pearson correlation coefficient of r_P=0.86 (N=1235, p<0.0001). Thus, although the Ponte Redonda data does not represent the total volume of freshwater flowing from the Vouga river into the Aveiro lagoon, it represents the main patterns of variation. In this sense, it was considered adequate for the present study, since the main objective is to evaluate trends and relations between the water quality variables and the main physical forcing. Mean monthly values of river flow in the Ponte Redonda station are presented in Figure IV.1.2.

Daily and monthly values of North Atlantic Oscillation (NAO) index, which represents the difference of atmospheric pressure at sea level between the Icelandic low and the Azores high, were obtained from the NOAA website (http://www.cpc.ncep.noaa.gov/products/precip/CWlink/pna/nao.shtml, Figure IV.1.3).

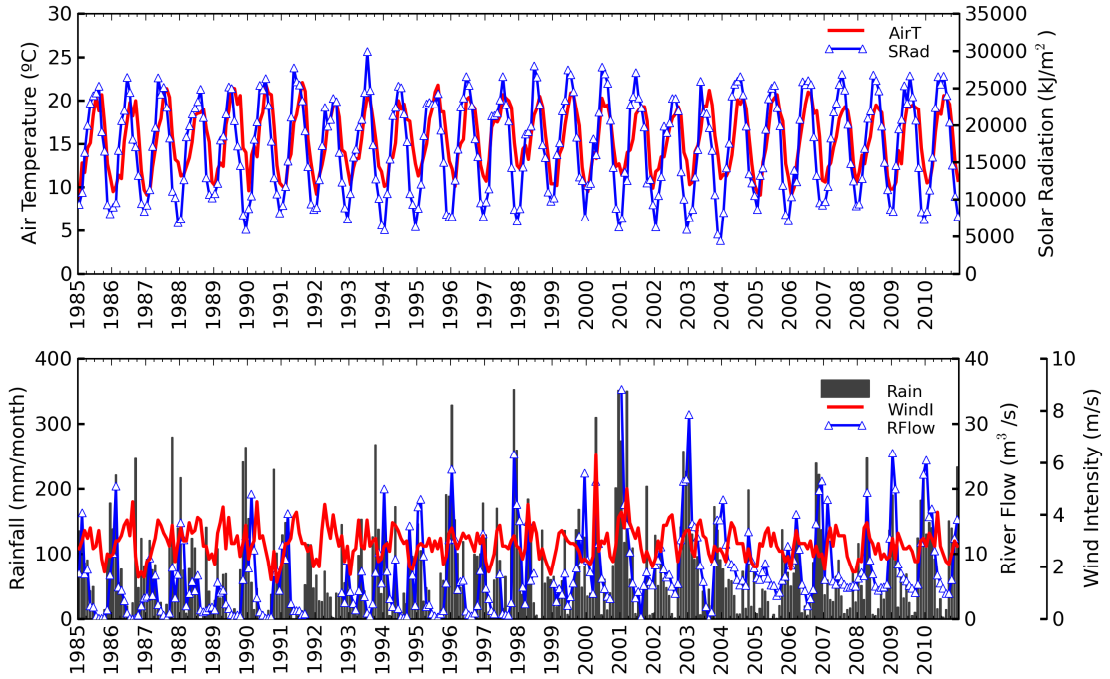

Figure IV.1.2. Monthly values of the time series of atmospheric parameters measured at the University of Aveiro meteorological station (Rain – total monthly rainfall; WindI – monthly mean wind intensity; AirT – monthly mean air temperature; SRad – monthly mean total solar radiation) and of monthly mean river flow measured at Ponte Redonda, from 1985 to 2010.

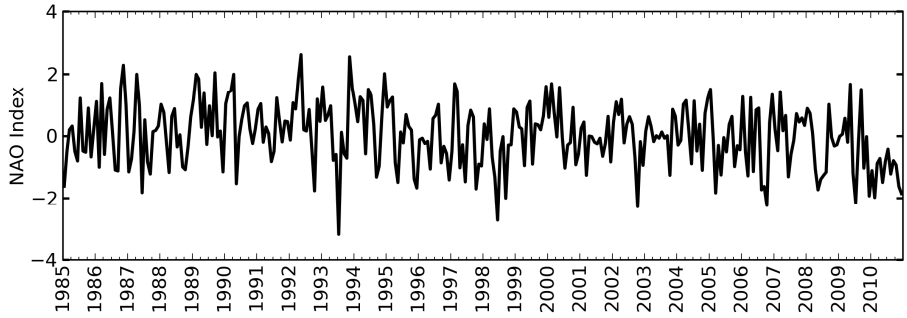

Figure IV.1.3. Monthly NAO index from 1985 to 2010.

Water quality parameters were obtained from the monitoring program "Monitoring the Marine Environment – POL-Aveiro" developed by the Instituto Hidrográfico (Palma *et al.*, 2000). This

program started in 1981 and includes the measurement of several physical, chemical and biological variables in the Aveiro lagoon. The monitoring stations, in a total of eleven, cover the main channels of the lagoon (Borges *et al.*, 2011). The periodicity of sampling changed through time and presently occurs twice a year, in summer and winter (Palma *et al.*, 2000; Borges *et al.*, 2011). All samples were collected during ebb conditions. Additional details from the sampling strategy and laboratorial analyses can be found in Borges *et al.* (2011). In the present study the period considered in the analyses ranges from 1985 to 2010, and includes the data obtained in the late winter (late January, February or March) and late summer seasons (late August, September or October). The following variables were selected for the data analyses (Figure IV.1.4): salinity, water temperature, chlorophyll *a* (used as a proxy for phytoplankton), dissolved oxygen and nutrients (ammonium, nitrates + nitrites, phosphates and silicates). In order to represent the spatial variability along the Aveiro lagoon the data from three sampling stations (RA) were acquired (Figure IV.1.1): i) station RA10, located near the mouth of the lagoon, aims to represent the oceanic/marine influence; ii) station RA4, located in the intermediate zone of the lagoon, in the S. Jacinto channel, which has the largest tidal prism (Dias, 2001), aims to represent an area of mixture between the freshwater and the marine water; and iii) station RA11, which is located near the riverine boundary of the lagoon under the influence of the Vouga river, which is the main river flowing to the lagoon (Dias *et al.*, 2000; Dias and Lopes, 2006). Accordingly to the spatial variability of the water quality variables during the sampling period (Borges *et al.*, 2011), these stations represent the main patterns observed in the lagoon.

IV.1.2.3 Data Analyses

The data analyses performed aimed to identify the main spatial and temporal patterns of the water quality along the Aveiro lagoon over the past 25-years, and to understand its variations in the scope of the variability of climatic and hydrological drivers and of the anthropogenic interventions in the lagoon. The datasets were summarized over the period 1985-2010 through basic statistics, including the determination of mean, median, minimum, maximum, standard deviation and percentile 90 values of each variable.

In order to evaluate the temporal variations at different scales (seasonal and long-term) autocorrelation and standardized anomalies were calculated. The stationarity of the water quality time series used in the autocorrelation analysis was achieved by differencing the series by a lag of 1. The standardized anomalies were computed at three temporal scales (McQuarters-Gollop *et al.,* 2008). For the seasonal variations or relative variations at short temporal scales (month or season), monthly values were used for the atmospheric and river flow data, while for the water quality the twice a year data were used. The anomalies computed were:

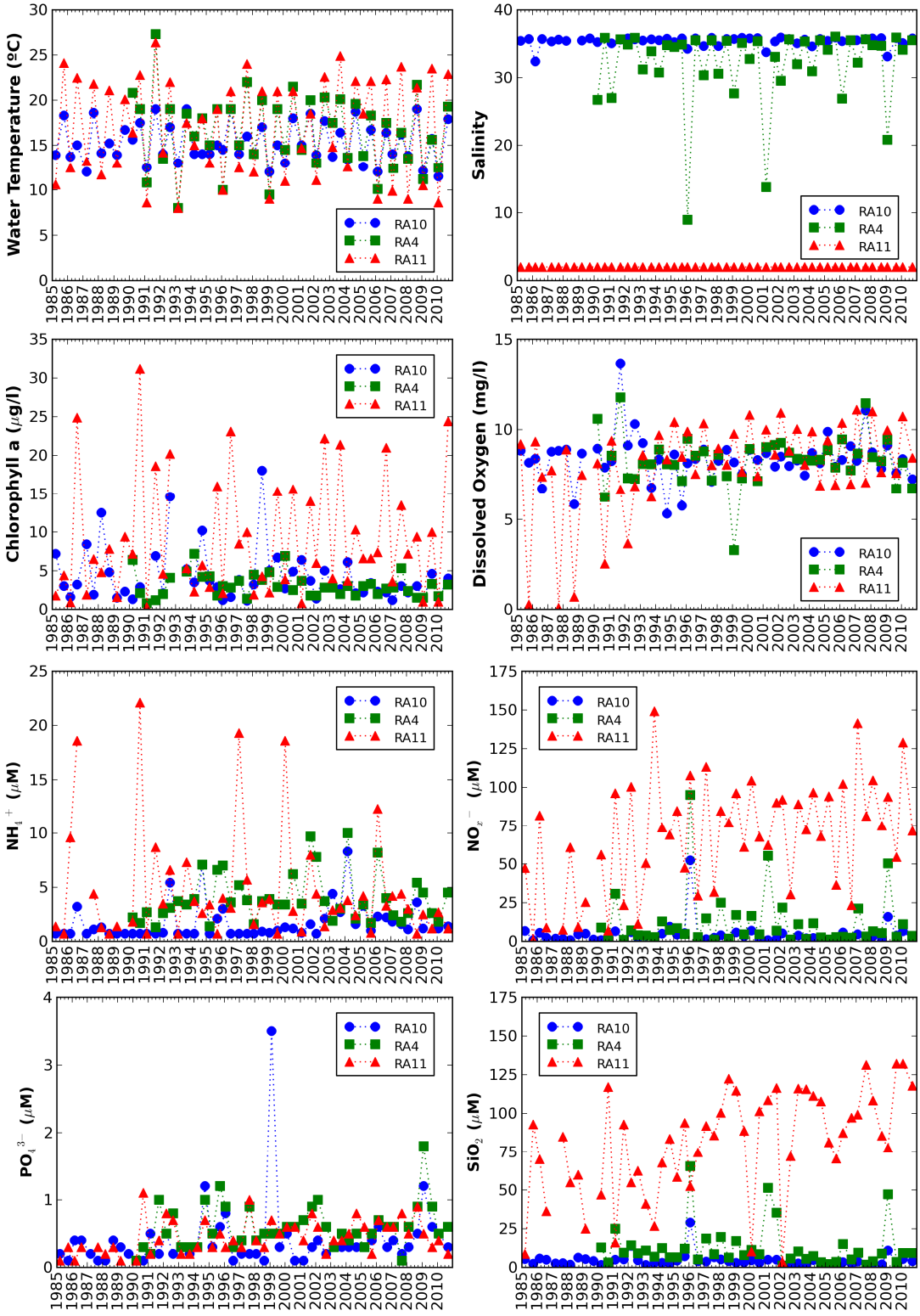

Figure IV.1.4. Time series of physical and bio-chemical parameters measured at three stations along the Ria de Aveiro (RA10, RA4 and RA11) from 1985 to 2010 (NH_4^+ – ammonium; NO_x^- – nitrates+nitrites; PO_4^{3-} - phosphates; SiO_2 - silicates).

i) the standardized monthly (atmospheric and river flow data) or seasonal (water quality data) anomaly (z_{mt}),

$$z_{mt} = \frac{x_{m\_25y} - \bar{x}_{25y}}{\sigma_{25y}} \quad \text{(IV.1.1)}$$

where x_{m_25y} is the long-term mean of each month or season, $\bar{x}_{25y}$ is the 25-years mean and σ_{25y} is the 25-years standard deviation;

ii) the standardized inter-annual anomaly (z_y),

$$z_y = \frac{x_y - \bar{x}_{25y}}{\sigma_{25y}} \quad \text{(IV.1.2)}$$

where x_y is the yearly mean of each year available;

and iii) the standardized individual monthly (atmospheric and river flow data) or seasonal (water quality data) anomaly (z_{m_y}),

$$z_{m\_y} = \frac{x_{m\_y} - \bar{x}_{m\_25y}}{\sigma_{m\_25y}} \quad \text{(IV.1.3)}$$

where x_{m_y} is the mean of each month or season of each year and σ_{m_25y} is the standard deviation of each month or season over the 25-years period.

The major changes in the atmospheric and river flow data over the 1985 to 2010 period were summarized with the cumulative sums method (CUSUM). The major long-term variations of the water quality variables were evaluated using an automatic sequential algorithm proposed by Rodionov (2004). The STARS (sequential t-test analysis of regime shifts) algorithm (available at http://www.beringclimate.noaa.gov/index.html) detects regime shifts based on the mean of consecutive regimes of the time series that are statistically significant according to the Student's *t*-test and computes a regime shift index (RSI). The sign of the RSI indicates the variation of the regime relative to the mean, while its absolute value specifies the magnitude of the shift. Rodionov and Overland (2005) applied this method to study the regime shifts of the Bering Sea ecosystem. More recently McQuarters-Gollop *et al.* (2008) used this algorithm to study the influence of the climate forcing on the chlorophyll *a* of the Black Sea. A detailed description of the STARS algorithm can be found in Rodionov (2004). In the present analysis a minimum regime length of 10 years was considered and two probability levels were evaluated (p=0.05 and p=0.10). The long-term trend of each variable was also assessed. Linear regression over the standardized individual monthly (atmospheric and river flow data) or seasonal (water quality data) anomalies, which correspond to the deseasonalised time series, was used.

In order to evaluate the main relations between the variables, Spearman rank (r_S) correlations were calculated. This correlation coefficient was chosen because it evaluates the relationship between the variables without making any assumptions about the nature of this relationship. The correlations among the atmospheric, river flow and NAO index data were based on the monthly values. For these variables, cross-correlation was performed over the monthly data to estimate the degree to which the time series correlate. Autocorrelation and trend were removed from the time series used in the cross-correlation analysis. For the correlations among the water quality and climatic variables, four different periods of integration were considered for the climatic and hydrological variables specification. These periods were the 8 days (Gameiro *et al*., 2007), 1 month, 3 months and 6 months before the sampling date, and aimed to evaluate the degree to which the previous climatic and hydrological variations influence the water quality, over time windows of different length. For each one of these periods mean values of air temperature, solar radiation, wind intensity and river flow, and accumulated rainfall were calculated. For the NAO index the daily value of the date of sampling was used. As multiple comparisons were performed in the correlation analysis, the Bonferroni correction (Morrison, 1976) was used.

Principal components analysis (PCA) was also used to investigate the relative importance of the water quality parameters, the similarities between years and the relations of each principal component with the climatic and hydrological variables, following an approach similar to the one described by Beaugrand *et al.* (2002). The results of this analysis revealed only trivial (seasonal) or redundant patterns relative to the ones evidenced by the other analyses performed and are not presented here.

IV.1.3 RESULTS

Results are presented in order to characterize the main spatial and temporal patterns of variation of the climatic, hydrological and water quality variables in the Aveiro lagoon over the 1985 to 2010 period. The relationships between these variables are also presented, providing fundamental information to understand the relative influence of climatic variability and anthropogenic interventions in the long-term evolution of the water quality in the lagoon. Complementary results are presented in Appendix III, including the descriptive statistics of all variables over the analysed period (Table AIII.1).

IV.1.3.1 Climatic and Hydrological Characterization

Air temperature and solar radiation exhibited an expected seasonal pattern (Figure IV.1.2), which is characterized by maximum standardized monthly anomalies during August and July,

respectively, and minimum standardized monthly anomalies in January and December. A positive correlation was found between these two variables (Table IV.1.1), which was maximum with a time lag of 1 month. In the 25-years period, 1989, 1995 and 1997 were the warmest years (Figure IV.1.5). The linear regression performed on the standardized individual monthly anomalies over 1985-2010 suggests a slightly upward trend, for both air temperature (0.1% year^{-1}) and solar radiation (0.6% year^{-1}). A more detailed analysis of the CUSUM results (Figure IV.1.5) evidences a global tendency for lower air temperatures between 1990 and 1995, followed by significantly warmer years until 1998 and alternations between colder and warmer years between 1998 and 2010. Solar radiation was significantly higher than the mean between 2004 and 2010, period during which most of the standardized individual monthly anomalies were positive (Figure IV.1.5).

As expected, rainfall varied seasonally (Figure IV.1.2), but inversely of air temperature and solar radiation (Table IV.1.1), with maximum standardized monthly anomalies occurring in late autumn and winter. The lowest rainfall was observed in 2004-2005, while 1996-1997 and 2000-2001 were rainy years (Figure IV.1.5). Regarding the tendencies, three distinct periods were observed (Figure IV.1.5): a period marked by a decrease in the rainfall until 1992, followed by a period of rainiest years with significant positive standardized anomalies until 2003 and then a period of drier years (2004-2008). Overall, during the 1985-2010 period, the linear regression of the deseasonalised time series suggests a slightly positive trend in rainfall (0.2% year^{-1}).

Similarly to rainfall, the river flow also presented an upward trend, in particular after 2000 (Figure IV.1.5). A positive correlation was found between the two variables (Table IV.1.1), which was maximal without any time lag. It should be noted that quantitatively this discharge does not represent the total Vouga river flow, but it is able to represent its main patterns as mentioned previously (section IV.1.2.2).

Table IV.1.1. Spearman rank correlations between atmospheric data (AirT – air temperature; SRad – solar radiation; Rain – rainfall; WindI – wind intensity), river flow (RFlow) and NAO index based on discrete data with no time lag (significant correlations with Bonferroni corrections are marked for *p<0.05, **p<0.01 and ***p<0.001).

	AirT	SRad	Rain	WindI	RFlow	NAO
AirT	1					
SRad	0.754***	1				
Rain	-0.481***	-0.640***	1			
WindI	0.171*	0.399***	-0.004	1		
RFlow	-0.594***	-0.515***	0.652***	0.075	1	
NAO	-0.173*	-0.092	-0.219**	-0.176**	-0.081	1

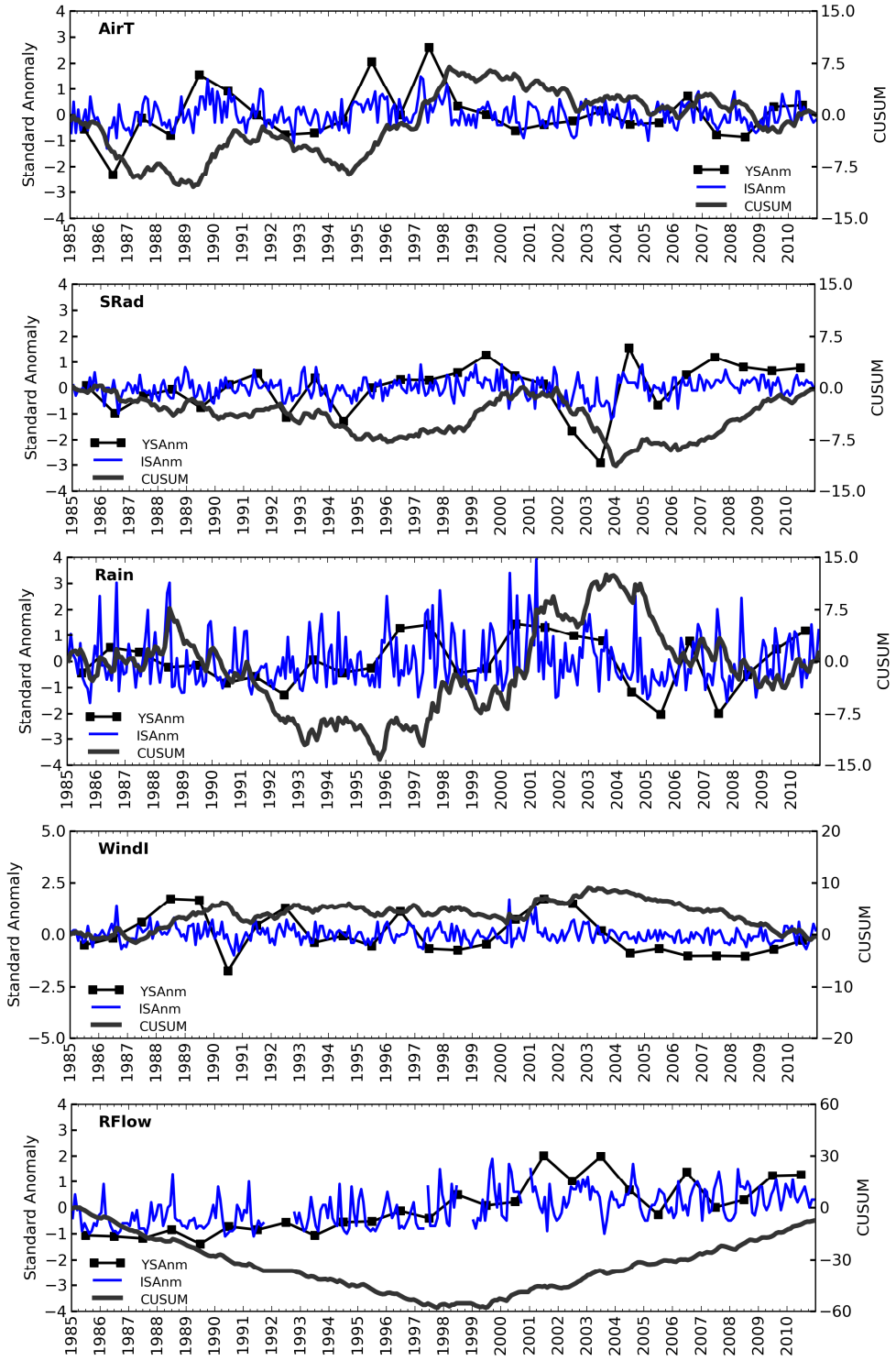

Figure IV.1.5. Standardized year anomaly (YSAnm), standardized individual monthly anomaly (ISAnm) and CUSUM for the atmospheric parameters and river flow from 1985 to 2010 (AirT – air temperature; SRad – solar radiation, Rain – rainfall; WindI – wind intensity; RFlow – river flow).

During the analyzed period, linear regression of the deseasonalised time series suggests a slight decrease in wind intensity, which is more evident after 2003 (Table IV.1.1).

The NAO index also presented a slight downward trend during the 1985 to 2010 period (Figure IV.1.3). Although significant correlations were found between this variable and the other climatic and hydrological variables, their magnitude is low (Table IV.1.1).

IV.1.3.2 Water Quality Variables Characterization

Salinity presented a spatial pattern along the three stations (Figure IV.1.4) with larger values in the downstream area of the Aveiro lagoon (station RA10) and smaller values upstream (station RA11), as expected. Station RA11, in particular, presented no significant variability of the salinity during the analyzed period and clear freshwater characteristics. Station RA4 presented the larger salinity amplitude (Table AIII.I, Appendix III), which evidences the combined influence of the tide and freshwater discharge in this station and its transition characteristics. Both RA10 and RA4 stations presented a marked seasonal pattern (Figure AIII.1, Appendix III), with lower salinities during winter and larger values during summer. Water temperature also presented a seasonal variation, with the larger temperatures occurring during summer (Figure AIII.1, Appendix III). A positive correlation was found between salinity and water temperature at station RA4 (Table IV.1.3). Both RA4 and RA11 presented the larger variations between the extreme values of water temperature (Table AIII.I, Appendix III), deriving from the lower depths of these areas and, consequently, the stronger influence of heat exchanges with the atmosphere.

Between 1985 and 2010, chlorophyll *a* presented a spatial gradient along the Aveiro lagoon, with higher concentrations in the upstream areas of lagoon. A seasonal variation of chlorophyll *a* was observed throughout all the RA stations (Figure AIII.2, Appendix 2), revealing the standardized seasonal anomalies larger chlorophyll *a* concentrations during the summer season, in particular at station RA11. The long-term variation of the chlorophyll *a* concentrations between 1985 and 2010 evidences a downward trend at both stations RA10 and RA4, while at station RA11 a slightly upward trend was observed (Figure IV.1.6). The downward trend at stations RA10 and RA4 was also identified by the RSI method (Figure IV.1.7 and Figure IV.1.8). At station RA10, a regime shift was identified in 2004, with a decrease in the mean concentrations of 2.4 $\mu g\ l^{-1}$. It should be noted that at this station the regime shift was only identified with p=0.10. At station RA4 the regime shift was identified earlier, in 2001, revealing a decrease in mean regime concentration of 1 $\mu g\ l^{-1}$. At these stations (RA10 and RA4), considering the Bonferroni correction, no significant correlations were found between chlorophyll *a* and inorganic nutrients (Table IV.1.2 and Table IV.1.3). At station RA11 chlorophyll *a* correlated negatively with nitrates + nitrites and dissolved oxygen (Table IV.1.4).

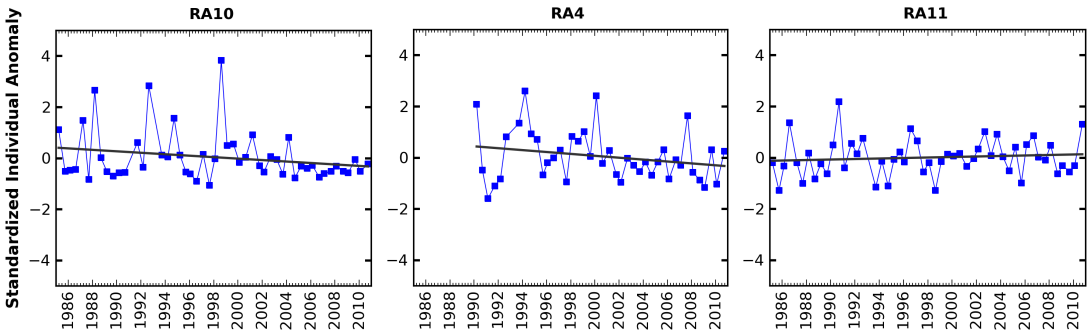

Figure IV.1.6. Chlorophyll *a* standardized individual seasonal anomalies (squared line) and linear correlation (solid line) at stations RA10, RA4 and RA11.

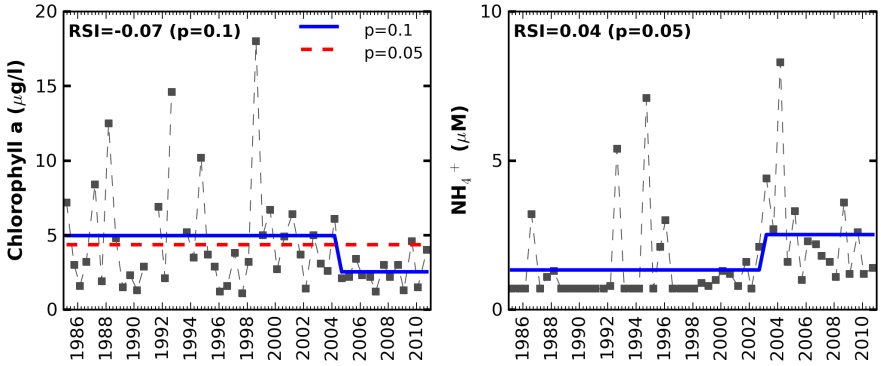

Figure IV.1.7. Shifts in chlorophyll *a* and ammonium (NH_4^+) concentrations at station RA10 (filled squares – variables concentration; solid and dashed line – regime mean; RSI – Regime Shift Index).

Mean dissolved oxygen concentrations were similar at all RA stations, of about 8 mg l^{-1}. Seasonally, there was a marked pattern at station RA11, with larger concentrations during winter, while at the other stations this pattern was not evident (Figure AIII.2, Appendix III).

At station RA11, dissolved oxygen correlated negatively with water temperature and positively with nitrates + nitrites (Table IV.1.4). At this station, dissolved oxygen concentrations remained relatively low until 1993, and overall, during the 1985-2010 period a positive trend was identified at this station. In particular, a regime shift was identified in 1994 (Figure IV.1.9), with an increase in the regime mean from 6.1 mg l^{-1} to 9.0 mg l^{-1}. At station RA4 a regime shift was identified in 2009, with a decrease of the dissolved oxygen concentrations (Figure IV.1.8).

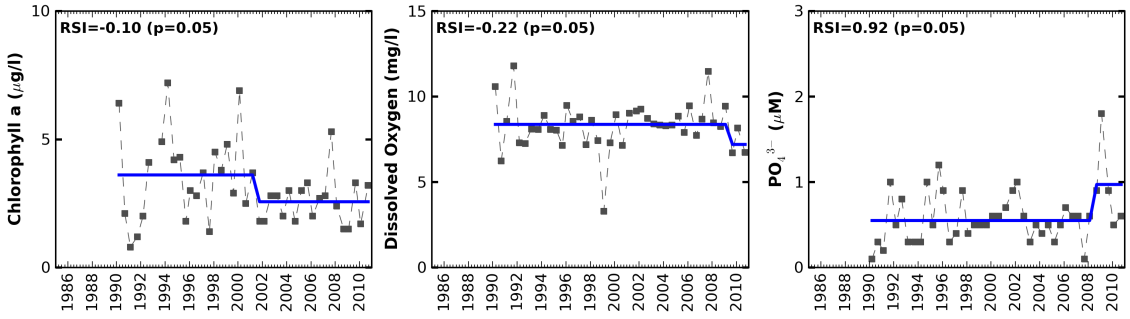

Figure IV.1.8. Shifts in chlorophyll *a*, dissolved oxygen and phosphates (PO_4^{3-}) concentrations at station RA4 (filled squares – variables concentration; solid line – regime mean; RSI – Regime Shift Index).

A spatial gradient was observed in the inorganic nutrients concentrations along the Aveiro lagoon, the larger concentrations occurring in the upstream area of the lagoon (station RA11), with the exception of phosphates. Phosphates mean concentrations were similar throughout all the RA stations (Table AIII.1, Appendix III). In terms of seasonal variation, nitrates + nitrites presented a marked seasonal pattern at all RA stations (Figure AIII.2, Appendix III), with larger concentrations during the winter season. At stations RA10 and RA11 results also evidenced a seasonal variation of ammonium concentration, which was not so evident at station RA4 (Figure AIII.2, Appendix III). At this station, silicates concentrations varied seasonally (Figure AIII.2, Appendix III), the larger concentrations occurring during the winter season. A positive correlation was found between silicates and nitrates + nitrites at stations RA10 and RA4 (Table IV.1.2 and Table IV.1.3). Phosphates did not present a defined seasonal pattern throughout all stations (Figure AIII.2, Appendix III). At station RA10, in particular, phosphates correlated positively with nitrates + nitrites (Table IV.1.2). Regarding the long-term variation of the inorganic nutrients in the Aveiro lagoon a regime shift, characterized by an increase in 2003 of ammonium, was identified at station RA10 (Figure IV.1.7). At this station, the linear regression over the deseasonalised time series also suggests an upward trend for phosphates and a downward trend for silicates. A regime shift, with a mean increase of about 0.4 μM of the phosphates concentration, was observed at station RA4 during 2008 (Figure IV.1.8). At this station, both ammonium and silicates presented a long-term trend similar to the one observed at RA10 station. At station RA11 two regimes shifts were identified for nitrates and nitrites (1993 and 2010) and silicates (1997 and 2009), both characterized by an increase of the concentrations of these nutrients (Figure IV.1.9). At this station two regime shifts were also observed for phosphates concentrations: a first shift in 1997, with an increase in the phosphates concentration, and an inverse shift in 2009 (Figure IV.1.9). Overall, during the 1985 and 2010 period, the linear regression analysis suggested a positive trend in the phosphates concentrations. Ammonium, at the RA11 station, presented a slightly downward trend.

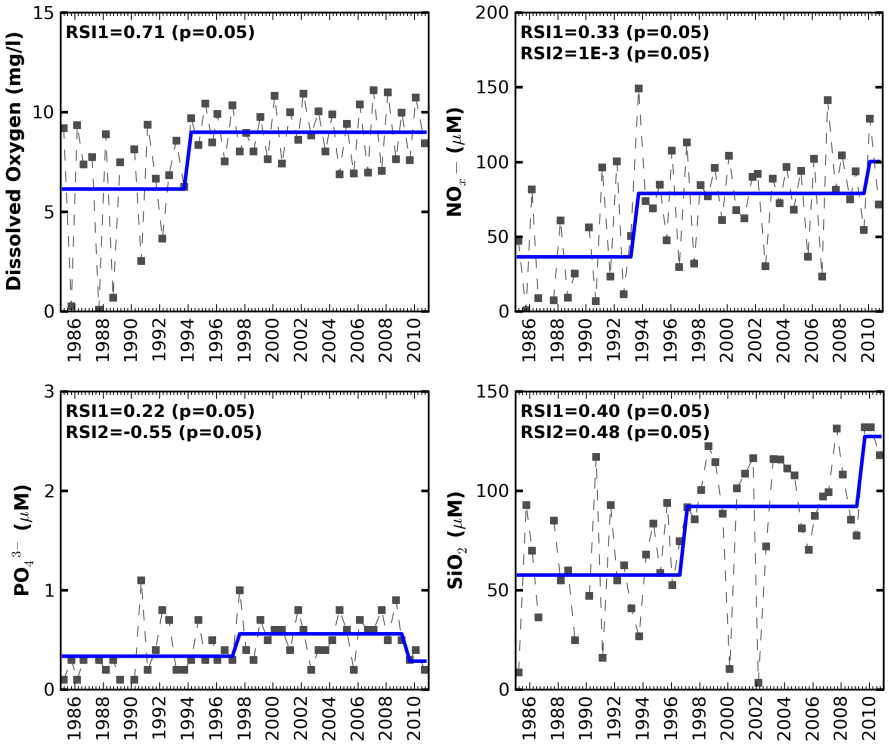

Figure IV.1.9. Shifts in dissolved oxygen, nitrates + nitrites (NO_x^-), phosphates (PO_4^{3-}) and silicates (SiO_2) concentrations at station RA11 (filled squares – variables concentration; solid line – regime mean; RSI – Regime Shift Index).

IV.1.3.3 Relationships Between Water Quality Variables and Climatic and Hydrological Factors

Relationships between the water quality and the climatic and hydrological variables are presented for the integration period of these last variables (8 days, 1 month, 3 months or 6 months; Table IV.1.2, Table IV.1.3 and Table IV.1.4). In these tables only the maximum correlation obtained for each pair of variables is given, separately for each station. Additional tables, including all the correlation values for all the periods evaluated, are presented in Appendix III (Table AIII.2 to Table AIII.13).

Salinity, at the downstream stations, and water temperature, at all stations, were significantly correlated with the atmospheric and river flow data, which puts in evidence the marked seasonal pattern of these variables and the influence of the climatic and hydrological drivers in establishing these properties.

No significant correlations were found between chlorophyll *a* and the physical parameters at stations RA10 and RA4. At station RA11, chlorophyll *a* correlated positively with air temperature, solar radiation and wind intensity, and negatively with rainfall and river discharge (Table IV.1.4), putting in evidence the seasonal variation of the biological activity. At this station,

the correlations found between the dissolved oxygen and the physical variables were opposite of those observed for chlorophyll *a* (Table IV.1.4). In general, the maximum correlations were found when considering the climatic and hydrological data integrated over 1 or 3 months prior to the sampling date of the water quality variables, suggesting different "time lags" between the bio-chemical and the physical processes.

Regarding nutrients, only nitrates + nitrites and silicates were significantly correlated ($p<0.05$, with Bonferroni correction) with some climatic and hydrological variables. Nitrates + nitrites were positively correlated with rainfall and river flow at stations RA4 and RA11 (Table IV.1.3 and Table IV.1.4). Silicates were positively correlated with rainfall, at station RA4 (Table IV.1.3). At this station, the maximum correlations occurred when considering the data from 3 months before the water quality sampling date.

Table IV.1.2. Spearman rank correlations between water quality variables at station RA10 (Salt – salinity, WTemp – water temperature, Chl a – chlorophyll *a*; DO – dissolved oxygen; NH_4^+ – ammonium; NO_x^- – nitrates+nitrites; PO_4^{3-} - phosphates; SiO_2 - silicates) and climatic and hydrological variables (AirT – air temperature; SRad – solar radiation; Rain – rainfall; WindI – wind intensity; RFlow – river flow; NAO – NAO index). Significant correlations for $p<0.05$ with Bonferroni correction are marked with *.

	Salt	WTemp	Chl a	DO	NH_4^+	NO_x^-	PO_4^{3-}	SiO_2
Salt	1							
WTemp	0.459	1						
Chl a	0.036	0.143	1					
DO	-0.357	-0.274	-0.036	1				
NH_4^+	0.049	0.019	0.064	-0.144	1			
NO_x^-	-0.159	-0.668*	-0.199	-0.112	0.026	1		
PO_4^{3-}	0.022	-0.492*	-0.251	-0.294	0.374	0.739*	1	
SiO_2	-0.278	-0.170	-0.077	-0.073	-0.144	0.516*	0.261	1
AirT	0.626* (1m)	0.850* (3m)	0.195 (8d)	-0.506* (6m)	0.147 (6m)	-0.555* (8d)	-0.439 (1m)	-0.129 (8d)
SRad	0.660* (3m)	0.746* (3m)	0.324 (1m)	-0.359 (6m)	0.175 (6m)	-0.554* (1m)	-0.385 (1m)	-0.286 (8d)
Rain	-0.658* (3m)	-0.620* (3m)	-0.225 (1m)	0.187 (3m)	-0.164 (3m)	0.464 (1m)	0.365 (1m)	0.336 (3m)
WindI	0.282 (6m)	0.759 (60)*	0.383 (6m)	-0.265 (6m)	-0.198 (8d)	-0.487* (6m)	-0.433 (6m)	0.268 (8d)
RFlow	-0.632* (3m)	-0.564* (1m)	-0.204 (1m)	0.435 (3m)	0.319 (6m)	0.374 (1m)	0.266 (8d)	0.205 (1m)
NAO	0.195	0.170	-0.134	0.106	-0.407	-0.085	-0.193	0.148

Table IV.1.3. Spearman rank correlations between water quality variables at station RA4 (Salt – salinity, WTemp – water temperature, Chl a – chlorophyll *a*; DO – dissolved oxygen; NH_4^+ – ammonium; NO_x^- – nitrates+nitrites; PO_4^{3-} - phosphates; SiO_2 - silicates) and climatic and hydrological variables (AirT – air temperature; SRad – solar radiation; Rain – rainfall; WindI – wind intensity; RFlow – river flow; NAO – NAO index). Significant correlations for p<0.05 with Bonferroni correction are marked with *.

	Salt	WTemp	Chl a	DO	NH_4^+	NO_x^-	PO_4^{3-}	SiO_2
Salt	1							
WTemp	0.607*	1						
Chl a	-0.086	-0.102	1					
DO	-0.499	-0.197	0.002	1				
NH_4^+	-0.330	-0.067	-0.114	0.022	1			
NO_x^-	-0.788*	-0.612*	0.185	0.310	0.187	1		
PO_4^{3-}	0.074	0.109	-0.398	-0.023	0.427	0.065	1	
SiO_2	-0.683*	-0.307	-0.012	0.271	0.241	0.639*	0.133	1
AirT	0.810* (8d)	0.857* (8d)	-0.212 (6m)	-0.405 (3m)	-0.196 (8d)	-0.710* (8d)	0.333 (6m)	-0.497 (8d)
SRad	0.799* (1m)	0.730* (1m)	-0.215 (6m)	-0.469 (1m)	-0.173 (8d)	-0.757* (1m)	0.299 (6m)	-0.569* (8d)
Rain	-0.809* (6m)	-0.557* (3m)	-0.252 (1m)	0.417 (3m)	0.329 (8d)	0.777* (3m)	0.294 (8d)	0.606* (3m)
WindI	0.515* (6m)	0.723* (6m)	-0.171 (8d)	0.196 (8d)	0.272 (8d)	-0.433 (6m)	0.382 (8d)	0.449 (8d)
RFlow	-0.664* (3m)	-0.543* (1m)	0.195 (3m)	0.487 (3m)	-0.096 (3m)	0.711* (3m)	0.006 (8d)	0.434 (3m)
NAO	0.123	0.322	-0.055 (8d)	-0.012	-0.129	-0.089	-0.197	-0.038

Table IV.1.4. Spearman rank correlations between water quality variables at station RA11 (Salt – salinity, WTemp – water temperature, Chl a – chlorophyll *a*; DO – dissolved oxygen; NH_4^+ – ammonium; NO_x^- – nitrates+nitrites; PO_4^{3-} - phosphates; SiO_2 - silicates) and climatic and hydrological variables (AirT – air temperature; SRad – solar radiation; Rain – rainfall; WindI – wind intensity; RFlow – river flow; NAO – NAO index). Significant correlations for p<0.05 with Bonferroni correction are marked with *.

	Salt	WTemp	Chl a	DO	NH_4^+	NO_x^-	PO_4^{3-}	SiO_2
Salt	-							
WTemp	-	1						
Chl a	-	0.740*	1					
DO	-	-0.733*	-0.484*	1				
NH_4^+	-	-0.002	0.131	0.106	1			
NO_x^-	-	-0.657*	-0.480*	0.692*	0.264	1		
PO_4^{3-}	-	0.136	0.294	-0.020	0.338	0.164	1	
SiO_2	-	0.312	0.246	-0.008	0.012	0.070	0.393	1
AirT	-	0.924* (8d)	0.690* (8d)	-0.722* (1m)	-0.131 (3m)	-0.670* (1m)	0.229 (6m)	0.402 (6m)
SRad	-	0.800* (1m)	0.724* (1m)	-0.745* (3m)	-0.245 (8d)	-0.674* (8d)	0.325 (6m)	0.420 (6m)
Rain	-	-0.732* (3m)	-0.698* (3m)	0.706* (3m)	-0.065 (1m)	0.601* (3m)	-0.204 (3m)	-0.214 (6m)
WindI	-	0.670* (6m)	0.530* (6m)	-0.600* (6m)	-0.158 (8d)	-0.601* (6m)	-0.189 (3m)	-0.390 (8d)
RFlow	-	-0.642* (3m)	-0.646* (1m)	0.764* (3m)	0.025 (3m)	0.683* (8d)	-0.092 (3m)	0.101 (6m)
NAO	-	0.111	0.115	-0.082	0.216	-0.035	0.029	-0.074

IV.1.4 DISCUSSION

During the past 25 years the Aveiro lagoon underwent several modifications due to the development of economic activities, the implementation of management measures or even occurring naturally due to the intrinsic nature of this estuarine system (Figure IV.1.10). The construction of an integrated domestic and industrial wastewater treatment and disposal system, which start operating in 2000 and discharges the treated effluents in the Atlantic ocean, is an example of these changes. Previously, the wastewater treatment plants in the lagoon were scarce and during several years untreated or poorly treated domestic and industrial effluents were discharged directly in the lagoon. Some major changes also occurred near the inlet, namely the construction of the North pierheard and the dredging of the channels for navigation, which affected the circulation in the lagoon. As a consequence of the modifications that happened in the Aveiro lagoon between 1985 and 2010, changes in the ecosystem and water quality dynamics of this system were expected to occur. Estuarine ecosystems are also influenced by climatic and hydrological factors and the natural variations of these drivers may affect their dynamics (e.g. Gameiro *et al.*, 2007). A long-term analysis of the chlorophyll *a*, dissolved oxygen and inorganic nutrients in the Aveiro lagoon, covering a period of anthropogenic modifications and different climatic and hydrological conditions contributes to the understanding of the relative role of these drivers in this type of estuarine systems.

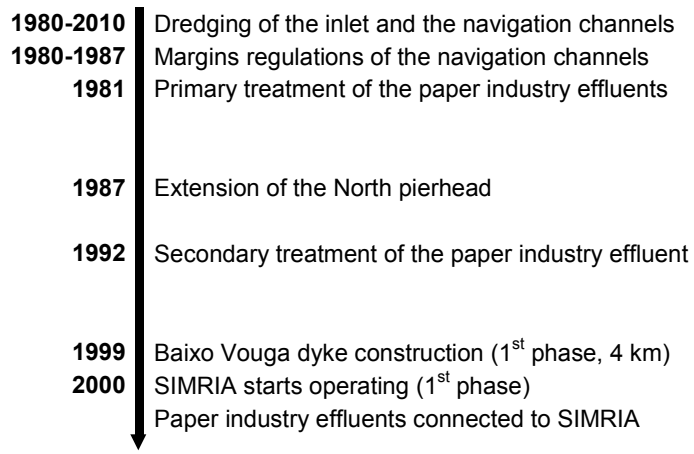

Figure IV.1.10. Timeline of some anthropogenic interventions in the Aveiro lagoon in the past 30 years.

Nutrient enrichment related with human disturbances has been pointed as one of the main causes of cultural eutrophication in estuaries (e.g. Cloern, 2001). In the Aveiro lagoon, with exception of phosphates, inorganic nutrients presented a well-defined seasonal pattern characterized by larger concentrations during the winter season. Inorganic nutrients

concentrations were within the range of variation observed in other estuaries (e.g. Harding, 1994; Cabeçadas *et al.*, 1999; Barbosa *et al.*, 2010; Gameiro and Brotas, 2010).

Ammonium and phosphates were not significantly related to the climatic and hydrological drivers, namely rainfall or the freshwater discharge, throughout all the area of the Aveiro lagoon. This suggests that in the lagoon the river discharge was not the main source of ammonium and phosphates, which may come from anthropogenic sources (e.g. domestic or industrial effluents discharges) or sediments resuspension. Some studies also suggest that excretions of zooplankton may be an important source of ammonium and phosphorus in estuaries and coastal areas (Ikeda *et al.*, 1982). In the downstream area of the lagoon, an upward trend characterized the long-term variation of these two nutrients. In particular, the increasing shifts observed after 2000, both in ammonium and phosphates, were not expected. The first stage of the SIMRIA wastewater treatment system started operating in 2000 and a decrease of these nutrients was expected to occur. In the upstream area of the lagoon, the long-term mean concentrations of ammonium presented a slightly downward trend in the 25-years period, while alternations occurred in phosphates.

Silicates presented an inverse long-term trend relative to ammonium and phosphates in the downstream area of the lagoon. Freshwater discharge from upstream rivers is the major source of silica to estuaries (Ji, 2008). This was also evident in the Aveiro lagoon, where silicates were brought from the river towards the inlet. Larger concentrations of silicates downstream occurred during the rainier periods (winter of 1996, 2001 and 2009), and positive correlations were found with rainfall. As silicates in the water bodies come from the weathering of terrestrial rocks (e.g. Statham, 2012), the intense rainfall winter of 2001 followed by very wet years in 2004, 2005 and 2007 could be associated with the decrease in silicates in the downstream area of the lagoon. However, in the upstream area of the lagoon silicates presented an upward trend between 1985 and 2010 and two increasing shifts occurred (1997 and 2009). This suggests that some retention may be happening in the upstream area of the lagoon. The construction of infrastructures that retain freshwater upstream (e.g. dams, dykes) may influence the volume of freshwater reaching the downstream area of the estuary and, consequently, silicates concentrations (e.g. Rocha *et al.*, 2002; Li *et al.*, 2007). In the upstream area of the Aveiro lagoon two dyke systems are used during the dry season to prevent the salinity intrusion, allowing agricultural activities and the operation a paper mill in the margins of the Vouga river (Plano de Bacia Hidrográfica do Rio Vouga, 1999). These dykes limit partly the freshwater progression downstream: the first dyke influences the Antuã river discharge, while the paper mill dyke influences the Vouga river discharge. The paper mill, in particular, pumps water from the Vouga river and, until the recent connection to the SIMRIA system in 2000 (Portucel Soporcel, 2009), also discharged its treated effluents in the river. This shunting of river water to the sewage system reduces the river flow, which has been previously identified as a risk (Plano de

Bacia Hidrográfica do Rio Vouga, 1999), and may also be contributing for the decrease of silicates transported downstream.

Another potential cause affecting silicates concentrations downstream may be deepening of the inlet of the Aveiro lagoon (maintained artificially through dredging) that occurred between 1987 and 2001 (Silva and Leitão, 2011). This deepening led to an increase in the tidal prism (Silva and Leitão, 2011) and in the tidal amplitude (Araújo *et al.*, 2008), which may promote a larger transport offshore of silicates and more dilution by seawater (e.g. Valiela and Costa, 1988; Ruiz *et al.*, 1998). Pereira *et al.* (2011) also suggested an offshore transport of silicates in the Aveiro lagoon. However, it should be noted that silicates were the only nutrient that presented this decreasing pattern downstream.

Regarding nitrates + nitrites, with exception of the upstream area, no significant trends occurred in the past 25-years. The concentration of nitrates + nitrites in the Aveiro lagoon was mainly controlled by climate, namely by rainfall and river discharge. Larger concentrations of nitrates + nitrites in the downstream area occurred during intense rainfall periods (e.g. 1996, 2001 and 2009), evidencing the role of the freshwater discharge in controlling the downstream transport of these nutrients. The increasing trend of nitrates + nitrites observed in the upper limit of the Aveiro lagoon was probably related with the simultaneous increase in the dissolved oxygen in this area, which provided the aerobic conditions needed for nitrification.

The riverine station experienced some hypoxia episodes until 1993. These episodes were characterized by dissolved oxygen concentrations lower than 3 mg l^{-1} (Nezlin *et al.*, 2009) and occurred mainly during the summer season. The occurrence of these conditions only during the summer and the relations found between dissolved oxygen and the river discharge put in evidence the role of the freshwater discharge in promoting the water renewal at this site. A regime shift with an increase in the dissolved oxygen was predicted in 1994. Although a negative correlation was found in this station between dissolved oxygen and chlorophyll *a*, evidencing large oxygen consumption during periods of increased primary productivity, most of the hypoxia episodes were not associated with the larger concentrations of chlorophyll *a*. In particular, chlorophyll *a* patterns remained almost unchanged at this station in the past 25 years. The paper mill that operates near this site started the primary treatment of its effluents in 1981, while the secondary treatment only started in 1992 (Portucel Soporcel, personal communication). Secondary treatment is mainly associated with the removal of organic matter from the effluent and a direct relation seems to exist between the beginning of the secondary treatment of the paper mill effluent and the improvement of the dissolved oxygen concentrations in this site. The effects of lower dissolved oxygen concentrations that occurred in the upstream area of the lagoon until 1993 were not observed in the downstream areas, revealing that tide promotes an effective water renewal in these areas.

Chlorophyll *a* in the Aveiro lagoon presented a spatial pattern, with larger concentrations in the upstream area of the lagoon. Between 1985 and 2010 observed concentrations were within the range of variation registered in other Portuguese estuaries (e.g. Cabeçadas *et al.*, 1999; Barbosa *et al.*, 2010; Gameiro and Brotas, 2010). Some episodes, where chlorophyll *a* was larger than 10 mg l^{-1}, were associated with blooms (Sève, 1993; Sin *et al.*, 1999; Gameiro *et al.*, 2007). These blooms occurred mainly in the upstream station during the summer season (16 bloom episodes). Four blooms were observed near the inlet, which were probably associated with upwelling events, and none was registered in the middle area of the lagoon. The seasonal pattern of chlorophyll *a*, with larger concentrations during summer and lower during winter, was related with rainfall and water temperature, in particular in the upstream area of the lagoon. This suggests that at this station chlorophyll *a* variations were mostly driven by the atmospheric and hydrological variability. The higher temperature observed during the summer combined with the lower river discharges and, consequently, higher residence times promote hydrodynamic conditions that potentiate phytoplankton growth (e.g. Ferreira *et al.*, 2005). In particular, some of the lower concentrations of chlorophyll *a* occurred during the rainier periods, namely in the winter season of 2001 and 2009. Maximum correlations were found with the climatic and hydrological data integrated over periods of 1 to 3 months, evidencing a time lag between the physical forcing and the bio-chemical processes and the need to evaluate different temporal scales when performing this type of analyses.

In the downstream areas of the lagoon, chlorophyll *a* presented a downward trend in the past 25-years, and regime shifts occurred in 2004 (inlet station) and 2001 (transition station). Taking into account the role of nutrients in limiting phytoplankton growth (e.g. Padersen *et al.*, 1996; Yin *et al.*, 2000) half-saturation constants and nutrients ratios are often used to analyse limiting nutrients for phytoplankton growth (e.g. Dortch and Whitledge, 1992). Half-saturation constants estimations are vast (Chapter II), but the ones proposed by Fisher *et al.* (1988) were considered. The approach described by Dorthch and Whitledge (1992) was also considered to evaluate nutrients limitation. Dissolved inorganic nitrogen (DIN – sum of ammonium, nitrates and nitrites) limitation (DIN<1 μM, N/P<10 and Si/N>1) was never observed at the downstream stations during the analysed period. At the inlet station, phosphates limiting conditions (PO_4^{3-} <0.2 μM, N/P>30 and Si/P>3) were found four times (three of them before 2000), while at the transition station these conditions were found three times (February 1990, February 1991, and September 2007). Silicates presented a downward trend at these two stations and concentrations below the reported half-saturation constant of 5 μM were observed. In the transition station these low silicate concentrations occurred mostly after 2000, while near the inlet they were observed from 1985 to 2010. Silicates limiting conditions (SiO_2<2.0 μM, Si/N<1, Si/P<3) were found three times at these stations, all of them after 2000. Silicates concentrations

and the nutrient ratios at the downstream stations, suggest that the downward trend observed in chlorophyll *a* was probably associated with the similar trend observed in silicates.

Although silicates availability seems to be the main factor affecting the decrease of phytoplankton in the downstream area of the Aveiro lagoon, the deepening that occurred between 1987 and 2001 near the inlet may have contributed for a larger transport offshore. This deepening may also have contributed for sediment resuspension and, consequently, promoted a decrease in the light availability in the water column, limiting the phytoplankton growth (e.g. Alpine and Cloern, 1988; Gameiro *et al.*, 2011). Mean suspended particulate matter in the inlet of the Aveiro lagoon after 2000 was close (17.7-22.95 mg l^{-1}, Martins *et al.*, 2009) to those observed in the light limited Tagus estuary (30 mg l^{-1}; Gameiro and Brotas, 2010). Additionally, a possible influence of zooplankton grazing cannot be discarded, but there are not enough in situ data to study this hypothesis.

The decrease in silicates concentrations observed during the past 10 years in the downstream area of the Aveiro lagoon, combined with the increase in ammonium and phosphates, may represent a threat to the ecosystem health, as it may lead to changes in phytoplankton species composition, the appearance of novel and toxic phytoplankton blooms, modifications in the food web and reduced efficiency in the nutrients recycling and oxygen dynamics (Conley *et al.*, 1993). Moreover, as the Aveiro lagoon is a mesotidal estuary, may also present some susceptibility to nitrogen enrichment (Monbet, 1992).

In the upstream area of the lagoon, silicates and nitrates + nitrites were below the half-saturation constants only once, while phosphates concentrations were below 0.5 μM several times. The nutrient ratios also evidence a minor availability of phosphorus, when compared with nitrogen and silica, suggesting a phosphorus limited-growth in the upper area of the Aveiro lagoon.

The seasonal and spatial variations of nutrients will also influence the phytoplankton species composition and distribution. A seasonal pattern of phytoplankton assemblages in the Aveiro lagoon was proposed by Lopes *et al.* (2007a), dominated by diatoms from late autumn to spring and by chlorophytes from late spring to summer. The seasonal silicates variation observed in the 1985 to 2010 period, with lower concentrations of silicates during the summer season, is consistent with this pattern. A spatial gradient of phytoplankton species is also expected to occur. At the transition station N/P and Si/P tend to be lower during summer and larger during winter. This suggests that, during winter, due to the larger freshwater discharge the freshwater phytoplankton species tend to be further downstream in the lagoon, while, during the summer, the marine phytoplankton species tend to be further upstream. Two distinct communities of phytoplankton had already been identified in the Mira channel of the Aveiro lagoon by Resende *et al.* (2005): one near the downstream area of the Mira channel and dominated by marine species (e.g. *Auliscus sculptus*, *Chaetoceros densus*, *Surirella comis*), while further upstream

freshwater species were dominant (e.g. *Caloneis permagna*, *Cymbella tumida*, *Pinnularia stommatophora*).

IV.1.5 CONCLUSIONS

The analysis of the chlorophyll *a*, dissolved oxygen and inorganic nutrients in the Aveiro lagoon between 1985 and 2010 included a period of diverse anthropogenic modifications and different climatic and hydrological conditions, contributing to the understanding of the relative role of these drivers in the estuarine ecosystems dynamics. The seasonal, inter-annual and long-term trends observed in the Aveiro lagoon depended on the combined influence of both anthropogenic and climate forcing.

Seasonal variations were mostly associated with the seasonal variation of the main climatic and hydrological forcing. This seasonal pattern was particularly evident on nitrates + nitrites and silicates, which are transported downstream in the lagoon by the freshwater flow. In particular, a longitudinal gradient was found throughout the lagoon, characterized by larger concentrations of nutrients and chlorophyll *a* in the upstream areas, where the influence of the freshwater discharge is larger.

In the upstream area of the lagoon, chlorophyll *a* inter-annual variations were mostly driven by the climatic and hydrological variability. Chlorophyll *a* presented a downward trend in the downstream areas of the lagoon, with lower concentrations after 2000. These lower concentrations were probably associated with the simultaneous decrease in silicates concentrations, which may derive from some anthropogenic modifications that occurred in the lagoon. Future monitoring of this situation is needed, since the combined decrease of silicates with the observed increase of ammonium and phosphates in these areas may represent a threat for the ecosystem health.

The adoption of some environmental measures, as the use of secondary treatment of industrial effluents, allowed the system recovery from hypoxia conditions in the upstream area of the lagoon. The significant influence of these measures puts in evidence that some anthropogenic interventions may have a larger influence in the water quality and ecological dynamics of the lagoon, when compared with the system natural variability.

The analysis performed in this study evidenced the need for long-term monitoring and to combine both anthropogenic and climate drivers when assessing the water quality of estuarine ecosystems, in order to promote the sustainable management and development of these systems.

IV.1.6 REFERENCES

Almeida M A, Cunha MA, Alcântara F. Relationship of bacterioplankton production with primary production and respiration in a shallow estuarine system (Ria de Aveiro, NW Portugal). *Microbiological Research* **2005**, 160(3), 315-328.

Alpine AE, Cloern JE. Phytoplankton growth rates in a light-limited environment, San Francisco Bay. *Marine Ecology - Progress Series* **1988**, 44, 167-173.

Araújo IB, Dias JM, Pugh DT. Model simulations of tidal changes in a coastal lagoon, the Ria de Aveiro (Portugal). *Continental Shelf Research* **2008**, 28(8), 1010-1025.

Azevedo IC, Duarte PM, Bordalo AA. Understanding spatial and temporal dynamics of key environmental characteristics in a mesotidal Atlantic estuary (Douro, NW Portugal). *Estuarine, Coastal and Shelf Science* **2008**, 76(3), 620-633.

Barbier EB, Hacker SD, Kennedy C, Koch EW, Stier AC, Silliman BR. The value of estuarine and coastal ecosystem services. *Ecological Monographs* **2011**, 81(2), 169-193.

Barbosa AB, Domingues RB, Galvão HM. Environmental forcing of phytoplankton in a Mediterranean Estuary (Guadiana Estuary, South-western Iberia): a decadal study of anthropogenic and climatic influences. *Estuaries and Coasts* **2010**, 33, 324-341.

Baumert HZ, Petzoldt T. The role of temperature, cellular quota and nutrient concentrations for photosynthesis, growth and light–dark acclimation in phytoplankton. *Limnologica - Ecology and Management of Inland Waters* **2008**, 38(3–4), 313-326.

Beaugrand G, Reid PC, Ibañez F, Lindley JA, Edwards M. Reorganization of North Atlantic marine copepod biodiversity and climate. *Science* **2002**, 296 (5573), 1692-1694.

Borges C, Valença M, Palma C, Cruz I. Monitorização da qualidade ambiental das águas da Ria de Aveiro. In: Almeida A, Alves FL, Bernardes C, Dias JM, Gomes NCM, Pereira E, Queiroga H, Serôdio J, Vaz N (Eds.), Actas das Jornadas da Ria de Aveiro, **2011**, 265-273.

Boyer JN, Kelble CR, Ortner PB, Rudnick DT. Phytoplankton bloom status: Chlorophyll *a* biomass as an indicator of water quality condition in the southern estuaries of Florida, USA. *Ecological Indicators* **2009**, 9, 56-57.

Burkholder JM, Tomasko DA, Touchette BW. Seagrasses and eutrophication. *Journal of Experimental Marine Biology and Ecology* **2007**, 350(1–2), 46-72.

Cabeçadas G, Nogueira M, Brogueira MJ. Nutrient dynamics and productivity in three European estuaries. *Marine Pollution Bulletin* **1999**, 38(12), 1092–1096.

Cardoso PG, Pardal MA, Lillebø AI, Ferreira SM, Raffaelli D, Marques JC. Dynamic changes in seagrass assemblages under eutrophication and implications for recovery. *Journal of Experimental Marine Biology and Ecology* **2004**, 302(2), 233-248.

Cloern JE. Our evolving conceptual model of the coastal eutrophication problem, *Marine Ecology Progress Series* **2001**, 210, 223-253.

Conley DJ, Schelske CL, Stoermer EF. Modification of the biogeochemical cycle of silica with eutrophication. *Marine Ecology Progress Series* **1993**, 101, 179–192.

Cunha MA, Almeida MA, Alcântara F. Compartments of oxygen consumption in a tidal mesotrophic estuary. *Acta Oecologica* **1999**, 20(4), 227-235.

Dias, JM. Contribution to the study of the Ria de Aveiro hydrodynamics. PhD Thesis, Universidade de Aveiro, **2001**.

Dias JM, Lopes JF, Dekeyser I. Hydrological characterisation of Ria de Aveiro, Portugal, in early summer. *Oceanologica Acta* **1999**, 22(5), 473-485.

Dias JM, Lopes JF, Dekeyser I. Tidal propagation in Ria de Aveiro Lagoon, Portugal. *Physics and Chemistry of the Earth, Part B: Hydrology, Oceans and Atmosphere* **2000**, 25(4), 369-374.

Dias JM, Lopes JF. Implementation and assessment of hydrodynamic, salt and heat transport models: the case of Ria de Aveiro Lagoon (Portugal). *Environmental Modelling & Software* **2006**, 21(1), 1-15.

Dortch Q, Whitledge TE. Does nitrogen or silicon limit phytoplankton production in the Mississippi River plume and nearby regions? *Continental Shelf Research* **1992**, 12(11), 1293-1309.

Ferreira JG, Simas T, Nobre A, Silva MC, Shifferegger K, Lencart-Silva J. *Identification of sensitive areas and vulnerable zones in transitional and coastal portuguese systems*, INAG, **2003**, 151 pp.

Ferreira JG, Wolff WJ, Simas TC, Bricker SB. Does biodiversity of estuarine phytoplankton depend on hydrology? *Ecological Modelling* **2005**, 187, 513–523

Fisher TR, Harding Jr. LW, Stanley DW, Ward LG Phytoplankton, nutrients, and turbidity in the Chesapeake, Delaware, and Hudson estuaries. *Estuarine, Coastal and Shelf Science* **1988**, 27(1), 61–93.

Gameiro C, Brotas V. Patterns of phytoplankton variability in the Tagus Estuary. *Estuaries and Coasts* **2010**, 33, 311-323.

Gameiro C, Cartaxana P, Brotas V. Environmental drivers of phytoplankton distribution and composition in Tagus Estuary, Portugal. *Estuarine, Coastal and Shelf Science* **2007**, 75, 21-34.

Gameiro C, Zwolinski J, Brotas V. Light control on phytoplankton production in a shallow and turbid estuarine system. *Hydrobiologia* **2011**, 669,249–263.

Harding Jr LW. Long-term trends in the distribution of phytoplankton in Chesapeake Bay: roles of light, nutrients and streamflow. *Marine Ecology Progress Series* **1994**, 104, 267-291.

Ikeda T, Carleton JH, Mitchell AW, Dixon P. Ammonia and phosphate excretion by zooplankton from the inshore waters of the Great Barrier Reef. II. Their in situ contributions to nutrient regeneration. *Australian Journal of Marine and Freshwater Research* **1982**, 33(4), 683-698.

Ji Z-G. *Hydrodynamics and water quality – Modeling rivers, lakes and estuaries*. Wiley, USA, **2008**.

Kotta I, Simm M, Põllupüü M. Separate and interactive effects of eutrophication and climate variables on the ecosystems elements of the Gulf of Riga. *Estuarine, Coastal and Shelf Science* **2009**, 84, 509-518.

Lehtonen H, Urho I, Kjellman J. Responses of ruffe (*Gymnocephalus cernuus* (L.)) abundance to eutrophication. *Journal of Great Lakes Research* **1998**, 24(2), 1998, 285-292.

Li M, Xu K, Watanabe M, Chen Z. Long-term variations in dissolved silicate, nitrogen, and phosphorus flux from the Yangtze River into the East China Sea and impacts on estuarine ecosystem. *Estuarine, Coastal and Shelf Science* **2007**, 71(1–2), 3–12.

Lopes CB, Lillebø AI, Dias JM, Pereira E, Vale C, Duarte AC. Nutrient dynamics and seasonal succession of phytoplankton assemblages in a Southern European Estuary: Ria de Aveiro, Portugal. *Estuarine, Coastal and Shelf Science* **2007a**, 71(3-4), 480-490.

Lopes CB, Pereira ME, Vale C, Lillebø AI, Pardal MA, Duarte AC. Assessment of spatial environmental quality status in Ria de Aveiro. *Scientia Marina* **2007b**, 71(2), 293-304.

Martins V, Jesus CC, Abrantes I, Dias JM, Rocha F. Suspended particulate matter vs. bottom sediments in a mesotidal lagoon (Ria de Aveiro, Portugal). *Journal of Coastal Research* **2009**, SI56, 1370–1374.

McQuarters-Gollop A, Mee LD, Raitsos DE, Shapiro GI. Non-linearities, regime shifts and recovery: the recent influence of climate on Black Sea chlorophyll. *Journal of Marine Systems* **2008**, 74, 649-658.

Monbet Y. Control of phtytoplankton biomass in estuaries: a comparative analysis of microtidal and macrotidal estuaries. *Estuaries* **1992**, 15, 563-571.

Moreira MH, Queiroga H, Machado MM, Cunha MR. Environmental gradients in a southern europe estuarine system: Ria de Aveiro, Portugal. Implications for soft bottom macrofauna colonization. *Netherlands Journal of Aquatic Ecology* **1993**, 27, 465-482.

Morrison DF. *Multivariate statistical methods*. McGraw-Hill, NY, **1976**, 415 pp.

Nezlin NP, Kamer K, Hyde J, Stein ED. Dissolved oxygen dynamics in a eutrophic estuary, Upper Newport Bay, California. *Estuarine, Coastal and Shelf Science* **2009**, 82(1), 139-151.

Padersen MF, Borum J. Nutrient control of algal growth in estuarine waters. Nutrient limitation and the importance of nitrogen requirements and nitrogen storage among phytoplankton and species of macroalgae. *Marine Ecology Progress Series* **1996**, 142, 261-272.

Paerl HW, Dyble J, Moisander PH, Noble RT, Piehler MF, Pinckney JL, Steppe TF, Twomey L, Valdes LM. Microbial indicators of aquatic ecosystem change: current applications to eutrophication studies. *FEMS Microbiology Ecology* **2003**, 46, 233-246.

Palma C, Valença M, Silva PP, Biscaya JL. Monitoring the quality of the marine environment. *Journal of Environmental Monitoring* **2000**, 2, 512-516.

Pereira E, Lopes CB, Duarte AC. Monitorização do estado trófico da Ria de Aveiro no intervalo temporal entre 2000 e 2004: implicações na evolução da qualidade da água. In: Almeida A, Alves FL, Bernardes C, Dias JM, Gomes NCM, Pereira E, Queiroga H, Serôdio J, Vaz N (Eds.), Actas das Jornadas da Ria de Aveiro, **2011**, 258-264.

Pinckney JL, Paerl HW, Tester P, Richardson TL. The role of nutrient loading and eutrophication in estuarine ecology. *Environmental Health Perspectives* **2001**, 109(5), 699–706.

Plano de Bacia Hidrográfica do Rio Vouga. *Anexo 10, Qualidade dos Meios Hídricos*. Consórcio: Ambio, CHIRON, Agri.Pro, Drena, HCL, FBO Consultores, **1999**, 160 pp.

Polis Litoral – Ria de Aveiro. Intervenção de requalificação e valorização da Ria de Aveiro, Plano Estratégico. Polis Litoral – Ria de Aveiro, **2010**.

Portucel Soporcel. *Monografia da fábrica de Cacia – 2009*. Portocel-Soporcel, **2009**.

Queiroga H, Almeida MJ, Alpuim T, Flores AAV, Francisco S, Gonzalez-Gordillo JI, Miranda AI, Silva I, Paula J. Wind and tide control of megalopal supply to estuarine crab populations on the Portuguese west coast. *Marine Ecology Progress Series* **2006**, 307, *21-36.*

Rebelo, JE. The ichthyofauna and abiotic hydrological environment of the Ria de Aveiro, Portugal. *Estuaries and Coasts* **1992**, 15(3), 403-413.

Resende P, Azeiteiro U, Pereira MJ. Diatom ecological preferences in a shallow temperate estuary (Ria de Aveiro, Western Portugal). *Hydrobiologia* **2005**, 544, *77-88.*

Rocha C, Galvão H, Barbosa A. Role of transient silicon limitation in the development of cyanobacteria blooms in the Guadiana estuary, south-western Iberia. *Marine Ecology Progress Series* **2002**, 228, 35-45.

Rodionov SN, Overland JE. Application of a sequential regime shift detection method to the Bering Sea ecosystem. *ICES Journal of Marine Sciences* **2005**, 62, 328-332.

Rodionov SN. A sequential algorithm for testing climate regime shifts. *Geophysical Research Letters* **2004**, 31, 1-4.

Ruiz A, Franco J, Villate F. Microzooplankton grazing in the Estuary of Mundaka, Spain, and its impact on phytoplankton distribution along the salinity gradient. *Aquatic Microbial Ecology* **1998**, 14, 281-288.

Sampaio L. Processo sucessional de recolonização dos fundos dragados da Ria de Aveiro após o desassoreamento: comunidades macrobentónicas. MsC Thesis, University of Aveiro, **2001**, 87pp.

Scanes P, Coade G, Doherty M, Hill R. Evaluation of the utility of water quality based indicators of estuarine lagoon condition in NSW, Australia. *Estuarine, Coastal and Shelf Science* **2007**, 74(1–2), 306-319.

Sève MA. Diatom bloom in the tidal freshwater zone of a turbid and shallow estuary, Rupert Bay (James Bay, Canada). *Hydrobiologia* **1993**, 269-270, 225-233.

Silva A, Leitão P. Simulação das condições hidromorfológicas da barra da Ria de Aveiro e respectivos impactes nos prismas de maré. In: Almeida A, Alves FL, Bernardes C, Dias JM, Gomes NCM, Pereira E, Queiroga H, Serôdio J, Vaz N (Eds.), Actas das Jornadas da Ria de Aveiro, **2011**, 30-36.

Sin Y, Wetzel RL, Anderson IC. Spatial and temporal characteristics of nutrient and phytoplankton dynamics in the York River estuary, Virginia: analysis of long-term data. *Estuaries* **1999**, 22, 260-275.

Smayda TJ. Complexity in the eutrophication–harmful algal bloom relationship, with comment on the importance of grazing. *Harmful Algae* **2008**, 8(1), 140-151.

Statham PJ. Nutrients in estuaries — An overview and the potential impacts of climate change. *Science of Total Environment* **2012**, 434, 213-227.

Valiela I, Costa JE. Eutrophication of Buttermilk Bay, a cape cod coastal embayment: Concentrations of nutrients and watershed nutrient budgets. *Environmental Management* **1988**, 12(4), 539-553.

Yin K, Qian P-Y, Chen JC, Dennis Hsieh DPH, Harrison PJ. Dynamics of nutrients and phytoplankton biomass in the Pearl River estuary and adjacent waters of Hong Kong during

summer: preliminary evidence for phosphorus and silicon limitation. *Marine Ecology Progress Series* **2000**, 194, 295-305.

Yin K, Zhang J, Qian P-Y, Jian W, Huang L, Chen J, Wu MCS. Effect of wind events on phytoplankton blooms in the Pearl River estuary during summer. *Continental Shelf Research* **2004**, 24(16), 1909–1923

Zimmerman AR, Canuel EA. A geochemical record of eutrophication and anoxia in Chesapeake Bay sediments: anthropogenic influence on organic matter composition. *Marine Chemistry* **2000**, 69(1–2), 117-137.

CHAPTER V

INFLUENCE OF CLIMATE CHANGE AND ANTHROPOGENIC PRESSURES ON THE WATER QUALITY AND ECOLOGICAL DYNAMICS OF THE AVEIRO LAGOON

SECTION V.1

ON THE ROLE OF CLIMATE CHANGE AND ANTHROPOGENIC PRESSURES IN THE WATER QUALITY AND ECOLOGICAL DYNAMICS OF AN ESTUARINE ENVIRONMENT (MIRA CHANNEL, AVEIRO LAGOON, PORTUGAL)[V.1.1]

ABSTRACT

The Aveiro lagoon harbours one of the largest saltmarshes in Europe, with a significant role of ecological services, supporting at the same time several economic activities that might impact its water and ecological quality. Besides the pressures associated with human activities, the impacts of climate change in estuarine ecosystems are also matter of concern worldwide. This study aimed at evaluating the impacts of climate change and anthropogenic pressures on an estuarine environment, the Mira channel (Aveiro lagoon, Portugal), taking advantage of numerical modelling tools. A set of 1-year scenarios was established to study the individual and combined effects of: i) various components of climate change, including air temperature increase, changes in the precipitation regimes and sea level rise, and ii) anthropogenic pressures, including a proposed dredging plan, a marina construction and an emergency by-pass wastewater discharge. Results suggest that, in general, climate change overwhelms the effects of the analysed anthropogenic interventions. Overall results suggest that the circulation is one of the main drivers controlling the water quality and ecological dynamics along the Mira channel. Changes due to sea level rise are the ones that influence these dynamics the most, leading to a significant increase of salinity along the channel and a decrease of nutrients, chlorophyll *a* and dissolved oxygen throughout the year. During the summer season these effects may be enhanced by the reduction of the freshwater discharge. The predicted changes suggest a decrease of the primary production, which may affect the entire food web. Shifts on species composition and further progression upstream of marine species may also occur. These findings constitute a first contribution to the understanding of the relative role of climate change and anthropogenic pressures on the water and ecological quality of the Aveiro lagoon and should be further extended in future studies, to support the sustainable long-term management of this system.

[V.1.1] In preparation to: *Estuarine, Coastal and Shelf Science*.

KEYWORDS

Shallow and Temperate Estuaries, Chlorophyll *a*, Dissolved Oxygen, Nutrients, Climate Change, Sea Level Rise, Increased Air Temperature, Hydrological Regimes, Anthropogenic Interventions

V.1.1 INTRODUCTION

Climate change is a matter of concern and discussion worldwide. Although there are evidences that climate is changing (IPCC, 2007), the extent and impacts of these changes on aquatic systems remain poorly known. In the 20th century sea level has risen and changes in the wind patterns, precipitation and air temperature have occurred worldwide (IPPC, 2007). In Portugal, a rising of the mean air temperature occurred between 1910 and 1945, followed by a decrease from 1946 to 1975, and another increase between 1976 and 2010 (Miranda *et al.*, 2006; Vilão *et al.*, 2011). During the next century expected climate change may induce modifications in air temperature, wind patterns, hydrological regimes and sea level rise (Statham, 2012).

Estuaries, located at the sea-land interface, are areas particularly sensitive to climate change. They present important ecological and economic values, being one of the most productive ecosystems on Earth (Likens, 2010). Estuarine ecosystems supply multiple services (e.g. Barbier *et al.*, 2011), and support several human activities (e.g. marine transportation, navigation and harbours, recreational and commercial fishing, tourism, receiving waters for domestic and industrial wastewater effluents).

The knowledge and understanding of how climate change will affect the estuarine ecosystems remains scarce. Sea level rise impacts include: inundation of low-lying coastal areas and erosion of sandy beaches and barrier islands, altering geomorphological configurations and their associated sediment dynamics; landward intrusion of salt water in estuaries and aquifers; displacement of ecosystems and habitats loss; and increased vulnerability of the social infrastructure (Pethick, 2001; Lopes *et al.*, 2011). Besides these impacts, changes in the hydrological regimes and global warming may also promote: increased planktonic productivity during winter, shifts in the taxonomic composition of algal species, harmful or toxic algae blooms, introduction of invasive and/or toxic species, changes in the food web structure, acceleration in the nutrients recycling rates, bottom-water hypoxia and changes in the physiological response of the species (Rabalais *et al.*, 2009; Najjar *et al.*, 2010; Statham, 2012).

The role of climate change in the estuarine ecosystems dynamics and water quality should always be investigated in the scope of the system natural variability (Gameiro and Brotas, 2010) and taking into account direct anthropogenic pressures on these systems (e.g. Ducharne *et al.*, 2007). On the one hand, there is a strong interaction between the physical and the ecological processes in estuaries (James, 2002). Ecological processes are affected by light and nutrients availability, currents, water temperature and freshwater discharge, among others (e.g Ferreira *et al.*, 2005; Gameiro and Brotas, 2010). In this sense, the natural variability associated to these physical drivers will also influence the estuarine ecosystems dynamics. On the other hand, disturbance related with human activities within estuaries may also influence their ecological

quality, possibly contributing to a degradation of the ecosystem health. Some of the threats associated with anthropogenic pressures in estuaries are: human interventions, such as dredging and infrastructures construction, which influence the estuarine hydrodynamics and sediment dynamics (e.g. Zhong *et al.*, 2010); renovation of coastal structures, such as breakwaters, artificial reefs and sea walls (Science for Environment Policy, 2012); modifications of freshwater discharges by damming systems (Rocha *et al.*, 2002); agriculture effluents (Sebastiá *et al.*, 2012); wastewater discharges from domestic and/or industrial effluents, which can change the water balance by altering the quantity of water inflows and/or change the nutrients balance and enhance eutrophication (Huang *et al.*, 2003); and resources exploitation, such as fish and shellfish capture (Thom *et al.*, 1994).

The relative influence of anthropogenic activities, climatic variability and climate change in the estuarine ecosystems is a matter of concern (Cloern and Jassby, 2010; Paerl *et al.*, 2010), as it remains poorly known. Chust *et al.* (2009) found that the anthropogenic impacts in coastal and estuarine habitats overwhelmed the driving forces of natural erosive processes and global climate change in the Bay of Biscay (Spain) between 1954 and 2004. Grangeré *et al.* (2012) found that, on the west coast of the Cotentin peninsula (France), climatic factors act in synergy with anthropogenic factors (in particular, nutrient enrichment), while, on the east coast, the climatic factors influence was reduced by the anthropogenic factors. The predicted increase of human activities in estuaries (Rabalais *et al.*, 2009) associated with climate change may increase the vulnerability of these systems (Statham, 2012), and there is a need to integrate both the anthropogenic pressures and the system's response to the physical and climate drivers in order to develop an effective management strategy (Paerl, 2006; Ducharne *et al.*, 2007; Kotta *et al.*, 2009).

Duly validated numerical models are useful tools for studying the estuarine water quality dynamics as a response to its main drivers, as they allow the simulation of different scenarios of engineering interventions and expected climate impacts. Nowadays there are some well-established coupled hydrodynamic and ecological models, which include HEM-3D (Park *et al.*, 2005), PELAGOS (Vichi *et al.*, 2007), NEMURO (Kishi *et al.*, 2007) and ECO-SELFE (Rodrigues *et al.*, 2009; Chapter III, Section III.3, Rodrigues *et al.*, 2012), among others. Although some recent studies took advantage of numerical modelling to evaluate the ecosystem response to climate change (e.g. Denman and Peña, 2002; Hashioka and Yamanaka 2007; Neumann, 2010), few compared the relative role of climate drivers with anthropogenic-induced modifications, in particular in estuaries.

Thus, this study aims at investigating the impacts of climate change and anthropogenic pressures on an estuarine environment, through the simulation of a set of scenarios, using a coupled hydrodynamic and ecological model (ECO-SELFE). The Aveiro lagoon, located in the Northwest coast of Portugal (Figure V.1.1), is a temperate, mesotidal estuary that harbours one

of the largest saltmarshes areas in Europe, supporting at the same time several economic activities that might impact its ecological quality. This study focuses on one of the main channels of the lagoon (Mira channel), which behaves like a tidally and seasonally poikilohaline estuary (Moreira *et al.*, 1993), providing further understanding on the influence of the climate change and anthropogenic pressures in this type of environments.

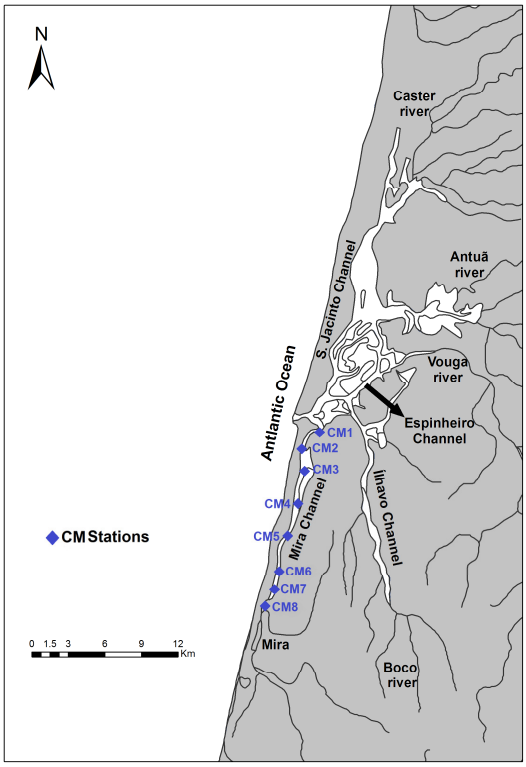

Figure V.1.1. Schematic overview of the Aveiro lagoon and location of the virtual stations.

V.1.2 METHODOLOGY

V.1.2.1 Study Area

The Aveiro lagoon (40º38'N, 8º45'W) is 45 km long and has a maximum width of 10 km. It covers an area that varies from 66 km^2 at low tide to 83 km^2 at high tide on spring tides (Dias and Lopes, 2006). This lagoon harbours several ecological relevant species of fauna and flora and, in particular, migratory birds. Simultaneously, it supports several economic activities (e.g. aquaculture, artisanal fishing, tourism, nautical and port activities, salt collection, industry), some of which contributed to the degradation of its ecological and water quality (e.g. Rebelo, 1992). Although Ferreira *et al.* (2003) has classified the lagoon with low overall eutrophic

condition (OEC) and low susceptibility index (US-NEEA index), the quality status within the lagoon may vary (Lopes *et al.,* 2007).

Morphologically, the lagoon is separated from the sea by a sandbar, connecting to it through an artificial inlet, and spreads over four main channels: in the south, the Mira and Ílhavo channels; in the centre, the Espinheiro channel; and in the north, the S. Jacinto channel. These channels, with exception of the Mira channel, have several shallow branches and interconnections, increasing the complexity of the Aveiro lagoon's dynamics and geometry (Dias *et al.*, 1999). The Mira channel, about 25 km long, may be considered a sub-estuarine system of the Ria de Aveiro (Leandro, 2008), behaving like a tidally and seasonally poikilohaline estuary (Moreira *et al.*, 1993). The lagoon is very shallow, with the exception of the inlet and the navigation channels, where maximum depths of about 20 m and 7 m (relative to mean sea level), respectively, are maintained artificially through dredging.

The circulation in the lagoon is mainly driven by the tide (Dias *et al.*, 1999). Tides are semi-diurnal, ranging from 0.6 m in neap tides to 3.2 m in spring tides at the mouth (Dias *et al.*, 2000). The lagoon is mesotidal with a mean tidal range of 2 m (Dias *et al.*, 2000). The mean tidal prism at the inlet is of about $70x10^6$ m^3 on spring tides, 10% of which flows to the Mira channel (Dias, 2001). The freshwater input to the lagoon is relatively small (of about 1.8×10^6 m^3 during a tidal cycle – Dias, 2001). The main sources of freshwater to the lagoon are the rivers Vouga and Antuã (Dias *et al.*, 2000; Dias and Lopes, 2006). In the other channels, the river flows are lower. Some uncertainty remains about the volume of freshwater that reaches the lagoon, mainly due to the lack of recent data. Annual average flows found in the literature vary from 29-50 m^3 s^{-1} for the Vouga river, and from 2-5 m^3 s^{-1} for the Antuã river (Dias and Lopes, 2006; Dias *et al.*, 2000). In the Mira channel, in particular, the freshwater flow is poorly known (Dias and Lopes, 2006). According to Dias *et al.* (2001), residence times in the lagoon vary from less than 2 days near the mouth to more than 1 week in the upstream areas of the channels.

V.1.2.2 Scenarios Definition

A set of eleven scenarios was established to study the effects of: i) climate change, including the increase in air temperature, changes in the precipitation regimes and sea level rise, ii) anthropogenic pressures, including a recently proposed dredging plan, the construction of a marina and an emergency by-pass wastewater discharge; and iii) combined anthropogenic and climate change. The number of scenarios was established in order to provide information about a wide range of driving factors, but also taking into account the computational time requirements associated with the application of a three-dimensional, fully coupled hydrodynamic and ecological model.

All downgrades of the IPCC climate change scenarios predict a significant air temperature rise by 2100 in Portugal, with increases in the mean air temperature ranging from 2 ºC to about 9 C (Miranda *et al.*, 2006). Taking into account the seasonal variation, maximum increases are predicted for the summer season (Miranda *et al.*, 2006). Two scenarios were established based on the seasonal variation (spring, summer, autumn and winter seasons) of air temperature predicted by the global circulation model HadCM3 for one point located in the centre of Portugal (Miranda *et al.*, 2006). The first scenario was based on the predictions presented by Miranda *et al.* (2006) for the scenario SRES (Special Report on Emission Scenario) B2, while the second scenario derived from scenario SRES A2 (Table V.1.1, Table V.1.2).

Table V.1.1. Scenarios SRES (Special Report on Emission Scenario) definition (Nakicenovic *et al.*, 2000).

Scenario	Definition
SRES A1	A future world of very rapid economic growth, global population that peaks in mid-century and declines thereafter, and rapid introduction of new and more efficient technologies.
SRES B1	A convergent world with the same global population as in the A1 storyline but with rapid changes in economic structures toward a service and information economy, with reductions in material intensity, and the introduction of clean and resource-efficient technologies.
SRES A2	A very heterogeneous world with continuously increasing global population and regionally oriented economic growth.
SRES B2	A world in which the emphasis is on local solutions to economic, social, and environmental sustainability, with continuously increasing population (lower than A2) and intermediate economic development.

Expected changes in the hydrological regimes in Portugal are more uncertain than those for air temperature (Miranda *et al.*, 2006). For Portugal, precipitation scenarios for 2100 predict a reduction over the mainland during spring, summer and autumn, which is within the range of 20 to 40% of the present values, and is larger in the southern region. In the winter an increase in precipitation may occur (Miranda *et al.*, 2006). As for air temperature, two seasonally varying hydrological scenarios were also established based on the predictions of Miranda *et al.* (2006) for the scenarios SRES B2 and A2 (Table V.1.2). For the hydrological scenarios, it was assumed that changes in the precipitation regimes would directly affect river flows, based on the positive correlation found between these two variables in the Aveiro lagoon, described in Chapter IV (correlation coefficient of 0.652, with $p<0.001$).

Several studies aimed at evaluating the sea level rise in the Portuguese coast by 2100 and the range of predicted values is wide: 0.14-0.57 m (Dias and Taborda, 1988), 0.05-0.20 m (Araújo, 2005), 0.47 (0.19-0.75) m (Antunes and Taborda, 2009), and 0.28, 0.35 and 0.42 m (Lopes *et al.*, 2011). In the establishment of sea level rise scenarios for the present study, two scenarios were considered, corresponding to the predictions of Lopes *et al.* (2011). These predictions were based on scenarios SRES B1 (sea level rise of 0.28±0.02 m) and A2 (sea level rise of

0.42±0.02 m) – Table V.1.1, Table V.1.2 – and were chosen since they were determined for the Aveiro coast.

The definition of the anthropogenic scenarios took into account the activities developed in the Aveiro lagoon, and the predicted or proposed modifications regarding these activities. These scenarios also include the failure of the wastewater systems. Three scenarios were considered (Table V.1.2): i) the implementation of a dredging plan, ii) a marina construction in the downstream area of the Mira channel, and iii) an emergency discharge of untreated domestic effluents near Costa Nova due to a failure of the interceptor system.

Additionally, in order to evaluate the combined influence of anthropogenic pressures and climates changes, two scenarios were established for this purpose (Table V.1.2): i) combining the rising air temperature and the dredging plan implementation, and ii) combining the changes in the hydrological regimes and the marina construction.

Table V.1.2. Scenarios description.

Scenario		Description[1,2]	Reference
S0	Reference	Established based on mean values of historical data	-
S1	Air temperature rise: SRES B2	Seasonal air temperature rise – spring: +2.2 ºC; summer: +6.1 ºC; autumn: +3.8 ºC; winter: +2.2 ºC	Miranda *et al.*, 2006
S2	Air temperature rise: SRES A2	Seasonal air temperature rise – spring: +3.8 ºC; summer: +8.8 ºC; autumn: +5 ºC; winter: +2.9 ºC	Miranda *et al.*, 2006
S3	Changes in hydrological regimes: SRES B2	Seasonal variation – spring: -2.7%; summer: -40 %; autumn: -13 %; winter: +20 %	Miranda *et al.*, 2006
S4	Changes in hydrological regimes: SRES A2	Seasonal variation – spring: -46%; summer: -56 %; autumn: -31 %; winter: -4 %	Miranda *et al.*, 2006
S5	Sea level rise: SRES B1	Sea level rise of 0.28 m	Lopes *et al.*, 2011
S6	Sea level rise: SRES A2	Sea level rise of 0.42 m	Lopes *et al.*, 2011
S7	Dredging plan	Implementation of a dredging plan in some of the main channels of the Aveiro lagoon, including the Mira channel	-
S8	Marina construction	Construction of a marina in the downstream area of the Mira channel	Ecossitema and Impacte, 2003
S9	Emergency discharge	Emergency discharge of untreated domestic effluents near Costa Nova due to a failure of the interceptor	-
S10	Combined scenario: S2 + S7	Combines scenarios S2 and S7	-
S11	Combined scenario: S3 + S8	Combines scenarios S3 and S8	-

[1]*Spring*: March, April, May; *Summer*: June, July, August; *Autumn*: September, October, November; *Winter*: December, January, February.

[2]Variations are relative to the reference scenario.

V.1.2.3 Model Description and Setup

V.1.2.3.1 ECO-SELFE DESCRIPTION

ECO-SELFE (Rodrigues *et al.*, 2009; Chapter III, Section III.3, Rodrigues *et al.*, 2012) is a three-dimensional unstructured grid fully coupled hydrodynamic and ecological model, which couples the hydrodynamic model SELFE (Zhang and Baptista, 2008) and an ecological model extended from EcoSim 2.0 (Bisset *et al.*, 2004). The parallel version of the coupled model (version 3.1d, available at www.stccmop.org/CORIE/modeling/selfe/) was used in this study, which allowed a significant improvement of the computational efficiency relative to the serial version of the model (Rodrigues *et al.*, 2009).

SELFE was developed for the baroclinic simulation from rivers to oceans and solves the three-dimensional shallow-waters equations, with the hydrostatic and Boussinesq approximations, for the free-surface elevation, water velocity, salinity and water temperature. The model includes a user-defined transport module, allowing the solution of the transport equation for any user-specified tracer:

$$\frac{\partial C}{\partial t} + u\frac{\partial C}{\partial x} + v\frac{\partial C}{\partial y} + w\frac{\partial C}{\partial z} = \frac{\partial}{\partial z}\left(\kappa\frac{\partial C}{\partial z}\right) + F_c + \Lambda C \qquad \text{(V.1.1)}$$

where C is a generic tracer, (u,v,w) is the velocity, κ is the vertical eddy diffusivity, Fc is the horizontal diffusion and ΛC are the sources and sinks. The hydrodynamic and ecological models are coupled through the sources and sinks terms of Equation V.1.1, which are calculated by the ecological model (Figure V.1.2).

The ecological model was extended from EcoSim 2.0 to account for the simulation of several groups of zooplankton (Rodrigues *et al.*, 2008) and the oxygen cycle (Rodrigues *et al.*, 2012). In its base formulation EcoSim2.0 simulates several ecological tracers (phytoplankton, bacterioplankton, dissolved and particulate organic matter, inorganic nutrients and dissolved inorganic carbon) for the carbon, nitrogen, phosphorus, silica and iron cycles. The extension of the model included the simulation of zooplankton, dissolved oxygen and chemical oxygen demand.

ECO-SELFE is also coupled to a near field model, based on the RSB model (Roberts *et al.*, 1989a,b), which allows for a detailed simulation of local discharges (Chapter III, Section III.1).

Numerically, ECO-SELFE uses finite-elements and finite-volumes schemes. The advection of salinity and temperature is solved either with Eulerian-Lagragian Methods (ELM), upwind or Total Variation Diminishing (TVD) schemes, while for the ecological tracers only upwind and TVD schemes are available. The domain is discretized horizontally with unstructured triangular grids and vertically with hybrid coordinates (*S* coordinates and *Z* coordinates), allowing for a high flexibility in both dimensions.

Detailed descriptions of the model formulation can be found in Bisset *et al.* (2004), Rodrigues *et al.* (2008, 2009, 2012) and Zhang and Baptista (2008).

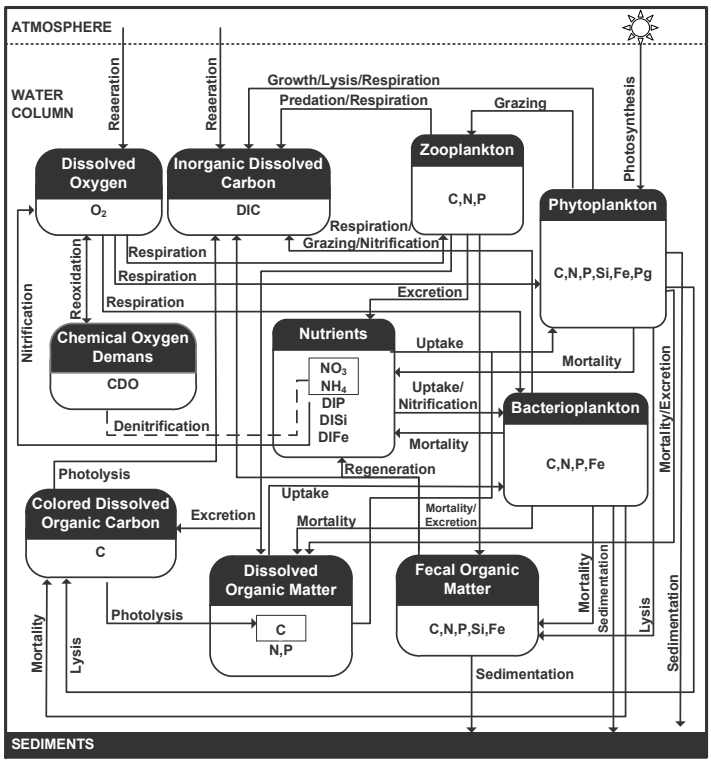

Figure V.1.2. Schematic overview of the sources and sink terms of the ecological model (C – carbon; N – nitrogen; P – phosphorus; Si – silica, Fe – iron; O_2 – oxygen).

V.1.2.3.2 MODEL SETUP

A two-step approach was used to optimize computational times (Rodrigues *et al.*, 2012): first hydrodynamic simulations were performed for the entire Aveiro lagoon domain; then, the coupled hydrodynamic-ecological model was used for the simulations in the Mira channel. ECO-SELFE has been previously validated in the Aveiro lagoon and, in particular, in the Mira channel (Rodrigues *et al.*, 2012) and a similar setup was used in the present study. A reference scenario was established and a set of eleven simulations was performed based on the anthropogenic, climate and combined scenarios described in section V.1.2.2. In each of these eleven scenarios, the evaluated parameters were changed from the reference scenario. In each case, simulations were performed for a 1-year period, in 2100.

Hydrodynamic simulations were performed with a horizontal grid of about 31000 nodes, with a resolution varying from 1.5 km in the coastal area to 2 m in the narrow channels (Figure V.1.3). The hydrodynamic grid was updated according to the scenario simulated (Figure V.1.3). For the sea level rise scenarios, the grid was extended to cover possible flooded areas (about 115000

nodes) and was previously validated with the two-dimensional version of SELFE (Fortunato *et al.*, submitted). The marina scenario grid was constructed based on the proposed project presented in the environmental impact study (Ecossistema and Impacte, 2003). Bathymetry was updated from Rodrigues *et al.* (2012; Chapter III, Section III.3) based on recent data for: the Mira channel between Costa Nova and Vagueira (2008) and between Vagueira and Areão (2011); the S. Jacinto channel (2008); and the Ílhavo channel (2011). For the dredging scenario, bathymetry was set based on a proposed dredging plan from the Polis Litoral Ria de Aveiro, S.A. Vertically, 7 equally spaced *S* levels were used. A spatially varying bottom roughness was considered, based on Dias and Lopes (2006). The Generic Length Scale KKL model with Kantha & Clayson's stability function was used for turbulence closure. The time step was set to 30 seconds and all simulations were performed with a warm-up period of 2 days.

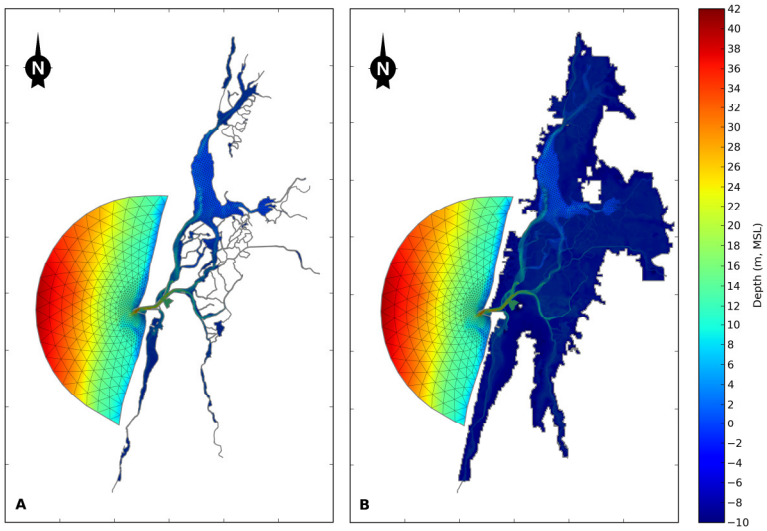

Figure V.1.3. Hydrodynamic horizontal grid and bathymetry for the Aveiro lagoon (MSL – mean sea level): A) reference scenario, B) sea level rise scenarios.

Six open boundaries were considered. At the oceanic boundary the model was forced with 14 tidal constituents (Z0, MSF, O1, K1, P1, Q1, M2, S2, N2, K2, M4, MN4, MS4 and M6) from the regional model of Fortunato *et al.* (2002). The riverine boundaries (Vouga, Antuã, Boco and Caster and Mira) were forced with monthly varying flows, determined based on historical data (Rodrigues *et al.,* 2009, 2012). Initial conditions of salinity and temperature were set to vary spatially to speed up the computations. At the oceanic boundary salinity was forced to remain constant at 36 and temperature was forced with climatological data from the Levitus atlas (http://www.cdc.noaa.gov). At the river boundaries, salinity was set constant at 0 and temperature was forced using an approach similar to the one described for the river flows. Surface heat exchanges between water and atmosphere were simulated with the model of

Zheng *et al.* (1998). Monthly atmospheric forcing was determined based on historical data from 1985 to 2010 from the University of Aveiro meteorological station and from the NCEP Reanalysis Database (http://www.esrl.noaa.gov/psd/).

For the simulations of ECO-SELFE along the Mira channel, a horizontal grid of about 12000 nodes was used (Figure V.1.4). This grid was updated according to the scenario simulated (Figure V.1.4). The downstream boundary was forced with the water levels and three-dimensional current velocities, salinities and temperatures obtained from the hydrodynamic simulations. The upstream boundary was forced similarly as described for the hydrodynamic model. Initial conditions for the ecological tracers were set similar to the approach used in Rodrigues *et al.* (2009, 2012 – Chapter III, Section III.3). Monthly varying boundary conditions were set based on historical data from previous field campaigns and from the S. Tomé station, located further upstream of the Mira channel (http://snirh.pt), for chlorophyll *a*, ammonium, nitrates + nitrites, phosphates, silicates and dissolved oxygen (Chapter III, Section III.3, Rodrigues *et al.*, 2012). For the other ecological variables, monthly-varying boundary conditions were determined as in Rodrigues *et al.* (2009). Input parameters of the ecological model were set as proposed by Rodrigues *et al.* (2009, 2012; Chapter III, Section III.3), based on the validation with several field campaigns.

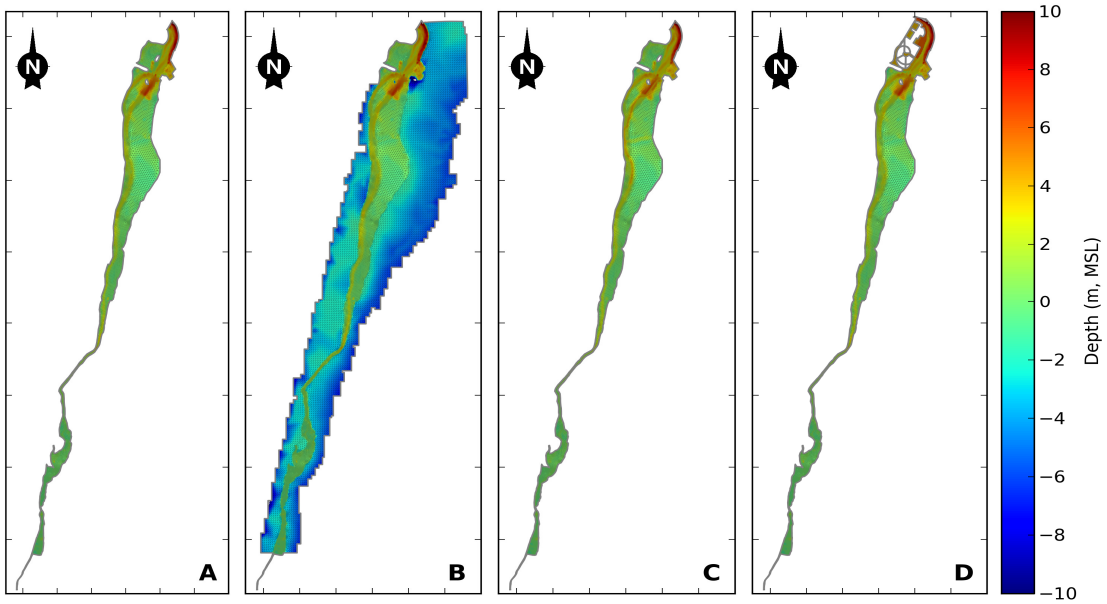

Figure V.1.4. Hydrodynamic-ecological horizontal grid and bathymetry for the Mira channel (MSL – mean sea level): A) reference scenario, B) sea level rise scenarios, C) dredging scenario, and D) marina construction scenario. Additional views for grids C and D are presented in Appendix IV.

The near field module of ECO-SELFE (described in Chapter III, Section III.2) was used to simulate emergency wastewater discharges, considering one emergency discharge in each one

of the seasons (spring, summer, autumn and winter). For the emergency discharge, a 24 hours failure period was considered. The mean discharge flow was set to $6x10^{-3}$ m^3 s^{-1}, which was estimated based on the population from Barra and Costa Nova served by this sub-system, of about 2500 habitants (Queiroga *et al.*, 2001; http://www.ine.pt – 2001 Censos Data). Concentrations of ammonium, nitrates and phosphates in the discharge were of 3500 μM, 5 μM and 70 μM, respectively, estimated based on typical concentrations measured on untreated domestic effluents.

V.1.2.4 Methodology for the Analysis of Model Results

Results were analysed based on the annual variation and the seasonal means for spring (March, April and May), summer (June, July and August), autumn (September, October and November) and winter (December, January and February). For the entire domain and for each season, the mean absolute difference from the reference scenario was computed. For the ecological tracers, the mean relative difference (i.e. the mean absolute difference divided by the concentration in the reference scenario) was also computed. The annual variation was evaluated over a set of virtual stations distributed along the channel (Figure V.1.1), at two depths (20 cm above the bottom and 20 cm below the surface).

V.1.3 RESULTS

Complementary results, namely mean, minimum and maximum annual values of each variable at each virtual station, are presented in Appendix IV.

V.1.3.1 Salinity and Water Temperature

Sea level rise scenarios (simulations S5 and S6) lead to the larger differences in the salinity from the reference scenario. A significant increase of the salinity occurs along the channel (Figure V.1.5), in particular in the middle and upstream areas, due to the increased volume of marine water reaching these areas. This larger volume of marine water increases the wetted cross-section, promoting a reduction of the residual velocity and hampering the progression downstream of the freshwater flow. Sea level rises of 0.28 m and 0.42 m lead to a similar mean increase of the water levels from downstream until the middle of the channel. Further upstream the mean water level increases are lower, of about 0.10 m and 0.25 m, respectively. The salinity increase due to sea level rise occurs throughout all seasons. Mean differences from the reference scenario are larger in the spring and summer, when the freshwater discharge is lower, and can reach values of 12-20 in the middle and upper areas of the Mira channel (Figure V.1.5;

Table AIV.1, Appendix IV). The annual variation of the salinity puts in evidence a significant increase of the extreme values in these areas due to sea level rise (Figure V.1.6). During the summer season the range of variation of the salinity increases from 0-20 in the reference scenario to 10-30 in the sea level rise scenarios; in the winter season, the maximum values of salinity also increase (Figure V.1.6). Between the two evaluated sea level rise scenarios, the salinity differences are relatively small and a non-linear increase of this variable with sea level rise is observed. Hong and Shen (2012) also suggested an increase of the salinity in the Chesapeake Bay estuary (USA) due to sea level rise. However, the salinity increase predicted for this estuary for a sea level rise of 0.30 m is significantly lower than the one predicted here to the Aveiro lagoon. This derives from the depth differences between these two estuaries, as the Aveiro lagoon is very shallow, and puts in evidence a higher impact of sea level rise in shallow estuaries.

The changes in the hydrological regimes scenarios also influence significantly the salinity along the Mira channel. The larger mean differences occur during the spring for scenario SRES A2 (simulation S4) and during the summer for both scenarios (simulation S3 and S4) – Figure V.1.7. During these periods the reductions of the freshwater discharge flowing into the channel are of about 40%-55%, which corresponds to a river flow smaller than 1 $m^3 s^{-1}$. This flow reduction hampers the freshwater progression downstream and allows a larger tidal propagation, promoting the salinity increase along the channel. However, the mean differences in the salinity relative to the reference scenario are much smaller than those predicted for the sea level rise scenarios. During summer, in the upstream areas of the channel, salinity minimum values increase from 5 in the reference scenario to about 15 due to the decrease of the freshwater discharge (Figure V.1.6). Predictions based on scenario SRES B2 suggest an increase of the precipitation of about 20% in the winter season (Miranda *et al.*, 2006), which leads to a small decrease (of about 2) of the salinity downstream (Figure V.1.7; Table AIV.1, Appendix IV).

All the other scenarios lead to mean differences of the salinity ranging from -2 to 2 relative to the reference scenario (Table AIV.1, Appendix IV). The exceptions are some specific areas located near the head of the channel, where a mean salinity increase of about 3-5 is observed in the dredging scenarios. This increase is associated with the deepening of the channel, which increases the tidal amplitude upstream, and puts in evidence the role of circulation and their forcings in controlling the salinity along the channel. However, the magnitude of the salinity changes is very small compared with the previous drivers.

Regarding water temperature, the largest differences relative to the reference scenario are observed in the air temperature rise scenarios (simulations 1, 2 and 14), namely during the summer months (Table AIV.1, Appendix IV). The largest differences are predicted for the SRES A2 scenario, for which the predicted increase in the air temperature near the centre of the

Portuguese coast is of 8.8 ºC during the summer season (Miranda *et al.*, 2006). This increase in the air temperature leads to mean increases in the water temperature of about 3 ºC to 4ºC relative to the reference scenario in the shallow areas of the channel, located upstream (Figure V.1.8). In these areas there is a significant influence of the heat exchanges with the atmosphere, promoting a larger increase in the water temperature. In the shallow areas of the channel, maximum values of water temperature vary from about 24 ºC in the reference scenario to 26.5 ºC and 27.5 ºC in the simulations S1 (scenario SRES B2) and S2 (scenario SRES A2), respectively (Figure V.1.9). Downstream, where depths are larger (of about 8 m) and the influence of the oceanic water is stronger, the differences are slightly smaller, of about 1.5 ºC to 2 ºC (Figure V.1.9), putting in evidence the larger influence that climate change may have in shallower estuaries. Minimum values of water temperature increase by about 0.5 ºC relative to the reference scenario, as the predicted rise in air temperature is smaller during winter.

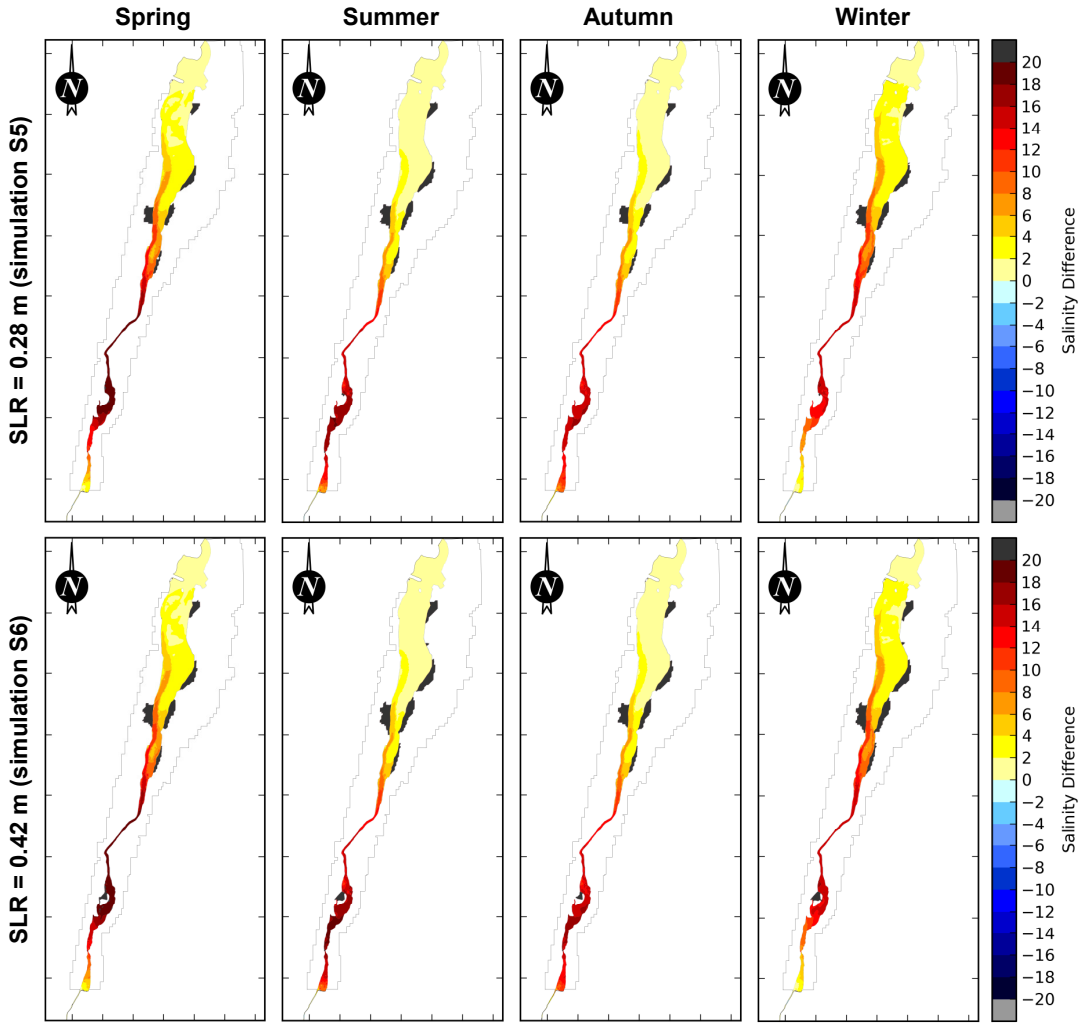

Figure V.1.5. Salinity mean absolute differences (depth-averaged) from the reference scenario due to sea level rise (SLR) of 0.28 m (simulation S5) and of 0.42 m (simulation S6) in spring, summer, autumn and winter seasons. Dark grey represents new flooded areas, while light grey represents new dry areas.

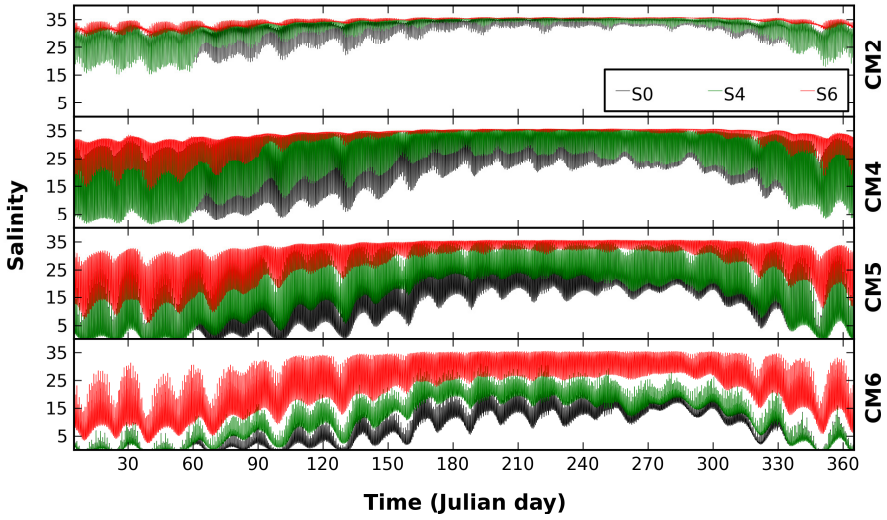

Figure V.1.6. Annual variation of surface salinity at the virtual stations for the reference simulation (S0), changes in the hydrological regimes based on SRES A2 (simulation S4) and sea level rise of 0.42 m (simulation S6) scenarios.

For all the other scenarios, differences in the water temperature are of about -1 ºC to 1 ºC relative to the reference scenario (Table AIV.1, Appendix IV). Although relatively small, the differences observed due to sea level rise and changes in the hydrological regimes put in evidence the balance established between the marine and the freshwater waters. In the present simulations, boundary conditions in the air temperature rise scenarios were assumed to be similar to those in the reference scenario. However, taking into account the water temperature increase within the channel due to air temperature rise, it would be expected that temperature of the water flowing into the channel will also rise. This effect could contribute to an increase of the predicted water temperature in these scenarios. The linkage between large scales ocean models and hydrological models predicting water temperature due to global warming should, thus, be taken into account in future research.

Regarding the relative role of climate change and anthropogenic pressures in establishing salinity and water temperature along the Mira channel, the combined climate and anthropogenic scenarios S11 (changes in the hydrological regimes + marina construction) and S10 (dredging + air temperature increase) put in evidence the larger influence of the climate forcing (Figure V.1.10). A particular effect should be noted in simulation S10, as channels' dredging reduces the water temperature along the Mira channel: the combined influence of dredging and air temperature increase (simulation S10) promotes smaller increases in the water temperature than the air temperature increase scenario alone (Figure V.1.10), and reveals the need of considering multiple drivers in this type of analysis.

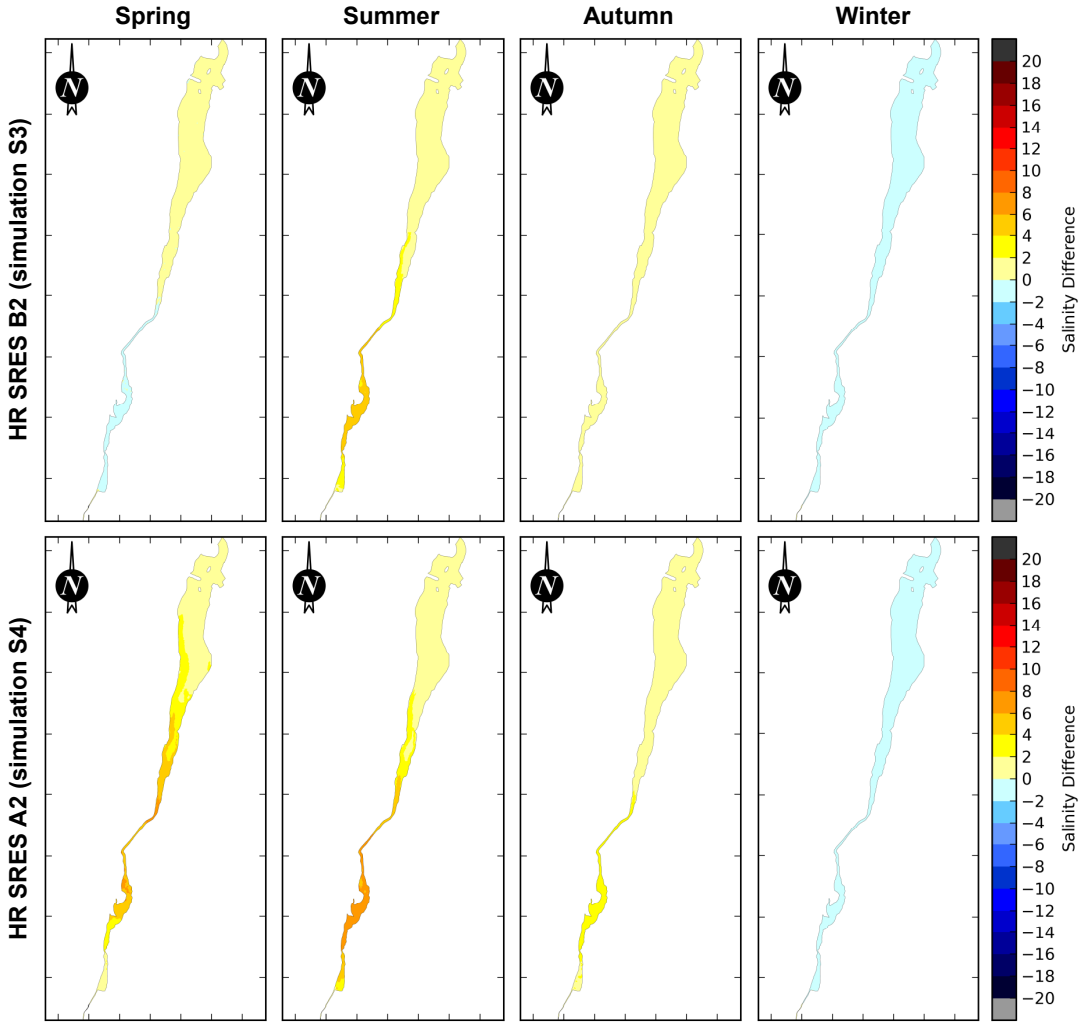

Figure V.1.7. Salinity mean absolute differences (depth-averaged) from the reference scenario due to changes in the hydrological regimes (HR) based on scenarios SRES B2 (simulation S3) and SRES A2 (simulation S4) in spring, summer, autumn and winter seasons. Dark grey represents new flooded areas, while light grey represents new dry areas.

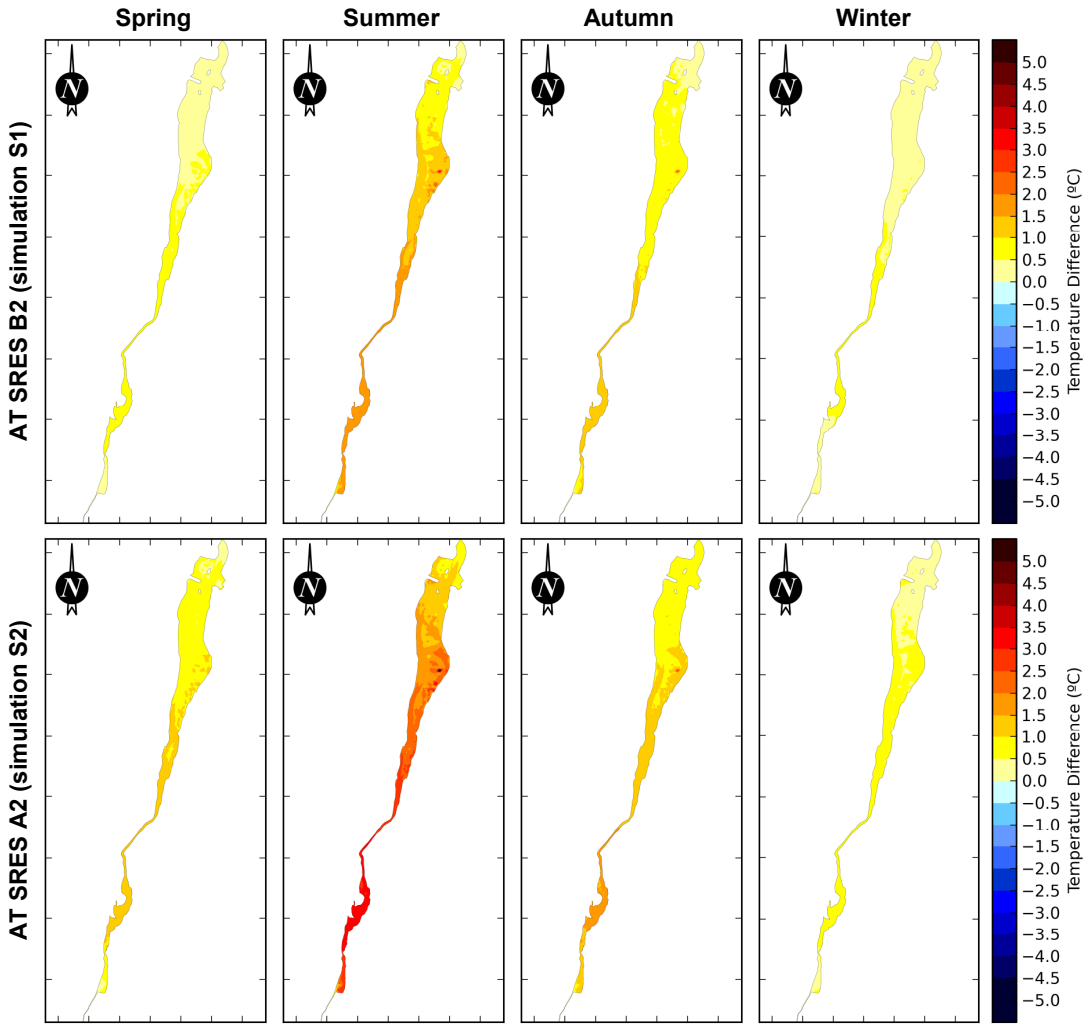

Figure V.1.8. Water temperature mean absolute differences (depth-averaged) from the reference scenario due to the rise of air temperature (AT) based on scenarios SRES B2 (simulation S1) and SRES A2 (simulation S2) in spring, summer, autumn and winter seasons.

Combined scenarios of climate change were not evaluated in the present study, although some synergistic effects would be expected. The combined effect of sea level rise with the reduction of the freshwater discharge during the summer will enhance the hampering of the freshwater progression downstream and favour the increase of the salinity in the upstream areas of the channel. Moreover, this effect may also contribute to increase the residence times (e.g. potentiating the increase of water temperature). During summer, the increase of salinity may also be potentiated due to the increase of air temperature, which favours the evaporation processes. This process may have a significant influence in the Aveiro lagoon due to its lower depths (Rodrigues *et al.*, 2009), and should be further investigated.

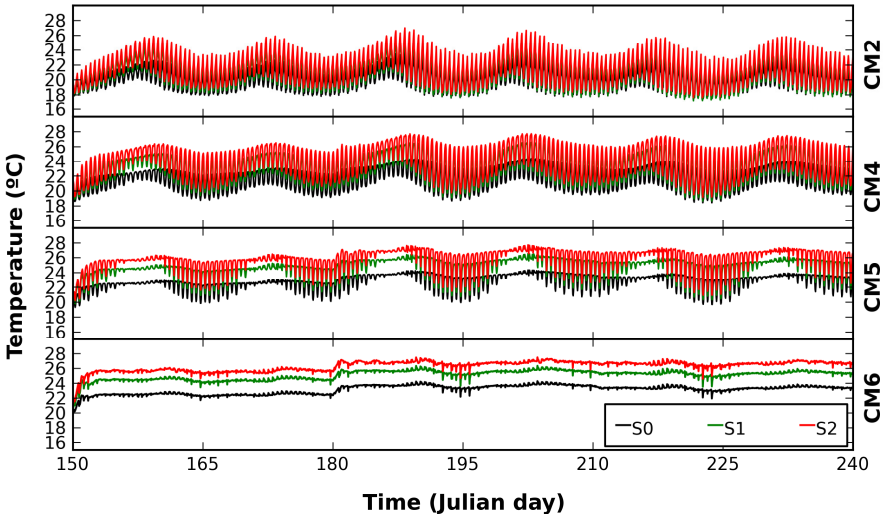

Figure V.1.9. Water temperature variation at the surface during the summer (June, July and August months) at the virtual stations for the reference (simulation S0), increase in air temperature based on SRES B2 (simulation S1) and increase in air temperature based on SRES A2 (simulation S2) scenarios.

V.1.3.2 Chlorophyll *a*, Dissolved Oxygen and Nutrients

A significant decrease of the chlorophyll *a* concentrations is predicted due to sea level rise (simulations S5 and S6). For these scenarios, changes on chlorophyll *a* concentrations occur throughout all seasons, with more significance during spring and winter (Figure V.1.11). Reductions are similar for both sea level rise of 0.28 m and 0.42 m scenarios (Table AIV.3, Appendix IV). Predicted reductions from the reference scenario are of about 40% to 50% in some regions of the channel. In the upstream areas, the range of variation of chlorophyll *a* during spring is reduced from 5-18 $\mu g\ l^{-1}$ in the reference scenario to 1-12 $\mu g\ l^{-1}$ in the sea level rise scenarios (Figure V.1.12). Downstream, chlorophyll *a* concentrations during spring are reduced to less than 2 $\mu g\ l^{-1}$ due to sea level rise (Figure V.1.12). This reduction of chlorophyll *a* due to sea level rise derives from the larger volume of marine water that enters the channel, which has lower concentrations of chlorophyll *a* and promotes a larger dilution. Associated with the decrease of chlorophyll *a*, a decrease of the dissolved oxygen, about 1 $mg\ l^{-1}$ in the upstream stations, also occurs in the scenarios of sea level rise (Figure V.1.13). These are, in fact, the only scenarios that affect significantly dissolved oxygen, as for all the other scenarios, the differences from the reference scenario are relatively small (Table AIV.3, Appendix IV), suggesting a similar influence of both air temperature rise and changes in the hydrological regimes on the dissolved oxygen concentrations (Figure V.1.13; Table AIV.3, Appendix IV).

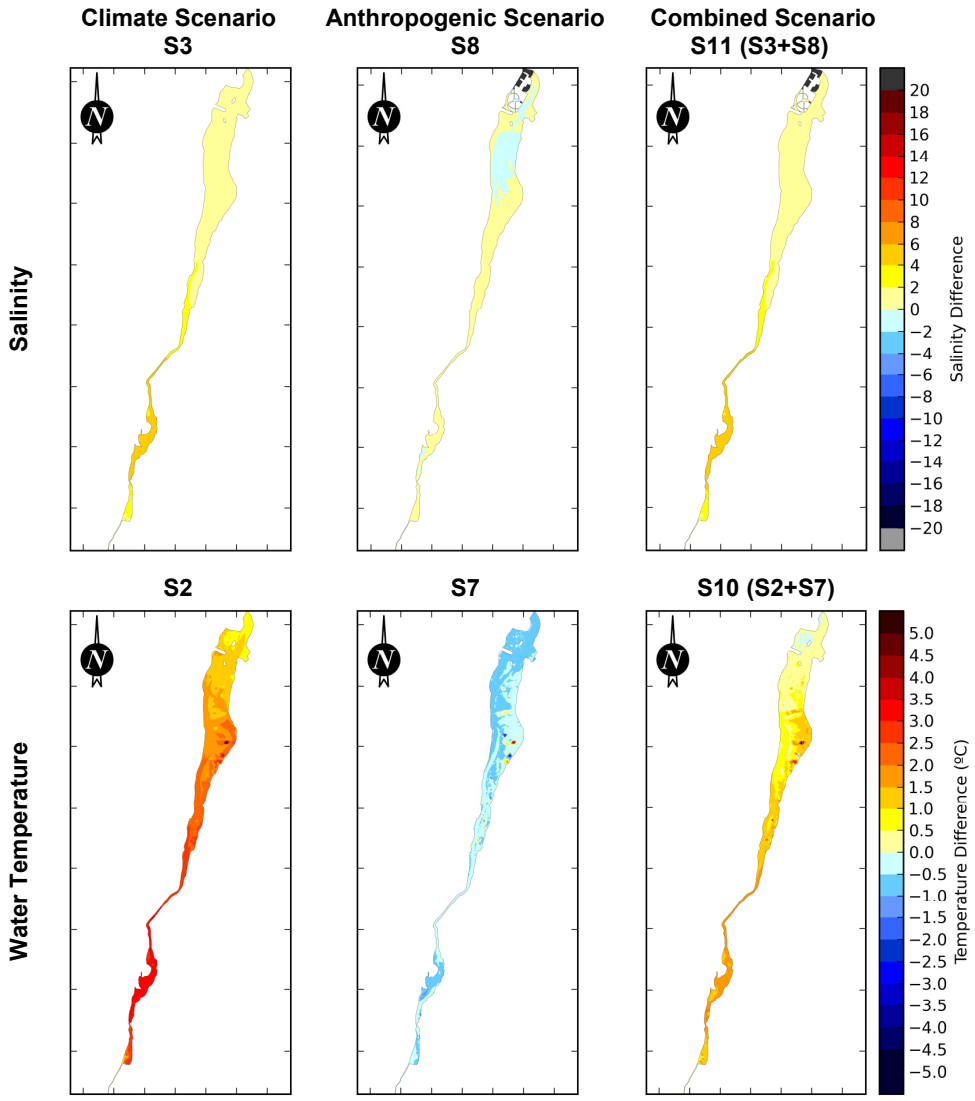

Figure V.1.10. Relative influence of climate and anthropogenic changes on salinity and water temperature: mean absolute differences (depth-averaged) from the reference scenario during the summer season. Salinity comparisons are presented for changes in hydrological regimes based on SRES B2 (simulation S3), marina construction (simulation S8) and combined (simulation S11) scenarios. Water temperature comparisons are presented for the increase in air temperature based on SRES A2 (simulation S2), dredging (simulation S7) and combined and combined (simulation S10) scenarios. Dark grey represents new flooded areas, while light grey represents new dry areas.

Regarding the changes in the hydrological regimes, changes in chlorophyll *a* are more evident when the predicted reduction of the freshwater discharge is larger. In particular, for the scenario SRES A2 (simulation S4), the larger reductions of chlorophyll *a* occur during spring and summer (Figure V.1.11), leading to a decrease from the reference scenario of about 5 $\mu g\ l^{-1}$ (Figure V.1.12). The predicted decrease in the chlorophyll *a* derives from the decrease of the freshwater

discharge itself, as larger concentrations of chlorophyll a occur in the upstream areas of the channel (Chapter III, Section III.3, Rodrigues *et al.*, 2012), and also from the decrease in the nutrients flowing to the system (Figure V.1.15) . In winter, in particular for scenario SRES B2 (simulation S3), there is a slight increase in the chlorophyll *a* and nutrients, which reveals an increase of the primary production.

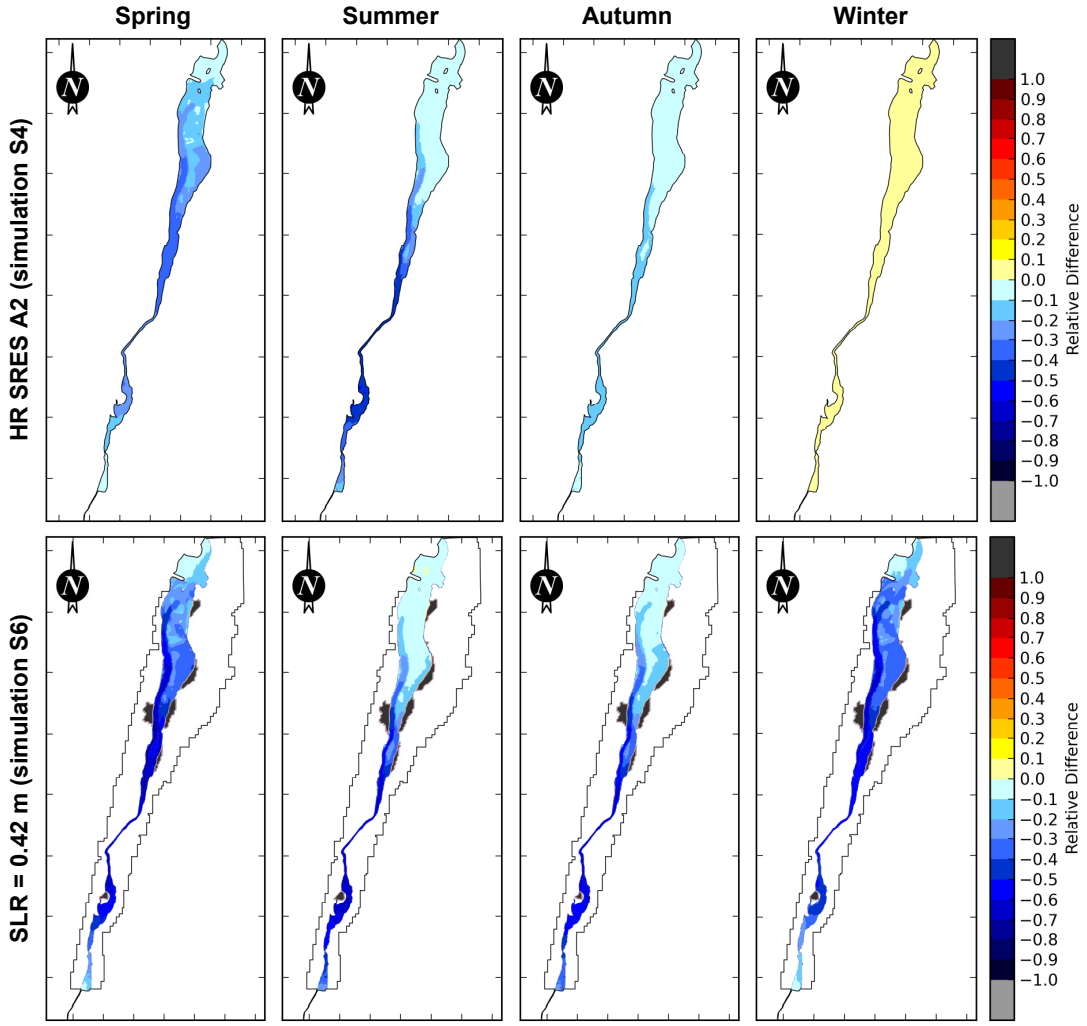

Figure V.1.11. Chlorophyll *a* mean relative differences (depth-averaged) from the reference scenario due to changes in the hydrological regimes (HR) based on scenarios SRES A2 (simulation S4) and sea level rise of 0.42 m (simulation S6) in spring, summer, autumn and winter seasons. Dark grey represents new flooded areas, while light grey represents new dry areas.

For all the other scenarios the variations of chlorophyll *a* from the reference scenario are relatively small, of about -10 to +10%, with no significant influence on the annual mean, minimum and maximum concentrations (Table AIV.3, Appendix IV). In particular, for the air temperature rise scenarios, which could affect the species physiological responses, no

significant changes were observed in the chlorophyll *a* concentrations (Figure V.1.12; Table AIV.3, Appendix IV).

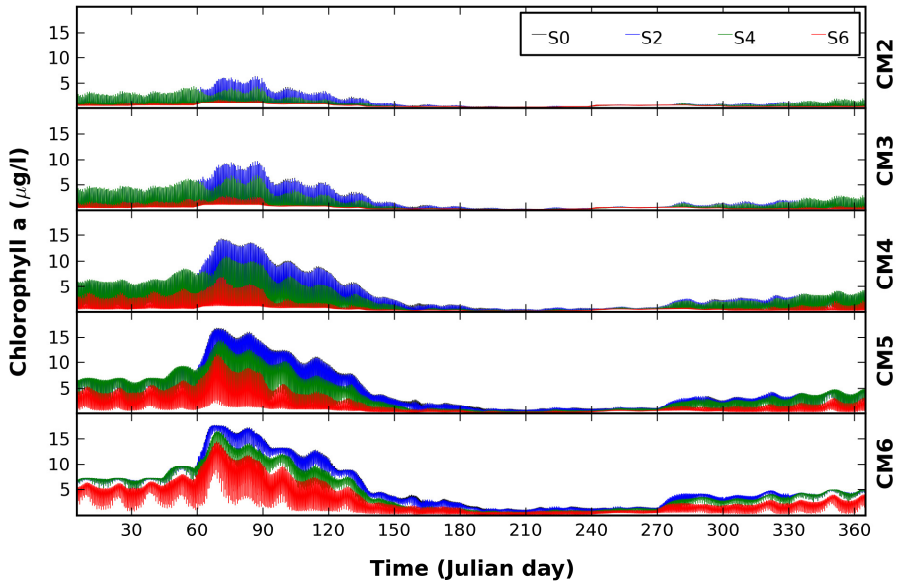

Figure V.1.12. Annual variation of surface chlorophyll *a* along the Mira channel for the reference simulation (S0), increase in air temperature based on SRES A2 (simulation S2), changes in the hydrological regimes based on SRES A2 (simulation S4) and sea level rise of 0.42 m (simulation S6) scenarios. Reference scenario time series (black line) is below simulation S2 time series (blue line).

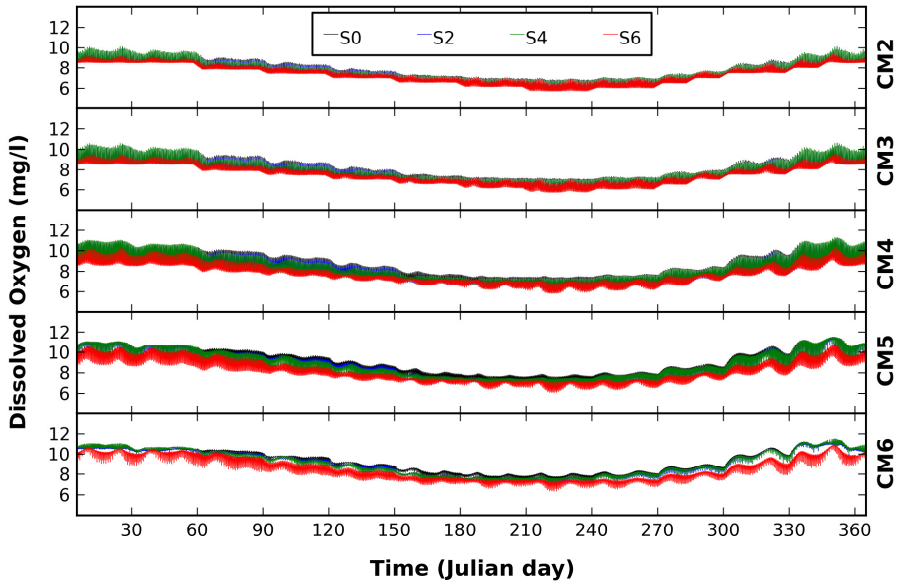

Figure V.1.13. Annual variation of surface dissolved oxygen along the Mira channel for the reference (simulation S0), increase in air temperature based on SRES A2 (simulation S2), changes in the hydrological regimes based on SRES A2 (simulation S4) and sea level rise of 0.42 m (simulation S6) scenarios. Reference scenario time series (black line) is below simulation S2 time series (blue line).

The combined influence of climate and anthropogenic drivers reveals that the effects of climate change on the chlorophyll *a* concentrations are larger than the marina construction (Figure V.1.14). In some dredged areas there are distinct effects: chlorophyll *a* concentration increases in the new dredged channel near Costa Nova, as there is a larger volume of water reaching this area, but minimum concentrations decrease upstream during high tide, as the deepening of the channel increases tidal amplitude in these areas. These effects put in evidence the role of circulation in establishing the water quality and ecological dynamics in this estuary. As the variations of chlorophyll *a* due to the anthropogenic interventions are relatively small when compared with the influence of sea level rise, it would be expected that the effects of sea level rise will overwhelm the ones of the analysed anthropogenic interventions.

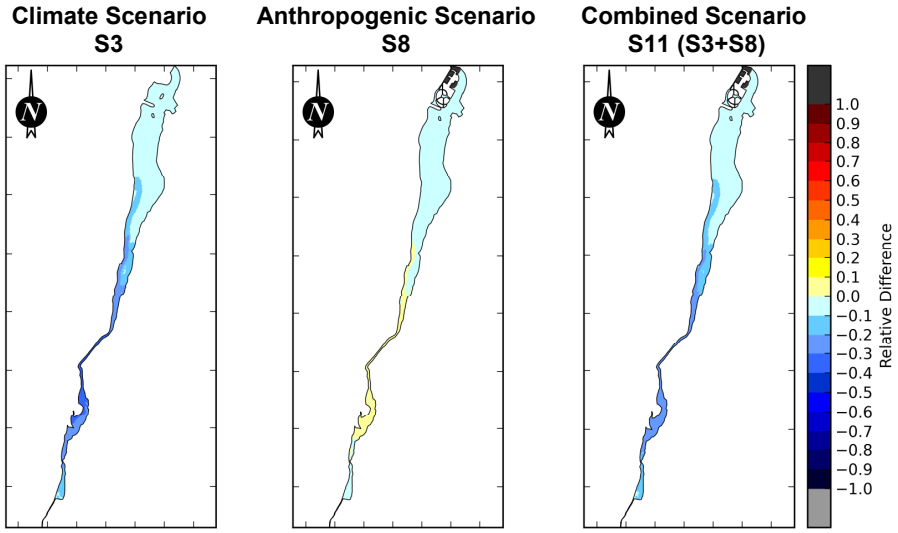

Figure V.1.14. Relative influence of climate and anthropogenic changes on chlorophyll *a*: mean absolute differences (depth-averaged) from the reference scenario during the summer season. Salinity comparisons are presented for changes in hydrological regimes based on SRES B2 (simulation S3), marina construction (simulation S8) and combined (simulation S11) scenarios. Water temperature comparisons are presented for the increase in air temperature based on SRES A2 (simulation S2), dredging (simulation S7) and combined (simulation S10) scenarios. Dark grey represents new flooded areas, while light grey represents new dry areas.

Regarding nutrients, sea level rise scenarios (0.28 m and 0.42 m) reveal a significant decrease of the concentrations along the Mira channel, in particular for ammonium, nitrates and silicates (Table AIV.2, Appendix IV). During spring, reductions from the reference scenario can reach values of about 30% due to the reduction of the freshwater discharge and of about 50% due to mean sea level rise of 0.42 m (Figure V.1.15). For the phosphates, the mean reductions are lower, of about 10% to 20% (Figure V.1.15). At the upstream stations, the annual variation of

the nutrients puts in evidence a reduction of ammonium maximum concentrations from about 16 μM in the reference scenario to about 9 μM due to sea level rise of 0.42 m (simulation S6) – Table AIV.2, Appendix IV. At the downstream stations, relative reductions of the ammonium maximum concentrations due to sea level rise are larger (of about 70%) – Table AIV.2, Appendix IV. As observed for chlorophyll *a*, these reductions on the nutrients concentrations derive from the larger volume of marine water flowing into the channel, which has lower nutrients concentrations and promotes a larger dilution.

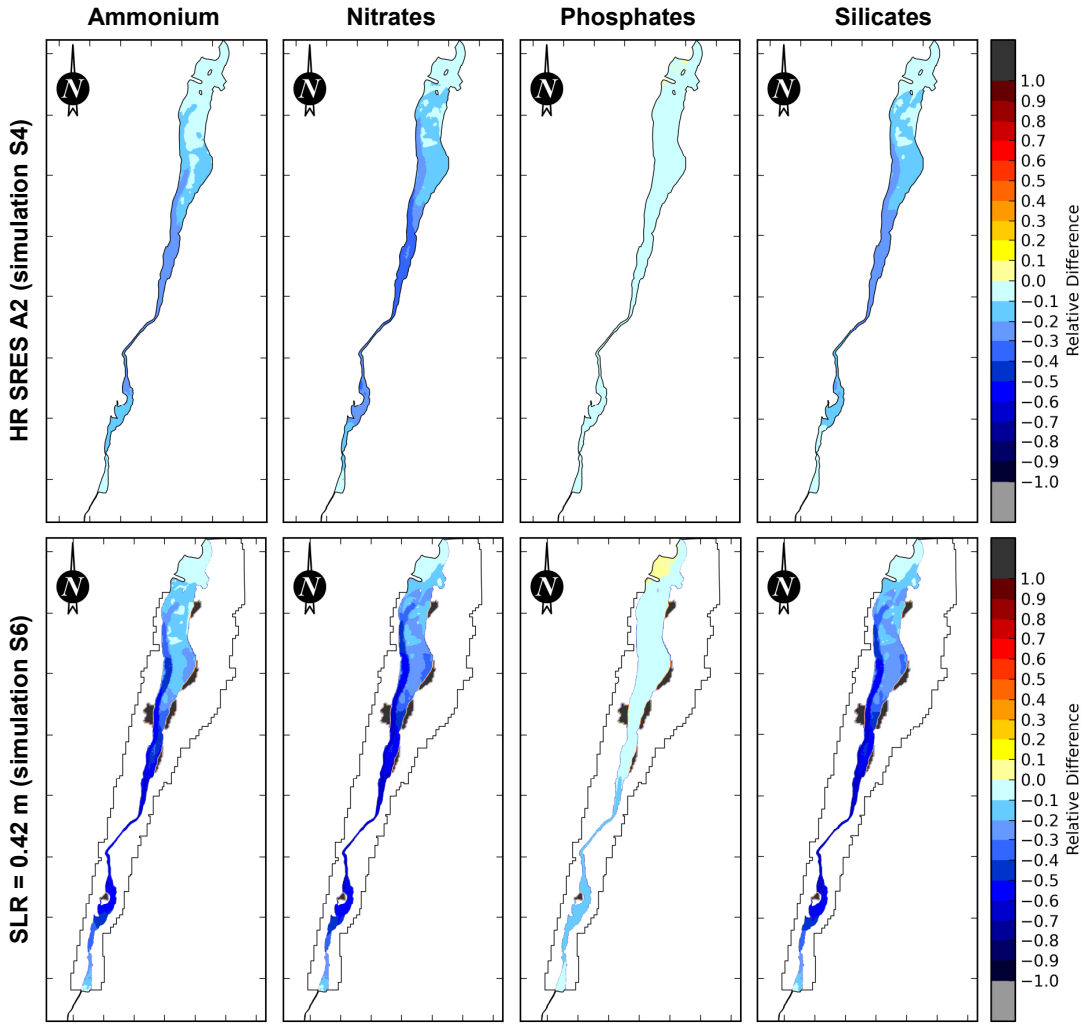

Figure V.1.15. Nutrients mean relative differences (depth-averaged) from the reference scenario due to changes in the hydrological regimes (HR) based on scenarios SRES A2 (simulation S4) and sea level rise of 0.42 m (simulation S6) in spring season. Dark grey represents new flooded areas, while light grey represents new dry areas.

Changes in the precipitation regimes also reduce the nutrients' concentrations, in particular during summer for both scenarios, and during spring for scenario SRES A2 (Table AIV.2,

Appendix IV). During the winter season, an increase of the nutrients concentrations is predicted by the scenario SRES B2, due to an increase of the freshwater discharge, which is one of the main sources of nutrients in the Aveiro lagoon (Lopes *et al.*, 2007; Chapter IV, Rodrigues *et al.*, in preparation). In particular, a negative correlation is observed between both nitrates and silicates and salinity, that has also been observed in previous studies (Chapter III, Section III.3, Rodrigues *et al.*, 2012; Chapter IV, Rodrigues *et al.*, in preparation), and puts in evidence the freshwater origin of these nutrients. This correlation may be used has an indicator of changes in these nutrients' concentrations when faster simulations are required.

Regarding the scenario of the emergency discharge (simulation S9), results show that the effects of this failure are local and constrained to the time of the failure, leading to increased concentrations of ammonium and phosphates. However, it should be noted that the period of failure considered was relatively small, and there is a significant increase of the population served by the system during the summer season, which may increase the predicted loadings in a failure situation.

V.1.4 DISCUSSION

Estuarine ecosystems dynamics and water quality are strongly dependent on the interplay between the physical, chemical and biological processes. Regarding the effects of climate change and anthropogenic pressures on these processes along a shallow temperate estuarine environment (Mira channel, Aveiro lagoon, Portugal), sea level rise followed by changes in the hydrological regimes were the drivers that lead to larger variations of the physical and water quality variables from the reference scenario. In particular, these climate scenarios are expected to have a larger influence on the estuarine water and ecological quality when compared with the anthropogenic scenarios analysed. The influence of these variations on the nutrients, primary production and food web, and species composition and distribution is discussed next. Although presented separately for the purposes of discussion, it should be noted that some of the expected shifts are correlated and, consequently, are likely to have a synergistic effect on the community.

V.1.4.1 Influence on Nutrients Concentrations

Nutrients are commonly used to assess the water quality and the lower trophic levels dynamics, namely phytoplankton dynamics, in estuarine systems (e.g. Crouzet *at al.*, 1999; Gameiro and Brotas, 2010). High loadings of nutrients, in particular nitrogen and phosphorus, are commonly associated with poor water quality and anthropogenic pressures in estuaries (Cloern, 2001).

Sea level rise scenarios (0.28 m and 0.42 m) put in evidence a significant decrease of the nutrients concentrations along the Mira channel, deriving from the larger volume of marine water flowing to the channel. For nitrates, silicates and ammonium the predicted reductions can reach values of less than 50% from the reference scenario. The computed concentrations in some of the downstream and middle areas of the channel in the sea level rise scenarios are lower than those observed near the inlet of the Aveiro lagoon over the past 25 years (Chapter IV, Rodrigues *et al.*, in preparation). A reduction of nutrients' concentrations was also predicted due to changes in the precipitation regimes, in particular during summer. However, the range of variation of nutrients concentrations in these scenarios is within the range observed over the past 25 years (Chapter IV, Rodrigues *et al.*, in preparation). For the scenario SRES B2, an increase of the nutrients concentrations is predicted during the winter season, due to the larger volume of freshwater flowing to channel.

As nutrients are one of the main factors limiting the growth of primary producers, the reductions of the nutrients levels are likely to promote shifts in the primary producers species composition. In particular, lower nutrient concentrations will probably cause a shift on phytoplankton community to species that are better adapted to lower nutrient conditions. During winter, the increase of the nutrients concentrations predicted for the scenario SRES B2 promotes a slight increase in the chlorophyll *a* (Figure V.1.11). An increase of the primary production during winter associated with a larger nutrients' availability due climate change was also suggested by Najjar *et al.* (2010) for the Chesapeake Bay (USA). During spring and summer, the combined effect of sea level rise and the reduction of the freshwater discharge will probably enhance the nutrients reductions along the channel. During winter, results suggest that sea level rise influence will be larger than the impact of the increase of the freshwater discharge. Moreover, as recent studies suggest that a mean sea level rise of about 1 m is likely to occur, this effect may be enhanced (e.g., Yates *et al.*, 2011, Sano *et al.*, 2011).

Another important aspect regarding nutrients long-term trends is the possible increase of the nutrients loadings due to an increase in human activity along the estuarine margins. Although there is some controversy, some authors argue that the increased population will likely intensify the eutrophication in coastal waters (Rabalais *et al.*, 2009). Changes in the nutrients concentrations flowing from the freshwater were not considered in the present study, but a scenario of a failure of the wastewater treatment system was evaluated. Both the reductions observed due to sea level rise and the local and constrained effects observed due to the failure of the wastewater treatment system suggest that, in this estuarine system, sea level rise will probably overwhelm the increase of nutrients loadings. Still, this influence should be further evaluated, combining scenarios of increased nutrients loadings with sea level rise and changes in the hydrological regimes.

The interactions between the sediments and the water column also require further research, as sediment resuspension is a potential source of nutrients (Gameiro and Brotas, 2010). Lopes *et al.* (2011) suggested that sea level rise will intensify the sediments fluxes in the downstream area of the Aveiro lagoon, promoting an increase of the erosion at the entrance of the lagoon and of the accretion inside the inlet. Moreover, changes of the sediments fluxes will also affect the bathymetry of the Aveiro lagoon and should also be taken into account in future studies of water quality and ecological dynamics of this estuarine system.

V.1.4.2 Influence on Chlorophyll *a*, Primary Production and Food Web

The significant decrease of the phytoplankton biomass associated to sea level rise indicates a decrease of primary production, as phytoplankton and microphytobenthos are the main primary producers in estuaries of temperate regions (Underwood and Kromkamp, 1999). Computed concentrations of chlorophyll *a* in the downstream and middle areas of the Mira channel are within the range of variation observed in the inlet of the Aveiro lagoon over the past 25 years and lower than those observed in the transition areas (Chapter IV, Rodrigues *et al.*, in preparation).

The predicted decrease of phytoplankton biomass, in particular due to sea level rise, might affect the food web structure. Results reveal a decrease of zooplankton biomass, which may also affect the higher trophic levels as less food will be available. As primary production in the downstream areas of estuaries is a sink of atmospheric carbon (Chen *et al.*, 2012), the reduction of primary production in estuarine systems may also reduce this effect. As discussed for nutrients, the combined effect of sea level rise with the decrease of the freshwater discharge due to changes in the hydrological regimes, in particular during spring and summer seasons, may enhance these effects.

Water temperature is an important driver of some physiological processes and responses of the species. Some authors suggest that global warming may change the species physiological response and phenology, promoting earlier spring blooms, among other effects (e.g. Hashioka and Yamanaka, 2007; Najjar *et al.*, 2010; Kromkamp and Engeland, 2010). In the North Pacific Ocean, Hashioka and Yamanaka (2007) found a decrease of the chlorophyll *a* and nutrients concentrations in 2100 associated with higher vertical stratification due to global warming. A shift of the dominant phytoplankton group from diatoms to other small phytoplankton species was also observed by these authors. The results obtained in the present study for air temperature rise scenarios reveal increases in the water temperature of 3ºC to 4ºC during the summer but small variations on the chlorophyll *a* concentrations from the reference scenario. Several reasons may explain these findings. First, no significant stratification was observed along the channel, both in the reference and in the simulated scenarios, as the Aveiro lagoon is

relatively shallow. This well-mixed environment allows nutrients' availability throughout the water column. Second, both phytoplankton and zooplankton growth rates increase with air temperature, suggesting a grazing control of the phytoplankton biomass and evidencing the complexity of the ecosystems response to the climate drivers and the requirement to consider different trophic levels in this type of studies. Third, only one phytoplankton group (diatoms) was simulated. In future research there is a need to include more primary producers to study the dynamics of the Aveiro lagoon, in particular macroalgae as they have an important role in the primary production in this system (Trancoso *et al.*, 2005). In the Chesapeake Bay estuary (USA), Najjar *et al.* (2010) suggested increased macroalgae productivity associated with global warming. Fourth, simulations were performed over a single year with the predicted conditions for the end of the 21st century. Longer simulations over the years from now till 2100 period are needed. However, very expensive computational times limit this type of applications. Moreover, species are also expected to evolve and adapt through time, and these behaviours are difficult to reproduce with numerical models.

V.1.4.3 Influence on Species Distribution and Composition

Salinity plays an important role in the biotic distribution within the estuaries and these correlations have been investigated in several studies (e.g. Wolf *et al.*, 2009). The Venice system, extended by Carriker (1967), is commonly used to classify the estuaries based on salinity. Five zones are identified: limnetic (freshwater, <0.5), oligohaline (0.5-5), mesohaline (5-18), polihaline (middle area, 18-25; lower area, 25-30), and euhaline (30-35). In the Aveiro lagoon, the phytoplankton (Resende *et al.*, 2005), zooplankton (Leandro, 2008) and benthic macrofauna (Moreira *et al.*, 1993) abundance and distribution have been studied along the salinity gradient established in the Mira channel. The mapping proposed in these studies for species composition and distribution, combined with the range of salinities observed, is presented in Table V.1.3. Based on that distribution for zooplankton and benthic macrofauna, Rodrigues *et al.* (2011) suggested that, during rainy periods, a larger expansion of estuarine species will occur downstream, while, during dry periods, marine species will progress further upstream.

As sea level scenarios suggest an increase in the salinity range in the middle and upper areas of the Mira channel, changes in the species' longitudinal distribution are likely to occur. Salinity may increase by about 12 to 20 in some middle and upstream areas of the channel, reaching values close to the ones observed presently in the downstream area. A classification of the Aveiro lagoon salinity based on the Venice's system for the sea level rise scenario of 0.42 m evidences an extension of the euhaline zone further upstream throughout the year (Figure V.1.16), when compared with the classification presented by Dias *et al*. (2011) based on 2001

data. Thus, an upstream progression of the marine species of phytoplankton, zooplankton and benthic macrofauna may occur along the Mira channel and the other branches of the Aveiro lagoon, as salinity increases due to sea level rise. Moreover, the increases of the volume of marine water within the estuary may also introduce more invasive or toxic coastal species, as proposed by Najjar *et al.* (2010) for the Chesapeake Bay estuary (USA). These effects may be enhanced when combined with the reductions predicted for the freshwater discharge, in particular during the summer season. Further research is needed in this area, in particular in long-term monitoring, to understand the species response to continuous environmental changes.

Table V.1.3. Zonation of the Mira channel based on phytoplankton, zooplankton and benthic macrofauna composition as proposed by Resede *et al.* (2005), Leandro (2008) and Moreira *et al.* (1993), respectively, and relationship with salinity based on the Venice system (extended from Rodrigues *et al.*, 2011).

Phytoplankton		Zooplankton		Benthic Macrofauna	
Zone and Species	**Salinity**	**Zone and Species**	**Salinity**	**Zone and Species**	**Salinity**
St1, Downstream Marine species dominance (e.g. *Auliscus sculptus*, *Chaetoceros densus*, *Surirella comis*)	18-37 (euhaline, polihaline)	Z1, downstream Marine species dominance (*Acartia clausi*)	25-35 (euhaline, lower polihaline)	GII, downstream Marine polyhaline species (*Urohoe brevicornis*, *Angulus tenuis*)	25-35 (euhaline, lower polihaline)
St3, middle area Freshwater species dominance (e.g. *Caloneis permagna*, *Cymbella tumida*, *Pinnularia stommatophora*)	0-33 (mean value of 15, mesohaline)	Z2, middle area Estuarine species dominance (*Acartia tonsa*)	5-25 (middle polihaline, mesohaline)	GI, along the channel Marine euryhaline and polyhaline species (*Scrobicularia plana*, *Tharyx marioni*, *Cerastoderme dulis*)	5-25 (middle polihaline, mesohaline)
-	-	Z3, upstream Low copepods abundance	0-5 (oligohaline, limnetic)	GII, upstream Estuarine and euryhaline limnic species (*Potamopyrgus jnkinsi*, *Corophium multisetosum*, *Chrinomidae*)	0-5 (oligohaline, limnetic)

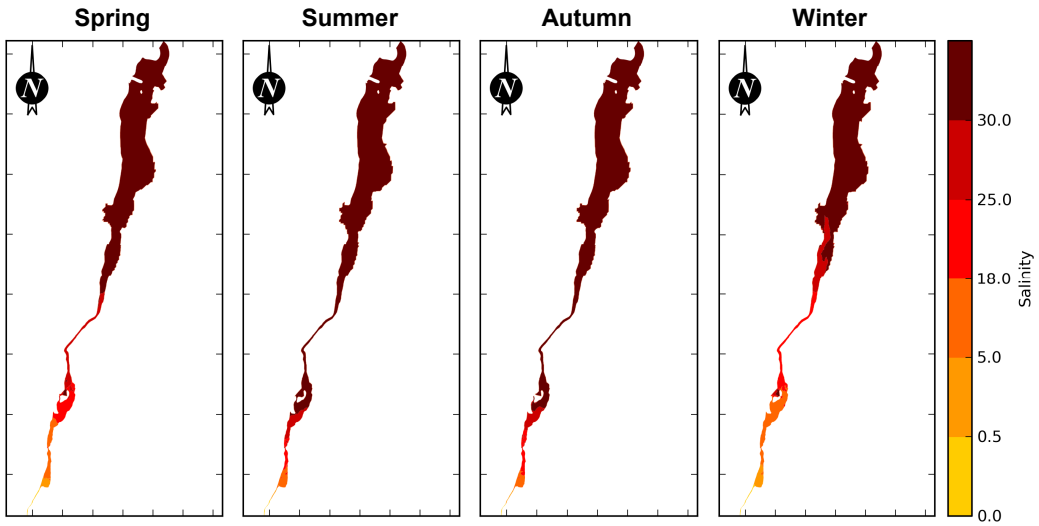

Figure V.1.16. Salinity seasonal zonation of the Mira channel based on the Venice system classification for the sea level rise scenario of 0.42 m.

V.1.5 CONCLUSIONS

Understanding the role of the main drivers of the estuarine ecosystems and water quality dynamics is fundamental for estuarine long-term management. The analysis of the relative influence of climate change, namely air temperature rise, changes in the hydrological regimes and sea level rise, and anthropogenic interventions along a estuarine environment provides useful insight in that direction. In the present study, a validated coupled three-dimensional hydrodynamic and ecological model (ECO-SELFE) was used to investigate several scenarios of climate change and anthropogenic interventions in a sub-estuarine environment of the Aveiro lagoon, the Mira channel. Besides providing useful knowledge for the long-term management of the Aveiro lagoon, this study also contributes for a better understanding of processes in shallow temperate estuaries, in general.

Sea level rise, followed by changes in the hydrological regimes, were the drivers that influenced most significantly the physical and the water quality variables, leading to the larger variations from the reference scenario. This influence, combined with some local variations due to dredging, brings into focus the important role of the circulation and their forcings in establishing the water quality and ecological dynamics in the Aveiro lagoon, in general, and in the Mira channel, in particular. The present study indicates that climate change is expected to have a much stronger impact on the dynamics and ecological quality of this system relative to the anthropogenic changes analysed.

A significant increase of the salinity in the middle and upstream areas of the channel, which can reach differences of more than 12-20 relative to the reference scenario, was predicted due to

sea level rise. Conversely, a significant decrease of nutrients, dissolved oxygen and chlorophyll *a* concentrations occurred throughout all seasons. These changes suggest reductions on the primary production, which may affect the food web, shifts on species composition and further progression upstream of marine species. Synergistic effects among climate drivers need further research, but sea level rise combined with the decrease of the freshwater discharge, in particular during summer, will probably enhance these changes. Regarding global warming, the major differences on water temperature occurred during summer for the worst scenario evaluated with increases of about 3ºC to 4ºC relative to the reference scenario. These changes in the water temperature lead to very small variations in the nutrients, dissolved oxygen and chlorophyll *a* concentrations from the reference scenario. These results suggest a grazing control of the phytoplankton and evidence the need to evaluate different trophic levels when performing this type of analyses.

The findings achieved in this study constitute a fist contribution to the analyses of the effects of climate change and anthropogenic pressures on the water quality and ecological dynamics of the Aveiro lagoon, helping in the development of long-term monitoring plans and management strategies for this system. Results also reveal that the effects of climate change can be more significant on shallow estuaries. Moreover, results put in evidence the need of multidisciplinary approaches when studying the estuarine ecosystems dynamics and the role of distinct drivers on water and ecological quality.

Another important aspect relates with the uncertainty of the future climate and the assumptions of the present analysis. Many of the available predictions suggest significant variations of the extreme values of the climate variables (Miranda *et al.*, 2006), which may enhance some of the effects revealed by the scenarios evaluated. These issues suggest that research in these areas should be continuous, based on the most recent knowledge, and developing information for the development of adaptive management strategies. In particular, future research should account for: morphological changes and sediments-water column dynamics; increased ecosystem complexity, by introducing more primary producers (namely macroalgae) and higher trophic levels; additional combined scenarios; and longer periods of simulation, allowing to evaluate the system evolution.

V.1.6 REFERENCES

Antunes C, Taborda R. Sea level at Cascais tide gauge: data, analysis and results. *Journal of Coastal Research* **2009**, SI 56, 218–222.

Araújo IGB. Sea level variability: examples from the Atlantic Coast of Europe. PhD thesis, University of Southampton, UK, **2005**.

Barbier EB, Hacker SD, Kennedy C, Koch EW, Stier AC, Silliman BR. The value of estuarine and coastal ecosystem services. *Ecological Monographs* **2011**, 81(2), 169-193.

Bisset WP, Debra S, Dye D. Ecological Simulation (EcoSim) 2.0 Technical Description, Tampa, Florida: Florida Environmental Research Institute, **2004**, 25 pp.

Carriker MR. Ecology of estuarine benthic invertebrates: A perspective. In: Lauff GH (Ed.), *Estuaries. American Association for the Advancement of Science* **1967**, 83, 442–487.

Chen C-TA, Huang T-H, Fu Y-H, Bai Y, He X. Strong sources of CO_2 in upper estuaries become sinks of CO_2 in large river plumes. *Current Opinion in Environmental Sustainability* **2012**, 4(2), 179-185.

Chust G, Borja A, Liria P, Galparsoro I, Marcos M, Caballero A, Castro R. Human impacts overwhelm the effects of sea-level rise on Basque coastal habitats (N Spain) between 1954 and 2004. *Estuarine, Coastal and Shelf Science* **2009**, 84(4), 453-462.

Cloern JE, Jassby AD. Patterns and scales of phytoplankton variability in estuarine-coastal systems. *Estuaries and Coasts* **2010**, 33, 230-241.

Cloern JE. Our evolving conceptual model of the coastal eutrophication problem. *Marine Ecology Progress Series* **2001**, 210, 223-253.

Crouzet P, Leonard J, Nixon S, Rees Y, Parr W, Laffon L, Bøgestrand J, Kristessen P, Lallana C, Izzo G, Bokn T, Back J, Lack TJ. *Nutrients in European ecosystems, Environmental Assessment Report nº 4*. European Environmental Agency, **1999** (http://www.eea.europa.eu/publications/ENVIASSRP04).

Denman KL Peña MA. The response of two coupled one-dimensional mixed layer/planktonic ecosystem models to climate change in the NE subarctic Pacific Ocean. *Deep Sea Research Part II: Topical Studies in Oceanography* **2002**, 49(24–25), 5739-5757.

Dias JA, Taborda R. Tidal gauge data in deducing secular trends of relative sea level and crustal movements in Portugal. *Journal of Coastal Research* **1992**, 8, 655–659.

Dias JM, Lopes JF, Dekeyser I. Hydrological characterisation of Ria de Aveiro, Portugal, in early summer. *Oceanologica Acta* **1999**, 22(5), 473-485.

Dias JM, Lopes JF, Dekeyser I. Lagrangian transport of particles in Ria de Aveiro lagoon, Portugal. *Physics and Chemistry of the Earth, Part B: Hydrology, Oceans and Atmosphere* **2001**, 26(9), 721-727.

Dias JM, Lopes JF, Dekeyser I. Tidal propagation in Ria de Aveiro lagoon, Portugal. *Physics and Chemistry of the Earth, Part B: Hydrology, Oceans and Atmosphere* **2000**, 25(4), 369-374.

Dias JM, Lopes JF. Implementation and assessment of hydrodynamic, salt and heat transport models: the case of Ria de Aveiro lagoon (Portugal). *Environmental Modelling & Software* **2006**, 21(1), 1-15.

Dias JM, Rodrigues M, Leandro S, Morgado F, Oliveira A, Queiroga H. Caracterização sinóptica dos gradientes ambientais na Ria de Aveiro. Parte I: salinidade e temperatura. In: Almeida A, Alves FL, Bernardes C, Dias JM, Gomes NCM, Pereira E, Queiroga H, Serôdio J, Vaz N (Eds.), Actas das Jornadas da Ria de Aveiro, **2011**,141-150.

Dias, JM. Contribution to the study of the Ria de Aveiro hydrodynamics. PhD Thesis, Universidade de Aveiro, **2001**.

Ducharne A, Baubion C, Beaudoin N, Benoit M, Billen G, Brisson N, Garnier J, Kieken H, Lebonvallet S, Ledoux E, Mary B, Mignolet C, Poux X, Sauboua E, Schott C, Théry S, Viennot P. Long term prospective of the Seine River system: confronting climatic and direct anthropogenic changes. *Science of the Total Environment* **2007**, 375(1-3), 292-311.

Ecossistema and Impacte – Ambiente e Desenvolvimento. Estudo de Impacte Ambiental da Marina da Barra, em fase de estudo prévio. Lisboa, **2003**.

Ferreira JG, Simas T, Nobre A, Silva MC, Shifferegger K, Lencart-Silva J. *Identification of sensitive areas and vulnerable zones in transitional and coastal portuguese systems*, INAG, **2003**, 151 pp.

Ferreira JG, Wolff WJ, Simas TC, Bricker SB. Does biodiversity of estuarine phytoplankton depend on hydrology? *Ecological Modelling* **2005**, 187, 513-523.

Fortunato AB, Pinto LL, Oliveira A, Ferreira JS. Tidally-generated shelf waves off the western Iberian coast. *Continental Shelf Research* **2002**, 22(14), 1935-1950.

Gameiro C, Brotas V. Patterns of phytoplankton variability in the Tagus Estuary. *Estuaries and Coasts* **2010**, 33, 311-323.

Grangeré K, Lefebvre S, Blin J-L. Spatial and temporal dynamics of biotic and abiotic features of temperate coastal ecosystems as revealed by a combination of ecological indicators. *Estuarine, Coastal and Shelf Science* **2012**, , 108, 109-118.

Hashioka T, Yamanaka Y. Ecosystem change in the western North Pacific associated with global warming using 3D-NEMURO. *Ecological Modelling* **2007**, 202, 95-104.

Hong B, Shen J. Responses of estuarine salinity and transport processes to potential future sea-level rise in the Chesapeake Bay. *Estuarine, Coastal and Shelf Science* **2012**, 104-105, 33-45.

Huang XP, Huang LM, Yue WZ. The characteristics of nutrients and eutrophication in the Pearl River estuary, South China. *Marine Pollution Bulletin* **2003**, 47(1-6), 30–36.

Intergovernmental Panel on Climate Change (IPCC). Climate Change 2007: The Physical Science Basis. UNEP and WMO, **2007** (http://www.ipcc.ch/SPM2feb07.pdf).

James ID. Modelling pollution dispersion, the ecosystem and water quality in coastal waters: a review. *Environmental Modelling & Software* **2002**, 17(4), 363-385.

Kishi MJ, Kashiwai M, Ware DM, Megrey BA, Eslinger DL, Werner FE, Noguchi-Aita M, Azumaya T, Fujii M, Hashimoto S, Huang D, Iizumi H, Ishida Y, Kang S, Kantakov GA, Kim H, Komatsu K, Navrotsky VV, Smith SL, Tadokoro K, Tsuda A, Yamamura O, Yamanaka Y, Yokouchi K, Yoshie N, Zhang J, Zuenko YI, Zvalinsky ZI. NEMURO – a lower trophic level model for the North Pacific marine ecosystem. *Ecological Modelling* **2007**, 202, 12-25.

Kotta I, Simm M, Põllupüü M. Separate and interactive effects of eutrophication and climate variables on the ecosystems elements of the Gulf of Riga. *Estuarine, Coastal and Shelf Science* **2009**, 84, 509-518.

Kromkamp JC, Engeland TV. Changes in phytoplankton biomass in the Western Scheldt estuary during the period 1978-2006. *Estuaries and Coasts* **2010**, 33, 270-285.

Leandro SM. Forçamento ambiental na abundância e produção de zooplâncton num gradiente estuarino. PhD Thesis, Universidade de Aveiro, **2008**.

Likens GE. *Plankton of Inland Waters*, Encyclopedia of Inland Waters, Elsevier, **2010**.

Lopes CB, Pereira ME, Vale C, Lillebø AI, Pardal MA, Duarte AC. Assessment of spatial environmental quality status in Ria de Aveiro. *Scientia Marina* **2007**, 71(2), 293-304.

Lopes CL, Silva PA, Dias JM, Rocha A, Picado A, Plecha S, Fortunato AB. Local sea level change scenarios for the end of the 21st century and potential physical impacts in the lower Ria de Aveiro (Portugal). *Continental Shelf Research* **2011**, 31(14), 1515-1526.

Miranda PMA, Valente MA, Tomé AR, Trigo R, Coelho MFES, Azevedo EB. *O clima de Portugal nos séculos XX e XXI. Alterações Climáticas em Portugal Cenários. Impactos e Medidas de Adaptação Projecto SIAM II*. Gradiva. Lisboa, **2006,** 169–208.

Moreira MH, Queiroga H, Machado MM, Cunha MR. Environmental gradients in a southern Europe estuarine system: Ria de Aveiro, Portugal. Implications for soft bottom macrofauna colonization. *Netherlands Journal of Aquatic Ecology* **1993**, 27, 465-482.

Najjar RG, Pyke CR, Adams MB, Breitburg D, Hershner C, Kemp M, Howarth R, Mulholland MR, Paolisso M, Secor D, Sellner K, Wardrop D, Wood R. Potential climate-change impacts on the Chesapeake Bay. *Estuarine, Coastal and Shelf Science* **2010**, 86(1), 1-20.

Nakicenovic N, Alcamo J, Davis G, de Vries B, Fenhann J, Gaffin S, Gregory K, Grübler A, Jung TY, Kram T, La Rovere EL, Michaelis L, Mori S, Morita T, Pepper W, Pitcher H, Price L, Riahi K, Roehrl A, Rogner H-H, Sankovski A, Schlesinger M, Shukla P, Smith S, Swart R,

van Rooijen S, Victor N, Dadi Z. Special Report on Emissions Scenarios: A Special Report of Working Group III of the Intergovernmental Panel on Climate Change, Cambridge University Press, Cambridge, United Kingdom, **2000**, 599 pp (http://www.grida.no/climate/ipcc/emission/index.htm).

Neumann T. Climate-change effects on the Baltic Sea ecosystem: A model study. *Journal of Marine Systems* **2010**, 81(3), 213-224.

Paerl HW, Rossignol KL, Hall SN, Peierls BL, Wetz MS. Phytoplankton community indicators of short- and long-term ecological change in the anthropogenically and climatically impacted Neuse River estuary, North Carolina, USA. *Estuaries and Coasts* **2010**, 33, 485-497.

Paerl HW. Assessing and managing nutrient-enhanced eutrophication in estuarine and coastal waters: Interactive effects of human and climatic perturbations. *Ecological Engineering* **2006**, 26(1), 40-54.

Park K, Jung H, Kim H, Ahn S. Three-dimensional hydrodynamic-eutrophication model (HEM-3D): application to Kwang-Yang Bay, Korea. *Marine Environmental Research* **2005**, 60(2), 171-193.

Pethick J. Coastal management and sea-level rise. *CATENA* **2001**, 42(2–4), 307-322.

Queiroga H, Neves R, Almeida A, Bernardes C, Calado A, Craveiro S, Cunha A, Delfino JP, Dias JM, Ferreira J, Figueiredo J, Henriques I, Leandro S, Leitão PC, Lindim C, Lopes JF, Morgado F, Oliveira M, Orgaz D, Pereira A, Pereira F, Pereira T, Pina P, Rodrigues M, Silva A, Talaia M, Tavares AL. *ModelRia – Modelização da qualidade da água da laguna da Ria de Aveiro. Relatório de progresso*. Universidade de Aveiro, Instituto Superior Técnico and Hidromod, **2001**.

Rabalais NN, Turner RE, Díaz RJ, Justić D. Global change and eutrophication of coastal waters. *ICES Journal of Marine Science* **2009**, 66, 1528-1537.

Rebelo JE. The ichthyofauna and abiotic hydrological environment of the Ria de Aveiro, Portugal. *Estuaries and Coasts* **1992**, 15(3), 403-413.

Resende P, Azeiteiro U, Pereira MJ. Diatom ecological preferences in a shallow temperate estuary (Ria de Aveiro, Western Portugal). *Hydrobiologia* **2005**, 544, *77-88.*

Roberts PJW, Snyder WH, Baumgartner DJ. Ocean outfalls. I: Submerged wastefield formation. *Journal of Hydraulic Engineering* **1989a**, 115(1), 1-25.

Roberts PJW, Snyder WH, Baumgartner DJ. Ocean outfalls. II: Spatial evolution of submerged wastefield. *Journal of Hydraulic Engineering* **1989b**, 115(1), 26-48.

Rocha C, Galvão H, Barbosa A. Role of transient silicon limitation in the development of cyanobacteria blooms in the Guadiana estuary, south-western Iberia. *Marine Ecology Progress Series* **2002**, 228, 35-45.

Rodrigues M, Dias JM, Leandro S, Morgado F, Cunha A, Almeida A, Oliveira A, Queiroga H. Caracterização sinóptica dos gradientes nos canais da Ria de Aveiro. Parte II: oxigénio, clorofila e zonação ecológica. In: Almeida A, Alves FL, Bernardes C, Dias JM, Gomes NCM, Pereira E, Queiroga H, Serôdio J, Vaz N (Eds.), Actas das Jornadas da Ria de Aveiro, **2011**, 151-158.

Rodrigues M, Oliveira A, Queiroga H, Fortunato AB, Zhang YJ. Three-dimensional modeling of the lower trophic levels in the Ria de Aveiro. *Ecological Modelling* **2009**, 220(9-10), 1274-1290.

Rodrigues M, Oliveira A, Queiroga H, Zhang YJ, Fortunato AB, Baptista AM. Integrating a circulation model and an ecological model to simulate the dynamics of zooplankton. In: Spaulding, M. (ed.), Estuarine and Coastal Modeling Conference Book, Proceedings of the Tenth International Conference, N.Y.: ASCE **2008**, 427-446.

Rodrigues M, Queiroga H, Brotas V, Oliveira A, Dolores M. Climatic and anthropogenic factors driving water quality variability in the Aveiro lagoon: 1985-2010 data analysis. In preparation to *Science of the Total Environment*.

Rodrigues M, Oliveira A, Queiroga H, Brotas V. Seasonal and diurnal water quality modelling along a salinity gradient (Mira channel, Aveiro lagoon, Portugal. *Procedia Environmental Sciences* **2012**, 899-918.

Sano M, Golshani A, Splinter KD, Strauss D, Thurston W, Tomlinson R. A detailed assessment of vulnerability to climate change in the Gold Coast, Australia. *Journal of Coastal Research* **2011**, SI 64, 245-249.

Science for Environment Policy. European Commission DG Environment News Alert Service, Issue 270. Ed. SCU, The University of the West of England, Bristol, **2012**.

Sebastiá M-T, Rodilla M, Sanchis J-A, Altur V, Gadea I, Falco S. Influence of nutrient inputs from a wetland dominated by agriculture on the phytoplankton community in a shallow harbour at the Spanish Mediterranean coast. *Agriculture, Ecosystems & Environment* **2012**, 152, 10-20.

Statham PJ. Nutrients in estuaries — An overview and the potential impacts of climate change. *Science of Total Environment* **2012**, 434, 213-227.

Thom RM, Parkwell TL, Niyogi DK, Shreffler DK. Effects of graveling on the primary productivity, respiration and nutrient flux of two estuarine tidal flats. *Marine Biology* **1994**, 118(2), 329-341.

Trancoso AR, Saraiva S, Fernandes L, Pina P, Leitão P, Neves R. Modelling macroalgae using a 3D hydrodynamic-ecological model in a shallow, temperate estuary. *Ecological Modelling* **2005**, 187, 232–246.

Underwood GJC, Kromkamp J. Primary production by phytoplankton and microphytobenthos in estuaries. *Advances in Ecological Research* **1999**, 29, 93-153.

Vichi M, Pinardi N, Masina S. A generalized model of pelagic biogeochemistry for the global ocean ecosystem. Part I: Theory. *Journal of Marine Systems* **2007**, 64, 89-109.

Vilão R, Venâncio C, Teixeira A, Gervásio I, Liberal P, Ribeiro R, Panão S. Relatório de Estado do Ambiente - Portugal 2011. Agência Portuguesa do Ambiente, Ministério da Agricultura, do Mar, do Ambiente e do Ordenamento do Território, **2011**, 200 pp.

Wolf B, Kiel E, Hagge A, Krieg H-J, Feld CK. Using the salinity preferences of benthic macroinvertebrates to classify running waters in brackish marshes in Germany. *Ecological Indicators* **2009**, 9, 837-847.

Yates ML, le Cozannet G, Lenôtre N. Quantifying errors in long-term coastal erosion and inundation hazard assessments. *Journal of Coastal Research* **2011**, SI64, 260-264.

Zhang Y, Baptista AM. SELFE: A semi-implicit Eulerian-Lagrangian finite-element model for cross-scale ocean circulation. *Ocean Modeling* **2008**, 21(3-4), 71-96.

Zhong J, Fan C, Zhang L, Hall E, Ding S, Li B, Liu G. Significance of dredging on sediment denitrification in Meiliang Bay, China: A year long simulation study. *Journal of Environmental Sciences* **2010**, 22(1), 68-75.

CHAPTER VI
CONCLUDING REMARKS AND CONSIDERATIONS FOR FUTURE RESEARCH

SECTION VI.1

MAJOR CONTRIBUTIONS

This study aimed at contributing to the current knowledge on the influence of climate change and anthropogenic interventions in estuaries and lagoons through the study of the Aveiro lagoon's water quality and ecological dynamics. The effects of climate change on the water quality and ecological dynamics of this lagoon, and the relative role of anthropogenic pressures, are poorly known. A combined approach of long time series data analysis, to account for the system natural variability, and high-resolution numerical modelling was used, aiming at: i) improving existing tools for ecological modelling at multi-scales, namely the fully coupled three-dimensional, unstructured grid, hydrodynamic and ecological model ECO-SELFE; ii) contributing to the robustness and usefulness of ecological modelling applications, through the representation of the relevant processes and the sensitivity analysis of the model input parameters; iii) evaluating the evolution over the past 25 years of the water quality in the Aveiro lagoon, through the statistical analysis of synoptic long-time series of atmospheric, hydrological, hydrodynamic, chemical and biological data; and iv) analysing the relative impacts of climate change and anthropogenic interventions on the water quality and ecological dynamics of the Aveiro lagoon, through the numerical simulation of a set of individual and combined scenarios.

Ecological models are useful tools to understand the ecosystems dynamics and to support management decisions. However, there are some difficulties in the implementation of these models in real systems that include: i) the requirement of the specification of many empirical parameters, which is one of the main sources of uncertainty in ecological modelling and may affect models robustness; and ii) the capacity to represent properly the multiple scales and processes of interest for water quality studies.

Regarding the first issue, the definition of the range of variation of ecological models' input parameters and the quantification of their influence on model predictions is essential to optimize the efforts of measuring the most important parameters. This study contributed in this direction through:

- a review of the values published in the literature for half-saturation constants for nutrients (nitrogen, phosphorous and silica) uptake by phytoplankton, and the definition of the respective ranges for estuarine environments. Besides contributing for the setting up of water quality and ecological models, the review of half-saturation constants is also of major relevance for phytoplankton dynamic studies;
- a sensitivity analysis on the influence of the several input parameters on phytoplankton results, using the ECO-SELFE model applied to the Aveiro lagoon. Phytoplankton

concentrations' simulated by ECO-SELFE presented lower sensitivity to the half-saturation constants for nutrients uptake, even within the range of variation observed for diatoms. On the contrary, the model was significantly influenced by the input parameters related to phytoplankton growth and zooplankton losses. Phytoplankton growth rate and zooplankton excretion and mortality rates, in particular, were the parameters that influenced the model results the most, the degree of their influence depending on the local concentrations of zooplankton and phytoplankton. Thus, the implementation of ecological models in real systems should account for a definition of phytoplankton and zooplankton parameters as accurate as possible, relying on site-specific data whenever they are available.

Regarding the second issue, the improvements and developments of ECO-SELFE performed in this study contributed for a better representation of the relevant processes from local to ocean scales, allowing multi-scale simulations, which are needed in water quality and ecological dynamic studies. Specific contributions included:

- the coupling of ECO-SELFE to a near field model (RSB model), which allows for the simulation of small scale, localized discharges for any given tracer. The coupling between the two models was done using a hybrid approach (i.e. the time-varying ambient currents and stratification predicted by the far field model are used to simulate the near field plume characteristics, which are then inputted in the far field model). The new model was validated through a set of synthetic tests for different environmental and discharge conditions. Results showed the ability of the coupled model to represent adequately the plume characteristics under different ambient and discharge situations, with mass errors generally smaller than 1%;
- the development of a methodology to handle the simulation of a large set of scenarios with a complex, computationally-intensive integrated hydrodynamic and ecological modelling system. The two-step modelling strategy used, performing the hydrodynamic simulations over the entire domain of the Aveiro lagoon and the coupled hydrodynamic-ecological simulations over the Mira channel, allowed the improvement of computational times and to focus the data acquisition efforts;
- the addition of the oxygen cycle (including the simulation of dissolved oxygen and chemical oxygen demand) to the existing cycles of ECO-SELFE (carbon, nitrogen, phosphorous, silica and iron), improving the range of applicability of this process-oriented model. The implemented formulation for the oxygen cycle was preliminarily validated in a small coastal stream, the Aljezur coastal stream, and thoroughly validated along a salinity gradient in the Aveiro lagoon (the Mira channel), establishing its usefulness for different coastal and estuarine systems. The validation of ECO-SELFE in the Aveiro lagoon was based on the methodology described above and was performed

at different temporal scales (diurnal and seasonal), relying on a set of specific campaigns. These 24-hour field campaigns in the Mira channel were designed to complement the existing data series and for model validation purposes, including the measurement of physical (river flow, water levels, currents velocities, water temperature and salinity), chemical (dissolved oxygen and nutrients) and biological parameters (chlorophyll *a*); Results showed the ability of the model to represent both the spatial and temporal patterns observed for the different variables, with differences generally smaller or similar to the ones achieved in this type of models (e.g. Lopes *et al.*, 2008; Fitzpatrick, 2009).

The patterns of variation of the water quality and ecological dynamics in the Aveiro lagoon, and their relationships with the climatic forcing and the anthropogenic interventions, were evaluated over different spatial and temporal scales. The past evolution, between 1985 and 2010, was analysed based on long time series that covered a period of diverse anthropogenic modifications undertaken in the lagoon and different climatic and hydrological conditions, contributing to the understanding of the relative role of these drivers. These data was complemented at small temporal scales by the targeted field campaigns developed during this thesis, which also contributed to increase the knowledge about the Aveiro lagoon's dynamics. The analysis of future evolution of the water quality and ecological dynamics in the Aveiro lagoon was based on a set of individual and combined scenarios of climate change (air temperature rise, changes in the precipitation regimes and sea level rise) and anthropogenic modifications/interventions (dredging, marina construction and emergency discharge of domestic effluents). This set of 1-year scenarios contributed for a first understanding of the possible effects of climate change and anthropogenic interventions in the Aveiro lagoon, producing useful knowledge regarding future management of this estuarine system and of shallow, temperate, estuaries, in general. Specific contributes included:

- the seasonal, inter-annual and long-term trends observed in the Aveiro lagoon over the past 25-years depended on the influence of both anthropogenic and climate forcings, evidencing the need to combine these different drivers when evaluating and developing management strategies for estuarine ecosystems;
- water dynamics, in particular the balance between tide and freshwater discharge, was found to have a main role in establishing the water quality and ecological dynamics in the lagoon. At the small temporal scales, namely at the diurnal scale, the patterns of variation of chlorophyll *a* and nutrients were mostly associated with the tidal dynamics, leading to the transport of the larger concentrations from upstream to downstream during the ebb. Seasonally, the variations were mostly associated with the seasonal variation of the main climatic and hydrological forcings, in particular, the freshwater discharge;

- in the upstream area of the lagoon, the inter-annual variations of chlorophyll *a* over the past 25-years were mostly driven by climatic variability and a slightly upward trend was observed. In this area, a recovery of the system from hypoxia conditions occurred after 1994 and derived from the beginning of the secondary treatment of the industrial effluents of a paper mill. These significant changes put in evidence that some anthropogenic interventions may have a larger influence in the water quality and ecological dynamics of the lagoon, when compared with the system's natural variability;
- in the downstream area of the lagoon, chlorophyll *a* presented a downward trend between 1985 and 2010, the lower concentrations occurring after 2000. This trend is expected to be associated with lower concentrations of silicates that occurred after 2000 in these areas, which may derive from some anthropogenic modifications (e.g. inlet's deepening) that occurred in the lagoon;
- the influence of climate change was found to overwhelm the effects of the anthropogenic interventions analysed, based on the scenarios simulated;
- the changes due to sea level rise were the ones that most influence the water quality and ecological dynamics in the Aveiro lagoon. Results suggested a significant decrease of nutrients, dissolved oxygen and chlorophyll *a* concentrations and a significant increase of the salinity (of more than 12-20 relative to the reference scenario) in the middle and upstream areas of the Mira channel, throughout all seasons. Results also reveal that the effects of climate change can be more significant on shallow estuaries The predicted changes may lead to reductions on the primary production, which may affect the food web, shifts on species composition and promote the progression upstream of marine species in the channels. Moreover, some recent studies suggest that sea level rise of about 1 m is likely to occur (e.g., Yates *et al.*, 2011, Sano *et al.*, 2011). This sea level rise corresponds to about twice of the maximum value evaluated here (0.42 m) and, thus, some of the identified effects might be enhanced. Synergistic effects between climate forcings need further research, however it would be expected that sea level rise combined with the decrease of the freshwater discharge, in particular during the summer season, will also enhance some of the mentioned effects;
- regarding global warming, the major differences on water temperature were found to occur during summer for the worst scenario evaluated, with increases of about 3ºC to 4ºC from the reference scenario. These changes in the water temperature led to very small variations in nutrients, dissolved oxygen and chlorophyll *a* concentrations from the reference scenario. Although an increase in the phytoplankton growth rate was identified, the zooplankton growth rate also increased evidencing a grazing control of the phytoplankton. This effect puts in evidence the complexity of evaluating the effects

of climate change on biological process and the need to consider different trophic levels in this type of studies.

As a final remark, the improvements and validation of ECO-SELFE accomplished with this study showed its usefulness and applicability as a supporting tool for the management of estuarine and coastal ecosystems and, in particular, in the study of the effects of climate change and anthropogenic pressures in the water quality and ecological dynamics of the Aveiro lagoon. Regarding these effects, the findings achieved in this study contribute for the development of long-term management and maintenance strategies in this estuarine system. These findings put in evidence the need to use multidisciplinary approaches, combining different drivers and establishing long-term robust monitoring plans, supported by data and numerical models, for a better understanding of the processes governing the water quality and ecological dynamics in estuarine systems. Future research in these areas of investigation is discussed in next section, regarding the improvement of some of the limitations and uncertainties identified in this study.

SECTION VI.2

CONSIDERATIONS FOR FUTURE RESEARCH

The research developed in the present thesis can be further continued focusing on different areas of investigation.

VI.2.1 WATER QUALITY AND ECOLOGICAL MODELS DEVELOPMENTS

Future research should account for the improvement of the processes simulated by the ecological and water quality models, and in particular by ECO-SELFE, at several levels.

One of these levels is the interaction sediments – water column, whose importance on ecological dynamics is well recognized in the estuarine and coastal areas (e.g. Simon, 1988; Reay *et al.*, 1995; Ji, 2008). Total suspended sediments in the water column influence water density and light penetration in the water column, which, in turn, affects several biological processes (e.g. Alpine and Cloern, 1988; Gameiro *et al.*, 2011). Nutrients, other chemical species and microorganisms concentrations in the water column are also influenced by suspended sediments, since they can attach to sediment particles and settle, or detach and become soluble or suspended in the water column (Ji, 2008). The fluxes between the bottom sediments and the overlaying water are relevant too. In particular, diagenesis in the sediments promotes the mineralisation of the organic matter and leads to a release of nutrients, like ammonium and phosphates, to the water column (e.g. Cabrita and Brotas, 2000; Qu *et al.*, 2003; Luff and Moll, 2004). Bottom sediments resuspension, occurring naturally or induced by human activities (e.g. dredging), is an important source of nutrients, other chemical species and microorganisms to the water column as well (e.g. Lohrer and Wetz, 2003; Gameiro *et al.*, 2007; Rehman and Soupin, 2009). Moreover, morphological changes of the bottom, which affect the patterns of circulation, may also influence the water quality and ecological dynamics in estuaries and coastal zones (e.g. Oliveira *et al.*, 2010).

Although the linkage between sediments and water column processes has been explored in some water quality and ecological dynamic models (e.g. Luff and Moll, 2004; Park *et al.*, 2005; Arndt *et al.*, 2011), most of these models rely only on water column processes (Luff and Moll, 2004), as the linkage between the two media is still difficult to quantify and very computationally demanding. Recent works on the understanding of this interaction (Li *et al.*, 2008) and the advances in parallel computation opens the path for the integration of this interaction in sophisticated, process-oriented three-dimensional models. Thus, future developments of these models should account for a more extensive use and representation of the interactions between

the sediments and the water column. ECO-SELFE, in particular, should be coupled to a sediment transport and morphodynamic model, as MORSELFE (Pinto *et al.*, in review), and extended to simulate the fluxes between the bottom sediments and the overlaying water column. In the Aveiro lagoon, in particular, this improvement is particularly relevant since: i) during the present study sediments resuspension was identified as a possible source of ammonium and phosphates in the lagoon; ii) will allow the simulation of other functional groups, as vascular plants, and iii) Lopes *et al.* (2011) suggested that sea level rise will affect sediments flux and bathymetry in the downstream area of the Aveiro lagoon, which will in turn change circulation patterns and, consequently, water quality and ecological dynamics in the lagoon, needing to be considered in future research of the system evolution and response to climate change.

Future developments in water quality and ecological modelling should consider additional functional groups on the lower trophic levels, namely other primary producers, like macroalgae, which are particularly relevant in the Aveiro lagoon (Trancoso *et al.*, 2005) and may also have an increased growth in estuaries due to global warming (Najjar *et al.*, 2010). The linkage to higher trophic levels and the extension to other components of the ecosystems should also be developed and evaluated. Saltmarshes, in particular, are an important habitat that provides multiple ecological services (Barbier *et al.*, 2011), and future efforts should rely on the simulation of these habitats evolution. The simulation of these habitats should account for the coupling between geomorphological and ecological processes and the feedbacks between them (Fagherazzi *et al.*, 2012). Although challenging from the numerical viewpoint, as the current knowledge of many of the processes involved is still scarce, the improvement of the capacity to simulate these habitats is fundamental (Fagherazzi *et al.*, 2012). This is particularly relevant in the Aveiro lagoon, as it harbours one of the largest saltmarshes in Europe. These developments are of particular relevance as they will allow a better understanding and quantification of the influence of the anthropogenic interventions and climate change throughout the different trophic levels of the estuarine ecosystems. In particular, they will allow a further comprehension of how the several functions and ecological services provided by these ecosystems would be affected by climate change, and support the implementation of more sustained management strategies.

VI.2.2 MODELS AS EFFECTIVE DECISION-SUPPORT TOOLS

An important area that requires future research in order to promote the use of water quality and ecological modelling as an effective and robust decision-support tool is *uncertainty*. The need to quantify, communicate and reduce uncertainty in water quality and ecological studies is well recognized (e.g. Ragas *et al.*, 1999; Refsgaard *et al.*, 2007; Ascough II *et al.*, 2008). However, the complexity of the several dimensions involved makes this a difficult and challenging process

(Ascough II *et al.*, 2008), which is often missed in water quality and ecological modelling. There are several sources of uncertainty (Ascough II *et al.*, 2008): knowledge uncertainty (e.g. processes parameterization, model structure, process understanding), variability uncertainty (natural, human, institutional and technological), decision-making uncertainty and linguistic uncertainty. In the context of the knowledge uncertainty, the increase of the model complexity, like the one proposed above (section VI.2.1), has associated an increase of the uncertainty of its predictions, since there is an increase of the number and interactions of processes that are simulated and, consequently, need to be parameterized. In long-term ecological studies, the lack of knowledge on how species will evolve and adapt through time, and the difficulty to reproduce these behaviours with numerical models (Atkins and Travis, 2010), are also additional sources of uncertainty. In the context of climate change, the natural variability of the climate and the doubt about the future climate increase the uncertainty of the predictions as well. Moreover, the strong interdependence between the physical, chemical and the biological processes and the cascade modelling approach used in water quality and ecological dynamics studies, combining different type of models (atmospheric, hydrodynamic, waves, morphodynamic and water quality and ecological models), represents also a major source of uncertainty in the predictions. This cascade modelling leads to uncertainty propagation (Rossa *et al.*, 2007). Thus, future model developments and applications should account for the quantification, communication and reduction of these different levels of uncertainty. This effort is of major relevance for the effective and sustained use of water quality and ecological models (like ECO-SELFE) as decision-support tools. Additionally, the incorporation of uncertainty in management plans will allow the adoption of adaptive management practices, which are essential from the long-term estuarine management perspective (Ascough II *et al.*, 2008).

VI.2.3 LONG-TERM MANAGEMENT OF ESTUARINE ECOSYSTEMS: MONITORING AND ANTICIPATING CHANGES

The concept of long-term management is essential for the sustainable development of estuarine ecosystems. In this context, the study of climate change and anthropogenic impacts in estuaries, and in particular in the Aveiro lagoon, should be continued, from both the monitoring and the modelling viewpoints.

The continuous and structured monitoring of estuarine ecosystems is a fundamental requirement to understand the systems natural variability and anticipate changes. In the Aveiro, lagoon the monitoring strategies combining physical (e.g. currents, river flow, air temperature), chemical (e.g. dissolved oxygen) and biological (e.g. chlorophyll *a*, zooplankton) variables were almost inexistent in the past years, and a continuous, integrated, monitoring strategy is needed. In particular, the identified trends in chlorophyll *a* and nutrients in the downstream areas of the

lagoon should be further investigated. The LTER-Ria de Aveiro project will contribute in this direction, but longer term monitoring is required.

Regarding the modelling dimension, future studies should account for the combination of more scenarios and for longer simulations, from the present till 2100, allowing a better understanding of the system evolution. The main limitation of these longer simulations is the very expensive computational demands of high-resolution hydrodynamic and ecological models. Thus, the improvement of the models' computational performance and, in particular of ECO-SELFE, should be explored in future research.

A real-time modelling approach and predictive capacity also constitutes a useful tool to support the management of estuarine ecosystems. Several water quality forecast systems have been proposed in the past (e.g. Lee et al., 2003; Kurunç *et al.*, 2005), but few were based on high-resolution, process-oriented models (e.g. http://ches.communitymodeling.org/models/ChesROMS/index.php; Baptista *et al.*, 2011). Nowcast-forecast water quality models allow: i) the continuous evaluation of the system behaviour; ii) to anticipate risk situations (e.g. eutrophication episodes, oxygen depletion); iii) to adapt the periodic monitoring strategies, as they cover broader spatial areas and temporal periods. In Portugal, these systems are still scarce and are mainly limited to the continental shelf and to the Tagus estuary. Combined with data allowing their continuous validation and improvement, and taking into account uncertainty as mentioned above (section VI.2.2), water quality and ecological high-resolution, process-oriented models, such as ECO-SELFE, can be used as operational tools for the long-term management of the Aveiro lagoon and of other estuarine ecosystems, in general.

REFERENCES

Alpine AE, Cloern JE. Phytoplankton growth rates in a light-limited environment, San Francisco Bay. *Marine Ecology - Progress Series* **1988**, 44, 167-173.

Arndt S, Lacroix G, Gypens N, Regnier P, Lancelot C. Nutrient dynamics and phytoplankton development along an estuary–coastal zone continuum: A model study. *Journal of Marine Systems* **2011**, 84(3-4), 49-66.

Ascough II JC, Maier HR, Ravalico JK, Strudley MW. Future research challenges for incorporation of uncertainty in environmental and ecological decision-making. *Ecological Modelling* **2008**, 219, 383-399.

Atkins KE, Travis JMJ. Local adaptation and the evolution of species' ranges under climate change. *Journal of Theoretical Biology* **2010**, 266(3), 449-457.

Baptista AM, Spitz YH, Needoba JA, Peterson TD, Zuber P, Herfort LM, Seaton CM, Cho KH, Welle P, Lopez JE. Collaboratory enabled ecological forecasts. Book of abstracts of ASLO Aquatic Sciences Meeting, **2011**, Puerto Rico.

Cabrita MT, Brotas V. Seasonal variation in denitrification and dissolved nitrogen fluxes in intertidal sediments of the Tagus estuary, Portugal. *Marine Ecology Progress Series* **2000**, 202, 51–65.

Fagherazzi S, Kirwan ML, Mudd SM, Guntenspergen GR, Temmerman S, D'Alpaos A, Koppel J, Rybczyk JM, Reyes E, Craft C, Clough J. Numerical models of salt marsh evolution: Ecological, geomorphic, and climatic factors. *Reviews of Geophysics* **2012**, 50, RG1002.

Fitzpatrick JJ. Assessing skill of estuarine and coastal eutrophication models for water quality managers. *Journal of Marine Systems* **2009**, 76, 195-211.

Gameiro C, Cartaxana P, Brotas V. Environmental drivers of phytoplankton distribution and composition in Tagus Estuary, Portugal. *Estuarine, Coastal and Shelf Science* **2007**, 75, 21-34.

Gameiro C, Zwolinski J, Brotas V. Light control on phytoplankton production in a shallow and turbid estuarine system. *Hydrobiologia* **2011**, 669,249–263.

Ji Z-G. *Hydrodynamics and water quality – Modeling rivers, lakes and estuaries*. Wiley, USA, **2008**.

Kurunç A, Yürekli K, Çevik O. Performance of two stochastic approaches for forecasting water quality and streamflow data from Yeşilırmak River, Turkey. *Environmental Modelling & Software* **2005**, 20(9), 1195-1200.

Lee JHW, Huang Y, Dickman M, Jayawardena AW. Neural network modelling of coastal algal blooms. *Ecological Modelling* **2003**, 159(2-3), 179-201.

Li Y, Brush MJ, Wang HV, Anderson IC, Sisson GM. Effects of benthic microalgae on eutrophication processes – a laboratory experiment and the model simulation. In: Estuarine and Coastal Modeling Conference Book, Proceedings of the Tenth International Conference, Ed.: Spaulding M, NY, ASCE, **2008**, 590-606.

Lohrer AM, Wetz JJ. Dredging-induced nutrient release from sediments to the water column in a southeastern saltmarsh tidal creek. *Marine Pollution Bulletin* **2003**, 46(9), 1156-1163.

Lopes CL, Silva PA, Dias JM, Rocha A, Picado A, Plecha S, Fortunato AB. Local sea level change scenarios for the end of the 21st century and potential physical impacts in the lower Ria de Aveiro (Portugal). *Continental Shelf Research* **2011**, 31(14), 1515-1526.

Lopes JF, Silva CI, Cardoso AC. Validation of a water quality model for the Ria de Aveiro lagoon, Portugal. *Environmental Modelling & Software* **2008**, 23, 479-494.

Luff R, Moll A. Seasonal dynamics of the North Sea sediments using a three-dimensional coupled sediment–water model system. *Continental Shelf Research* **2004**, 24(10), 1099-1127.

Najjar RG, Pyke CR, Adams MB, Breitburg D, Hershner C, Kemp M, Howarth R, Mulholland MR, Paolisso M, Secor D, Sellner K, Wardrop D, Wood R. Potential climate-change impacts on the Chesapeake Bay. *Estuarine, Coastal and Shelf Science* **2010**, 86(1), 1-20.

Oliveira A, Fortunato AB, Guerreiro M, Bertin X, Bruneau N, Rodrigues M, Taborda R, Andrade C, Silva AM, Antunes C, Freire P, Pedro LS, Dodet G, Loureiro C, Mendes A. Effect of inlet morphology and wave action on pollutant pathways and sediment dynamics in a coastal stream. Estuarine and Coastal Modeling - Proceedings of the Eleventh International Conference, Ed. Malcolm L. Spaulding, ASCE, **2010**, 601-620.

Park K, Jung H, Kim H, Ahn S. Three-dimensional hydrodynamic-eutrophication model (HEM-3D): application to Kwang-Yang Bay, Korea. *Marine Environmental Research* **2005**, 60(2), 171-193.

Pinto L, Fortunato AB, Zhang Y, Oliveira A, Sancho FEP. Development and validation of a three-dimensional morphodynamic modelling system for non-cohesive sediment. *Ocean Modelling*, in review.

Qu W, Morrison RJ, West RJ. Inorganic nutrient and oxygen fluxes across the sediment–water interface in the inshore macrophyte areas of a shallow estuary (Lake Illawarra, Australia). *Hydrobiologia* **2003**, 492 (1-3), 119-127.

Ragas AMJ, Etienne RS, Willemsen FH, Meent D. Assessing model uncertainty for environmental decision-making: a case study of the coherence of independently derived

environmental quality objectives for air and water. *Environmental Toxicology and Chemistry* **1999**, 18(8), 1856-1867.

Reay WG, Gallagher DL, Simmons GM. Sediment-water column oxygen and nutrient fluxes in nearshore environments of the lower Delmarva Peninsula, USA. *Marine Ecology Progress Series* **1995**, 118, 215-227.

Refsgaard JC, Sluijs JP, Højberg AL, Vanrollenghem PA. Uncertainty in the environmental modeling process – a framework and guidance. *Ecological Modelling & Software* **2007**, 22, 1543-1556.

Rehmann CR, Soupir ML. Importance of interactions between the water column and the sediment for microbial concentrations in streams. *Water Research* **2009**, 43(18), 4579-4589.

Rossa A, Liechti K, Zappa M, Bruen M, Germann U, Haase G, Keil C, Krahe P. The COST 731 action: a review of uncertainty propagation in advanced hydro-meteorological forecast systems. *Atmospheric Research* **2011**, 100(2-3), 150-167.

Sano M, Golshani A, Splinter KD, Strauss D, Thurston W, Tomlinson R. A detailed assessment of vulnerability to climate change in the Gold Coast, Australia. *Journal of Coastal Research* **2011**, SI 64, 245-249.

Simon NS. Nitrogen cycling between sediment and the shallow-water column in the transition zone of the Potomac River and estuary. I. Nitrate and ammonium fluxes. *Estuarine, Coastal and Shelf Science* **1988**, 26(5), 4083-497.

Trancoso AR, Saraiva S, Fernandes L, Pina P, Leitão P, Neves R. Modelling macroalgae using a 3D hydrodynamic-ecological model in a shallow, temperate estuary. *Ecological Modelling* **2005**, 187, 232–246.

Yates ML, le Cozannet G, Lenôtre N. Quantifying errors in long-term coastal erosion and inundation hazard assessments. *Journal of Coastal Research* **2011**, SI64, 260-264.

APPENDIX I
FIELD WORK DATA AND MONITORING STATIONS PHOTOS

AI.1 INTRODUCTION

This appendix presents some photos of the sampling stations and the complete set of the data collected during the dedicated field campaigns (March 2009, September 2009 and January 2010).

AI.2 MONITORING STATIONS PHOTOS

Samplings of physical, chemical and biological parameters were performed at four stations located along the Mira channel, namely stations EM1, EM2 and EM3 (Figure AI.1-Figure AI.3) and station EB (boat near Costa Nova). The main rivers, flowing into the Aveiro lagoon were also sampled: Poço da Cruz (Mira), Ouca (Boco), Angeja (Vouga), Estarreja (Antuã) and Ribeira-Ovar (Caster) – Figure AI.4.

Figure AI.1. Station EM1: Ponte do Areão.

Figure AI.2. Station EM2: Ponte da Vagueira.

Figure AI.3. Station EM3: Navio-Museu.

Figure AI.4. Riverine stations.

AI.3 DATA COLLECTED

The data collected during the field campaigns is presented in sections AI3.1 to AI3.10. At stations EM1 (Ponte do Areão), EM2 (Ponte da Vagueira) and EM3 (Navio-Museu) data was collected at two depths: bottom and surface. At stations EM1 and EM2 measurements were done about 20 cm below surface and about 20 cm above bottom. At station EM3 measurements were done about 20 cm and 5 m below surface. At station EB three depths were sampled: surface (about 20 cm below surface), mid-depth (about 1 m below surface) and bottom (about 2-3 m below surface). All data is presented at Portugal legal time (winter period: UTC; summer period: UTC+1 hour).

AI.3.1 Water Levels Variation

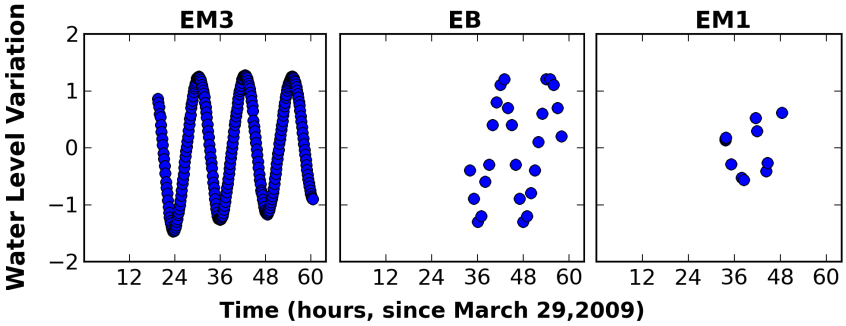

Figure AI.5. Water levels variation along the Mira channel: March 2009.

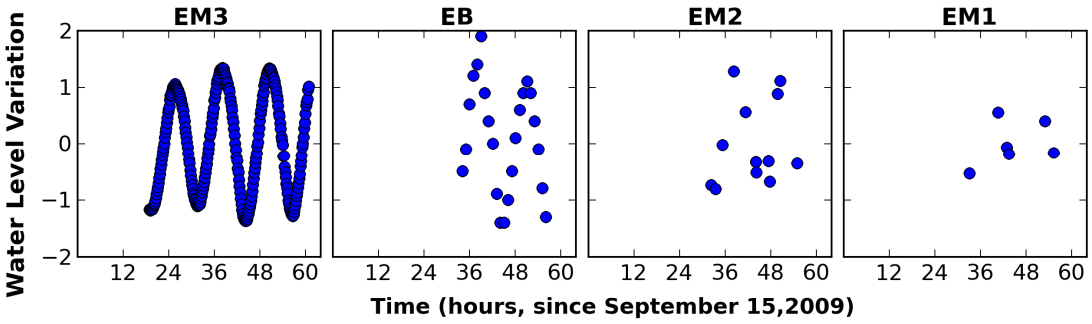

Figure AI.6. Water levels variation along the Mira channel: September 2009.

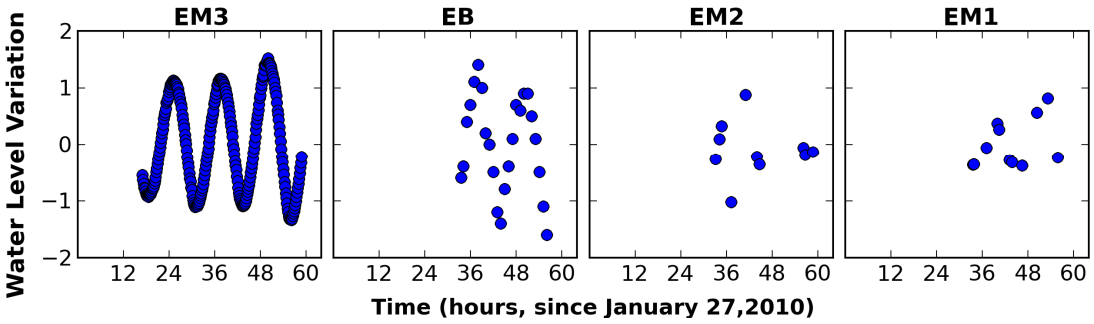

Figure AI.7. Water levels variation along the Mira channel: January 2010.

AI.3.2 Current Velocity

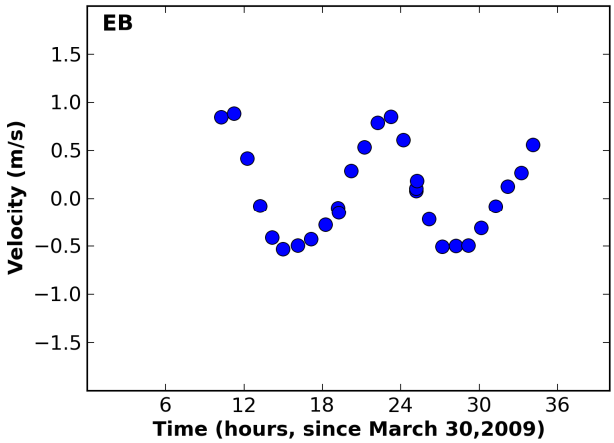

Figure AI.8. Current velocity at EB station (positive values represent flood and negative values represent ebb): March 2009.

AI.3.3 Salinity

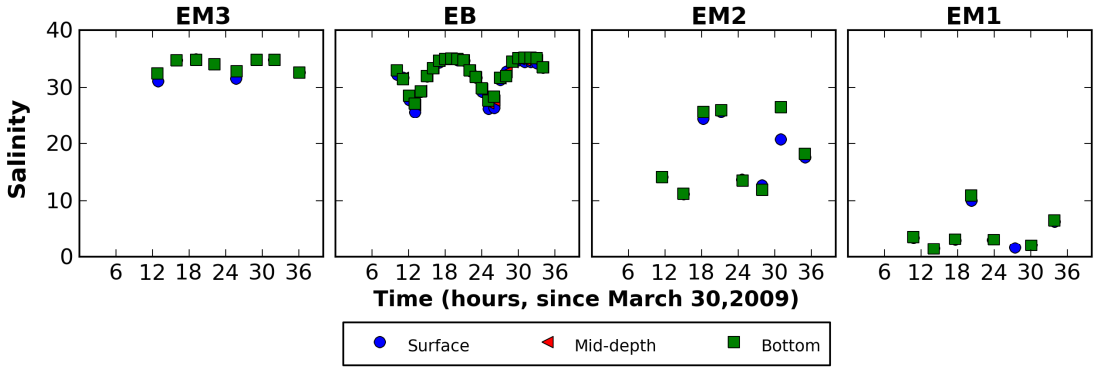

Figure AI.9. Salinity along the Mira channel: March 2009.

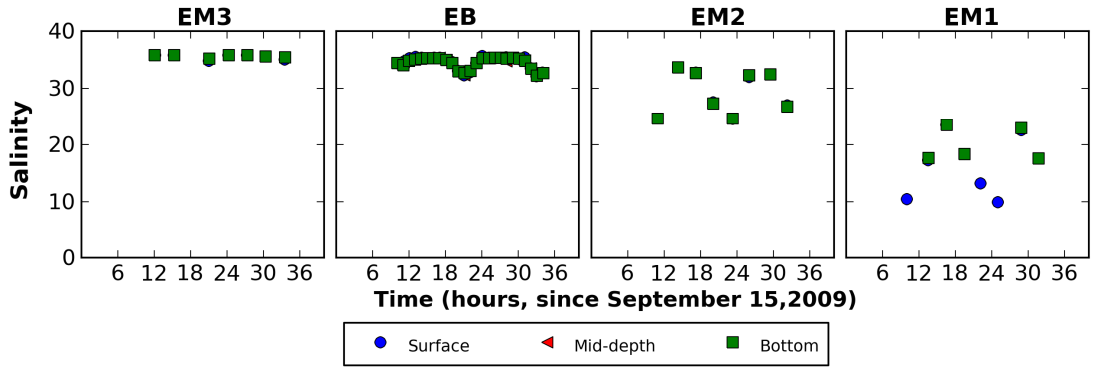

Figure AI.10. Salinity along the Mira channel: September 2009.

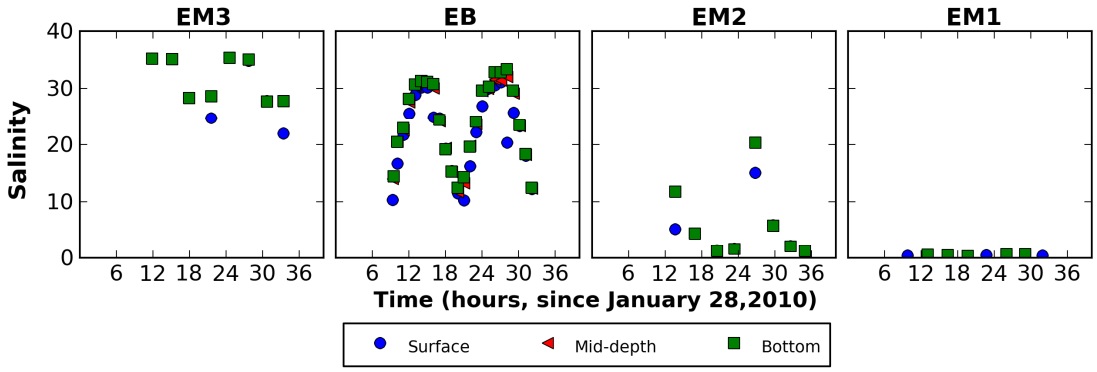

Figure AI.11. Salinity along the Mira channel: January 2010.

AI.3.4 Water Temperature

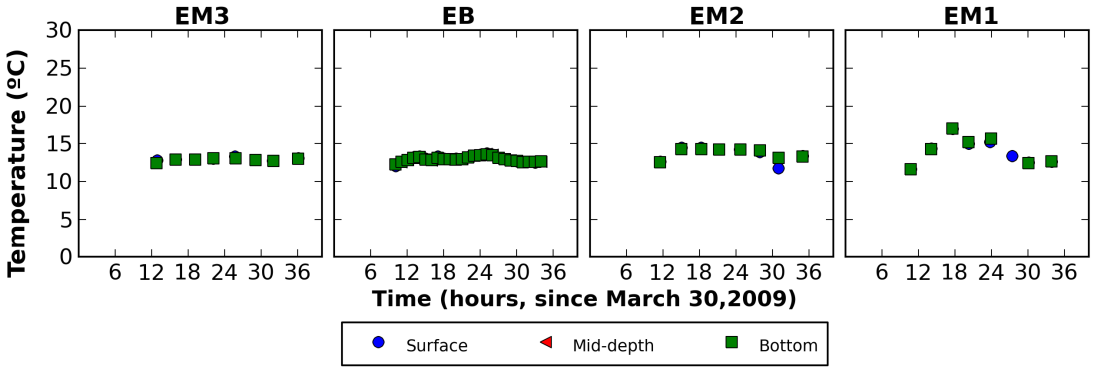

Figure AI.12. Water temperature along the Mira channel: March 2009.

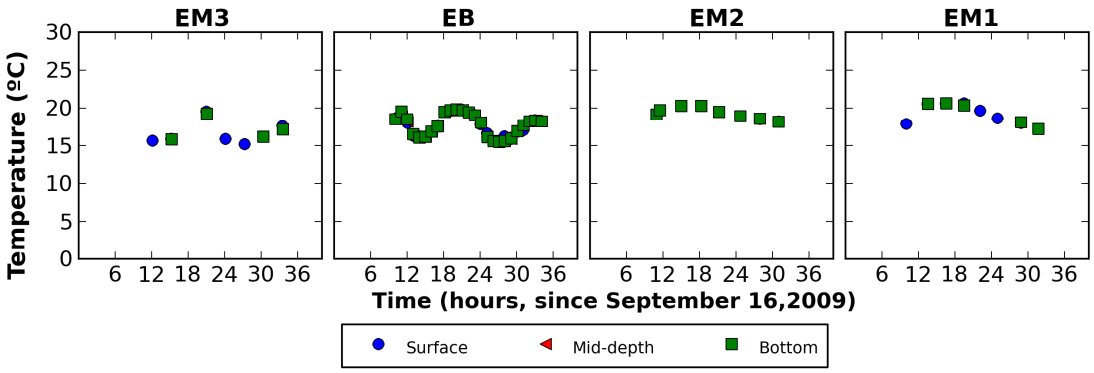

Figure AI.13. Water temperature along the Mira channel: September 2009.

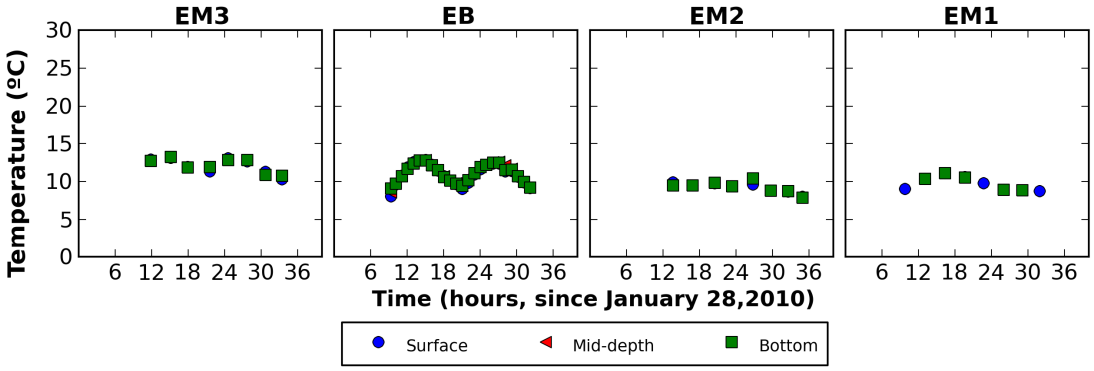

Figure AI.14. Water temperature along the Mira channel: January 2010.

AI.3.5 Chlorophyll *a*

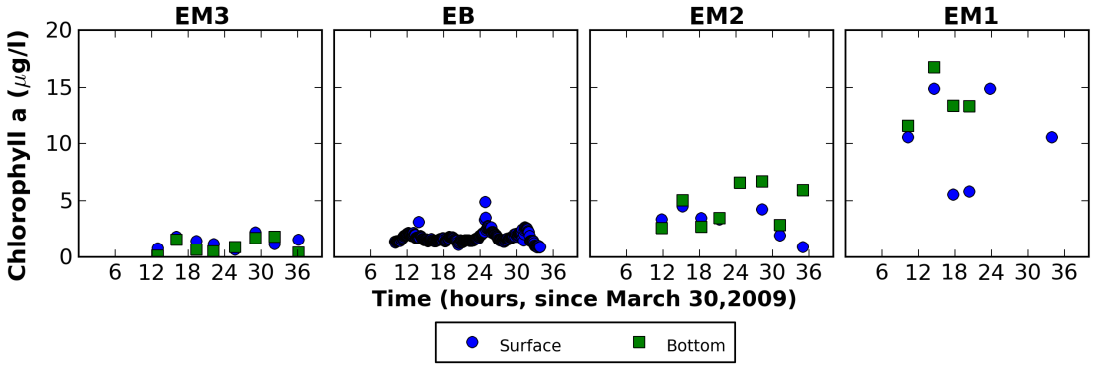

Figure AI.15. Chlorophyll *a* concentration along the Mira channel: March 2009.

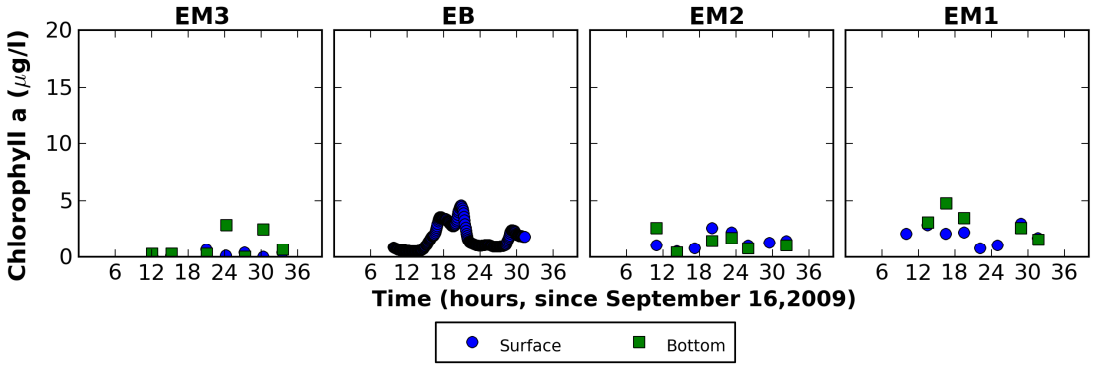

Figure AI.16. Chlorophyll *a* concentration along the Mira channel: September 2009.

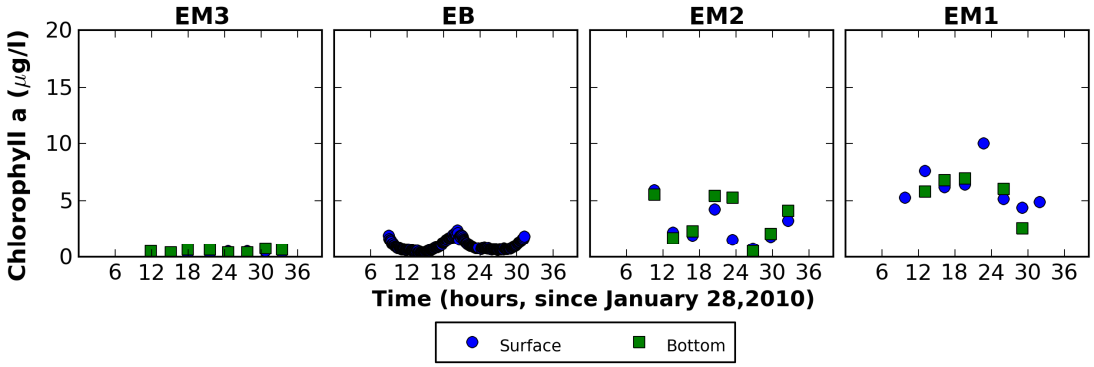

Figure AI.17. Chlorophyll *a* concentration along the Mira channel: January 2010.

AI.3.6 Dissolved Oxygen

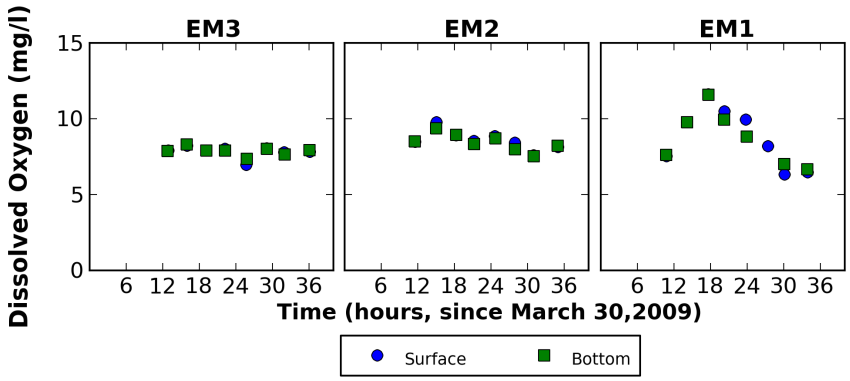

Figure AI.18. Dissolved oxygen concentration along the Mira channel: March 2009.

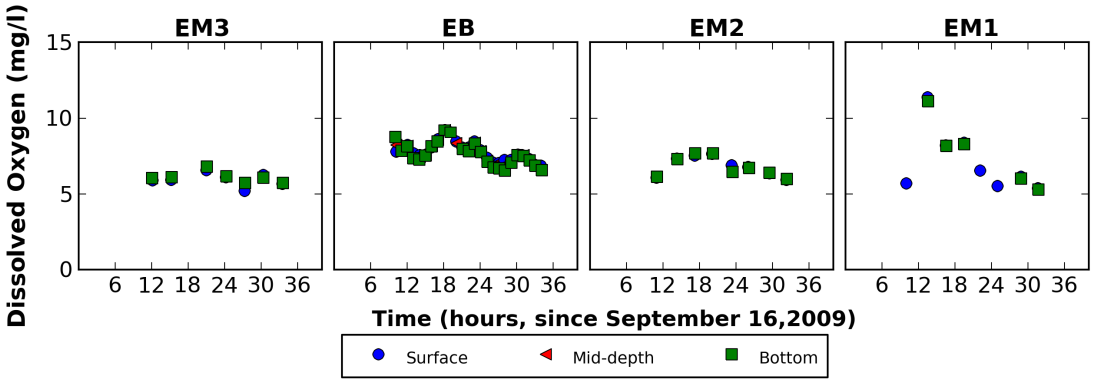

Figure AI.19. Dissolved oxygen concentration along the Mira channel: September 2009.

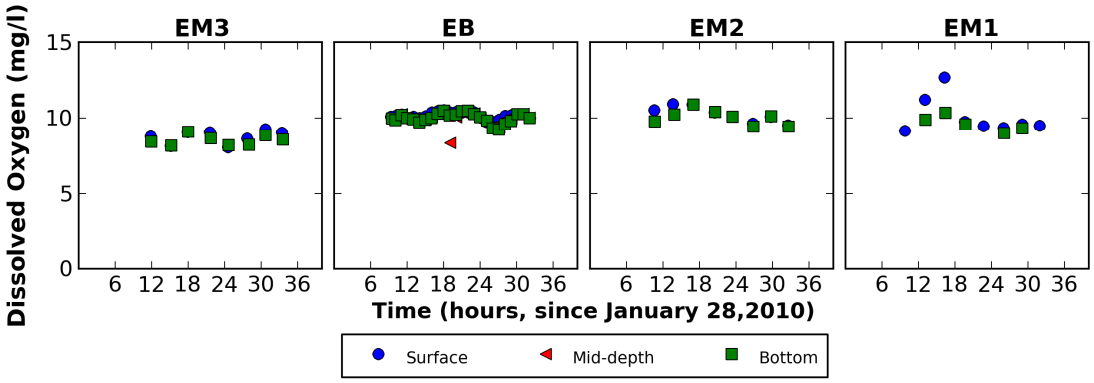

Figure AI.20. Dissolved oxygen concentration along the Mira channel: January 2010.

AI.3.7 Ammonium (NH_4^+)

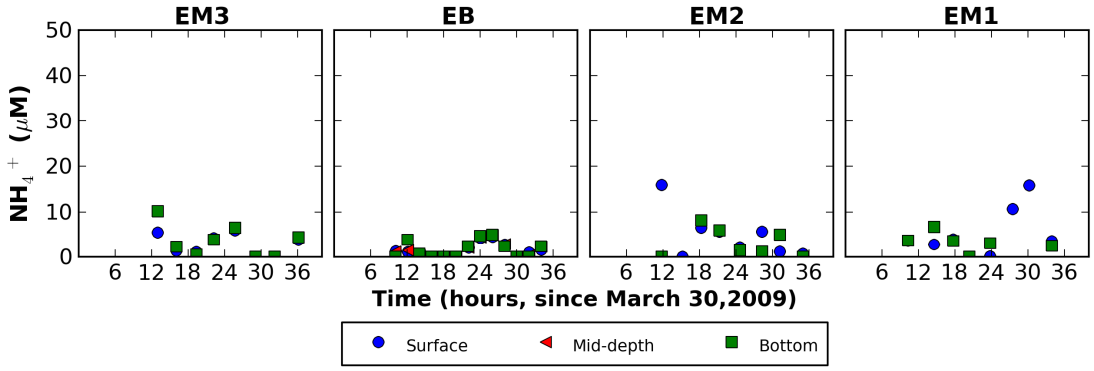

Figure AI.21. Ammonium concentration along the Mira channel: March 2009.

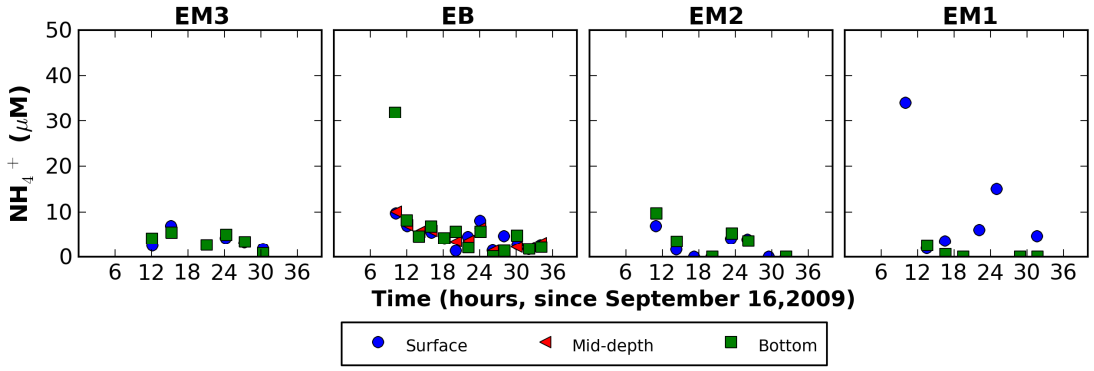

Figure AI.22. Ammonium concentration along the Mira channel: September 2009.

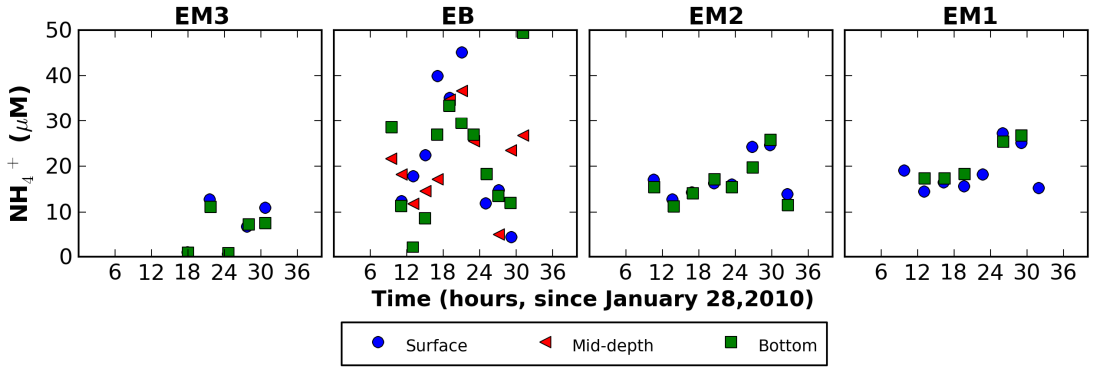

Figure AI.23. Ammonium concentration along the Mira channel: January 2010.

AI.3.8 Nitrates + nitrites (NO_3^-+NO_2^-)

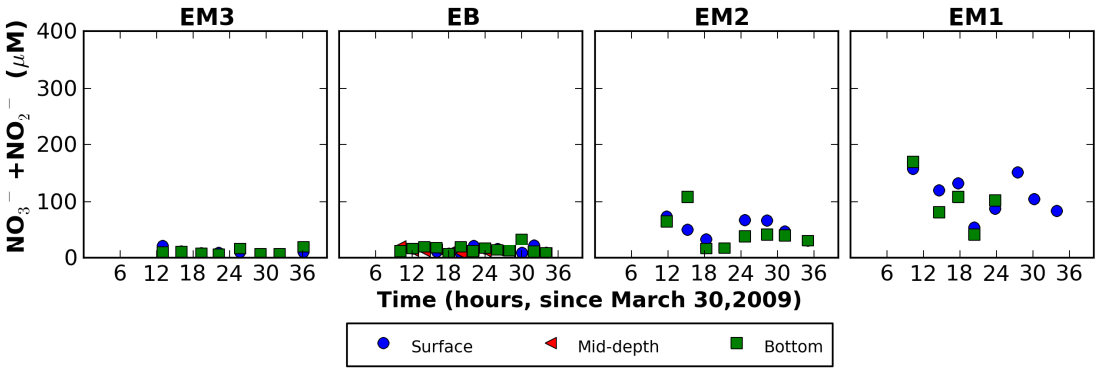

Figure AI.24. Nitrates + nitrites concentration along the Mira channel: March 2009.

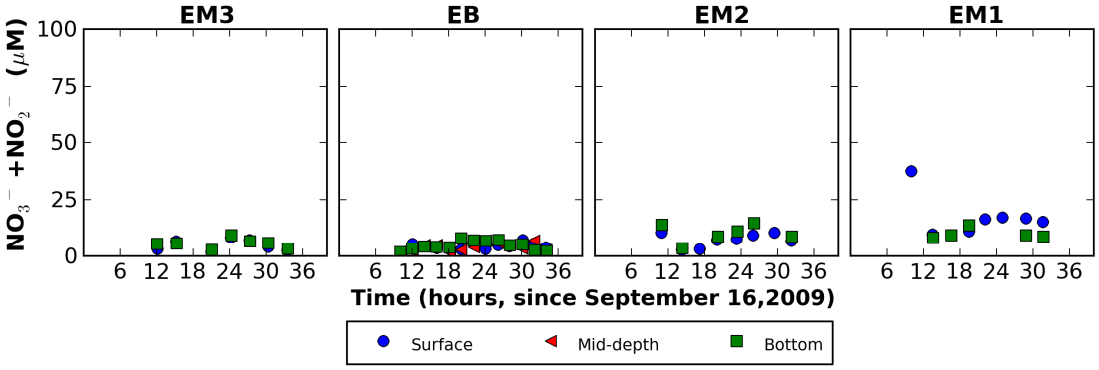

Figure AI.25. Nitrates + nitrites concentration along the Mira channel: September 2009.

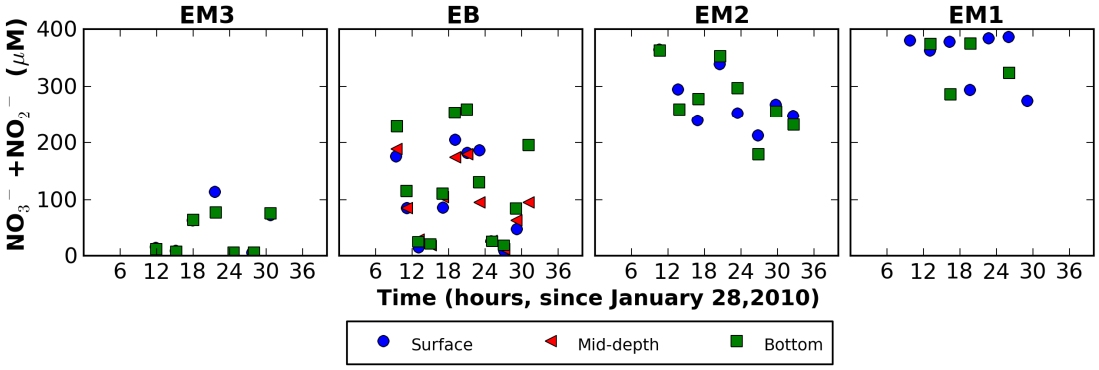

Figure AI.26. Nitrates + nitrites concentration along the Mira channel: January 2010.

AI.3.9 Phosphates (PO_4^{3-})

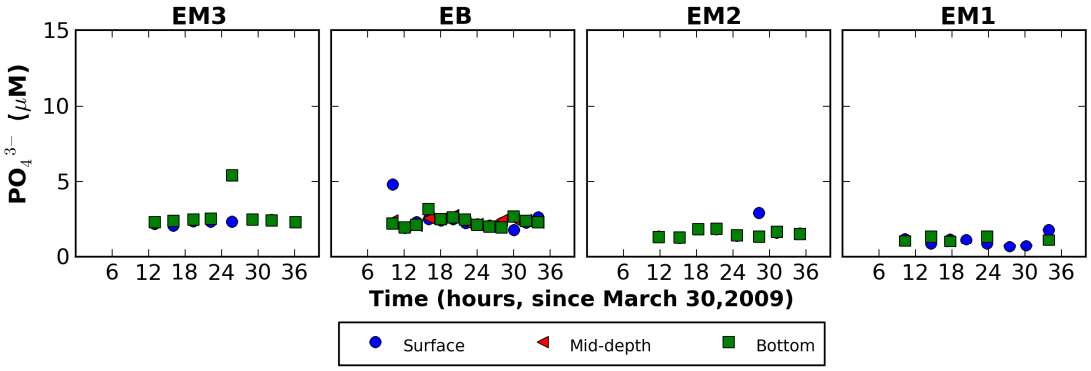

Figure AI.27. Phosphates concentration along the Mira channel: March 2009.

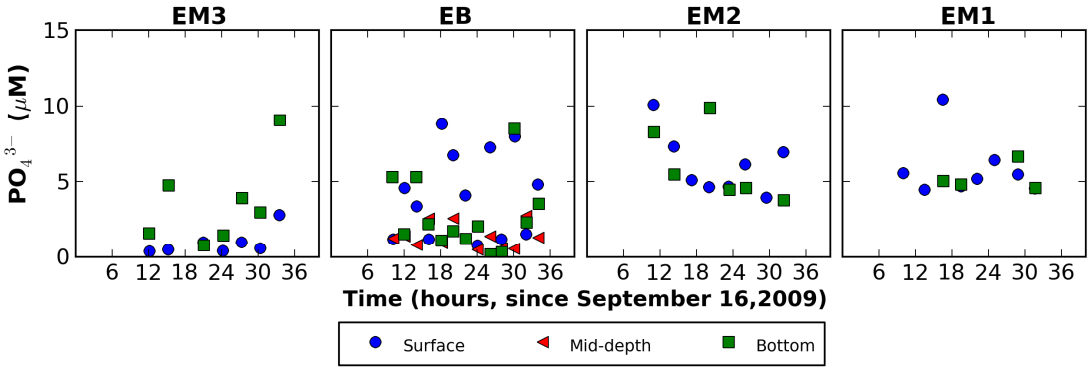

Figure AI.28. Phosphates concentration along the Mira channel: September 2009.

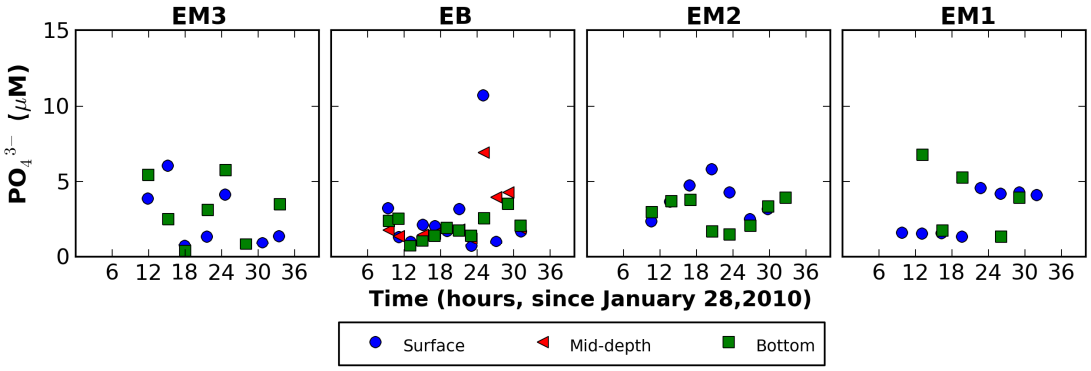

Figure AI.29. Phosphates concentration along the Mira channel: January 2010.

AI.3.10 Silicates (SiO_2)

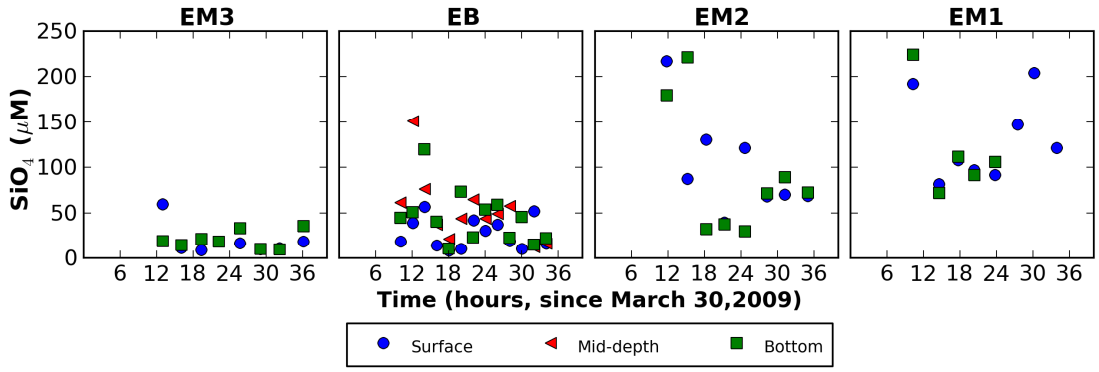

Figure AI.30. Silicates concentration along the Mira channel: March 2009.

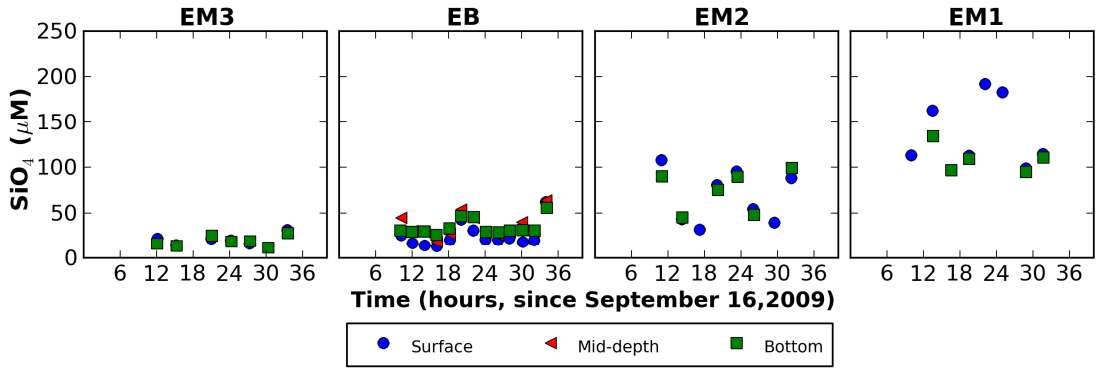

Figure AI.31. Silicates concentration along the Mira channel: September 2009.

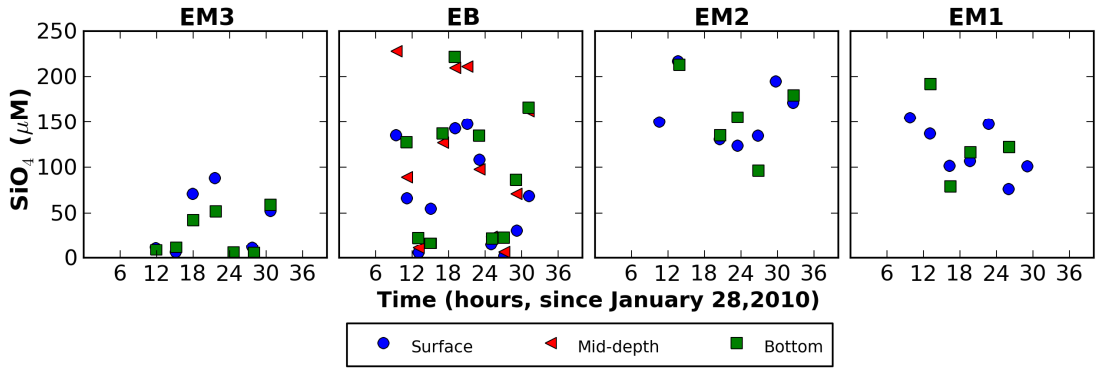

Figure AI.32. Silicates concentration along the Mira channel: January 2010.

AI.3.11 Riverine measurements

Table AI.1. River flows measured during the field campaigns.

	River Flow (m^3/s)		
	March 30, 2009	September 16, 2009	January 28, 2010
Mira	0.7	0.1	3.5
Boco	0.2	-	0.5
Vouga	32.0	-	39.0
Antuã	2.6	0.3	6.4
Caster	0.9	0.4	0.8

Table AI.2. Water properties measured at the riverine stations: March 30, 2009 (S – Salinity; T – Water temperature; DO – dissolved oxygen; Chl *a* – Chlorophyll *a*; NH_4^+ – Ammonium; NO_3^-+NO_2^- – Nitrates + Nitrites; PO_4^{3-} – Phosphates; SiO_2 – Silicates).

	Time	S	T (ºC)	DO (mg/l)	Chl *a* (µg/l)	NH_4^+ (µM)	NO_3^- +NO_2^- (µM)	PO_4^{3-} (µM)	SiO_2 (µM)
Mira	12:00	0.2	13.9	11.4	18.7	15.8	161.4	0.6	112.5
Boco	13:58	0.2	10.6	10.5	0.1	5.5	257.7	0.0	81.4
Vouga	15:40	0.1	13.7	11.6	4.0	1.7	76.0	0.3	124.4
Antuã	17:30	0.2	13.0	9.1	0.3	118.7	385.4	3.4	55.3
Caster	18:55	0.1	13.1	8.8	0.3	144.6	341.9	3.7	134.8

Table AI.3. Water properties measured at the riverine stations: September 16, 2009 (S – Salinity; T – Water temperature; DO – dissolved oxygen; Chl *a* – Chlorophyll *a*; NH_4^+ – Ammonium; NO_3^-+NO_2^- – Nitrates + Nitrites; PO_4^{3-} – Phosphates; SiO_2 – Silicates).

	Time	S	T (ºC)	DO (mg/l)	Chl *a* (µg/l)	NH_4^+ (µM)	NO_3^- +NO_2^- (µM)	PO_4^{3-} (µM)	SiO_2 (µM)
Mira	10:30	0.3	18.4	5.3	1.2	33.8	-99.0	18.1	70.6
Boco	-	-	-	-	-	-	-	-	-
Vouga	12:50	0.2	22.2	7.6	1.9	12.7	115.4	1.0	79.8
Antuã	15:00	0.0	18.2	8.6	0.8	16.8	615.8	0.6	173.2
Caster	16:15	0.2	19.9	7.3	1.0	400.2	1031.8	13.4	259.0

Table AI.4. Water properties measured at the riverine stations: January 28, 2010 (S – Salinity; T – Water temperature; DO – dissolved oxygen; Chl *a* – Chlorophyll *a*; NH_4^+ – Ammonium; NO_3^-+NO_2^- – Nitrates + Nitrites; PO_4^{3-} – Phosphates; SiO_2 – Silicates).

	Time	S	T (ºC)	DO (mg/l)	Chl *a* (μg/l)	NH_4^+ (μM)	NO_3^- +NO_2^- (μM)	PO_4^{3-} (μM)	SiO_2 (μM)
Mira	10:35	0.2	9.4	10.0	41.4	18.9	280.6	1.3	148.4
Boco	12:33	0.2	7.5	11.6	0.3	12.7	-	1.0	-
Vouga	14:45	0.1	9.0	11.3	0.5	7.7	216.0	0.9	42.9
Antuã	15:55	0.1	10.0	10.8	0.1	33.5	635.0	1.3	35.3
Caster	17:15	0.1	11.2	10.4	0.1	101.4	850.2	1.8	102.1

APPENDIX II

VALIDATION OF THE ECO-SELFE OXYGEN MODULE IN A SMALL COASTAL STREAM

AII.1 INTRODUCTION

The new formulation for the oxygen cycle implemented in the ECO-SELFE model was preliminarily validated in a small coastal stream (the Aljezur coastal stream, Southwest coast of Portugal), taking advantage of a set of data collected synoptically in this stream in the scope of the FCT-funded project MADyCOS (PTDC/ECM/66484/2006). This preliminary validation of the model in a different coastal system also contributes to show its applicability in other coastal and estuarine systems. However, the main goal of this application was to perform a preliminary validation of the implemented formulation for the oxygen cycle in a real system and, therefore, an extensive calibration and validation of ECO-SELFE in the Aljezur was not performed. Next sections describe briefly the study area, the field campaigns and the implementation of the model in the Aljezur coastal stream. Finally, section AII.5 presents and discusses the results for the field campaign of May 2008.

AII.2 STUDY AREA

The Aljezur stream, located in the southwest coast of Portugal (Figure AII.1A), has a high economic (tourism, aquaculture) and ecological importance. It is located within an environmentally protected area (*Southwest Alentejano and Costa Vicentina Natural Park*) and is part of the Natura 2000 classified network.

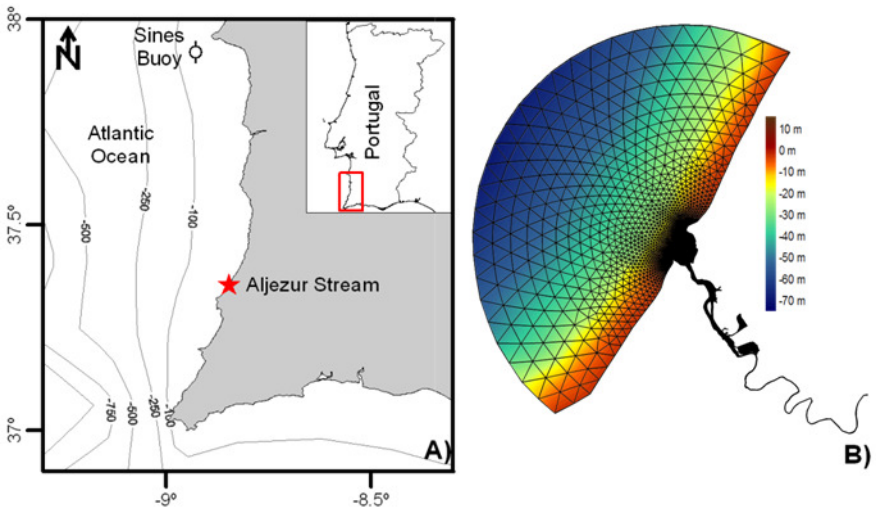

Figure AII.1. Aljezur coastal stream: A) location and B) horizontal grid (bathymetry, in meters, relative to MSL).

This coastal stream is about 34 km long (MAOT, 2000), 10-40 m wide and 1-3 m deep close to the mouth, where it reaches the Atlantic Ocean (Amoreira-sea beach). The stream's dynamics is challenging from a physical viewpoint, as it is strongly influenced by the combined effect of tides, waves, rivers flows and winds (Oliveira *et al.*, 2011; Rodrigues *et al.*, 2011). Its downstream end is tidal flood-dominated, presenting a brackish environment, with ebbs being significantly longer than floods. The yearly mean significant wave height is about 2 m, with waves predominantly from the NW/SW. The basin's drainage area is about 184 km^2 (Gama-Pereira, 2005). The stream is close to ephemeral, with almost no freshwater flow in the dry season, when it is dominated by the wastewater discharge and other urban sources, and with torrential flows during the rainy periods (Jacob *et al.*, 2010). Moreover, the stream's inlet also displays a significant morphological variability, as a result of the relative importance of tides, waves and river flows (Guerreiro, 2010), with occasional closures. Accordingly, it is not considered a real estuary, but a transition system (Gama-Pereira, 2005) that from an ecological point of view can be classified as a lagoon-estuarine environment (Fidalgo e Costa, 2003).

The basin land-use types are predominantly forest and agriculture. Artificial surfaces only occupy ca. 1% of the total area. The sanitary quality of its water is of key importance. In addition to being used for recreational activities, its downstream end is intensively used for bathing (Amoreira-river beach). The potential sources of water pollution are agriculture, farm animals, including swine farms and free-grazing cows, the Aljezur village, the wastewater treatment plant effluent and septic tanks from farms and dispersed houses.

AII.3 FIELD CAMPAIGNS

Five field surveys were undertaken to provide a preliminary understanding of the dependence of the hydrodynamics, fecal contamination and morphology in the Aljezur coastal stream on the river flow, tidal amplitude, wave regime and pollutant discharge characteristics. The field campaigns were carried out in May 6, 2008 (spring tide, end of maritime winter), September 11, 2008 (neap tide, end of maritime summer), May 12, 2009 (mean tide, end of maritime winter), September 8, 2009 (spring tide, end of maritime summer), and September 9, 2010 (spring tide, end of maritime summer). The preliminary validation of the oxygen formulation implemented in ECO-SELFE was performed with the May 2008 set of data, since only the 2008 field surveys had been undertaken at the date of this preliminary application. Synoptic measurements were performed during a tidal cycle (13 hours) at several stations distributed along 8 km in the stream (Figure AII.2). This set of field surveys included physical, chemical and biological parameters. The bathymetries of the inlet and beach were measured at each campaign using two Differential GPS (Topcon and Leica 1200). Tidal levels and wave heights were measured using graduate rulers and pressure sensors (LevelTroll 500, miniTroll, Infinity) with intervals that range from 30

minutes to 0.5 seconds. Current velocities were measured with intervals of 1 hour at stations 9 and 11, using two electromagnetic current meters and floats. Salinity, temperature and dissolved oxygen concentrations were measured every 30 minutes with probes (YSI 6820, YSI 556 and WTW) that were previously calibrated against standard solutions and inter-calibrated in the laboratory for stream water samples. Four water samples were collected below surface (~20-30 cm depth) at high and low water as well as at mid-ebb and mid-flood, at 10 different stations. In May 2008, these stations included the boundary stations (1A and 1B) upstream, the sewage treatment plant (station 2), the recreational area of the river and sea beaches (stations 8A, 9 and 17) and 2 stations along the stream (stations 5 and 7). Samples were analyzed for chlorophyll *a*, ammonium (NH_4^+), nitrates + nitrites (NO_3^-+NO_2^-), phosphates (PO_4^{3-}), silicates (SiO_2), fecal coliforms, fecal enterococcus, BOD_5 and total suspended solids, as described in Cravo *et al.* (2010). Sediment samples were also collected at the bed for grain size characterization.

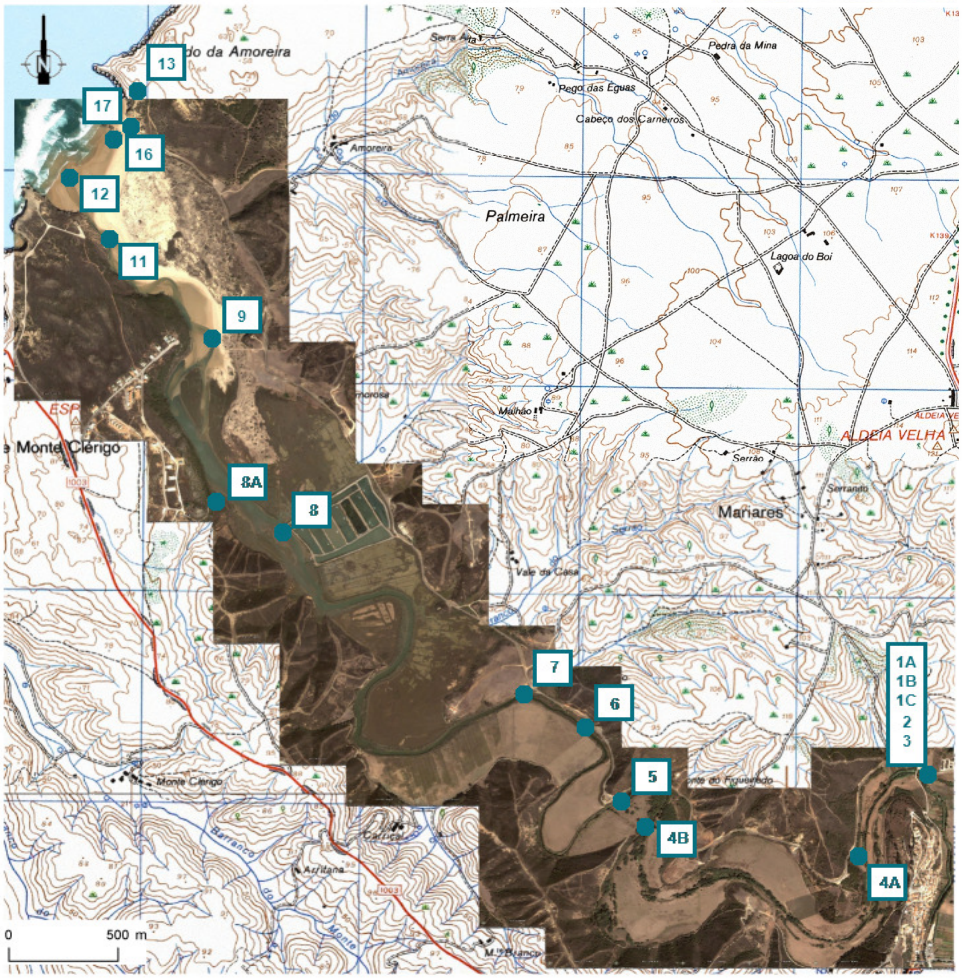

Figure AII.2. Location of the sampling stations along the Aljezur coastal stream.

AII.4 MODEL SETUP

The simulation was performed for a period of 12 days, starting 10 days before the field survey of May 2008 and allowing 2 days for spin-up. The horizontal domain was discretized with an unstructured grid with 41000 nodes, extending about 5 km into the coastal zone and 10 km from the inlet up to the upstream boundary (Figure AII.1B). The spatial resolution varies from 450 m in the coastal area to 2 m in the stream. The vertical domain was discretized using 11 equally spaced vertical *S* levels, since the stream is shallow. The bathymetry of the inlet was updated, based on the field surveys measurements done during the campaign (Figure AII.3). A spatially varying bottom roughness coefficient was used. The spatial variation of this parameter was set based on the characteristics of the bottom sediments present in the stream, which are mostly sandy in the lower estuary, with very significant bedforms, and a mixture of cohesive and non-cohesive sediments in the upper estuary (Freire *et al.*, 2011). The Generic Length Scale KKL turbulence closure scheme, with the Kantha & Clayson's stability function, was used. The time step was set to 5 seconds.

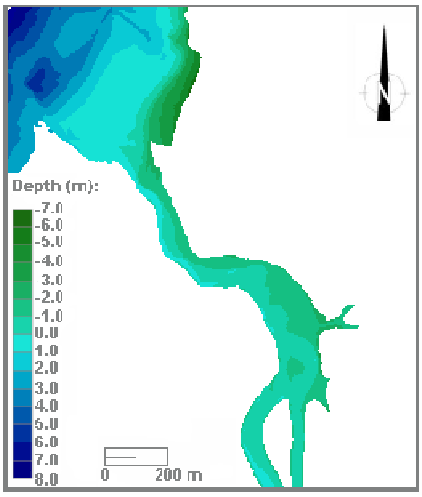

Figure AII.3. Bathymetry of the Aljezur coastal stream inlet in May 2008 (meters, MSL).

Two open boundaries were considered. At the ocean boundary the model was forced by tidal elevations from the regional model of Fortunato *et al.* (2002). Eleven tidal constituents were used: Z0, MSF, M2, S2, K2, N2, O1, K1, M4, MN4 and MS4. The effect of wave set-up and atmospheric pressure was parameterized through the Z0 constituent and was based on the results of the application of the morphodynamic model MORSYS2D to the Aljezur coastal stream (Oliveira *et al.*, 2010; Guerreiro, 2010). The river boundary was forced by a constant river flow of 0.15 $m^3 s^{-1}$, which was estimated based on water level and velocity measurements at the inflow boundary on the day of the campaign.

The temperature dynamics was simulated using the surface heat exchange model from Zheng *et al.* (1998). Based on the availability of data and information for the period of the simulation, several sources were considered for the atmospheric forcing: NCEP Reanalysis Data (http://www.esrl.noaa.gov/psd/), GFS model results (http://www.windguru.cz), SNIRH: *Sistema Nacional de Informação de Recursos Hídricos* database (http://snirh.pt) and data from the port of Sines.

Initial conditions for salinity were set to decrease from 36 in the coastal area to 0 at the river boundary. Salinity was set constant in time at both boundaries. Similarly, spatially varying initial conditions for temperature were used. The ocean boundary temperature was forced with data from the Sines's buoy (http://www.hidrografico.pt/). The river boundary temperature forcing was based on daily variation of the data measured at Station 3 during the field survey.

A detailed and extensive calibration and validation of the hydrodynamic model is presented by Rodrigues *et al.* (2011). The comparison between the hydrodynamic model predictions and the data for each station and variable was done using the relative mean average error (RMAE):

$$RMAE_i = \frac{1}{\overline{O}_{j,i}} \frac{1}{N} \sum_{n=1}^{N} \left| O_{j,i,n} - P_{j,i,n} \right| \qquad \text{(AII.1)}$$

where *i* is a given station, *j* is a given variable (water level, velocity, salinity and temperature), *n* is a given observation, *N* is the number of observations for each station and variable, *O* is the observed value and *P* is the predicted value.

Results show the ability of the model to represent the main circulation patterns and physical properties (salinity and temperature) along the stream (Figure AII.4 and Figure AII.5). Water level errors are of about 2-5%, velocity errors are about 13-16 cm s^{-1} (20-40%) and, generally, salinity and temperature errors are of 3% and 2-5%, respectively.

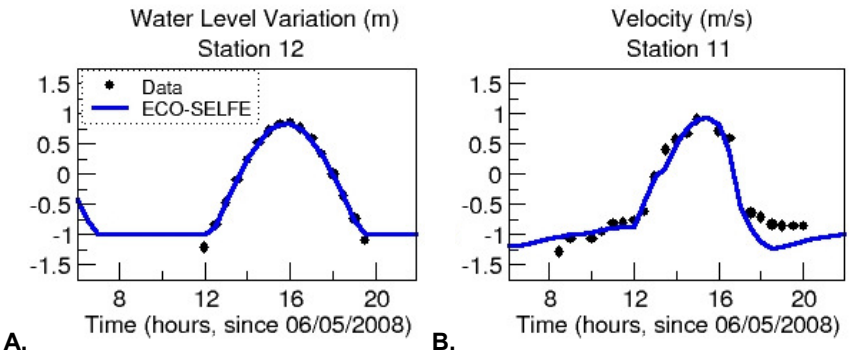

Figure AII.4. Comparison between data and model results along the tidal cycle: A) water level variation in station 12 and B) velocity in station 11 (positive values represent flood).

For the ecological tracers, initial conditions were set based on the average values of the variables measured during the 2008 field campaigns. The initial conditions for the other ecological variables were set as described in Rodrigues *et al.* (2009). At river and ocean boundaries, values for the variables measured during the field campaigns were derived from the measurements at station 3 and station 17, respectively. For the other variables the criteria used were similar to the ones adopted by Rodrigues *et al.* (2009). In this simulation only one phytoplankton group (diatoms) and one zooplankton group (copepods) were considered. Input parameters of the ecological model were set as presented in Rodrigues *et al.* (2009). The input parameters for the oxygen cycle processes added to the model are presented in Table III.3.1. The phytoplankton basal specific respiration rate considered in this simulation is 0.01 day^{-1}. The increase in the dissolved oxygen saturation concentration due to the wind was not considered.

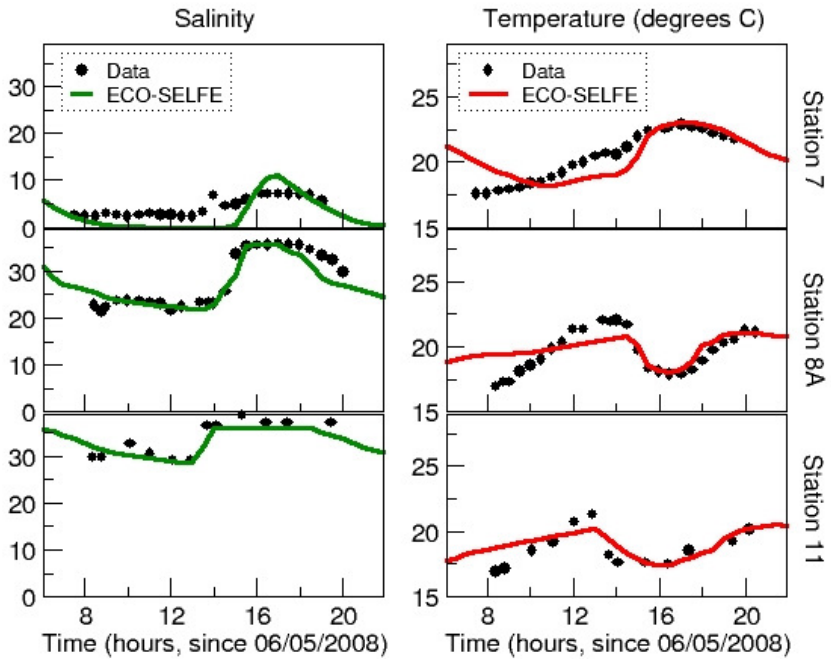

Figure AII.5. Comparison between data and model results along the tidal cycle: salinity and temperature variation in stations 7, 8A and 11.

AII.5 RESULTS AND DISCUSSION

The dissolved oxygen concentration along the Aljezur coastal stream in May 6, 2008 is presented in Figure AII.6. Results show the ability of ECO-SELFE to represent the variation of the dissolved oxygen along the tidal cycle with differences generally smaller than 1 mg l^{-1}. The exception is the variation of dissolved oxygen in station 7. Dissolved oxygen concentrations at this station present a larger range of variation during the tidal cycle (6-12.38 mg l^{-1}) than at the

other stations, a behavior that the model is able to represent. However, the model tends to overestimate dissolved oxygen concentrations at this station, with differences larger than 1 mg l^{-1}, in particular in early morning and early night.

At station 7, during the May 2008 field survey, chlorophyll *a* reached significantly large concentrations (average value of 96 μg l^{-1}; maximum value of 195 μg l^{-1}), which the model fails to represent (Figure AII.7). Cravo *et al.* (2010) suggested that these concentrations are associated with cyanobacteria, since silicates did not present concomitant variations. Thus, this may lead to the differences observed in station 7 for chlorophyll *a,* since diatoms were the only phytoplankton group simulated. Due to the interdependence between the variables and the ecological processes, this difference may also affect dissolved oxygen at this station. At the other stations, where differences between observed and simulated dissolved oxygen concentrations are smaller, ECO-SELFE provides a better representation of the observed chlorophyll *a* concentration with differences between the average values smaller than 1-2 μg l^{-1} (Figure AII.7A).

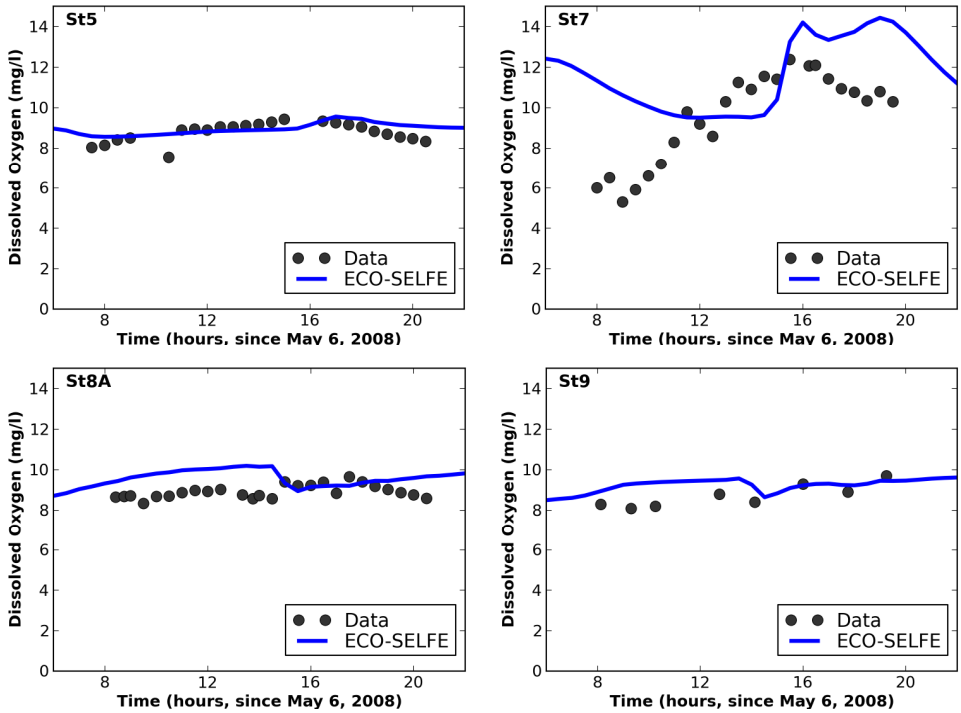

Figure AII.6. Dissolved oxygen concentration along the Aljezur coastal stream in May 2008: comparison between data and model results during the tidal cycle.

This interdependence between the ecological processes and variables is a fundamental and complex aspect in the establishment and evaluation of this type of models in real systems. Thus, nutrients concentrations should also be taken in account in this analysis. Results suggest

that the model is able to represent the main patterns observed along the stream, although it tends to underestimate ammonium and phosphate concentrations with differences of about 1 μM (Figure AII.8). These differences may also derive from additional sources that were not included in the model (e.g. diffuse sources from agriculture and cattle pastures).

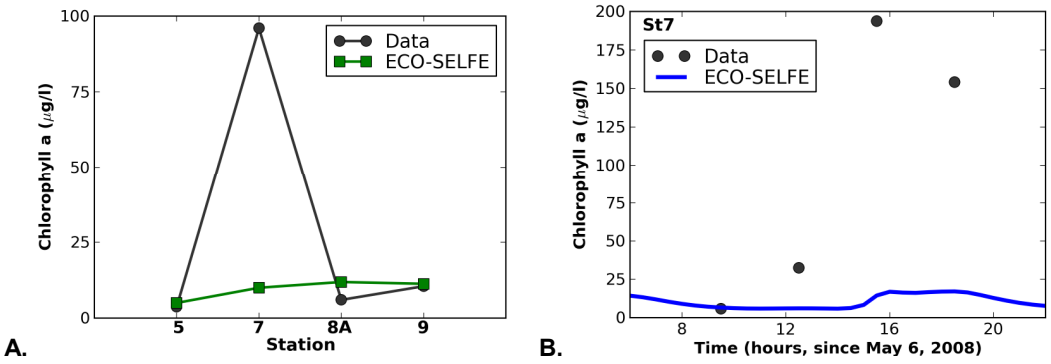

Figure AII.7. Comparison between data and model results of chlorophyll *a* concentration in May 2008: A) average values along the Aljezur coastal stream and B) variation during the tidal cycle in station 7.

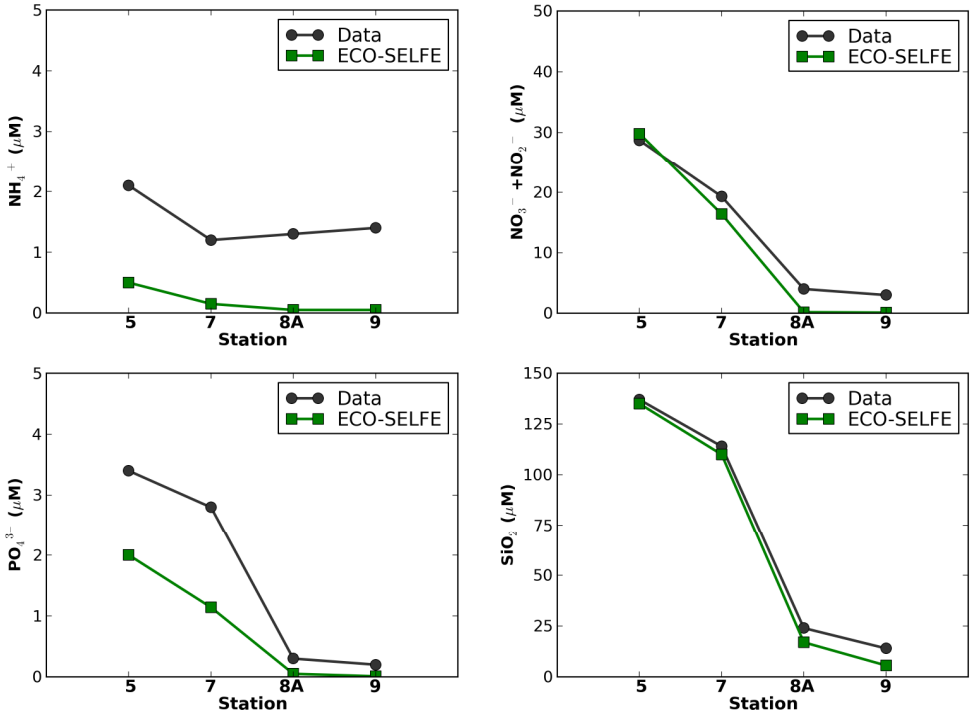

Figure AII.8. Nutrients (NH_4^+ - ammonium; NO_3^-+NO_2^- - nitrates + nitrites; PO_4^{3-} - phosphates; SiO_2 - silicates) average values along the Aljezur coastal stream in May 6, 2008: comparison between data and model results.

Another fundamental factor that may contribute to the differences observed between the data and the model results is parameterization used for the ecological model, since an intensive calibration procedure was not undertaken because the main goal of this application was to preliminarily validate the new formulation for the oxygen cycle implemented in ECO-SELFE in a real system. Thus, a more detailed calibration of the ecological model could contribute to improve the model results.

Overall, and considering the main goal of this preliminary application of ECO-SELFE to the Aljezur coastal stream, results show the ability of the new formulation implemented in the model to represent dissolved oxygen concentrations in a real system. It should however be mentioned that a more detailed application of this model in this coastal stream must account for a further exploitation of the ecological model parameterization, which will allow a more robust validation of ECO-SELFE in this system.

AII.6 REFERENCES

Cravo A, Menaia J, Napier V. A qualidade da água da ribeira de Aljezur, SW Portugal: seus efeitos nas águas balneares. 14º ENaSB /SILUBESA Encontro Nacional de Saneamento Básico / Simpósio Luso-Brasileiro de Engenharia Sanitária e Ambiental **2010**.

Fidalgo e Costa P. The oogenic cycle of Nereis diversicolor (O.F. Muller, 1776) (Annelida: Polycheta) in shallow water environments in south western Portugal. *Boletín Instituto Español de Oceanografia* **2003**, 19(1-4), 17-29.

Fortunato AB, Pinto LL, Oliveira A, Ferreira JS. Tidally-generated shelf waves off the western Iberian coast. *Continental and Shelf Research* **2002**, 22(14), 1935-1950.

Freire P, Taborda R, Bertin X, Fortunato AB, Andrade C, Oliveira A, Antunes C, Guerreiro M, Freitas CM, Nahon A, Silva AM, Rodrigues, M. Medium-term morphodynamic evolution of a small coastal stream. *Journal of Coastal Research* **2011**, SI 64, 666-670.

Gama-Pereira C. Dinâmica de sistemas sedimentares do litoral ocidental português a sul do Cabo Espichel. PhD Thesis, Universidade de Évora, **2005**.

Guerreiro, M. Morphodynamic modeling of the Aljezur inlet. M.Sc. Thesis, Universidade de Aveiro, **2010**.

Jacob J, Carvalho R, David L, Charneca N. Hydraulic Structures Design Data Provided by GIS Tools and Hydrologic Modelling – the Case of Aljezur Basin. In *Hydraulic Structures: Useful Water Harvesting Systems or Relics?*, Proc. of IJREWHS'10, Janssen R and Chanson H,

Eds.; Hydraulic Model Report CH80/10; School of Civil Engineering: The University of Queensland, Brisbane, Australia, **2010**, 157-164.

Ministério do Ambiente e do Ordenamento do Território (MAOT). *Plano de Bacia Hidrográfica das Ribeiras do Algarve, 1ª fase, Volume III*, Lisboa, Portugal, **2000**.

Oliveira A, Fortunato AB, Guerreiro M, Bertin X, Bruneau N, Rodrigues M, Taborda R, Andrade C, Silva AM, Antunes C, Freire P, Pedro LS, Dodet G, Loureiro C, Mendes A. Effect of inlet morphology and wave action on pollutant pathways and sediment dynamics in a coastal stream. Estuarine and Coastal Modeling - Proceedings of the Eleventh International Conference, Ed. Malcolm L. Spaulding, ASCE, **2010**, 601-620.

Oliveira A, Rodrigues M, Fortunato AB, Guerreiro, M. Impact of seasonal bathymetric changes and inlet morphology on the 3D water renewal and residence times of a small coastal stream. *Journal of Coastal Research* **2011**, SI 64, 1555-1559.

Rodrigues M, Oliveira A, Guerreiro M, Fortunato AB, Menaia J, David LM, Cravo A. Modeling fecal contamination in the Aljezur coastal stream (Portugal). *Ocean Dynamics* **2011**, 61(6), 841-856.

Rodrigues M, Oliveira A, Queiroga H, Fortunato AB, Zhang YJ. Three-dimensional modeling of the lower trophic levels in the Ria de Aveiro (Portugal). *Ecological Mode*lling **2009**, 220, 1274–1290.

Zheng X, Zhao M, Dickinson RE. Intercomparison of bulk aerodynamic algorithms for the computation of sea surface fluxes using TOGA COARE and TAO data. *Journal of Climate* **1998**, 11, 2628-2644.

APPENDIX III

COMPLEMENTARY RESULTS OF THE DATA ANALYSIS IN THE AVEIRO LAGOON BETWEEN 1985 AND 2010

AIII.1 COMPLEMENTARY RESULTS OF THE DATA ANALYSIS IN THE AVEIRO LAGOON BETWEEN 1985 AND 2010

Table AIII.1. Descriptive statistics based on discrete data for all variables (AirT – air temperature; SRad – solar radiation; Rain – rainfall; WindI – wind intensity; RFlow – river flow; NAO – NAO index; Salt – salinity, WTemp – water temperature, Chl a – chlorophyll *a*; DO – dissolved oxygen; NH_4^+ – ammonium; NO_x^- – nitrates + nitrites; PO_4^{3-} - phosphates; SiO_2 - silicates).

	N	Mean	Median	Minimum	Maximum	Standard Deviation	Percentile 90
AirT (ºC)	9496	15.5	15.6	1.0	29.5	4.2	20.5
SRad (kJ m^{-2})	9488	17171	16752	0	34539	7946	28511
Rain (mm day^{-1})	9490	3	0	0	88	7	9
WindI (m s^{-1})	9490	2.9	2.6	0	11.0	1.4	4.7
RFlow (m^3 s^{-1})	8513	7	5	0.01	125.6	9.3	15.2
NAO (-)	9494	-	-	-3.3	2.4	-	-
RA10 station							
Sal (-)	50	35.4	35.6	32.4	35.9	0.7	35.8
WTemp (ºC)	52	15.3	15.0	11.5	19.0	2.2	18.6
Chl a (μg l^{-1})	50	4.2	3.1	1.1	18.0	3.5	7.3
DO (mg l^{-1})	51	8.4	8.4	5.3	13.7	1.3	9.1
NH_4^+ (μM)	52	1.7	1.1	<0.7	8.3	1.6	3.3
NO_x^- (μM)	52	4.2	2.3	0.3	52.4	7.4	6.6
PO_4^{3-} (μM)	52	0.4	0.3	0.1	3.5	0.5	0.6
SiO_2 (μM)	52	4.3	3.5	0.1	28.9	4.2	6.2
RA4 station							
Sal (-)	42	32.0	34.6	8.9	36.0	5.8	35.6
WTemp (ºC)	42	16.4	17.0	8	27.3	4.1	20.8
Chl a (μg l^{-1})	41	3.1	2.8	0.8	7.2	1.5	4.9
DO (mg l^{-1})	42	8.3	8.3	3.3	11.8	1.4	9.4
NH_4^+ (μM)	42	4.0	3.5	1.3	10.0	2.2	7.1
NO_x^- (μM)	42	11.9	5.1	0.9	95.1	17.8	24.7
PO_4^{3-} (μM)	42	0.6	0.5	0.1	1.8	0.3	1.0
SiO_2 (μM)	42	12.8	9.0	1.1	65.4	13.6	24.5
RA11 station							
Sal (-)	52	<2.0	<2.0	<2.0	<2.0	-	<2.0
WTemp (ºC)	52	16.9	17.8	8	26.4	5.5	23.4
Chl a (μg l^{-1})	51	9.0	6.6	0.3	31.2	7.8	21.4
DO (mg l^{-1})	51	8.0	8.4	0.1	11.1	2.6	10.4
NH_4^+ (μM)	50	4.6	3.1	<0.7	22.1	5.1	9.9
NO_x^- (μM)	50	67.9	72.1	0.9	149.2	36.5	104.9
PO_4^{3-} (μM)	50	0.4	0.4	0.1	1.1	0.2	0.8
SiO_2 (μM)	50	80.2	85.6	3.5	132.1	34.2	117.2

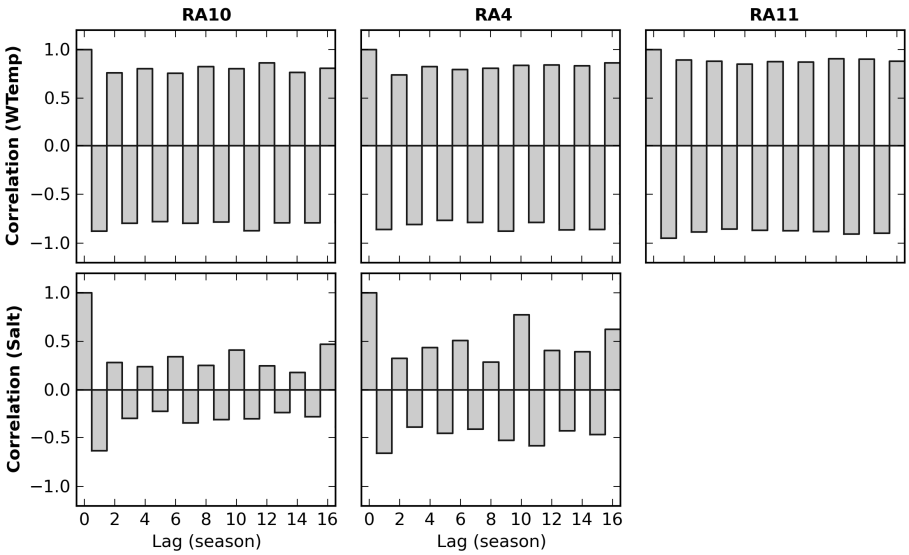

Figure AIII.1. Seasonal autocorrelation of water temperature (WTemp) and salinity (Salt) measured in the stations RA10, RA4 and RA11 along the Aveiro lagoon. Measurements of salinity at station RA11 present no variability through the time series.

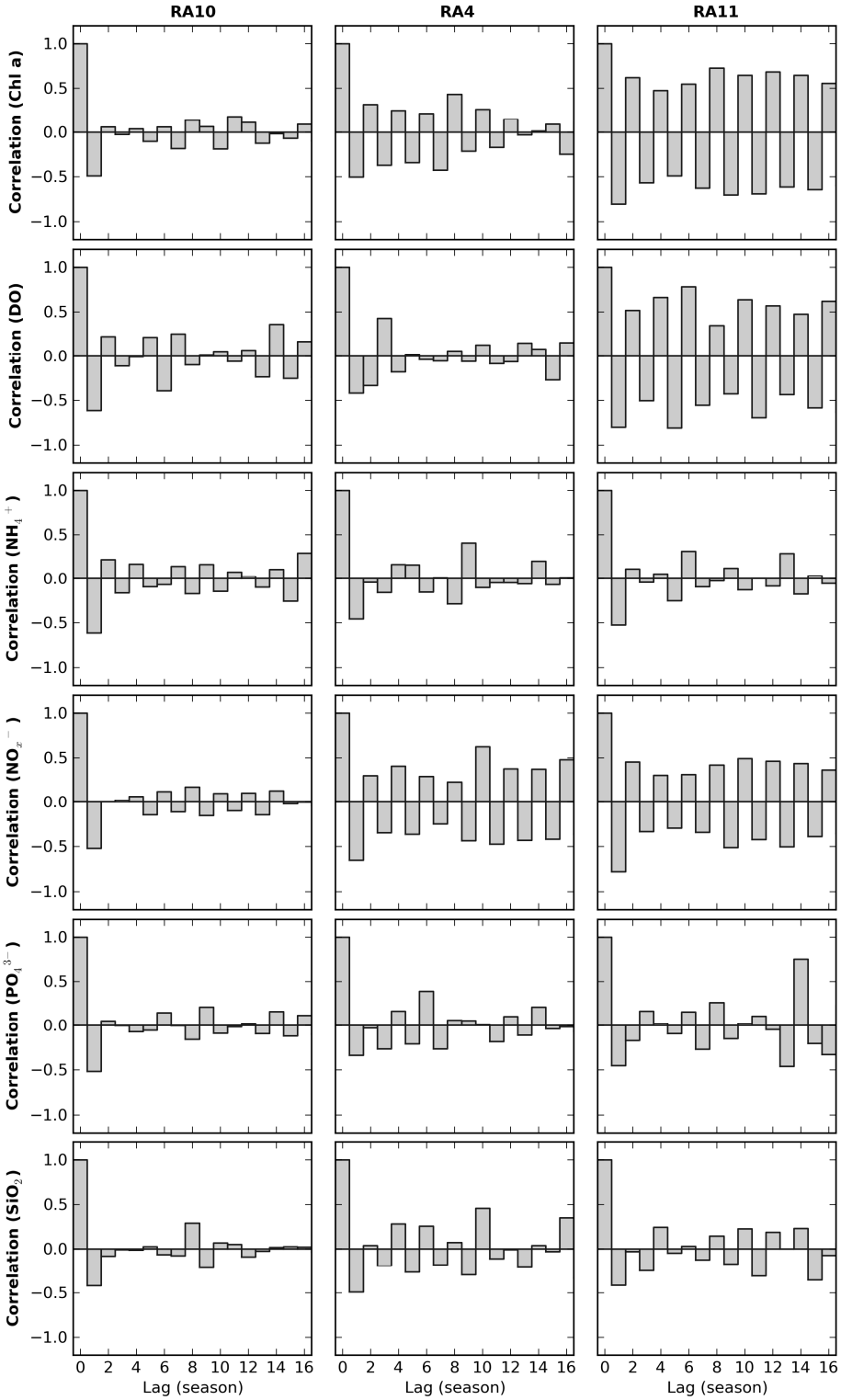

Figure AIII.2. Seasonal autocorrelation of bio-chemical parameters measured in the stations RA10, RA4 and RA11 along the Aveiro lagoon (Chl a – chlorophyll *a*; DO – dissolved oxygen; NH_4^+ – ammonium; NO_x^- – nitrates + nitrites; PO_4^{3-} - phosphates; SiO_2 - silicates).

Table AIII.2. Spearman rank correlations between water quality variables at station RA10 (Salt – salinity, WTemp – water temperature, Chl a – chlorophyll *a*; DO – dissolved oxygen; NH_4^+ – ammonium; NO_x^- – nitrates + nitrites; PO_4^{3-} - phosphates; SiO_2 - silicates) and climatic and hydrological variables integrated over an 8-days period prior to the water quality sampling date (AirT – air temperature; SRad – solar radiation; Rain – rainfall; WindI – wind intensity; RFlow – river flow). Significant correlations for $p<0.05$ with Bonferroni correction are marked with *.

	Salt	WTemp	Chl a	DO	NH_4^+	NO_x^-	PO_4^{3-}	SiO_2
AirT	0.531*	0.813*	0.195	-0.254	0.069	-0.555*	-0.402	-0.129
SRad	0.581*	0.549*	0.260	-0.100	0.013	-0.418	-0.354	-0.286
Rain	-0.296	-0.156	-0.088	-0.149	0.021	0.226	0.274	0.290
WindI	-0.028	-0.151	0.236	0.003	-0.198	0.234	0.100	0.268
RFlow	-0.499*	-0.422	-0.191	0.251	0.129	0.287	0.266	0.145

Table AIII.3. Spearman rank correlations between water quality variables at station RA10 (Salt – salinity, WTemp – water temperature, Chl a – chlorophyll *a*; DO – dissolved oxygen; NH_4^+ – ammonium; NO_x^- – nitrates + nitrites; PO_4^{3-} - phosphates; SiO_2 - silicates) and climatic and hydrological variables integrated over an 1-month period prior to the water quality sampling date (AirT – air temperature; SRad – solar radiation; Rain – rainfall; WindI – wind intensity; RFlow – river flow). Significant correlations for $p<0.05$ with Bonferroni correction are marked with *.

	Salt	WTemp	Chl a	DO	NH_4^+	NO_x^-	PO_4^{3-}	SiO_2
AirT	0.626*	0.830*	0.160	-0.368	-0.068	-0.506*	-0.439	-0.081
SRad	0.626*	0.733*	0.324	-0.218	0.130	-0.554*	-0.385	-0.239
Rain	-0.450	-0.424	-0.225	-0.127	-0.022	0.464	0.365	0.314
WindI	0.018	0.129	-0.003	-0.022	-0.025	0.052	-0.010	0.177
RFlow	-0.585*	-0.564*	-0.204	0.387	0.059	0.374	0.245	0.205

Table AIII.4. Spearman rank correlations between water quality variables at station RA10 (Salt – salinity, WTemp – water temperature, Chl a – chlorophyll *a*; DO – dissolved oxygen; NH_4^+ – ammonium; NO_x^- – nitrates + nitrites; PO_4^{3-} - phosphates; SiO_2 - silicates) and climatic and hydrological variables integrated over a 3-months period prior to the water quality sampling date (AirT – air temperature; SRad – solar radiation; Rain – rainfall; WindI – wind intensity; RFlow – river flow). Significant correlations for $p<0.05$ with Bonferroni correction are marked with *.

	Salt	WTemp	Chl a	DO	NH_4^+	NO_x^-	PO_4^{3-}	SiO_2
AirT	0.487*	0.850*	0.102	-0.429	0.072	-0.496*	-0.330	-0.092
SRad	0.660*	0.746*	0.272	-0.252	0.091	-0.529*	-0.314	-0.226
Rain	-0.658*	-0.620*	-0.156	0.187	-0.164	0.462	0.182	0.336
WindI	0.079	0.533*	0.313	-0.152	0.072	-0.333	-0.423	0.096
RFlow	-0.632*	-0.548*	-0.107	0.435	0.083	0.298	0.144	0.166

Table AIII.5. Spearman rank correlations between water quality variables at station RA10 (Salt – salinity, WTemp – water temperature, Chl a – chlorophyll *a*; DO – dissolved oxygen; NH_4^+ – ammonium; NO_x^- – nitrates + nitrites; PO_4^{3-} - phosphates; SiO_2 - silicates) and climatic and hydrological variables integrated over a 6-months period prior to the water quality sampling date (AirT – air temperature; SRad – solar radiation; Rain – rainfall; WindI – wind intensity; RFlow – river flow). Significant correlations for $p<0.05$ with Bonferroni correction are marked with *.

	Salt	WTemp	Chl a	DO	NH_4^+	NO_x^-	PO_4^{3-}	SiO_2
AirT	0.527*	0.742*	-0.012	-0.506*	0.147	-0.334	-0.113	-0.082
SRad	0.584*	0.717*	0.038	-0.359	0.175	-0.362	-0.067	-0.105
Rain	-0.581*	-0.521*	-0.107	0.187	-0.117	0.295	0.105	0.220
WindI	0.282	0.759*	0.383	-0.265	0.165	-0.487*	-0.433	-0.062
RFlow	-0.475	-0.321	-0.039	0.249	0.319	0.118	0.074	-0.036

Table AIII.6. Spearman rank correlations between water quality variables at station RA4 (Salt – salinity, WTemp – water temperature, Chl a – chlorophyll *a*; DO – dissolved oxygen; NH_4^+ – ammonium; NO_x^- – nitrates + nitrites; PO_4^{3-} - phosphates; SiO_2 - silicates) and climatic and hydrological variables integrated over an 8-days period prior to the water quality sampling date (AirT – air temperature; SRad – solar radiation; Rain – rainfall; WindI – wind intensity; RFlow – river flow). Significant correlations for $p<0.05$ with Bonferroni correction are marked with *.

	Salt	WTemp	Chl a	DO	NH_4^+	NO_x^-	PO_4^{3-}	SiO_2
AirT	0.810*	0.857*	-0.039	-0.301	-0.196	-0.710*	0.116	-0.497
SRad	0.779*	0.665*	0.047	-0.460	-0.173	-0.666*	-0.009	-0.569*
Rain	-0.424	-0.183	-0.105	0.234	0.329	0.437	0.294	0.484
WindI	-0.381	-0.305	-0.171	0.196	0.272	0.374	0.382	0.449
RFlow	-0.627*	-0.461	0.020	0.468	-0.062	0.629*	0.006	0.399

Table AIII.7. Spearman rank correlations between water quality variables at station RA4 (Salt – salinity, WTemp – water temperature, Chl a – chlorophyll *a*; DO – dissolved oxygen; NH_4^+ – ammonium; NO_x^- – nitrates + nitrites; PO_4^{3-} - phosphates; SiO_2 - silicates) and climatic and hydrological variables integrated over an 1-month period prior to the water quality sampling date (AirT – air temperature; SRad – solar radiation; Rain – rainfall; WindI – wind intensity; RFlow – river flow). Significant correlations for $p<0.05$ with Bonferroni correction are marked with *.

	Salt	WTemp	Chl a	DO	NH_4^+	NO_x^-	PO_4^{3-}	SiO_2
AirT	0.737*	0.836*	-0.087	-0.374	-0.107	-0.638*	0.173	-0.407
SRad	0.799*	0.730*	0.004	-0.469	-0.028	-0.757*	0.024	-0.549*
Rain	-0.632*	-0.390	-0.252	0.167	0.212	0.632*	0.190	0.532*
WindI	-0.080	-0.055	0.140	0.134	0.050	0.173	0.180	0.000
RFlow	-0.647*	-0.543*	0.082	0.468	-0.089	0.705*	-0.008	0.370

Table AIII.8. Spearman rank correlations between water quality variables at station RA4 (Salt – salinity, WTemp – water temperature, Chl a – chlorophyll *a*; DO – dissolved oxygen; NH_4^+ – ammonium; NO_x^- – nitrates + nitrites; PO_4^{3-} - phosphates; SiO_2 - silicates) and climatic and hydrological variables integrated over a 3-months period prior to the water quality sampling date (AirT – air temperature; SRad – solar radiation; Rain – rainfall; WindI – wind intensity; RFlow – river flow). Significant correlations for $p<0.05$ with Bonferroni correction are marked with *.

	Salt	WTemp	Chl a	DO	NH_4^+	NO_x^-	PO_4^{3-}	SiO_2
AirT	0.706*	0.757*	-0.140	-0.405	-0.140	-0.603*	0.183	-0.362
SRad	0.775*	0.686*	-0.019	-0.466	-0.054	-0.733*	0.017	-0.557*
Rain	-0.786*	-0.557*	0.147	0.417	0.014	0.777*	-0.121	0.606*
WindI	0.327	0.487	0.169	0.023	-0.154	-0.258	0.066	-0.133
RFlow	-0.664*	-0.528*	0.195	0.487	-0.096	0.711*	-0.128	0.434

Table AIII.9. Spearman rank correlations between water quality variables at station RA4 (Salt – salinity, WTemp – water temperature, Chl a – chlorophyll *a*; DO – dissolved oxygen; NH_4^+ – ammonium; NO_x^- – nitrates + nitrites; PO_4^{3-} - phosphates; SiO_2 - silicates) and climatic and hydrological variables integrated over a 6-months period prior to the water quality sampling date (AirT – air temperature; SRad – solar radiation; Rain – rainfall; WindI – wind intensity; RFlow – river flow). Significant correlations for $p<0.05$ with Bonferroni correction are marked with *.

	Salt	WTemp	Chl a	DO	NH_4^+	NO_x^-	PO_4^{3-}	SiO_2
AirT	0.664*	0.680	-0.212	-0.393	-0.047	-0.541*	0.333	-0.323
SRad	0.721*	0.582	-0.215	-0.340	-0.040	-0.609*	0.299	-0.429
Rain	-0.809*	-0.453	0.204	0.352	0.109	0.766*	-0.219	0.601*
WindI	0.515*	0.726*	0.094	-0.104	-0.069	-0.433	0.141	-0.209
RFlow	-0.455	-0.219	0.192	0.351	-0.030	0.481	-0.073	0.205

Table AIII.10. Spearman rank correlations between water quality variables at station RA11 (Salt – salinity, WTemp – water temperature, Chl a – chlorophyll *a*; DO – dissolved oxygen; NH_4^+ – ammonium; NO_x^- – nitrates + nitrites; PO_4^{3-} - phosphates; SiO_2 - silicates) and climatic and hydrological variables integrated over an 8-days period prior to the water quality sampling date (AirT – air temperature; SRad – solar radiation; Rain – rainfall; WindI – wind intensity; RFlow – river flow). Significant correlations for $p<0.05$ with Bonferroni correction are marked with *.

	Salt	WTemp	Chl a	DO	NH_4^+	NO_x^-	PO_4^{3-}	SiO_2
AirT	-	0.924*	0.690*	-0.719*	-0.060	-0.628*	0.121	0.307
SRad	-	0.653*	0.560*	-0.623*	-0.245	-0.674*	-0.009	0.090
Rain	-	-0.431	-0.354	0.349	0.053	0.413	0.042	-0.118
WindI	-	-0.242	-0.149	-0.002	-0.158	-0.157	-0.094	-0.390
RFlow	-	-0.557*	-0.497*	0.617*	0.020	0.683*	-0.002	-0.001

Table AIII.11. Spearman rank correlations between water quality variables at station RA11 (Salt – salinity, WTemp – water temperature, Chl a – chlorophyll *a*; DO – dissolved oxygen; NH_4^+ – ammonium; NO_x^- – nitrates + nitrites; PO_4^{3-} - phosphates; SiO_2 - silicates) and climatic and hydrological variables integrated over an 1-month period prior to the water quality sampling date (AirT – air temperature; SRad – solar radiation; Rain – rainfall; WindI – wind intensity; RFlow – river flow). Significant correlations for p<0.05 with Bonferroni correction are marked with *.

	Salt	WTemp	Chl a	DO	NH_4^+	NO_x^-	PO_4^{3-}	SiO_2
AirT	-	0.849*	0.690*	-0.722*	-0.100	-0.670*	0.077	0.257
SRad	-	0.800*	0.724*	-0.719*	-0.157	-0.645*	0.132	0.195
Rain	-	-0.574*	-0.532*	0.509*	-0.065	0.554*	-0.012	0.001
WindI	-	0.093	-0.064	-0.216	-0.128	-0.292	-0.164	-0.311
RFlow	-	-0.639*	-0.646*	0.695*	-0.025	0.597*	-0.075	-0.047

Table AIII.12. Spearman rank correlations between water quality variables at station RA11 (Salt – salinity, WTemp – water temperature, Chl a – chlorophyll *a*; DO – dissolved oxygen; NH_4^+ – ammonium; NO_x^- – nitrates + nitrites; PO_4^{3-} - phosphates; SiO_2 - silicates) and climatic and hydrological variables integrated over a 3-months period prior to the water quality sampling date (AirT – air temperature; SRad – solar radiation; Rain – rainfall; WindI – wind intensity; RFlow – river flow). Significant correlations for p<0.05 with Bonferroni correction are marked with *.

	Salt	WTemp	Chl a	DO	NH_4^+	NO_x^-	PO_4^{3-}	SiO_2
AirT	-	0.769*	0.666*	-0.647*	-0.131	-0.566*	0.105	0.391
SRad	-	0.772*	0.680*	-0.745*	-0.119	-0.550*	0.159	0.203
Rain	-	-0.732*	-0.698*	0.706*	0.013	0.601*	-0.204	-0.109
WindI	-	0.446	0.245	-0.381	-0.085	-0.482*	-0.189	-0.008
RFlow	-	-0.642*	-0.619*	0.764*	0.025	0.633*	-0.092	-0.006

Table AIII.13. Spearman rank correlations between water quality variables at station RA11 (Salt – salinity, WTemp – water temperature, Chl a – chlorophyll *a*; DO – dissolved oxygen; NH_4^+ – ammonium; NO_x^- – nitrates + nitrites; PO_4^{3-} - phosphates; SiO_2 - silicates) and climatic and hydrological variables integrated over a 6-months period prior to the water quality sampling date (AirT – air temperature; SRad – solar radiation; Rain – rainfall; WindI – wind intensity; RFlow – river flow). Significant correlations for p<0.05 with Bonferroni correction are marked with *.

	Salt	WTemp	Chl a	DO	NH_4^+	NO_x^-	PO_4^{3-}	SiO_2
AirT	-	0.701*	0.666*	-0.532*	-0.038	-0.404	0.229	0.402
SRad	-	0.700*	0.655*	-0.609*	-0.012	-0.373	0.325	0.420
Rain	-	-0.673*	-0.647*	0.610*	0.016	0.561*	-0.186	-0.214
WindI	-	0.670*	0.530*	-0.600*	-0.090	-0.601*	0.007	0.158
RFlow	-	-0.389	-0.403	0.644*	-0.021	0.447	-0.023	0.101

APPENDIX IV

COMPLEMENTARY RESULTS OF THE ANALYSIS OF THE INFLUENCE OF CLIMATE CHANGE AND ANTHROPOGENIC PRESSURES IN THE AVEIRO LAGOON

AIV.1 COMPLEMENTARY RESULTS OF THE ANALYSIS OF THE INFLUENCE OF CLIMATE CHANGE AND ANTHROPOGENIC PRESSURES IN THE AVEIRO LAGOON

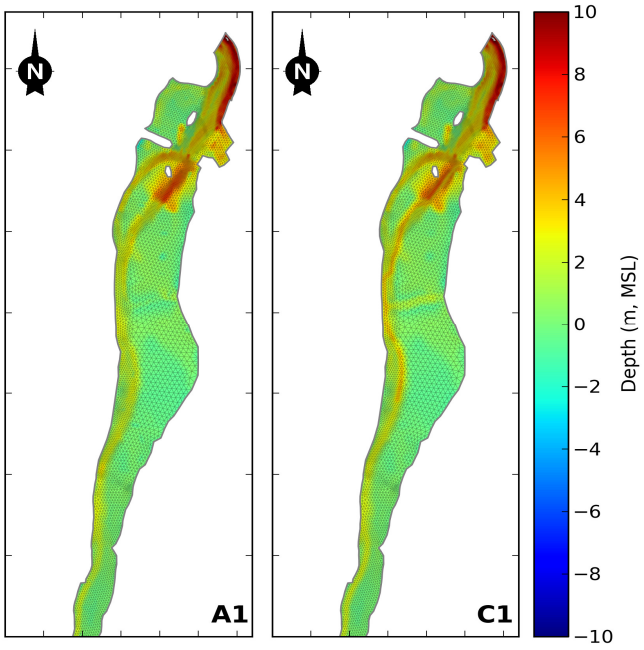

Figure AIV.1. Detailed view of the hydrodynamic-ecological horizontal grid and bathymetry in the downstream area of the Mira channel (MSL – mean sea level): reference (A1) and dredging (C1) scenarios.

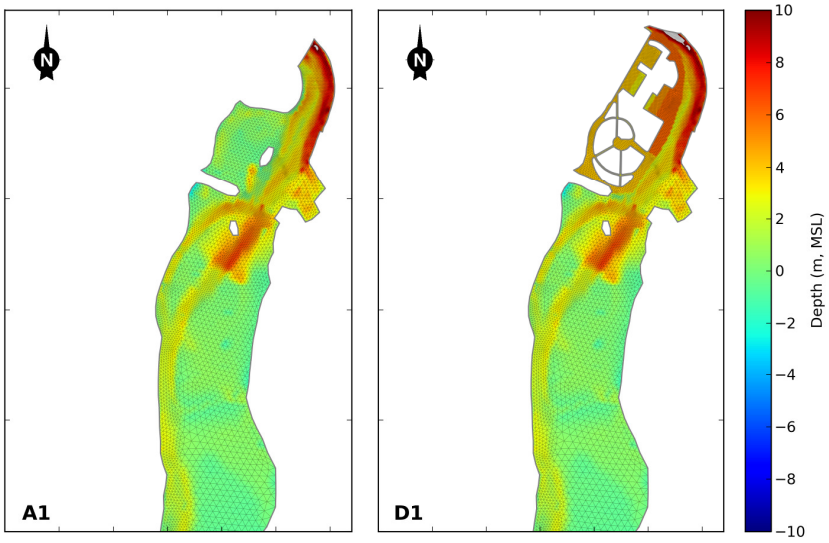

Figure AIV.2. Detailed view of the hydrodynamic-ecological horizontal grid and bathymetry in the downstream area of the Mira channel (MSL – mean sea level): reference (A1) and marina construction (D1) scenarios.

Table AIV.1. Mean (minimum and maximum) surface annual salinity and water temperature at CM stations. Relative difference from the reference scenario is represented by the colorbar.

Scenario	CM2	CM3	CM4	CM5	CM6	CM7
Salinity						
S0	32.0 (15.7-35.7)	30.1 (9.0-35.5)	24.7 (1.4-35.1)	14.8 (0.0-34.4)	7.8 (0.0-27.3)	3.4 (0.0-19.8)
S1	31.8 (15.1-35.7)	29.9 (8.6-35.5)	24.5 (1.2-35.0)	14.5 (0.0-34.3)	7.4 (0.0-26.8)	3.1 (0.0-19.0)
S2	31.8 (15.1-35.6)	29.9 (8.5-35.5)	24.5 (1.2-35.0)	14.5 (0.0-34.2)	7.4 (0.0-26.0)	3.2 (0.0-18.9)
S3	32.0 (13.5-35.8)	30.2 (7.1-35.7)	25.1 (0.7-35.4)	15.9 (0.0-35.0)	9.4 (0.0-30.4)	4.8 (0.0-24.3)
S4	32.8 (15.3-35.8)	31.3 (8.7-35.8)	26.9 (1.2-35.5)	18.4 (0.0-35.1)	11.6 (0.0-31.1)	6.1 (0.0-24.7)
S5	34.5 (28.2-35.9)	34.2 (24.1-35.9)	33.1 (12.2-35.7)	29.8 (4.3-35.7)	23.6 (1.6-35.7)	18.2 (0.3-34.7)
S6	34.5 (28.5-35.9)	34.1 (24.9-35.8)	33.1 (13.6-35.7)	29.9 (6.0-35.6)	24.0 (2.5-35.6)	19.4 (0.7-34.5)
S7	32.2 (16.5-35.6)	30.3 (8.1-35.5)	25.8 (1.6-35.0)	17.1 (0.0-34.3)	10.6 (0.0-31.2)	4.4 (0.0-24.1)
S8	31.9 (15.9-35.6)	30.1 (9.2-35.4)	24.8 (1.4-35.0)	14.9 (0.0-34.4)	7.9 (0.0-27.2)	3.5 (0.0-19.8)
S9	31.9 (15.5-35.7)	30.0 (8.8-35.5)	24.6 (1.3-35.1)	14.6 (0.0-34.3)	7.5 (0.0-26.8)	3.4 (0.0-19.4)
S10	32.1 (16.2-35.5)	30.1 (7.8-35.4)	25.5 (1.6-34.9)	16.7 (0.0-34.2)	10.1 (0.0-31.1)	4.0 (0.0-23.2)
S11	31.9 (13.8-35.7)	30.2 (7.2-35.6)	25.2 (0.7-35.3)	16.1 (0.0-35.0)	9.7 (0.0-30.4)	5.0 (0.0-24.6)
Water Temperature (ºC)						
S0	16.4 (9.4-23.8)	16.5 (9.1-24.2)	16.6 (8.9-24.4)	16.9 (8.9-24.4)	17.0 (8.9-24.3)	17.4 (9.0-24.1)
S1	16.9 (9.9-25.9)	17.2 (9.5-26.3)	17.5 (9.3-26.6)	18.0 (9.3-26.6)	18.1 (9.3-26.4)	18.4 (9.4-26.1)
S2	17.3 (10.0-27.0)	17.6 (9.6-27.5)	18.0 (9.4-27.7)	18.5 (9.4-27.7)	18.7 (9.4-27.5)	18.9 (9.5-27.3)
S3	16.3 (9.4-23.8)	16.4 (9.1-24.2)	16.6 (9.0-24.5)	16.9 (9.0-24.5)	17.1 (9.0-24.4)	17.5 (9.1-24.1)
S4	16.3 (9.4-23.9)	16.4 (9.1-24.2)	16.6 (8.9-24.5)	16.9 (8.9-24.4)	17.0 (8.9-24.4)	17.4 (9.0-24.1)
S5	16.1 (9.5-23.4)	16.2 (9.3-23.8)	16.4 (9.1-24.3)	16.7 (9.1-24.3)	16.9 (9.0-24.4)	17.1 (9.2-24.3)
S6	16.0 (9.5-23.4)	16.1 (9.3-23.9)	16.4 (9.2-24.3)	16.7 (9.2-24.4)	16.9 (9.1-24.4)	17.1 (9.3-24.3)
S7	16.0 (9.5-23.7)	16.2 (9.2-24.3)	16.4 (9.1-24.5)	16.8 (9.2-24.4)	16.9 (9.1-24.4)	17.3 (9.3-24.3)
S8	16.3 (9.5-23.8)	16.5 (9.1-24.2)	16.6 (8.9-24.4)	16.9 (8.9-24.4)	17.0 (8.9-24.3)	17.4 (9.0-24.1)
S9	15.9 (7.9-21.0)	15.8 (7.3-21.1)	15.5 (6.9-21.2)	15.0 (6.8-21.2)	14.6 (6.8-21.2)	15.3 (7.1-21.1)
S10	16.6 (10.0-25.7)	16.9 (9.7-26.5)	17.3 (9.6-26.6)	17.9 (9.6-26.5)	18.0 (9.5-26.5)	18.3 (9.7-26.3)
S11	16.1 (9.5-23.8)	16.3 (9.3-24.2)	16.5 (9.2-24.5)	16.8 (9.3-24.5)	17.0 (9.3-24.4)	17.1 (9.4-24.1)

Relative difference from the reference scenario	<-1	[-1, -0.6[	[-0.6, -0.4[	[-0.4, -0.2[	[-0.2, 0[	0	]0, 0.2]	]0.2, 0.4]	]0.4, 0.6]	]0.6, 1]	>1

Table AIV.2. Mean (minimum and maximum) surface annual concentrations of nutrients at CM stations. Relative difference from the reference scenario is represented by the colorbar.

Scenario	CM2	CM3	CM4	CM5	CM6	CM7
Ammonium (μM)						
S0	2.5 (1.1-11.7)	3.2 (1.2-16.2)	5.4 (1.3-21.2)	9.6 (1.6-22.1)	12.9 (5.0-22.2)	15.7 (7.3-26.8)
S1	2.5 (1.1-12.1)	3.2 (1.2-16.5)	5.4 (1.3-21.3)	9.7 (1.6-22.1)	13.1 (5.1-22.2)	15.8 (7.3-26.9)
S2	2.5 (1.1-12.1)	3.2 (1.2-16.5)	5.4 (1.3-21.3)	9.7 (1.6-22.1)	13.1 (5.1-22.2)	15.7 (7.2-26.5)
S3	2.5 (1.1-12.9)	3.2 (1.2-17.3)	5.2 (1.3-21.6)	9.0 (1.6-22.1)	12.0 (4.3-22.4)	14.8 (6.8-25.7)
S4	2.4 (1.1-11.9)	2.9 (1.2-16.3)	4.7 (1.3-21.3)	8.2 (1.4-22.1)	11.1 (2.9-22.2)	14.1 (4.7-25.5)
S5	1.9 (1.0-4.0)	2.0 (1.0-6.5)	2.4 (1.0-14.5)	3.8 (1.2-19.4)	6.5 (1.3-21.1)	9.0 (2.0-22.3)
S6	1.9 (1.0-3.9)	2.0 (1.0-6.1)	2.4 (1.0-13.6)	3.8 (1.2-18.3)	6.4 (1.3-20.6)	8.5 (2.0-22.0)
S7	2.5 (1.1-10.7)	3.2 (1.1-16.5)	5.1 (1.2-21.0)	9.1 (1.6-22.1)	12.1 (3.0-22.4)	15.6 (6.4-27.1)
S8	2.5 (1.2-11.7)	3.2 (1.3-16.2)	5.4 (1.3-21.2)	9.6 (1.6-22.1)	12.9 (5.0-22.2)	15.7 (7.3-26.8)
S9	2.6 (1.1-11.7)	3.3 (1.2-16.3)	5.6 (1.3-21.2)	10.1 (1.8-22.1)	13.5 (5.6-22.2)	15.9 (8.3-26.1)
S10	2.5 (1.1-10.9)	3.2 (1.1-16.7)	5.2 (1.2-21.1)	9.2 (1.6-22.1)	12.3 (3.1-22.4)	15.8 (6.6-27.2)
S11	2.6 (1.2-12.9)	3.2 (1.3-17.3)	5.3 (1.4-21.6)	9.1 (1.8-22.1)	12.1 (4.3-22.4)	14.9 (6.9-25.6)
Nitrates (μM)						
S0	23.3 (3.2-138.8)	28.8 (3.2-194.7)	46.8 (3.2-273.1)	82.4 (3.6-317.6)	113.5 (6.0-344.9)	141.0 (8.0-361.9)
S1	23.6 (3.3-140.3)	29.1 (3.3-196.6)	47.4 (3.3-274.2)	83.5 (3.6-317.6)	115.6 (6.3-345.5)	142.5 (8.6-362.1)
S2	23.6 (3.3-138.2)	29.1 (3.3-195.9)	47.4 (3.3-273.9)	83.5 (3.7-317.2)	115.7 (6.4-345.8)	142.4 (8.6-362.0)
S3	24.2 (3.1-154.5)	30.2 (3.1-212.6)	48.9 (3.1-292.3)	84.3 (3.2-327.5)	113.5 (5.3-350.6)	138.9 (7.3-365.2)
S4	22.6 (3.1-141.1)	27.3 (3.1-197.7)	42.8 (3.1-276.1)	74.0 (3.2-319.1)	102.3 (5.4-345.7)	131.0 (7.2-362.4)
S5	18.2 (2.8-56.6)	18.6 (2.7-82.8)	23.1 (2.6-183.3)	38.7 (2.6-267.7)	68.5 (2.6-315.3)	91.1 (3.7-349.9)
S6	18.2 (2.8-57.0)	18.6 (2.6-80.4)	22.7 (2.6-169.7)	37.9 (2.6-249.2)	66.4 (2.6-305.0)	86.1 (3.7-344.2)
S7	23.0 (3.2-147.3)	29.2 (3.2-214.4)	46.2 (3.2-282.8)	82.0 (3.5-336.6)	111.6 (5.0-351.0)	144.1 (7.6-368.8)
S8	23.2 (3.1-139.9)	28.7 (3.1-195.2)	46.7 (3.1-273.1)	82.2 (3.5-317.6)	113.6 (5.8-344.9)	140.9 (7.9-361.9)
S9	23.5 (3.2-140.6)	29.0 (3.2-197.8)	47.1 (3.2-273.5)	82.8 (3.6-317.7)	114.6 (6.4-344.9)	141.3 (8.5-361.9)
S10	23.2 (3.3-148.9)	29.6 (3.3-217.0)	46.8 (3.3-283.4)	83.3 (3.6-336.5)	113.8 (5.3-351.0)	145.8 (8.1-368.8)
S11	24.0 (3.0-153.2)	29.9 (3.0-212.0)	48.5 (3.0-291.8)	83.7 (3.1-327.3)	112.9 (5.2-350.8)	138.4 (7.0-365.3)
Phosphates (μM)						
S0	2.6 (2.0-4.0)	2.7 (1.6-5.0)	3.2 (1.2-6.6)	4.1 (1.1-7.9)	4.9 (1.0-9.3)	5.6 (1.0-11.4)
S1	2.6 (2.0-4.1)	2.7 (1.6-5.0)	3.2 (1.2-6.7)	4.2 (1.0-8.1)	5.0 (1.0-9.5)	5.7 (1.0-11.4)
S2	2.6 (2.0-4.1)	2.7 (1.6-5.0)	3.2 (1.2-6.6)	4.2 (1.1-8.1)	5.0 (1.0-9.4)	5.6 (1.0-11.3)
S3	2.6 (2.0-4.2)	2.7 (1.6-5.2)	3.1 (1.3-6.3)	3.9 (1.1-7.5)	4.7 (1.0-8.7)	5.4 (1.0-11.0)
S4	2.6 (2.2-4.1)	2.7 (1.9-5.0)	3.0 (1.6-6.1)	3.8 (1.3-7.2)	4.5 (1.2-8.6)	5.3 (1.1-11.0)
S5	2.5 (2.2-3.0)	2.5 (2.2-3.2)	2.5 (2.1-3.9)	2.8 (1.8-4.8)	3.3 (1.5-6.0)	3.8 (1.2-8.0)
S6	2.5 (2.2-3.0)	2.5 (2.2-3.2)	2.6 (2.1-3.8)	2.8 (1.8-4.8)	3.3 (1.6-6.0)	3.7 (1.3-7.6)
S7	2.6 (2.0-4.0)	2.7 (1.7-5.1)	3.1 (1.3-6.4)	3.9 (1.1-7.6)	4.6 (1.1-8.8)	5.5 (1.1-11.3)
S8	2.6 (2.0-4.1)	2.7 (1.6-5.1)	3.2 (1.2-6.6)	4.1 (1.1-7.9)	4.9 (1.0-9.3)	5.6 (1.0-11.3)
S9	2.6 (2.0-4.1)	2.7 (1.6-5.1)	3.2 (1.3-6.7)	4.2 (1.1-8.2)	5.0 (1.1-9.4)	5.6 (1.1-11.0)
S10	2.6 (2.0-4.0)	2.7 (1.6-5.1)	3.1 (1.3-6.4)	4.0 (1.1-7.7)	4.7 (1.1-9.0)	5.6 (1.1-11.3)
S11	2.6 (2.0-4.2)	2.7 (1.6-5.2)	3.1 (1.3-6.3)	3.9 (1.1-7.5)	4.7 (1.0-8.6)	5.4 (1.0-11.0)
Silicates (μM)						
S0	30.0 (19.1-113.0)	39.0 (19.1-150.1)	67.5 (19.3-192.1)	120.7 (22.4-199.3)	157.8 (59.1-199.4)	181.0 (98.0-199.8)
S1	30.3 (19.0-116.1)	39.5 (19.1-152.8)	68.4 (19.4-192.8)	122.4 (22.6-199.4)	160.2 (61.5-199.4)	182.6 (101.8-199.8)
S2	30.4 (19.1-116.5)	39.6 (19.1-153.0)	68.5 (19.4-192.8)	122.3 (22.7-199.4)	160.1 (65.3-199.4)	182.0 (102.2-199.8)
S3	30.1 (19.0-123.3)	38.8 (19.1-159.9)	65.9 (19.2-195.4)	115.5 (21.5-199.4)	149.9 (45.1-199.6)	174.1 (76.2-199.8)
S4	27.8 (19.0-114.6)	35.0 (19.1-151.6)	58.1 (19.2-192.7)	103.4 (21.4-199.3)	138.7 (41.9-199.4)	167.5 (74.6-199.8)
S5	21.7 (18.9-49.1)	22.6 (18.9-70.2)	28.0 (18.9-136.5)	45.4 (18.9-177.4)	77.9 (19.0-191.2)	106.0 (23.9-197.8)
S6	21.7 (18.9-48.2)	22.7 (18.9-66.7)	27.9 (18.9-129.3)	44.9 (18.9-168.4)	75.8 (19.1-186.3)	99.5 (24.9-195.7)
S7	28.6 (19.1-108.5)	37.8 (19.1-155.0)	61.7 (19.2-190.6)	108.7 (21.4-199.1)	143.1 (37.9-199.4)	176.4 (75.1-199.9)
S8	30.3 (19.1-113.2)	39.4 (19.2-150.1)	67.7 (19.5-192.0)	120.6 (22.5-199.4)	157.7 (60.0-199.6)	180.9 (97.8-199.8)
S9	30.2 (19.1-113.9)	39.5 (19.1-150.9)	68.4 (19.3-192.2)	122.2 (23.0-199.3)	159.7 (62.2-199.5)	181.2 (99.8-199.8)
S10	29.0 (19.1-109.9)	38.3 (19.1-156.6)	62.7 (19.2-191.1)	110.6 (21.6-199.1)	145.9 (37.5-199.3)	178.4 (79.2-199.9)
S11	30.4 (19.0-123.2)	39.1 (19.1-159.6)	65.7 (19.3-195.3)	114.7 (21.5-199.7)	149.0 (45.3-199.8)	173.3 (74.9-199.8)

Relative difference from the reference scenario	<-1	[-1, -0.6[	[-0.6, -0.4[	[-0.4, -0.2[	[-0.2, 0[	0	]0, 0.2]	]0.2, 0.4]	]0.4, 0.6]	]0.6, 1]	>1

Table AIV.3. Mean (minimum and maximum) surface annual concentrations of chlorophyll *a* and dissolved oxygen at CM stations. Relative difference from the reference scenario is represented by the colorbar.

Scenario	CM2	CM3	CM4	CM5	CM6	CM7
Chlorophyll *a* (μg l^{-1})						
S0	0.8 (0.2-6.4)	1.1 (0.2-9.7)	2.1 (0.2-14.3)	4.0 (0.2-16.8)	5.4 (0.4-17.7)	6.5 (0.8-18.2)
S1	0.8 (0.2-6.4)	1.1 (0.2-9.7)	2.1 (0.2-14.3)	4.0 (0.2-16.8)	5.4 (0.4-17.7)	6.5 (0.7-18.2)
S2	0.8 (0.2-6.3)	1.1 (0.2-9.7)	2.1 (0.2-14.2)	3.9 (0.2-16.7)	5.4 (0.3-17.7)	6.4 (0.6-18.2)
S3	0.8 (0.2-6.3)	1.1 (0.2-9.6)	2.1 (0.2-14.2)	3.9 (0.2-16.8)	5.3 (0.3-17.7)	6.3 (0.4-18.2)
S4	0.7 (0.2-4.4)	0.9 (0.2-6.9)	1.7 (0.2-11.0)	3.2 (0.2-14.5)	4.5 (0.2-16.6)	5.8 (0.4-17.8)
S5	0.5 (0.1-1.8)	0.5 (0.1-2.9)	0.8 (0.1-7.5)	1.5 (0.1-12.6)	2.8 (0.1-15.2)	3.9 (0.2-17.4)
S6	0.5 (0.1-1.7)	0.5 (0.1-2.8)	0.7 (0.1-6.9)	1.4 (0.1-11.6)	2.7 (0.1-14.4)	3.7 (0.2-17.4)
S7	0.8 (0.2-6.5)	1.1 (0.2-10.2)	2.0 (0.2-14.2)	3.8 (0.2-17.3)	5.1 (0.3-17.9)	6.5 (0.7-18.5)
S8	0.8 (0.2-6.4)	1.1 (0.2-9.8)	2.1 (0.2-14.3)	4.0 (0.2-16.8)	5.4 (0.4-17.7)	6.5 (0.8-18.2)
S9	0.8 (0.2-6.7)	1.1 (0.2-10.2)	2.2 (0.2-14.3)	4.1 (0.2-16.8)	5.6 (0.5-17.7)	6.6 (0.9-18.2)
S10	0.8 (0.2-6.5)	1.1 (0.2-10.2)	2.0 (0.2-14.2)	3.8 (0.2-17.3)	5.2 (0.3-17.8)	6.6 (0.7-18.5)
S11	0.8 (0.2-6.3)	1.1 (0.2-9.8)	2.1 (0.2-14.3)	3.9 (0.2-16.9)	5.2 (0.3-17.8)	6.3 (0.5-18.3)
Dissolved Oxygen (mg l^{-1})						
S0	7.5 (5.7-10.1)	7.7 (5.8-10.6)	8.2 (5.8-11.3)	8.9 (6.2-11.5)	9.3 (7.1-11.5)	9.3 (7.5-11.3)
S1	7.5 (5.7-10.0)	7.7 (5.8-10.6)	8.1 (5.8-11.2)	8.8 (6.2-11.4)	9.1 (7.0-11.4)	9.2 (7.4-11.2)
S2	7.5 (5.7-10.0)	7.6 (5.8-10.5)	8.1 (5.8-11.2)	8.7 (6.2-11.4)	9.1 (6.9-11.4)	9.1 (7.3-11.2)
S3	7.5 (5.7-10.2)	7.7 (5.8-10.8)	8.2 (5.8-11.3)	8.8 (6.2-11.4)	9.2 (7.0-11.4)	9.3 (7.4-11.3)
S4	7.5 (5.7-10.1)	7.7 (5.8-10.7)	8.1 (5.8-11.3)	8.7 (6.2-11.5)	9.1 (6.9-11.5)	9.2 (7.3-11.3)
S5	7.4 (5.7-9.4)	7.5 (5.7-9.6)	7.7 (5.8-10.5)	8.1 (6.1-11.0)	8.5 (6.3-11.1)	8.8 (6.8-11.0)
S6	7.4 (5.7-9.4)	7.5 (5.7-9.6)	7.7 (5.8-10.4)	8.1 (6.1-10.8)	8.5 (6.3-10.9)	8.7 (6.8-10.9)
S7	7.5 (5.7-10.0)	7.8 (5.8-10.8)	8.2 (5.8-11.3)	8.9 (6.2-11.5)	9.2 (6.9-11.5)	9.4 (7.4-11.4)
S8	7.6 (5.8-10.3)	7.8 (5.8-10.8)	8.3 (5.9-11.5)	9.0 (6.3-11.8)	9.4 (7.2-11.8)	9.4 (7.6-11.5)
S9	7.6 (5.7-10.7)	7.8 (5.8-10.8)	8.3 (5.8-10.5)	9.0 (6.3-11.8)	9.4 (7.2-11.8)	9.4 (7.6-11.5)
S10	7.5 (5.7-10.0)	7.7 (5.8-10.7)	8.1 (5.8-11.3)	8.7 (6.2-11.4)	9.1 (6.8-11.4)	9.3 (7.3-11.3)
S11	7.6 (5.8-10.4)	7.8 (5.8-10.9)	8.3 (5.9-11.5)	9.0 (6.3-11.6)	9.3 (7.1-11.6)	9.4 (7.5-11.4)

Relative difference from the reference scenario	<-1	[-1, -0.6[	[-0.6, -0.4[	[-0.4, -0.2[	[-0.2, 0[	0	]0, 0.2]	]0.2, 0.4]	]0.4, 0.6]	]0.6, 1]	>1